
# Reliable Control of Power Electronic based Power Systems

Steinkohl, Joachim

*DOI (link to publication from Publisher):*
10.54337/aau443229854

*Publication date:*
2021

*Document Version*
Publisher's PDF, also known as Version of record

# RELIABLE CONTROL OF POWER ELECTRONIC BASED POWER SYSTEMS

**BY**
**JOACHIM STEINKOHL**

DISSERTATION SUBMITTED 2021

AALBORG UNIVERSITY
DENMARK

# Reliable Control of Power Electronic based Power Systems

Ph.D. Dissertation

Joachim Steinkohl

Dissertation submitted March, 2021

Dissertation submitted: March, 2021

PhD supervisor: Professor Frede Blaabjerg
Aalborg University

Assistant PhD supervisors: Professor Xiongfei Wang
Aalborg University

Associate Professor Pooya Davari
Aalborg University

PhD committee: Associate Professor Florin Iov (chairman)
Aalborg University

Professor Monti, Antonello
RWTH Aachen

Professor Yilu Liu
The University of Tennessee

PhD Series: Faculty of Engineering and Science, Aalborg University

Department: Department of Energy Technology

ISSN (online): 2446-1636
ISBN (online): 978-87-7210-917-6

Published by:
Aalborg University Press
Kroghstræde 3
DK – 9220 Aalborg Ø
Phone: +45 99407140
aauf@forlag.aau.dk
forlag.aau.dk



Printed in Denmark by Rosendahls, 2021

# Abstract

The transition to a full-renewable based power system is currently under process. The ambitious goals of many countries to limit the usage of carbon-based generation units causes the power systems all over the world to be in the most severe change since their beginning. The increasing integration of power-electronic based power generation units influences the power system's ability to operate in a reliable way. Therefore, transmission system operators have to rethink their decisions on planning and operating the power grid.

Previously dominated by a limited number of central power plants, are power systems now including new generation systems, which are decentralized and operate dependent on the current weather conditions. The arising issues include the lack of system inertia, faster rates of power changes, or harmonic interaction, just to mention a few challenges. However, installing power electronic-based units also allows controlling the system much more flexible than ever before. Controls in the units can be adapted in an infinite number of ways to benefit the power system.

FACTS (Flexible AC Transmission Systems) are known to be the fastest units in the power grid to supply reactive power for voltage control. This allows to more reliably connect renewable power plants, such as offshore wind farms, but also to improve the supply of certain loads, such as remote cities or oil-rigs. The installation of more of these units can highly benefit the system operation. It has to be guaranteed that they all contribute with respect to each other when multiple units are in close proximity. Otherwise, these units can cause interactions between each other, causing undesired voltage fluctuations. Thus, the need for a correct adaption of these units arises when they are being used more and more in modern power grids.

This Ph.D. project focuses on the interactions between these kinds of units. It is determined how different units have to adapt to the reactive power support of other FACTS devices without communication between them. It is shown that the currently used method in the industry is not sufficient to reliably maintain the dynamic response. A control scheme is proposed, which allows adapting the FACTS units to changes in the power grid during operation and other units nearby. This is required when these units are being used

more frequently in modern power grids.

Moreover is the reliable control of the system frequency one of the main challenges when it comes to a full-renewable power system. Micro-grids, where the system is highly limited in space, can already be controlled by power converters. Power systems under transition have to operate in compliance with the existing equipment, such as the remaining generation units and the protection system. Renewable power sources, and especially wind power plants, have the potential to support or even replace conventional generation units for frequency supports. Wind power plants can curtail their output power to keep reserve available, or they can even utilize the rotational energy in the blades to provide short-term frequency support. The transmission system operator now has the challenging task of determining which kind of controls are needed to allow for the reliable control of the system frequency. Therefore it is important to assess the influence of incorporating these new controls into the operational frequency reliability assessment. This also requires the system operators to determine, which controls are optimal for their specific grid conditions.

In order to tackle the issues mentioned above, this Ph.D. project discusses methods, which enable to include wind power plant frequency support into the reliability assessment with all required time-frames. Also, a methodology to find the optimal frequency management is proposed in this project, which allows system operators to compare different strategies easily. System operators are always challenged to find the right balance between gains in frequency quality versus the over-usage of frequency controls and thereby loss of energy production.

# Resumé

Overgangen til et fuldt vedvarende energi-basered elnet er allerede fuldt i gang. Mange landes ambitiøse mål om at begrænse brugen af kulstofbaserede kraftværker er den største forandring elnettene verden over nogensinde har været i. Den stigende integration af effektelektronikbaserede enheder påvirker elnettets evne til at fungere pålideligt. Derfor er operatører af transmissionssystemet nødt til at genoverveje den måde de planlægger og driver elnettet på.

Tidligere var elnettet domineret af et begrænset antal centrale kraftværker, men i dag inkluderer elnettet nye generatorsystemer, som er decentraliserede og fungerer afhængigt af de aktuelle vejrforhold. Dette giver problemer såsom en mangel på systeminerti, hurtigere lastændringer eller harmonisk interaktion. Imidlertid giver brugen af effektelektronikenheder også styringen af systemet meget mere fleksibilitet end nogensinde før. Kontrollen af enhederne kan tilpasses på et uendeligt antal måder til gavn for elnettet.

FACTS-enheder er kendt for at være de hurtigste enheder i elnettet til at bidrage til reaktiv effekt til spændingskontrol. De kan bruges til at forbinde vedvarende kraftværker, som havmølleparker, men også til at levere strøm til belastninger som fjerntliggende byer eller olierigge. Installation af flere af disse enheder kan i høj grad gavne systemets drift. Det skal garanteres, at de alle bidrager optimalt, når flere enheder er i nærheden. Ellers kan disse enheder interagere med hinanden og forårsage uønskede spændingsudsving og der opstår et behov for en korrekt tilpasning af disse enheder, når de bruges mere og mere i moderne elnet.

Dette Ph.D. projekt fokuserer på interaktionen mellem denne slags enheder. I projektet bestemmes det, hvordan forskellige enheder skal tilpasse sig den reaktive understøttelse sammen med andre FACTS-enheder og uden kommunikation imellem dem. Der vises at den aktuelt anvendte metode ikke er tilstrækkelig pålidelig til at opretholde den dynamiske respons. Der foreslås derfor et kontrolsystem, der gør det muligt at tilpasse FACTS-enhederne passivt til ændringer i elnettet under drift og til andre enheder sammen i nærheden. Dette bliver mere påkrævet, når disse enheder bruges oftere i moderne elnet.

Desuden er en pålidelige kontrol af systemfrekvensen en af de største udfordringer, når det kommer til et fuldt vedvarende energi baseret elsystem. Mikro-net, hvor systemet er meget begrænset i størrelse, kan allerede styres af effektomformere. Strømsystemer under overgangen til vedvarende energi skal fungere i overensstemmelse med det eksisterende udstyr, såsom konventionelle produktionsenheder eller beskyttelsessystemet. Vedvarende energikilder og især vindkraftværker har potentialet til at understøtte eller endda erstatte konventionelle generatorer som frekvensstyring. Vindkraftværker kan ved at begrænse deres udgangseffekt holde en effekt-reserve tilgængelig, eller de kan endda udnytte rotationsenergien i bladene til at yde kortvarig frekvensstøtte. Operatøren af transmissionssystemet har nu den udfordrende opgave at bestemme, hvilken type kontrol, der er behov for, for at muliggøre pålidelig kontrol af systemfrekvensen. Derfor er det vigtigt at vurdere indflydelsen af at indarbejde disse nye kontrol method i den vurderingen af den operationelle frekvenssikkerhed. Dette kræver også at operatørerne bestemmer, hvilken kontrol der er optimal for deres specifikke net forhold.

For at løse ovennævnte emner diskuterer dette Ph.D. projekt metoder, som gør det muligt at inkludere vindkraftværkernes frekvensstøtte i pålidelighedsvurderingen med alle krævede tidsrammer. Der foreslås en metode til at finde den optimale frekvensstyring. Dette giver operatører mulighed for nemt at sammenligne forskellige styre strategier. Systemoperatører udfordres altid ved at finde den rette balance mellem gevinster i frekvenskvalitet mod overforbrug af frekvensstyring, som reducerer energi produktionen.

# Contents

# Preface

This dissertation summarizes the outcomes of the Ph.D. project "Reliable Control of Power Electronic based Power Systems," carried out at the Department of Energy Technology, Aalborg University, Denmark. This Ph.D. project is supported by the Villum Foundation Denmark through the Reliable Power Electronic based Power Systems (REPEPS) project. The author would like to acknowledge the above-mentioned institutions.

I would like to begin by expressing my sincere gratitude and appreciation to my supervisor Professor Frede Blaabjerg, for his continuous guidance, encouragement, and patience throughout the entire Ph.D. study. His valuable expertise and recommendations have been essential in completing this thesis. I would also like to express my deepest gratitude to my co-supervisors, Professor Xiongfei Wang and Pooya Davari, whose constant support and guidance helped me overcome all the challenges encountered throughout this project.

I also want to thank Torsten Lund, and Germán Claudio Tarnowski, for their valuable inputs and collaboration during my stay at Vestas A/S in Aarhus.

A special thank you to all my colleagues at the Department of Energy Technology, Aalborg University, and especially to Mads, Shih-Feng, Martin and Martin, for all their suggestions and fruitful discussions.

Finally, I would like to express my most sincere gratitude to my wife, Emily Steinkohl, and my daughter Nora Leni Steinkohl for their continuous support, encouragement, and for always being there for me. None of this would have been possible without you.

Joachim Steinkohl
Aalborg University, March 25, 2021

# Part I

# Report

# Chapter 1

# Introduction

## 1.1 Background

The power system is in the biggest transition of its history. The global challenge of changing the power generation from fossil-based over to renewable-based energy sources is the political aim, which has also been defined in the United Nations Framework Convention on Climate Change (UNFCCC) agreement, better known as the Paris Agreement [1]. To stop the process of global warming, all parts of the energy sector have to change severely. This reaches from the way houses are isolated and heated, over the electrification of the transport sector, to the usage of renewable energy sources in the power system generation. This transition has already begun, but the targets for the renewable energy production have been set more ambitiously in the past years.

Denmark, and other countries, have set ambitious goals for the transition of their energy production and usage to reduce their impact on climate change. The phase-out of all coal power shall be done in 2030, and a renewable share of 55 % of the total energy consumption. The full transition to renewable energy production is aimed to be reached in 2050 [2]. The main driver for renewable energy is supposed to be wind power in Denmark, while in other countries it will be based on solar power. Large areas in the surrounding seas are supposed to be available for offshore wind power production.

The German government has also set its renewable energy share goals ambitiously. A share of at least 60 % renewable power shall be reached. The biggest contributor is foreseen to be offshore wind power, as it is an economic and socially acceptable solution. Laws currently limit the further increase of onshore production capacity, not allowing new units close to housing areas, and solar power is limited by the financial aspects and by the limited solar

radiation throughout the year [3].

The renewable sources are mainly injecting their produced power through power electronic converters. These converters use semiconductors in order to convert and transfer energy from one voltage level to another. They have seen large technological development over the last decades and are used in generation units, and equipment in the transmission grid. Converter-based units are also more and more connecting the system loads, such as motor drives, to the power grid. This means their increasing influence on the system operation can be seen already and will only grow further during the transition to a carbon-free energy system.

Multiple effects occur when more and more power electronic-based generation units are installed in the power system. Local voltage changes, depending on the actual power injection, occur in the distribution grid at lines with these generation units [4]. The changing power generation units may have a severe effect on the power flow through transmission lines and, therefore, on the system protection during transient events [5–7]. The converter-based generation units can further affect the system harmonics as different time constants and controller designs in the converters can interfere with other equipment in the system, causing higher system penetration with harmonics in the power grid [8–10]. Also, the system frequency control is affected by the higher integration of converter-based units, as it reduces the need for conventional units and thereby decreasing the natural power system inertia [11]. Therefore, the controller design has to incorporate these effects, trying to mitigate all of the new challenges.

Renewable energy sources also have the challenge that the system operators cannot control when they have their power output to the grid. In conventional power systems, transmission system operators (TSOs) control, at a certain degree, when which generators contribute to the supply of the loads. Some units are used for the supply of the base load, which is demanded almost all year long, other units are then responsible to supply the higher demand throughout the system operation. However, the power production of renewable plants depends on the weather conditions; it does not follow the demand from the system loads. An example of system load and wind injection over several days is shown in Fig.1.1. The net load is hereby defined as the difference between the system load and the provided wind power. Therefore, the net load has to be provided by conventional generation units.

The volatile nature of these generation units challenges the maintenance of the stable grid operation with all its aspects. The changes in power in-feeds change the local grid voltage around the renewable generation units faster than before, the active power balancing does not only have to balance changes in loads, but also has to balance the changes in renewable power supply. Also, the protection system has to adapt, as converter-based units change the way

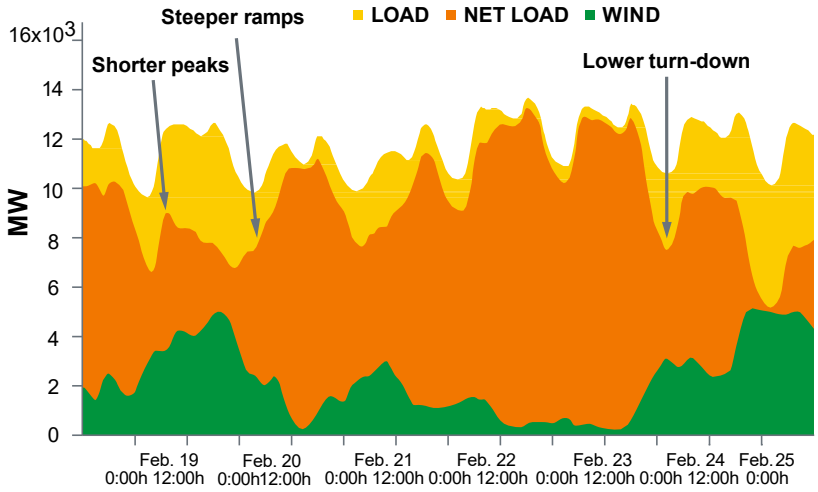


**Fig. 1.1:** System load and wind power injection over several days in the USA Eastern Grid 2010 [12].

fault currents are behaving, and therefore also have to consider how these situations have to be managed in the future.

The transmission system operators are responsible for the safe operation of the power system. System operators worldwide are concerned about how the transition to a renewable source-based power system has to be managed throughout the system operation to keep the power system reliable [13–16]. Some of these challenges in the transition to a modern power grid are further discussed in the following sections.

### 1.1.1 Power system reliability

Power system reliability describes the system's capability to maintain its functions under any circumstances [17]. It can be separated into two main assessments. The first one is the system adequacy; the other one is the security of the power system. These two aspects are illustrated in Fig. 1.2 [18].

The two main aspects are further described in the following sections.

#### Power system adequacy

The system adequacy describes the ability of the power system to fulfill its targets under steady-state operations [19]. This describes the planning of transmission lines, generation units, or the optimal placement of voltage control devices. The well-known N-1 criterion is also a part of the adequacy of the power system. It describes the system's ability to perform its steady-state

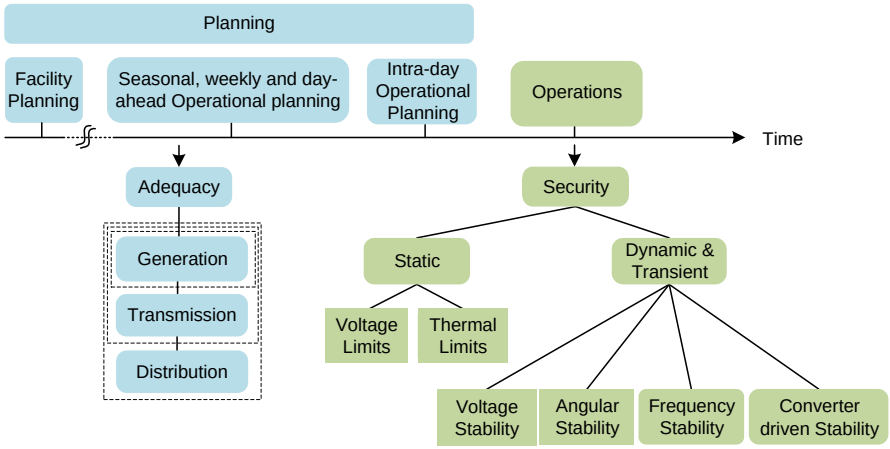


**Fig. 1.2:** Reliability evaluation framework in modern power systems [18].

tasks after the failure of any critical equipment [20]. Adequacy is mainly determined when system changes are planned to see how these changes are affecting the system's performance. Suppose the system load increases over time, the TSO has to ensure that the generating capacity can still supply the increased demand at any time throughout the grid operation. This is the same for the transmission system. With increasing system demand, the transmission lines and their capacities also have to be checked to guarantee reliable system operation. Otherwise, the lines could trip, e.g., due to over-currents. Nevertheless, the adequacy can also describe the ability of the system to react to minor frequency changes, as they can occur after load changes and when renewable power injection changes. Another aspect of the system adequacy is the optimal sharing of equipment load to ensure minimum equipment damage and a longer overall system lifetime. The system adequacy assessment in its three different hierarchical levels is described in [17, 20–22].

The power system adequacy changes due to renewable power generating units in many aspects. One important field of interest is determination, how much renewable generation can replace conventional generation units, still keeping all loads served throughout the system operation [23, 24]. This requires reliability models of the renewable units, determining their available power during every hour of the year and their availability in terms of failures for wind power plants [25–29] and photovoltaic power plants [30–32].

Another field of interest is evaluating the reactive power system support with the fast-changing renewable generation units. Flexible AC transmission systems (FACTS) have proven to be a reliable equipment type, allowing to control the voltage at the transmission level. The determination of how many units are required, the sizing of the units, and their optimal placement is a

field of wide interest that is also a part of the power system adequacy [33–37].

These are just some of the issues that renewable generation units can cause. Their grid interactions and the adequate design of the power system is a much more complicated issue, which the transmission and distribution system operators have to evaluate.

**Power system security**

The security of the power system describes the capability of the power system to withstand any contingency. It is analyzing the system dynamics that occur when, e.g., equipment fails. The security analyzes the different effects, depending on the kind of contingency that occurs. The system security incorporates the system's capability to maintain a stable frequency, voltage, and angle following any disturbance. It describes how well the system can handle any contingency that causes a severe active power imbalance and a significant frequency deviation. These severe frequency deviations occur seldom and are mainly caused by equipment failures, such as the loss of a generation unit or the loss of a heavily loaded transmission line [38].

The secure system operation has different internal time frames. Static security describes the dynamic capability of the system to operate in a steady-state after the initial control of a contingency. This incorporates voltage violations and line over-loading. These events might cause consecutive failures due to, for example, further line tripping. The dynamic security describes the system performance during a contingency. It determines if critical system states or oscillations occur. This can be the reaction to a change in the system frequency and the actions performed by the frequency controls. Nevertheless, this can also be reactions to voltage disturbances, such as reactive power actions. Also, angular security, meaning the capability of the generation units to stay synchronized to the power grid during transients, is a part of this field.

System operators assess the system's operational security by monitoring the power system state. The system operator can influence the system with remedial actions changing the transmission system or the behavior of the connected equipment. The different hierarchical levels of the power system and the system operator's actions are shown in Fig. 1.3. The 'Plant Level' describes the injected active and reactive powers by the conventional and renewable generation units. Also, the system loads and other equipment, such as FACTS, capacitor banks, or HVDC units, are modeled in this hierarchical level. The 'System Level' describes the transmission system with its power flows and voltages. The TSO determines the state of the system in the 'ICT-Level' (Information and Communication Technology Level) to assess, which actions are required to take during operation to ensure a reliable grid operation.

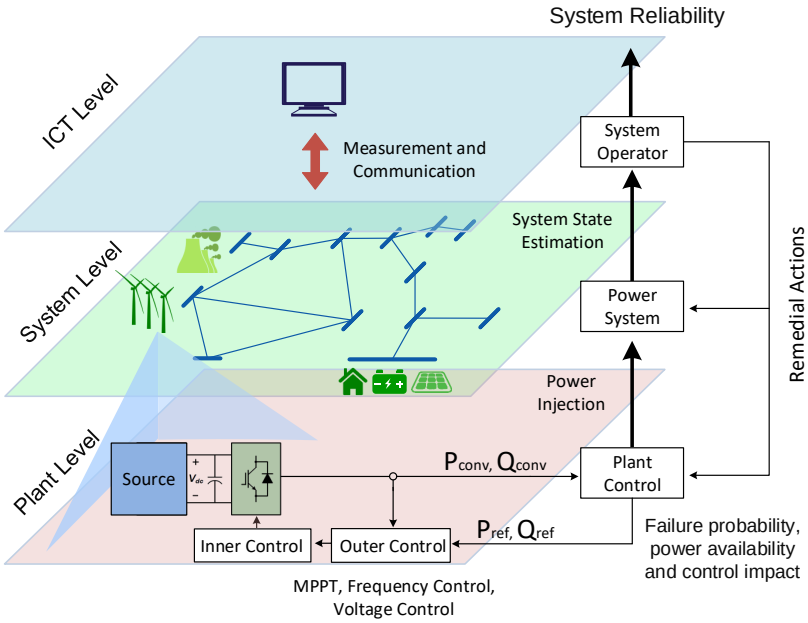


**Fig. 1.3:** The different hierarchical system levels describing the operator's actions to enhance the system operational reliability [J2].

As renewable generation units are becoming more and more dominant in the power system, it is crucial to use their full capabilities to enhance the secure operation of the power grid in order to increase the penetration level of these units. This can be optimal control and placement of voltage controllers or reactive power injection into grid faults. Nevertheless, one of the main issues is the reduced system inertia, causing faster and more severe frequency violations on the power system [13–16].

The Ph.D. thesis works in dynamic power system security. The aim is to assess and enhance the operation of the modern power grid. A fast but nevertheless stable controller design in the voltage controlling units is one of the key enablers of wider usage of renewable power. The issues with the voltage control and the options, power electronic-based units offer in this field are further discussed in Section 1.1.2. The influence of renewable power generation on frequency reliability is discussed in Section 1.1.3 and Section 1.1.4. This is done with a special focus on wind power plants, as they are the main contributors of renewable power generation in many countries worldwide.

### 1.1.2 Reliable system voltage

The voltage in the conventional power system is mainly controlled by the installed generation units [39]. The generators are controlled to maintain a stable voltage in a given operating range for all customers and other equipment connected to the power system. The generation units are responsible for balancing the reactive power needs at their location, keeping the system voltage in the operative band. The system voltage maintenance during operation is essential, as the connected equipment in the power grid is designed to withstand a certain over-voltage level before failing. During phases of under-voltage is the equipment unable to perform its tasks as designed.

The grid voltage is affected by changes during the system operation. These changes can be transient events or changes in the power system power flows, causing a voltage change over the line [39]. Generation units affect the system voltage with their injected active and reactive power. The power flow from a generation unit to the rest of the power grid causes a voltage deviation over the connecting impedance $Z_{Grid}$. This is illustrated in Fig. 1.4, where the injected generator current, $I_{Grid}$, causes a deviation between the grid voltage $V_1$ and the voltage at the generator bus $V_2$.

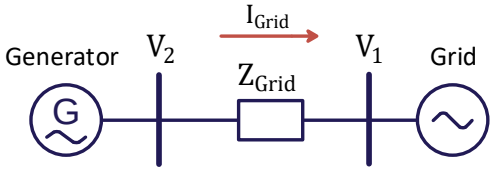


**Fig. 1.4:** Voltage impact of a generation unit providing active and reactive power.

This voltage change over a transmission line $\Delta V$ is described by the product of injected current and the line impedance:

$$\Delta V = I_{Grid} \cdot Z = I_{Grid} \cdot (R_{Grid} \cos\phi + X_{Grid} \sin\phi) \tag{1.1}$$

This relationship can also be expressed in the vector diagram illustrated in Fig. 1.5. It shows the dependence between the flowing currents and the resulting voltage change.

The stiffness of the power grid in the context of voltage control is expressed with short circuit level, $SCL$. The relationship between the $SCL$ and the transmission line impedance is dependent on the nominal grid voltage, $U_N$, as described in (1.2) [40].

$$SCL = \sqrt{3}\frac{U_N^2}{Z_{Grid}} \tag{1.2}$$

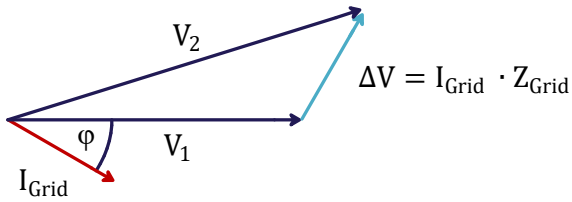


**Fig. 1.5:** Voltage vector diagram, describing the voltage drop over a line.

The transmission line impedance causes voltage changes to be a local issue. Deviations in the grid voltage only propagate a certain distance from their point of origin. The balancing of reactive power demand and supply as a voltage control must be addressed locally to keep the system voltage in the normal operating band at all locations. Renewable power generation may change the way the voltage behaves significantly. Changes in power flows are more rapid, and the voltage control has to incorporate this.

**Voltage-related challenges in modern power systems**

The transition to more power electronic converter-based generation and transmission units changes the behavior of the system voltage. The active power changes in modern grids are faster. Natural phenomena, such as clouds on photovoltaic generation units and wind speed changes, influence the active power injection from these renewable plants, as also illustrated in Fig. 1.1. This means a more volatile grid voltage during the operation, as mentioned by TSOs [14].

The local grid voltage can then leave the normal operating band before the conventional controls react. This operating band is defined in the system operator's policies and the grid codes for the connected equipment. The grid codes define for each country the protection functions required in generation units. In the Danish grid code for wind power plants [41], the protective functions regarding the system voltage are separated into two steps like shown in Fig. 1.6. Step 1 requires the wind power plants to remain operational for 60 seconds. Step 2 allows to disconnect the units after 200 ms.

Distant locations of renewable energy sources extend this issue, as lines with high impedance are more vulnerable to voltage fluctuations, as described in (1.1). Offshore and remote onshore wind power plants are connected via long transmission lines, causing high impedance and more severe voltage changes due to active power changes.

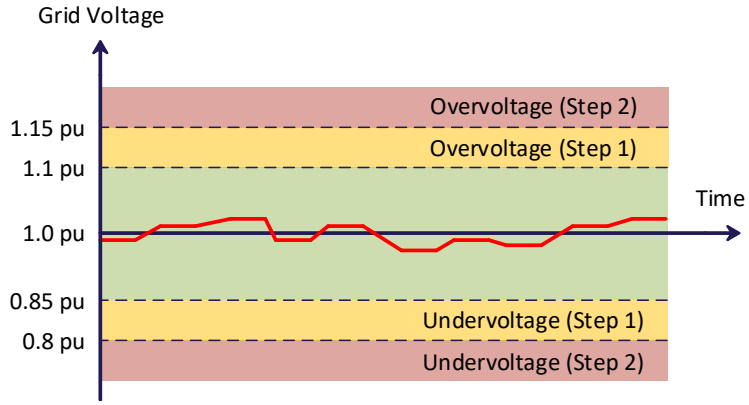


**Fig. 1.6:** Voltage-related protection functions in wind power plants [41].

### Grid voltage control in modern power grids

The control of system voltage is under severe changes due to the renewable, decentralized power generation units. A line that usually feeds local loads can now be turned into a grid feeding line when new wind power plants or photovoltaic units are connected. Additionally, the reduced number of running generation units can limit an area's reactive power capability.

There are voltage controlling devices installed in the system to overcome some of these issues. Tap-changing transformers can change their winding configurations during operation to adjust to new grid situations. Reactors and capacitor units are installed, which can be activated and deactivated by the TSO or automatically, depending on the local voltage [39,42]. These control options are well established but too slow for the fast voltage fluctuations, and they are not always at the locations of renewable power generation.

Renewable generation units are nowadays capable and also required to assist in the control of the grid voltage. Two strategies are implemented, active power ramp rates and reactive power voltage control. Modern grid codes require renewable generation units to limit the rate of active power change. The local grid voltage changes then slower and voltage deviations can be measured and controlled back into the allowed operational band. The second strategy is the controlled usage of reactive power to perform voltage control. This can be done by modern converter-based units that control their injected active and reactive currents within certain limitations. The contribution of renewable generation units to the system voltage is highly beneficial. However, it changes the way grid voltage is controlled significantly. The used controls have to be chosen carefully and with respect to the units' capabilities. The dynamics of voltage controls in wind power plants are highly limited by the communication between the wind power plant controller and the wind

turbines, restricting the response time of these units.

Advanced and fast voltage controlling devices are FACTS. These devices are installed in the transmission system and provide stabilizing controls. There are two different topologies of FACTS units used for the reliable control of the local grid voltage [40, 43, 44].

One type consists of thyristor-based power electronics. Typically, thyristor-switched capacitors (TSC) are used together with thyristor-controlled reactors (TCR) [44]. This allows operating capacitive or inductive, dependent on the grid voltage. To the power grid, these units act as reactance or as a capacitor. The reactive current injected into the grid depends on the actual grid voltage amplitude, making the reactive current dependent on the grid voltage. This limits the unit's capability during very low grid voltages. A voltage drop by 0.5 pu causes the available reactive power to be only 0.25 pu.

The other often used topology is a STATCOM, a Static Synchronous Compensator. This kind of unit is based on voltage source converters, often a multilevel voltage source converter. These control the converter output voltage to provide or consume reactive current. STATCOMs are the more advanced and more complex units out of the two topologies. STATCOMs are used in the thesis to improve voltage control. However, the shown interactions (Chapter 2) and the adjustments required to obtain a reliable voltage control (Chapter 3) can also be applied for other topologies.

**STATCOMs for local voltage control**

The main advantage of STATCOMs is their dynamic capability of controlling the voltage at the connecting bus. These units are the fastest FACTS units for voltage control, which are currently available [43, 44]. They can control the reactive current output, making them capable of providing the rated reactive current, even during very low grid voltages. Therefore, these units often are installed together with wind power plants, providing the local voltage control, as shown in Fig. 1.7. However, they can also contribute to the voltage at weak locations in the power grid, such as remote cities with long lines to the main power grid.

Changes in the system load or the injected active power by the wind power plant cause changes in $P_{Grid}$ and $Q_{Grid}$. This affects the voltage at the point of connection $V_{Grid}$. The STATCOM measures $V_{Grid}$ and uses it as an input for the voltage controller. The voltage controller determines the required reactive power support, $Q_{STATCOM}$ to stabilize the grid voltage.

The converter current output is realized by the voltage drop $\Delta V_{Arm}$ over the connected reactor $X_{STATCOM}$, as shown in Fig. 1.8. This voltage drop $\Delta V_{Arm}$ is the difference between the phase to phase voltage at the low voltage side of the coupling transformer, $V_{LV}$, and the produced converter voltage $V_{Conv}$ [45].

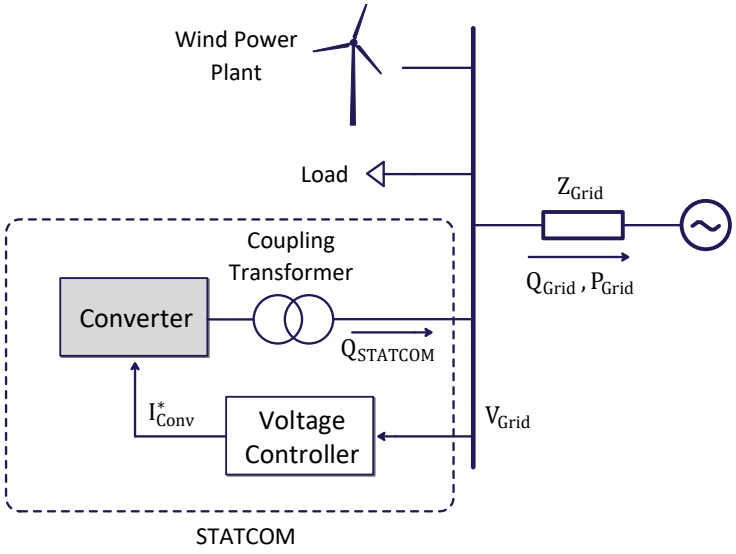


**Fig. 1.7:** STATCOM installation in a power grid to control the voltage for loads or connected wind power plants.

The equation for the resulting converter current is given in:

$$I_{Conv} = \frac{\Delta V_{Arm}}{jX_{STATCOM}} \tag{1.3}$$

Fig. 1.8 shows one of the three legs, or arms, of the converter, connected in a delta configuration. The three converter arms provide their respective converter arm currents. The current flowing into the coupling transformer results from these converter currents. The three-line diagram of a STATCOM is shown in Fig. 1.10, with the phase currents $I_A$, $I_B$, and $I_C$ flowing into the coupling transformer.

In the end, provide STATCOMs reactive power, $Q_{STATCOM}$, to the connecting high voltage bus for local voltage control [45]. The current controller is assumed to be much faster than the voltage control loop, which is the main focus in Chapter 2 and Chapter 3. Therefore, the current control is neglected in the analysis. The demanded and the produced converter currents are identical for the rest of this thesis.

$$I^*_{Conv} = I_{Conv} \tag{1.4}$$

The wider usage of these units can solve many voltage-related issues in power-electronic-based power systems, but their control must be carefully designed. Otherwise, these units may cause dynamic voltage issues leading to abnormal grid voltages and even instability [46]. The rest of the thesis

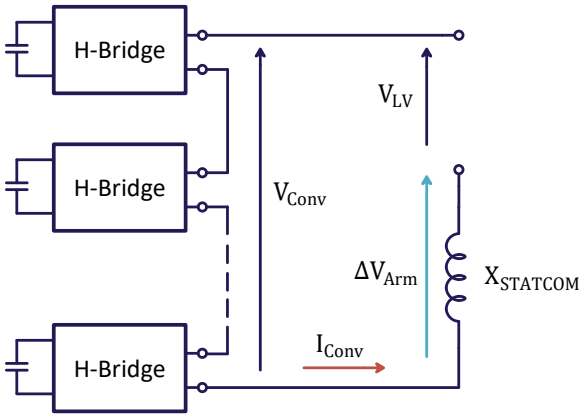


**Fig. 1.8:** One STATCOM converter arm, providing converter current via the reactance $X_{STATCOM}$.

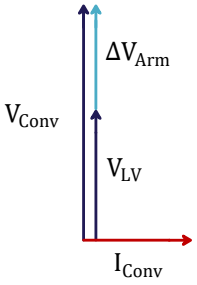


**Fig. 1.9:** STATCOM vector diagram.

focuses on STATCOMs. However, the shown principles and the controller proposals can also be applied for other topologies, providing voltage control in the same time frame.

With the wider integration of FACTS units, they are becoming a dominant factor in the voltage control of modern power grids. They can be utilized with or without renewable generation units, whenever there is a need for more reactive power support. However, are there still challenges in the voltage controller design and the coordination between multiple fast voltage controlling units that have not been there in the conventional power grid.

The arising voltage controller issues are further described in Chapter 2 and Chapter 3. Chapter 2 focuses on the interaction of STATCOMs operating in parallel, where multiple units have to be coordinated to control the voltage reliably. Chapter 3 proposes a way to determine the strength of the power grid regarding the voltage control, to improve the dynamic reactive power response of these units.

### 1.1.3 System frequency in modern power grids

The maintenance of the system frequency is one of the main tasks of power system operation. The power system frequency is not fixed, but it is dependent on the balance of active power throughout the grid operation. Whenever the produced and consumed power are imbalanced, a frequency deviation occurs. Often, throughout the operation, this deviation is just minor. However, it can be dangerous for the system if the active power imbalance is severe.

The power system frequency is a global indication of the energy balance, meaning that all generation units in a synchronous area have to provide the

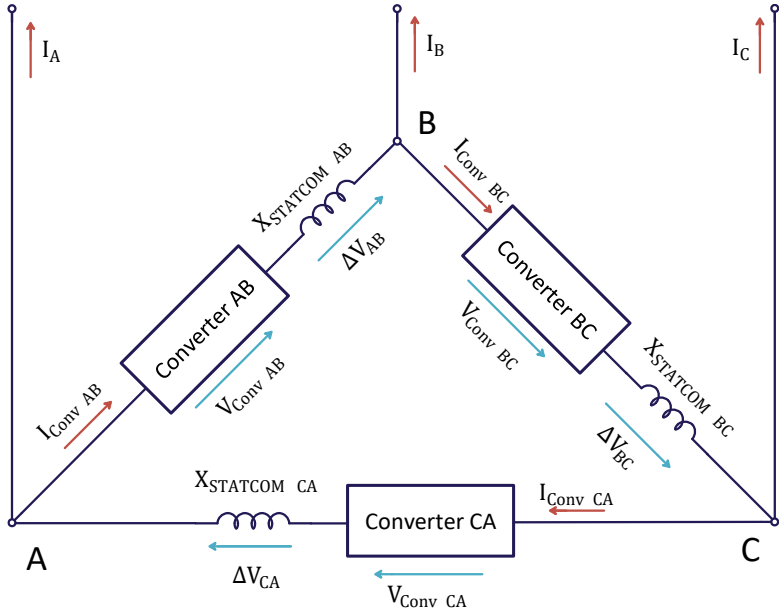


**Fig. 1.10:** Three-line diagram of a STATCOM converter [43].

amount of energy that the system loads consume. The total rated power of conventional generation units $S_B$ and their total time constant $H$ define the inertia of the power system, meaning the stiffness of the system frequency to active power imbalances between the generated power ($P_{Gen}$) and the consumed power ($P_{Load}$). The system frequency follows the power system swing equation (1.5) [39].

$$\dot{f}_{Grid} = (P_{Gen} - P_{Load}) \cdot \frac{f_n}{2 S_B H} \tag{1.5}$$

The swing equation is the result of the physics of the synchronous machines that react naturally with the rotational energy to voltage angle deviations at their point of common coupling. The total system inertia is the addition of the inertia of all independent generation units that are currently in operation.

$$S_B H = \sum_{i=1}^{N} S_{B\,i} \cdot H_i \tag{1.6}$$

High system inertia means a very stiff grid frequency and a low rate of change of frequency (RoCoF) after an active power imbalance, as it can be explained by looking at (1.5), and it can be seen in Fig. 1.11. This value has

a severe impact on the frequency control, as the inertia gives more time to react before a critical frequency deviation is reached.

Active power reserves are set in place that detect frequency deviations and counteract them with a change in active power delivery. The fastest one, the primary reserve, is based on a proportional controller, resulting in a frequency deviation when the controller is settled. Afterwards, to bring the frequency back to the nominal value, secondary and tertiary frequency controls are activated, restoring the system frequency [39]. Such a frequency behavior after a generator outage is shown in Fig. 1.11.

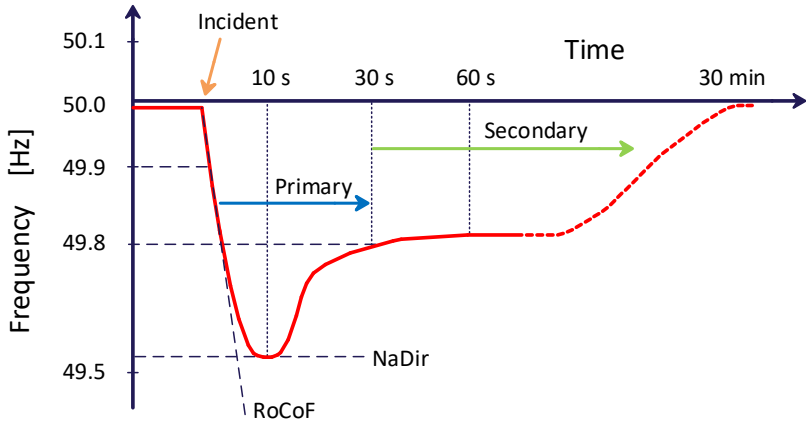


**Fig. 1.11:** Power system frequency during the loss of a generation unit.

The design of the primary reserve is, together with the system inertia, responsible for the NaDir, the maximum frequency deviation during an event, like also shown in Fig. 1.11. The needed amount of primary reserve is determined by the reference incident [47]. This is the worst-case contingency in a grid that is possible to occur during the weakest possible grid condition during operation. In the central Europe synchronous area, this is defined as the loss of 3000 MW of generation. The primary reserve is designed to control the frequency before the under-frequency load shedding is activated. In Central Europe, the load curtailment begins at a frequency below 49 Hz; the primary reserve is designed to have a maximum frequency drop of only 800 mHz, in order to have a safety margin included [48].

The well-established frequency controls are now under increasing pressure, as the renewable power injection is reducing the inertia of the system by replacing conventional units. The ambitious replacement of fossil-based units with renewable sources is decreasing the system inertia, making the frequency more volatile. Therefore, many TSOs are concerned about the changes in system reliability with the higher renewable power penetration, mostly the reduced inertia, and the following increased RoCoF [13, 14, 49].

**Frequency-related issues in modern power grids**

Converter-based units affect the system frequency behavior during an active power imbalance severely and put the system at higher risk of failures. The dynamics of the first dynamic phase after a frequency disturbance are typically described with two critical measures that influence the power system controls and protection systems.

The NaDir is measured in many units that are connected to the power grid. It has a significant impact on the system load, and on the protection system of generation units and converter-based units. The NaDir is used in protection relais to disconnect shares of the system loads when the frequency drops severely. This is described in the respective TSO policies [48]. Reaching too high or too low values of NaDir causes the protective functions in generation units to activate, which causes them to disconnect from the grid before being damaged.

Converter-based generation units also use the NaDir to determine their state of operation. In the earlier grid codes, these units were meant to disconnect when the frequency has left the normal operating range [14]. Then, the conventional system established the active power balance and restored the system frequency. Afterwards, the converter-based units were allowed to reconnect to the stable system. However, this is not beneficial in the operation when the penetration of renewable units increases. Today, these units supply large shares of the demand, it is not allowed to disconnect anymore, as this would mean a severe loss of active power supply, followed by a drop in system frequency. Therefore, the frequency-protection functions and requirements in grid codes are radically changed, allowing for a wider operation band and functions, supporting active power balancing [41, 50, 51].

The RoCoF in the power system is also a value that is used widely for protective functions. Generation units are mechanically damaged when they are changed in their rotational speed too fast. Therefore, they require the RoCoF to be below a certain threshold [52]. The RoCoF is also often used in converter-based units as detection of islanded operation. Converter-based units are required to disconnect from the power grid in case of islanded operation. A high RoCof indicates small system inertia, so the units estimate that the system size is severely reduced and split up [53–55]. This is done to ensure a safe and controlled restart of the power grid after a blackout. Islands of active power production put the restoration process and the involved personal in danger. So an increased RoCoF during the system operation can cause an uncoordinated deactivation of all types of generation equipment.

Already now, to mitigate these issues, TSOs have the option to curtail the active power in-feed by converter-based units in steady-state. This allows conventional generation units to maintain in operation, ensuring at least a minimum reserve of the system inertia [56]; however, other reasons demand

the curtailment of wind power plants during the system operation [57]. The level of the maximum allowed penetration is different for all synchronous areas. In the Irish power grid, this converter-based penetration level is measured with the SNSP (System Non-Synchronous Penetration) [58]. The SNSP incorporates the converter share in the power grid depending on the current system load, and the interconnection to other countries via HVDC lines, also being counted as non-synchronous penetration when feeding into the grid. This SNSP value is used in the system operation to identify weak grid conditions and to activate different counteractions to ensure reliable system operation. Other countries utilize the remaining system inertia as a measure of the system's operational safety. In the ENTSO-E power grid, minimum system inertia is taken as a design value to calculate the required primary reserve in the grid at any given time, so the TSOs aim not to violate this design value [47].

Despite the efforts in the frequency controls so far, the even higher renewable energy share goal put the system under higher pressure. Conventional frequency reserves may not be sufficient to maintain these thresholds in a reliable way when the renewable share increases further. However, power electronic converters are also capable of contributing to a reliable system frequency, as they can also contribute to the reliable system voltage. Battery systems are already contributing to the controls of frequency in some countries. They provide fast frequency controls with rise times that are much faster than the primary reserve is capable of [59]. However, the wind power plant's usage for frequency controls is limited for now, but it is of increasing interest. Some frequency controls are already in place, and some just under development, are explained in the following.

**Frequency control in wind power plants**

For the frequency security of the power system, the focus is set to wind power integrated systems, as they contribute majorly to the high share of renewable power production. Also, wind power plants are capable of a wide range of frequency controls, which allows them to more actively participate in frequency control strategies. They can curtail their active power production, but they also have the potential to produce additional power for short periods of time. This means the frequency supporting controls can be designed in many different ways, depending on the control target.

These additional frequency controls extend the options for TSOs to ensure reliable maintenance of the system frequency, as shown in Fig. 1.12. Several services can be realized on the system demand side, such as the underfrequency load shedding (UFLS), and the demand response (DR), as well as planned activation, and deactivation of system load.

Frequency controllers in converters are widely utilized all over the world.

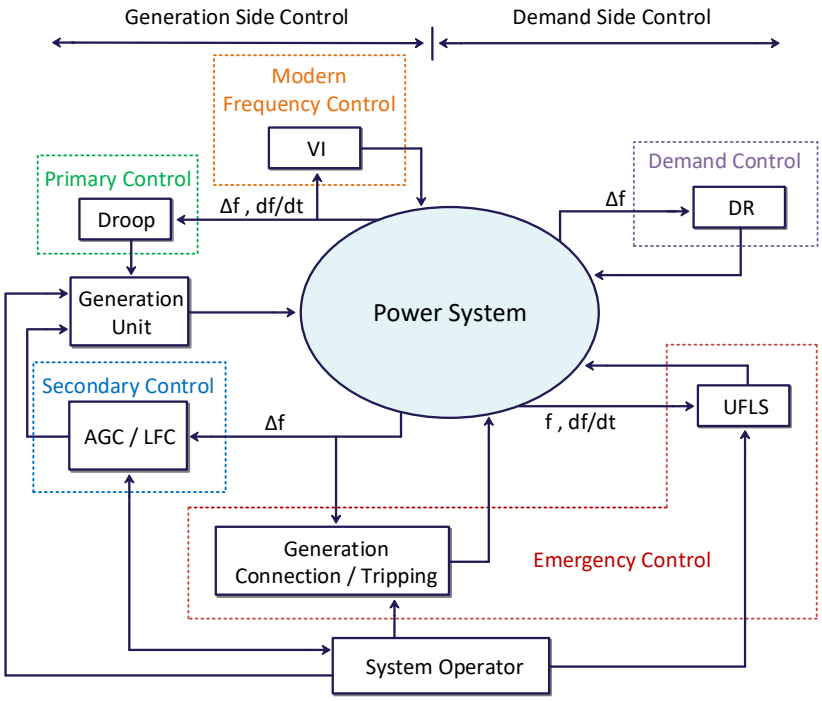


**Fig. 1.12:** Possible frequency controls TSOs have for enhancing the system frequency, with the additional services converters are capable of supplying.

The system frequency is measured, following the requirements from the grid codes. The frequency is often measured within ten cycles, so 200 ms in central Europe with 50 Hz nominal frequency [60]. Wind power plants realize their frequency controls not in the turbine control but in the central Wind Power Plant Controller (WPPC). There, the frequency, voltage, active and reactive power are measured. After that are the reference values for the active and reactive powers for the single turbines dispatched and then communicated to the units, as shown in Fig. 1.13.

The frequency deviation from the nominal value is used to create a change in the active power reference value inside the converter controller. There are already grid codes in place that require this kind of control from wind farms and photovoltaic plants. Some examples are the Danish, the Irish, and the German grid codes, which require a frequency response, an active power curtailment during over-frequency events [41, 50, 51]. The Danish grid code for wind power plants is shown as an example in Fig. 1.14. This is referred to as 'frequency response.'

Converter-based renewable power generators are typically designed to operate at the maximum power point to produce as much energy as possible

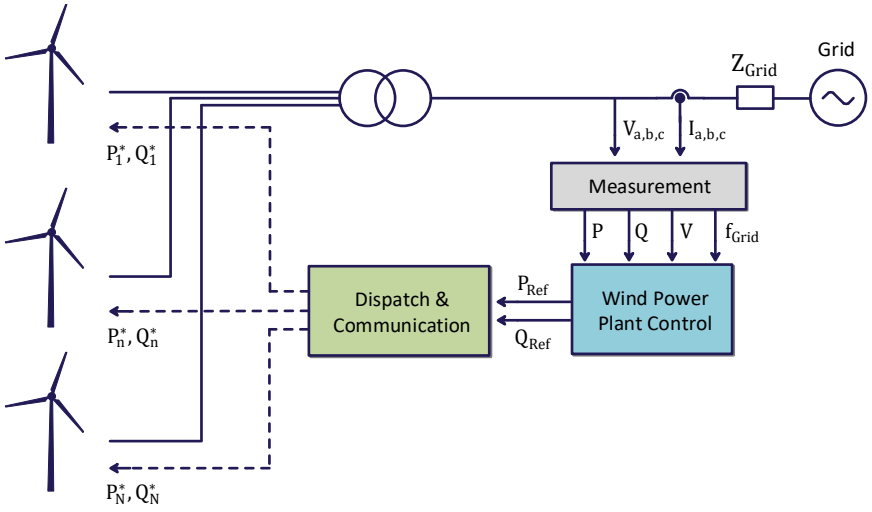


**Fig. 1.13:** Wind power plant control overview.

with the available natural resource. This implicates that renewable sources are not used for under-frequency assistance, as there is no additional energy available to inject into the system, when operating at their maximum power point. Nevertheless, these generation units can curtail their power output in steady-state operation in order to have additional power available when demanded by the grid. This is nowadays demanded in grid codes of countries where the wind power injection is dominating, such as in Denmark. The Danish TSO, Energinet, requires that a frequency control has to be available in the wind power plants, to be activated on demand. This frequency control (shown in Fig. 1.14) requires an active power curtailment in steady-state to have additional power available when requested.

The exact dynamics, and the allowed time for setpoint changes, are defined in the grid code. This control scheme can be activated by the system operator when the wind power injection is very high, and the inertia provided by the conventional units is relatively low. However, it is not activated automatically. An agreement between the system operator and the wind power plant operator has to be made to compensate for the not-produced power and for providing the service. The power curtailment during steady-state will reduce the amount of energy that the wind power plants produce, making additional power available when the demand exceeds the generation, e.g., after a generator outage.

When comparing Fig. 1.14 and Fig. 1.15, it can be seen that the number of variables that determine the control behavior has increased. This means that the system operator can severely change how the frequency control impacts

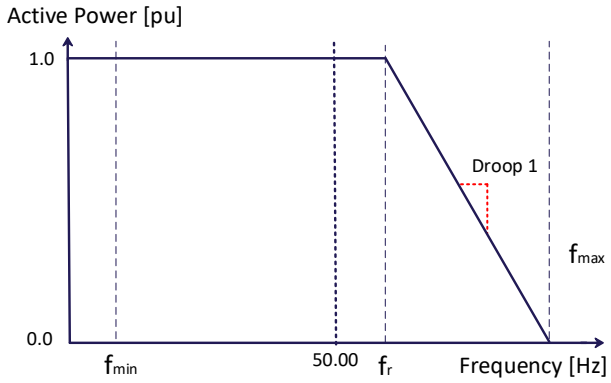


**Fig. 1.14:** 'Frequency response' in the Danish grid code for wind power plants [41].

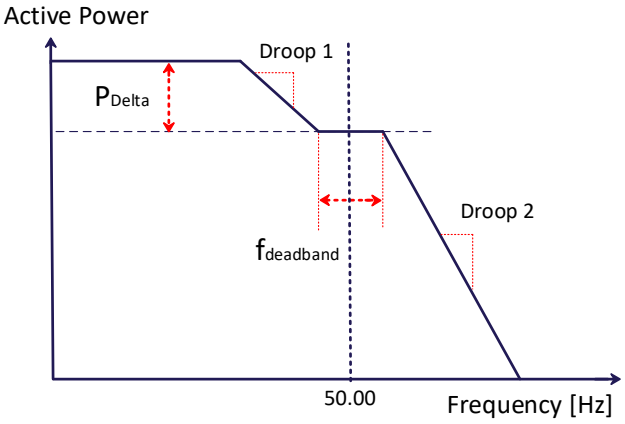


**Fig. 1.15:** 'Frequency Control' in the Danish grid code for wind power plants [41].

the frequency during a disturbance. This opens the question, when and how to reliably utilize this new flexibility.

Other more advanced frequency controls are being developed for wind power plants, aiming to directly mitigate the issues with the reduction of inertia in the power system. This is especially the increase in the RoCoF with all the associated effects. New, proposed converter controls are described, e.g., as virtual synchronous machines (VSMs). Other, similar controls are called power-synchronization or inertia-emulating controls. These controls impact the internal controller structure, requiring severe research in implementing a stable and safe control [61–67]. Such controls mimic the internal physics of synchronous machines to provide an active power change due to a frequency change in the power system. An example control structure for such a system

is given in Fig. 1.16.

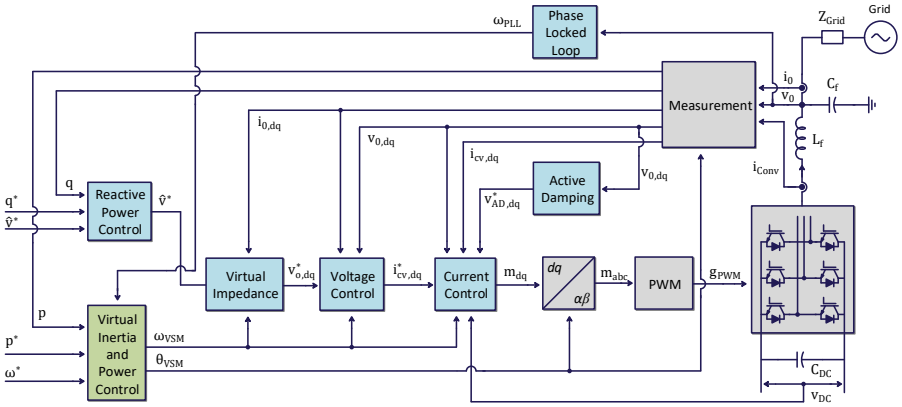


**Fig. 1.16:** Virtual synchronous machine control [68].

The frequency control block diagram of these VSMs is shown in Fig. 1.17, where the active power balance is achieved by changing the output voltage angle, dependent on an internal frequency value.

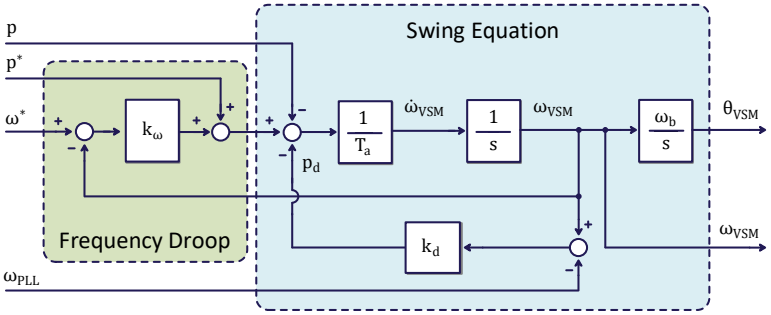


**Fig. 1.17:** Virtual inertia emulating block in a VSM [68].

This kind of control seems promising for the usage in converter-based generation units. Still, these units are limited in their capability of providing additional power reserves. Wind power plants have the potential to provide additional power for a short term by utilizing the rotational energy of the blades, or by including energy storage equipment.

To see the impact of additional frequency controls in wind power plants, one can decide only to consider the reference incident given for the respective synchronous region. The dynamic simulation of the reference incident is evaluated to prove the stability and the performance of the proposed frequency control [61, 69–74]. This is an important part, but the frequency control impact on the operational system reliability has to be evaluated as well.

This allows determining the effect of the control during different states of the system operation.

So one open question is whether these controller options are enough to prevent abnormal frequency conditions, and what are the drawbacks that the TSOs, and in the end, the customers, will have to pay? The curtailment of power during over-frequency events may not occur many times throughout the operation every year. However, this curtailment would mean a severe reduction in overall energy production from the wind power plant. This has to be compensated by the TSO, which may increase the system costs. The impact of any kind of control on the system performance can be determined in a reliability assessment that estimates the healthy system conditions and the disturbances, allowing to estimate the number of abnormal events, and the energy required for frequency control purposes during the power system operation.

### 1.1.4 Operational frequency reliability

The performance of the power system during its operation can be analyzed doing a reliability assessment. This assessment analyzes the frequency behavior throughout the system operation and the efforts of the frequency controls to maintain it. The analysis can assist in finding the balance between a high-quality system frequency and the costs of maintaining it. This type of analysis estimates the system performance for every hour of the year with the different amounts of system loads, available renewable power, and conventional generation units in operation.

System operators measure their system performance and evaluate the frequency quality. All frequency deviations of more than 200 mHz are counted as abnormal and bring the system to an alarmed state in the ENTSO-E synchronous area [75]. The power system's frequency quality is recorded by the system operator, counting the number and duration of these abnormal frequency states throughout the system operation. This verifies if the used controls are sufficient for the reliable system operation or if remedial actions have to be changed to mitigate the abnormal states. Other measures that can indicate how the system performed are the amount of energy used for frequency control or the number of and severity of under-frequency load shedding operations per year. The used energy can be seen as the cost that has to be spent to get a more reliable power system. If the TSO decides to increase its primary reserve severely, then many, if not all, abnormal frequency events can be avoided. Nevertheless, this may come with a very high cost, that the customers must pay. This is indicated in Fig. 1.18, even if the cost can not always be reflected with actual money, but also with a better or poorer system performance.

As these events are rare, it is recommended to simulate and study the

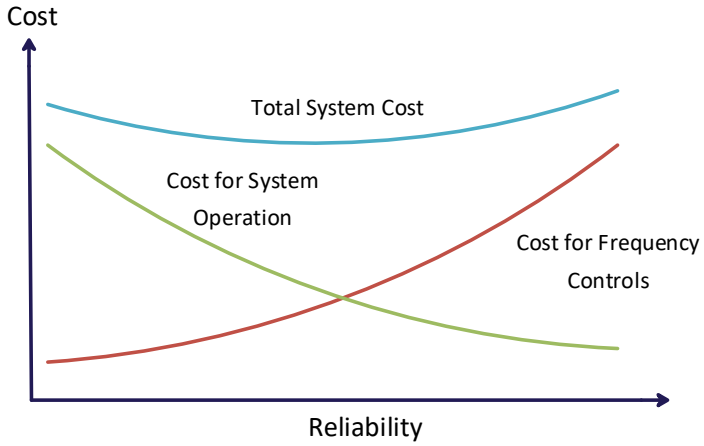


**Fig. 1.18:** TSOs balance the cost of frequency controls and the cost of abnormal frequency events.

impact of a control change on these indices. The design, and the criteria, how the system performance is measured, has a wide field of interest. The assessment design has to be chosen carefully to have a valid result, how the system performance is impacted by the tested system change.

**Impact of converter-based units on the system frequency security**

Renewable power penetration and imports from HV-DC lines reduce the number of running generation units. The decreasing system inertia is causing faster frequency changes in power systems. This makes it more likely that abnormal frequency states occur, and it also increases the duration of the abnormal frequency states.

As it is done in research today, the assessment is suitable for determining the impact of this change of the equipment. It is also suitable for testing slight changes in the frequency control strategy, such as an increase in spinning reserve, or a changed level of allowed renewable penetration. However, the assessment is not yet suitable to utilize the level of freedom the system operators have today, or to adapt the frequency behavior of these units.

This freedom is based on the ability to change their controls, depending on the grid-side demand; some, but not all are listed below:

- Different frequency control schemes inside the units.
- Flexibility in the settings of these control schemes.
- Activation and deactivation of the different control schemes during operation.

The wider usage of power electronic converters allows for adaptions to changes in system conditions with a level of flexibility that has never been seen before. TSOs do not only have to consider the amount of primary reserve for their fast frequency security but they can influence how many converter-based units shall contribute to achieve a more reliable system frequency. TSOs can adapt the control strategies and the control settings to their needs for the most reliable operation of their power system. In order to choose a combined frequency control strategy that utilizes primary and secondary reserves combined with converter-based units, the assessment procedure has to change accordingly to evaluate a much wider range of different operational strategies. Then it is possible to find the most reliable combination of frequency controls for the system operation.

## 1.2 Project Motivation

As presented in the previous sections, several challenges arise when the power system operation has to be maintained with high reliability in a mainly renewable generation-based power system. Hence, during the transition towards this state, it is important to safely be able to operate the power system.

Firstly, the need for a stable voltage control without major interference of multiple, decentralized units is one important topic in a grid with many converter-based generation units. Careful design and tuning of these controls are of high importance, as otherwise controller instabilities and danger to the equipment will occur. This includes well-designed controls for single units, but a particular focus is set to the interaction of multiple units close to each other. Controls that allow for reliable coordination of multiple units without communication are needed with a higher number of voltage controlling units operating in parallel.

Secondly, the system frequency has to be maintained. As the changes in operation throughout the year are changing significantly, it is crucial to measure the impact of modern frequency controls on the reliability of the system. Whereas every power system is specific in its topology and with regards to its frequency controls, the process of assessing the system frequency quality needs to be generalized. The assessment of a renewable-based system has to be changed from classical power systems, as new system states and contingencies have to be taken into account.

Finally, the design of new frequency controller structures and tuning rules is also an important part of further integrating power electronic-based generation units into the power system. Only when the frequency control is maintained, not only by the conventional units but also by the converter-based units, a wider integration will be possible. The controls have to ensure a safe operation in a worst-case scenario, but they also have to perform well

throughout a variety of system contingencies.

## 1.3 Project Objectives and Limitations

### 1.3.1 Research Questions and Objectives

Keeping in mind the main goal of having a higher share of power electronic systems, and inherently a cost-efficient and reliable operation of the power system, the main objective of this Ph.D. project can be defined as finding control and assessment methods that are needed to replace wide parts of the conventional power generation units with power electronic-based generation units. As a result, the research question arises:

- How can the power system be operated with a highly converter-based power system?

This leads to the following subsequent research questions:

- How can the voltage control be adapted in a fast-changing power system?
- Is it possible to avoid negative controller interaction between multiple voltage controlling units?
- What has to be done to correctly assess the frequency reliability in a power system that is more and more penetrated by power-electronic converter-based units with renewable power sources?
- What are suitable frequency control structures in power electronic-based generation units for modern power systems, and which tuning rules have to be applied when having these in operation in order to keep high system reliability?

Based on the above-raised questions, the following objectives can be set for this Ph.D. project:

**Find suitable voltage control methods for power-electronic-based power systems**

Due to the local effect of voltage controls and the dependency on the power system's local strength, it is important that voltage control units, such as FACTS units, can quickly adapt to system changes. Only then they can perform well. This is becoming more urgent with a broader integration of converter-based units, as the system changes can be faster, e.g., due to fast-changing weather conditions. More and more FACTS units are being installed in the power grid, which can cause controller instabilities and equipment damage. Controls have to be found that can adapt to changes in the

power system strength and they have to be adaptive to other voltage controlling units close nearby.

**Investigate the assessment methods of the operational frequency reliability with a higher penetration of renewables**

The assessment of the system frequency reliability has to incorporate the variety of operation possibilities in the system, as well as the possible system contingencies. Both are highly dependent on the level of integration of renewables into the power system. New system states arise, and new frequency controls are introduced in modern converter-based generation units. The assessment of the power system frequency has to incorporate the new states, and it has to be ensured that the assessment of the system is taking all these changes into account.

**Assess the impact of modern frequency controls on the power systems frequency reliability**

The introduction of modern frequency controls into the power system severely changes the behavior of the system during power system contingencies. The study aims to find control structures and rules to tune the controls in order to keep the system frequency healthy during the operation of the power grid. This includes a comparison of different controller topologies and their impact on the frequency. But also the impact of different control settings within the control schemes to find suitable controls under various operational conditions are of importance.

### 1.3.2 Limitations

The project is limited in terms of voltage control to STATCOM units, but the findings can also be used for other, comparably fast voltage controlling units. The type of unit is not the critical factor, as the control and methodology can also be used in generation units, HV-DC units, or other FACTS equipment. The interaction of voltage controllers with different dynamics is not considered in this study. It is assumed that the discussed control is the fastest one in the grid area, as this is state of the art.

Limitations regarding the frequency controls of a modern power system are given by the reduced system models. Only wind power sources in the power system are analyzed; the usage of battery systems, as well as photovoltaic units, is not studied. The power system is also not modeled with different types of demand control. Only the frequency-dependent power consumption, as well as the under-frequency load shedding, are part of this analysis. In the modern power system, they can be important parts of the wider integration of renewable energy. Modern generation scheduling strategies allow a vast integration of renewables already, but this thesis focuses on

the effect of modern frequency controls inside the converter-based sources. Otherwise, the effect of these modern frequency controls is not specific to be measured if multiple factors are tuned simultaneously for power system operation.

## 1.4 Thesis Outline

The outcomes and results of this Ph.D. project are summarized in the form of a Ph.D. thesis based on a collection of papers. The thesis is structured in two main parts: the report and the selected publications. The report consists of a brief summary of the main research carried out within this project, while the selected publications include the published paper outcomes of this Ph.D. study.

The main structure of the thesis, together with the relation between the report and the selected publications, is shown in Fig. 1.19.

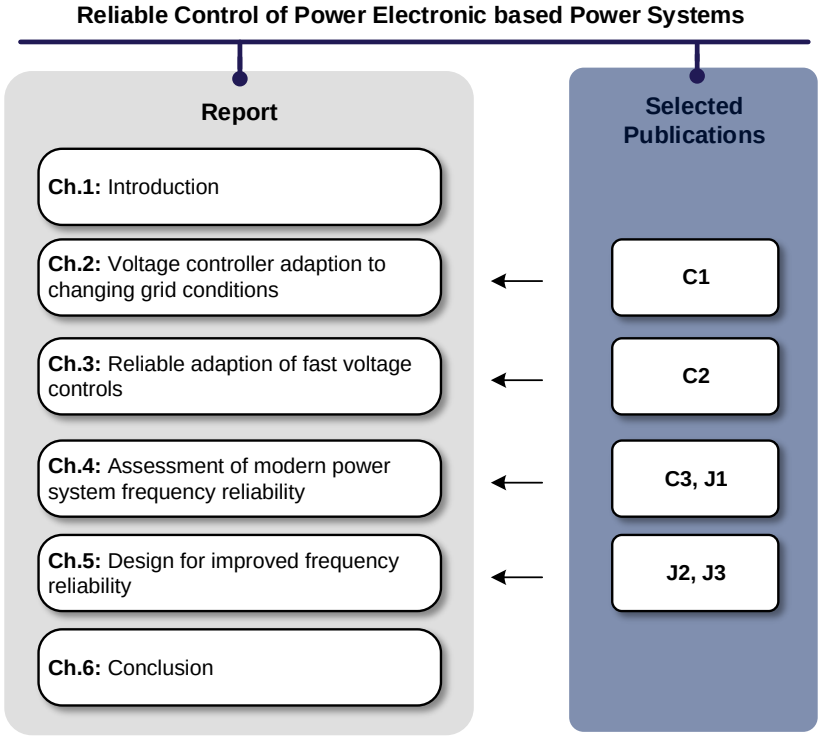


**Fig. 1.19:** Main thesis structure and the correlation between the report and selected publications (Cx: Conference paper, Jx: Journal paper, and x indicates its assigned number).

The report is organized into six main chapters. In Chapter 1, an introduc-

tion to the Ph.D. study is given by discussing the background and the main motivation behind this project.

Chapter 2 presents the design of the voltage controller adaption to changes in the power grid. This is done especially with respect to the interaction of multiple voltage controlling units which are close to each other, as they can otherwise cause voltage issues.

Afterwards, Chapter 3 presents a voltage control strategy in power electronic-based units that gives a fast but stable power grid voltage. This will allow a wider integration of renewable energy sources into the power grid by mitigating instabilities and controller oscillations.

Chapter 4 introduces new reliability indices, allowing an evaluation of the operational reliability of the system with wind power plants contributing to frequency controls. This is needed, as the introduction of new equipment and their controls severely change the system behavior during the operation of the power grid. Also, the accuracy of the assessment procedure is determined to ensure, that the system reliability is estimated fast, but still correct.

The design for better frequency reliability, together with a method to compare different frequency managements, are presented in Chapter 5. This allows system operators to determine the best-suited frequency controls and operational decisions for when to utilize them in their power grid. The rapid evaluation, which frequency management allows for the most reliable operation of the power system enables system operators to include wind power plants into their frequency management strategy.

Finally, the main contributions of this Ph.D. study are summarized in Chapter 6, and some future research perspectives are proposed.

## 1.5 List of Publications

The research outcomes of the Ph.D. project have been disseminated in different forms of publications: journal papers (Jx), and conference proceedings (Cx), as listed below. Nonetheless, only a selected few (e.g., Cx, and Jx) are summarized and considered within this Ph.D. dissertation, which is based on a collection of papers.

Publications in Peer-Reviewed Journals

Publications in Peer-Reviewed Conferences

The below-mentioned conference publications published in the Ph.D. study time are not considered/summarized in this Ph.D. thesis:

J1 **J. Steinkohl**, X. Wang, P. Davari, and F. Blaabjerg, "Assessment Accuracy of Power System Frequency Security with Additional Frequency Controls in Wind Turbines," *IET Renewable Power Generation*, 2021, In Press.

J2 **J. Steinkohl**, X. Wang, P. Davari, F. Blaabjerg, and S. Peyghami, "Frequency-Security Constrained Control of Power Electronic-Based Generation Systems," *IET Renewable Power Generation*, 2021, In Press.

J3 **J. Steinkohl**, X. Wang, P. Davari, F. Blaabjerg, and S. Peyghami, "Fuzzy-Based Frequency Security Evaluation of Wind-Integrated Power Systems," *IET Energy Systems Integration*, 2021, In Review.

C1 **J. Steinkohl** and X. Wang, "Tuning of Voltage Controller Gain for Multiple STATCOM Systems," in *2018 IEEE 19th Workshop on Control and Modeling for Power Electronics (COMPEL)*. Padua, Italy, IEEE, 2017, pp. 1–6.

C2 **J. Steinkohl** and X. Wang, "Gain Optimization for STATCOM Voltage Control under Various Grid Conditions," in *2018 20th European Conference on Power Electronics and Applications (EPE'18 ECCE Europe)*. Riga, Latvia, IEEE, 2018, pp. 1–6.

C3 **J. Steinkohl**, X. Wang, P. Davari, and F. Blaabjerg, "A Frequency Security Analysis of Wind Integrated Power Systems with Frequency Controls," in *Proceedings of 18th Wind Integration Workshop*. Dublin, Ireland, Energynautics, 2019, pp. 1–8.

**J. Steinkohl**, M.G. Taul, X. Wang and F. Blaabjerg, "A Synchronization Method for Grid Converters with Enhanced Small-Signal and Transient Dynamics," in *2018 IEEE 19th Workshop on Control and Modeling for Power Electronics (COMPEL)*. Padua, Italy, IEEE, 2017, pp. 1–7.

**J. Steinkohl**, X. Wang, P. Davari, and F. Blaabjerg, "Analysis of linear Phase-Locked Loops in Grid-Connected Power Converters," in *2019 21th European Conference on Power Electronics and Applications (EPE'19 ECCE Europe)*. Genova, Italy, IEEE, 2019, pp. 1–10.

# Chapter 2

# Voltage controller adaption to changing grid conditions

## 2.1 Background and Motivation

As described in Section 1.1.2 are STATCOMs used to control the grid voltage with their reactive current input. They are often used in combination with wind power plants or to ensure the reliable supply of remote loads. A simplified Single-Line diagram of a STATCOM unit in a power system is shown in Fig. 2.1. The power grid is represented with a voltage source behind an impedance $Z_{Grid}$. The STATCOM injects reactive power, $Q_{STATCOM}$, dependent on the measured grid voltage $V_{Grid}$ and the set reference voltage $V_{Ref}$. The grid impedance $Z_{Grid}$ determines the ratio between the injected reactive power and in the measured grid voltage change, expressed with the short-circuit-level, SCL, as discussed in Section 1.1.2.

The STATCOM assists, due to its dynamic reactive power injection, with renewable power integration and with the reliable supply of system loads. STATCOMs are used because of their fast response time and the capability of providing reactive current in very low voltage conditions, as discussed in Section 1.1.2. The details of the voltage controller and the upcoming issues with the voltage control in modern power grids are discussed in the following.

### 2.1.1 STATCOM voltage controller

A typical voltage control scheme for STATCOM units is shown in Fig. 2.2. STATCOMs typically use a proportional-integral controller (PI-controller) to adjust the reactive current output to deviations between $V_{Ref}$ and the measured $V_{Grid}$. Also, a Droop control is utilized to incorporate the used reac-

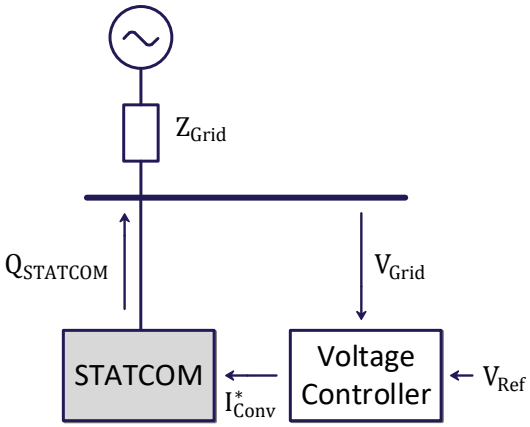


**Fig. 2.1:** Single-Line diagram of a STATCOM unit.

tive power during grid voltage disturbances, applying the voltage reference change $\Delta V_{Droop}$ in steady-state, allowing the coordination with other STATCOMs, and with slower voltage controlling units, which can return the voltage back to the nominal value [43].

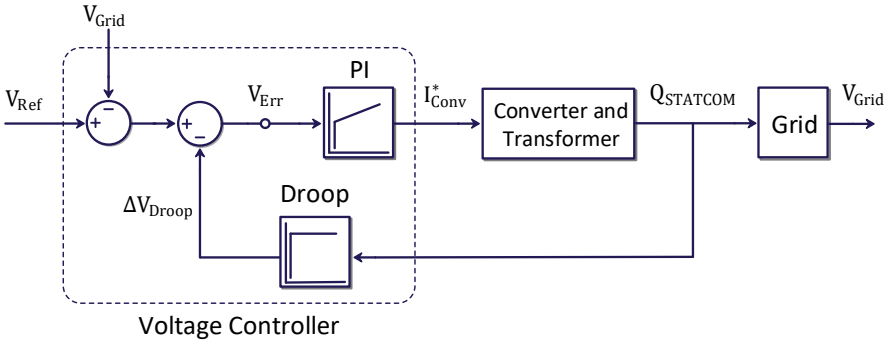


**Fig. 2.2:** STATCOM voltage control scheme [C1].

The PI-controller utilized for the voltage control in Fig. 2.2 is described in the form of:

$$I^*_{Conv} = V_{Err} \cdot Gain \cdot \left(1 + \frac{1}{T_n \cdot s}\right) \tag{2.1}$$

The converter and its current-control are neglected for this voltage control, as it is much faster and does not interfere with the analyzed voltage control, as mentioned in Section 1.1.2. The coupling transformer determines the ratio between the reactive current on the converter side and the reactive

power on its high voltage side. The transformer ratio is fixed in the following analysis, as the voltage controller dynamics around the nominal grid voltage are determined. The SCL in Fig. 2.2 describes the relationship between the injected reactive current and the induced voltage change in the connected bus.

The Gain in the PI-controller adjusts the STATCOM response to changes in the Droop and SCL during operation. The relationship between them can be expressed by (2.2) [46]. Adapting the Gain allows constant STATCOM response to deviations in the grid voltage, even if the system operator changes the grid configuration, e.g., by opening or closing nearby transmission lines, which is affecting the SCL.

$$Gain \propto \frac{1}{\frac{1}{SCL} + \frac{Droop}{Q_{\mathrm{NOM}}}} \tag{2.2}$$

When multiple STATCOMs are installed in one power grid, they all provide reactive power support to control the grid voltage. It has been reported that the parallel operation of FACTS causes interactions leading to unreliable voltage controller performance [46]. The interactions of multiple STATCOMs providing voltage support are discussed in more detail in Section 2.1.2.

### 2.1.2 STATCOM voltage controller interactions

When two or more STATCOM units are installed in close proximity, then they all measure disturbances in the grid voltage and react according to their controller settings. These units then inject all reactive power, aiming to control the grid voltage back to the reference value with respect to the Droop setting. A simplified Single-Line diagram of the analyzed installation is shown in Fig. 2.3. Two units are installed at the same grid location. Both units experience the same SCL in the surrounding grid and measure the same system voltage $V_{Grid}$.

The system details used in the simulation are reported in Table 2.1.

**Table 2.1:** Simulated system data.

| | Description | Value |
|---|---|---|
| SCL | Short Circuit Level | 10 GVA |
| $U_N$ | Nominal System Voltage | 220 kV |
| $Q_{NOM}$ | STATCOM Rated Power | 100 MVar |

The reactive powers from both units, $Q_{STATCOM1}$ and $Q_{STATCOM2}$, affect the measured grid voltage during dynamic events. The combined reactive powers from the units cause an over-compensation of the grid voltage when

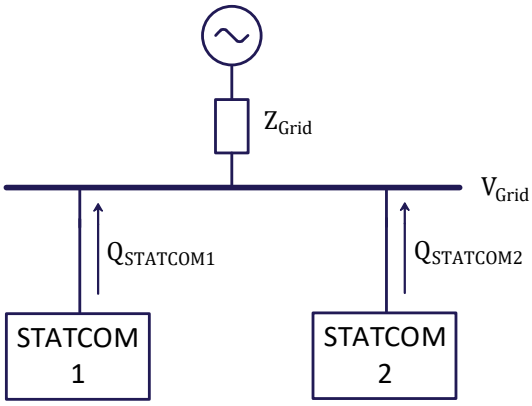


**Fig. 2.3:** Single-Line diagram of two identical STATCOM units installed at one bus

the controllers are not aware of the other units. Voltage overshoots or even instabilities can occur, meaning that the voltage is controlled as required [46].

The system from Fig. 2.3 is simulated to show the interactions between STATCOMs. The STATCOMs in the simulation have the Droop set to 4%. During the simulation, the voltage reference value is changed in both units simultaneously from 1 pu to 0.95 pu.

The response with only one STATCOM in operation with the Gain as calculated by (2.2) is shown as a comparison. The results are shown in Fig. 2.4. It can be seen that the voltage is controlled too fast, causing a severe drop in grid voltage with an overshoot of 22%, when both STATCOMs are in operation.

In Fig. 2.5 are the simulation results shown where the two STATCOMs control a deviation in the grid voltage. With only one unit in operation is the grid voltage restored as required. With both STATCOMs in operation, however, it causes an over-compensation of the disturbance in the initial phase of the controller response.

Therefore, the Gain value used in the PI-controller has to be reduced, slowing the controller down when multiple STATCOMs are in service [46,76]. In Section 2.1.3 it is shown how this Gain reduction is done currently and also why the current solution does not allow for a reliable coordination of STATCOMs.

### 2.1.3 State of the art for adapting multiple STATCOMs

To coordinate multiple STATCOMs, it has been proposed to slow all controllers down. The PI-controller Gain is reduced with a constant factor when multiple units operate close together, as shown in (2.3) [46].

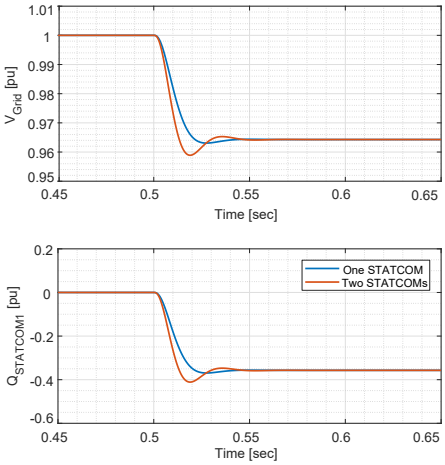


**Fig. 2.4:** Influence of a second STATCOM on the voltage controller dynamics during a voltage reference step test.

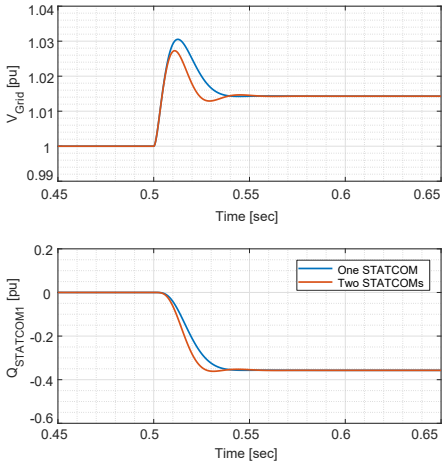


**Fig. 2.5:** Influence of a second STATCOM on the voltage controller dynamics during a grid voltage change.

$$Gain \propto K_3 \cdot \frac{1}{\frac{1}{SCL} + \frac{Droop}{Q_{\mathrm{NOM}}}} \tag{2.3}$$

The constant factor of 0.55 is proposed for $K_3$, when two identical units are installed at one bus.

$$Gain \propto 0.55 \cdot \frac{1}{\frac{1}{SCL} + \frac{Droop}{Q_{\mathrm{NOM}}}} \tag{2.4}$$

The calculation of the Gain is verified in simulation to determine its impact on the STATCOM during the above-shown conditions. The simulation contains again two parallel STATCOM units at the same location with the same power rating and Droop setting, as used in Section 2.1.2. The system data from Table 2.1 is used again. The Gain in both STATCOMs is calculated as proposed in (2.4).

A change in the voltage reference value is applied to see the STATCOM response in Fig. 2.6. During the simulation, the voltage reference value is changed in both STATCOMs simultaneously from 1 pu to 0.95 pu. The Droop setting is varied during the simulations to determine its impact on the controller dynamics. Fig. 2.7 shows the controller performance during voltage disturbances in the simulated power grid. Again, different Droop values are used. Grid voltage deviations are the most common situation for a STATCOM under operation, as the voltage reference value is not varied with a step during operation.

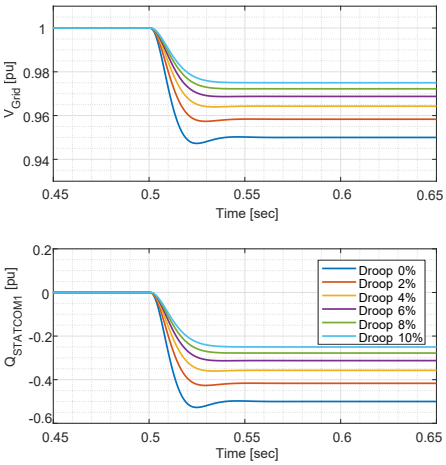


**Fig. 2.6:** Simulation of two STATCOM units during a voltage reference change, with the Gain calculation from (2.4).

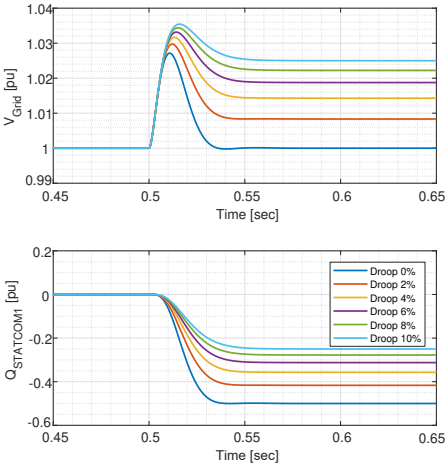


**Fig. 2.7:** Simulation of two STATCOM units during a grid voltage disturbance, with the Gain calculation from (2.4).

The simulation results in Fig. 2.6 and Fig. 2.7 show that the controller performance is dependent on the used Droop values. The step-response time is not constant, but varies with the Droop settings. Also, the control of grid voltage deviations is not done with constant dynamic behavior. Higher Droop values slow the control down and the steady-state voltage after the disturbances is reached later.

The Gain reduction with a constant factor from (2.4) reduces the negative effect of the second STATCOM, but the voltage controller dynamics change with the different controller settings. The used calculation of the Gain value is therefore not allowing for constant voltage control. In [46], it has also not been discussed how the value for $K_3$ has to be set under different conditions, such as when the installation of STATCOMs are not at one bus but at different locations. Then, their effect on each other depends on the grid impedance between them.

### 2.1.4 Open issues for the reliable voltage control

The coordination of multiple FACTS units is still an open issue that has to be solved in modern power grids. The number of fast voltage controlling devices based on power electronics is only increasing due to the transition, the power system is in at the moment. The main questions that have to be answered for reliable voltage control under these conditions are:

- How STATCOMs, installed in the same proximity, interact with each other?

- How is the STATCOM interaction affecting the Gain calculation for keeping the voltage control dynamics constant?
- How do STATCOM units adapt to each other when they are located at different locations?

To solve these issues, the voltage controller Gain calculation for a single STATCOM unit leading to (2.2) is discussed in Section 2.2. Afterward, in Section 2.3, a second unit is considered, and its influence on the grid voltage during dynamic events is considered. The Gain calculation is then extended with more units, with different rated powers of the units and the STATCOM's placement at different locations in the grid.

## 2.2 Gain calculation for a single unit

The controller Gain of a single STATCOM unit installed in a power grid, as shown in Fig. 2.1, is described in this Section. The controller Gain is calculated by determining the change between several points of operation. Fig. 2.8 shows the steady-state points of operation after an initial voltage disturbance. In the figure, the system is initially in a steady-state condition at $OP\,1$, where $V_{Grid}$ and the reference voltage are identical at $V_1$. The reactive power of the STATCOM unit is at 0 pu. A voltage disturbance $\Delta V_0$ is applied to the grid voltage. The STATCOM measures this voltage deviation and injects reactive power to restore the system voltage to the reference value. The STATCOM injects capacitive reactive power in this case, as the voltage drops. The grid voltage follows then the 'Grid Line' according to the amount of injected reactive power. SCL defines the 'Grid Line'. The stronger the grid, the more reactive power by the STATCOM unit is required to influence the grid voltage. In this case, the curve has to be drawn more flat.

All voltage values are normalized with the nominal grid voltage at the point of connection. The reactive power by the STATCOM is related to the nominal STATCOM reactive power to compare units with different rated powers later in the analysis.

Without Droop control, the STATCOM injects reactive power until the steady-state point $OP_2$ is reached. In this case, there is no change in $V_{Ref}$ due to the Droop control. $\Delta V_{Droop}$, as well as $\Delta Q_{Droop}$ are then zero. The required reactive power $Q_{STATCOM}$ is $Q_2$. The Gain in the STATCOM has to be set proportional to the required change in the reactive power output $Q_{STATCOM}$ to reach $OP_2$ after the initial voltage disturbance $\Delta V_0$.

$$Gain \propto \frac{Q_{STATCOM}}{\Delta V_0} \tag{2.5}$$

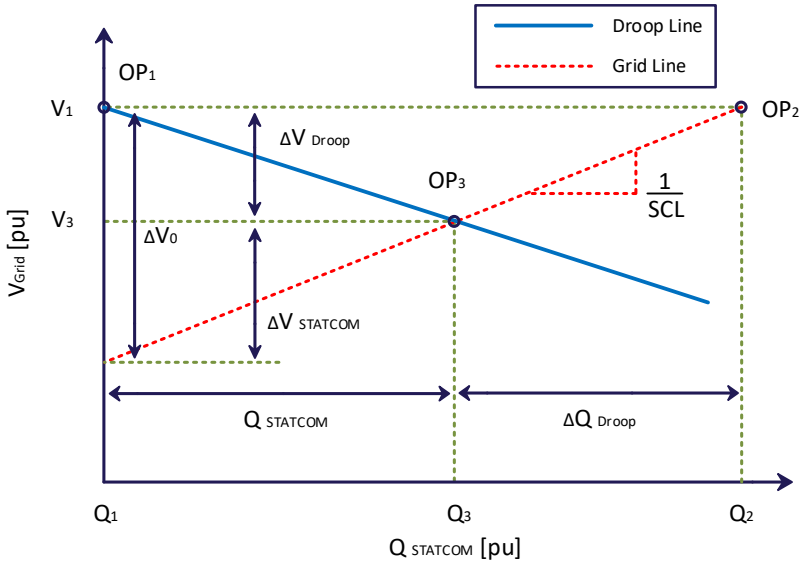


**Fig. 2.8:** Finding a voltage operating point for one STATCOM unit [C1].

The relationship between the reactive power required, SCL, and the initial grid voltage change can be described by:

$$\Delta V_0 = \Delta V_{STATCOM} = \frac{Q_{STATCOM}}{SCL} \tag{2.6}$$

When combining (2.5) and (2.6), the required Gain value for the PI-controller can be calculated.

$$Gain \propto \frac{Q_{STATCOM}}{\Delta V_0} = SCL \tag{2.7}$$

So the higher SCL is, the higher the controller Gain has to be to ensure constant controller performance.

However, with Droop control, the initial voltage deviation $\Delta V_0$ is not compensated in total by the STATCOM, returning the voltage to the reference value. The Droop control changes $V_{Ref}$ by $\Delta V_{Droop}$, according to the 'Droop Line' in Fig. 2.8 before being used as PI-controller input. The Droop control reduces the required reactive power output by $\Delta Q_{Droop}$. The reactive power $Q_{STATCOM}$ required to reach the steady-state operation point $OP_3$ is then $Q_3$. It is dependent on SCL and the Droop setting.

The change in $V_{Ref}$ due to the Droop control is described by (2.8).

$$\Delta V_{Droop} = Q_{STATCOM} \cdot \frac{Droop}{Q_{NOM}} \tag{2.8}$$

The voltage change due to the STATCOM reactive power is therefore not as described in (2.6), but given as:

$$\Delta V_{STATCOM} = \frac{Q_{STATCOM}}{SCL} = \Delta V_0 - Q_{STATCOM} \cdot \frac{Droop}{Q_{NOM}} \tag{2.9}$$

Only this voltage change is to be compensated for by the reactive power in the STATCOM unit, resulting in:

$$\frac{Q_{STATCOM}}{SCL} = \Delta V_0 - Q_{STATCOM} \cdot \frac{Droop}{Q_{NOM}} \tag{2.10}$$

and

$$\Delta V_0 = \frac{Q_{STATCOM}}{SCL} + Q_{STATCOM} \cdot \frac{Droop}{Q_{NOM}} \tag{2.11}$$

The initial voltage disturbance $\Delta V_0$ is substituted by (2.5) and solved to express the required unit Gain value, resulting in (2.2). With this, the STATCOM unit can adapt the Gain to changes in the SCL and on changes in the Droop setting. (2.2) is already state of the art for the PI-controller adaption [46, 76, 77]. Hence, the equations leading to it are later adapted when there exist additional STATCOMs nearby. This is elaborated in Section 2.3.

## 2.3 Gain adaption with multiple STATCOM units

In this Section, the influence of two or more STATCOM units close to each other and the influence on the Gain calculation is discussed. This is required to allow stable controller performance under various grid conditions. The Gain calculation is initially shown with a simple system setup, where two identical units are installed at the same bus. This is described in Section 2.3.1. Afterward, the effect of even more units is calculated. The calculation is extended to incorporate the possibility of units with unequal rated powers in Section 2.3.2. Finally, the influence of different locations of the units is shown in Section 2.3.3. This leads to a generalized calculation of the required Gain value.

The Gain calculations in this Section are in part also presented in [C1]. However, the calculations from Section 2.3.3 are not shown in [C1] due to space limitations.

### 2.3.1 Gain adaption with identical units at one bus

Typically, when two units are installed at one bus, they operate in a combined control scheme, such as a Master-Slave relationship. However, it can also occur that the communication link between the units breaks. The system

should then still operate reliably and not cause voltage control issues, such as overshoots and oscillations. The installation of two identical units with the same power rating and the same Droop setting at the same bus is considered in this Section before generalizing it. The Single-Line diagram of this setup is shown in Fig. 2.3.

Fig. 2.9 shows how to redraw Fig. 2.8 in respect to the interaction with the second STATCOM unit. $\Delta V_{Droop\,1}$ is the voltage reference change inside STATCOM 1 following its Droop-characteristic. However, in this case contribute both STATCOMs with their reactive powers. The voltage rise $\Delta V_{STATCOM\,1}$ measured by STATCOM 1 is the result of both reactive powers $Q_{STATCOM\,1}$ and $Q_{STATCOM\,2}$.

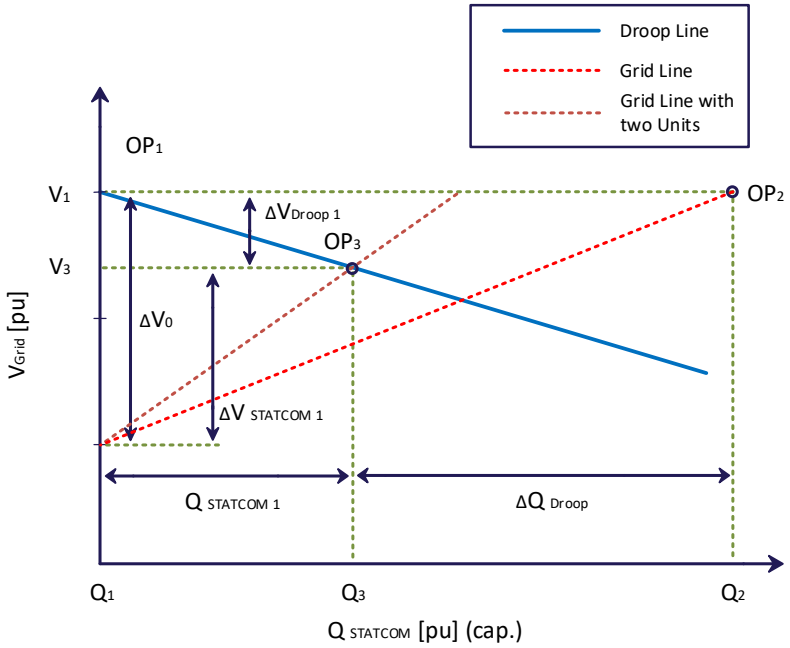


**Fig. 2.9:** Finding a voltage operating point for two STATCOM units installed at one bus [C1].

With two STATCOMs installed at one bus, the equation for $\Delta V_{STATCOM\,1}$, (2.9), changes as the second STATCOM also contributes to the voltage control with its reactive power injection $Q_{STATCOM\,2}$. This causes the voltage increase $\Delta V_{STATCOM\,1}$ to be dependent on both reactive powers following the 'Grid Line'.

$$\Delta V_{STATCOM\,1} = \frac{Q_{STATCOM\,1} + Q_{STATCOM\,2}}{SCL} = \Delta V_0 - Q_{STATCOM\,1} \cdot \frac{Droop}{Q_{NOM\,1}} \tag{2.12}$$

The same equation can be made for the second STATCOM, which is also measuring the voltage lift by both STATCOMs, but only varying its Droop-based voltage reference change according to its own reactive power output.

$$\Delta V_{STATCOM\,2} = \frac{Q_{STATCOM\,1} + Q_{STATCOM\,2}}{SCL} = \Delta V_0 - Q_{STATCOM\,2} \cdot \frac{Droop}{Q_{NOM\,2}} \tag{2.13}$$

In the first case are STATCOM 1 and STATCOM 2 identical, they have the same rated power, resulting in:

$$Q_{NOM\,2} = Q_{NOM\,1} = Q_{NOM} \tag{2.14}$$

The initial voltage disturbance $\Delta V_0$ is substituted by (2.5) as before. (2.12) and (2.13) can then be solved to calculate the Gain with two identical units, as in the system shown in Fig. 2.3. This is described in more detail in [C1]. The Gain calculation for a constant response of a two-unit system is shown in (2.15) [C1]. It is the same for STATCOM 1 and STATCOM 2.

$$Gain \propto \frac{1}{\frac{1}{\frac{1}{2}SCL} + \frac{Droop}{Q_{NOM}}} \tag{2.15}$$

Both units 'split up' the value of SCL to reduce their Gain. The Gain calculation from (2.15) is simulated in a two-STATCOM simulation, as in Section 2.1.3. The STATCOMs receive a voltage reference change at the same time from 1 pu to 0.95 pu. Different Droop settings are used and the dynamic controller performance is shown in Fig. 2.10. It can be seen that the controller dynamics are now constant, allowing a stable control of this system.

The simulation results from Fig. 2.11 show the same two STATCOM system during deviations in the grid voltage. The dynamic performance is again constant for all used Droop settings, so the coordination of the STATCOMs is done correctly, and the voltage is controlled reliably.

The same equations for the steady-state grid voltage can be derived when even more independent STATCOMs are located at one bus. Then, the voltage after a disturbance is the result of the combined effort of all STATCOMs. In [C1], it is shown that the number of identical STATCOMs, $X$, can be used to determine their influences on the grid voltage. $X$ is then used to incorporate the reactive powers of all STATCOMs in (2.13).

$$\Delta V_{STATCOM\,1} = \frac{X \cdot Q_{STATCOM\,1}}{SCL} = \Delta V_0 - Q_{STATCOM\,1} \cdot \frac{Droop}{Q_{NOM\,1}} \tag{2.16}$$

The PI-controller Gain can then be calculated by (2.17), allowing for constant response times for multiple STATCOMs during operation [C1].

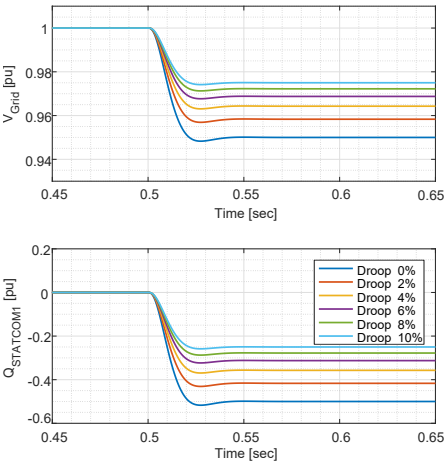


**Fig. 2.10:** Simulation of two STATCOM units during a voltage reference change with the proposed Gain calculation.

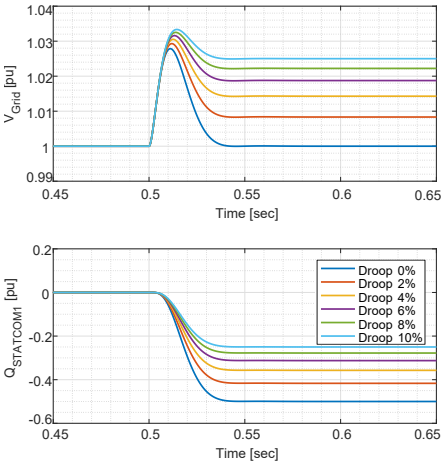


**Fig. 2.11:** Simulation of two STATCOM units during a grid voltage change with the proposed Gain calculation.

$$Gain \propto \frac{1}{\frac{1}{SCL} \cdot X + \frac{Droop}{Q_{NOM}}} \tag{2.17}$$

Another possibility is the installation of STATCOMs with different power ratings. The different rated powers affect the amount of reactive power supplied by the STATCOMs according to their Droop control, meaning (2.14) is not valid anymore. This is considered in the following Section to determine the correct Gain calculation to allow for a reliable grid voltage control.

### 2.3.2 Gain adaption with different units at one bus

STATCOMs with different rated reactive powers can be installed in one bus. This is shown in the Single-Line diagram in Fig 2.12. The Gain has to incorporate this, as the rated powers significantly influence the Droop control, determining the steady-state operating point. The Droop value is constant throughout the STATCOMs, allowing the optimal share of used reactive powers by the STATCOMs [39].

The Gain calculations from Section 2.3.1 are redone to incorporate the STATCOM's rated power. With this, the steady-state operation of the STATCOMs can be determined by (2.12) and (2.13). However, when solving the equations, the nominal powers have an influence on the factor, that 'splits-up' the SCL between the STATCOMs. The Gain values for two STATCOMs are then calculated by:

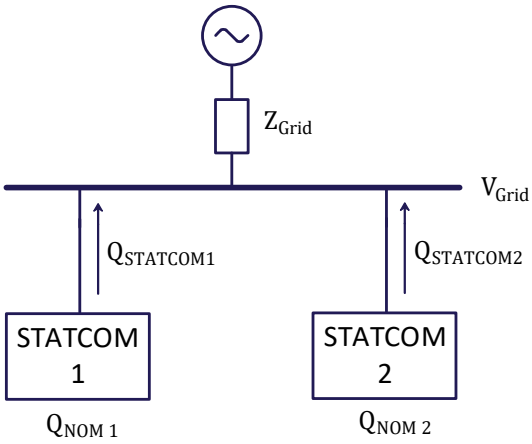


**Fig. 2.12:** Single-Line diagram of two STATCOM units with different rated powers installed at one bus.

$$Gain_1 \propto \frac{1}{\frac{1}{SCL} \cdot \frac{Q_{NOM1}+Q_{NOM2}}{Q_{\mathrm{NOM}1}} + \frac{Droop}{Q_{NOM1}}} \tag{2.18}$$

and

$$Gain_2 \propto \frac{1}{\frac{1}{SCL} \cdot \frac{Q_{NOM1}+Q_{NOM2}}{Q_{NOM2}} + \frac{Droop}{Q_{NOM2}}} \tag{2.19}$$

The presented equations are again described in more detail in [C1]. The STATCOMs' different rated powers cause the SCL to be 'split-up' with a certain share between the STATCOMs in the Gain calculation. With even more units, (2.19) has to be extended into:

$$Gain_i \propto \frac{1}{\frac{1}{SCL} \cdot \frac{\sum_{i=1}^{N} Q_{NOMi}}{Q_{NOMi}} + \frac{Droop}{Q_{NOMi}}} \tag{2.20}$$

The factor $X$ from (2.17) can be rewritten from the number of STATCOMs to incorporate the different rated powers as:

$$X_i = \frac{\sum_{i=1}^{N} Q_{NOMi}}{Q_{NOMi}} \tag{2.21}$$

When the STATCOMs have the same rated powers, (2.21) can still be used, only resulting in the number of units. With this Gain calculation, is it possible to guarantee a reliable controller response to the deviations in the grid voltage

and steps in the reference voltage value. This is verified by simulation, with the rated power of STATCOM 2 being reduced from 100 MVar to 50 MVar. For STATCOM 1 $X$ is therefore set to two thirds. STATCOM 2 has $X$ set as one third, as this is the ratio between the rated powers.

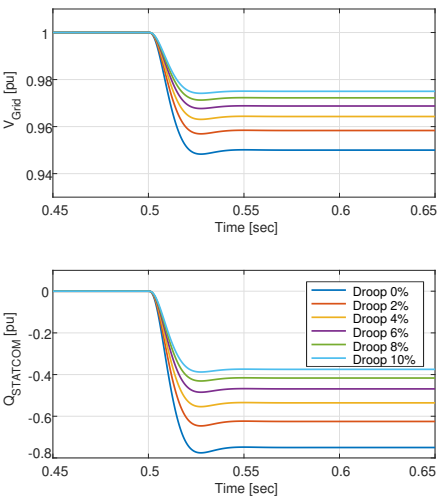


**Fig. 2.13:** Influence of a second STATCOM with different rated powers during a voltage reference step test.

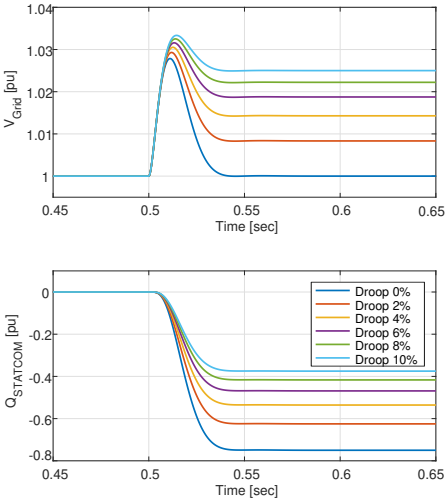


**Fig. 2.14:** Influence of a second STATCOM with different rated powers during a grid voltage change.

The simulation results in Fig. 2.13 and Fig. 2.14 show that STATCOM 1 injects more reactive power than before in Section 2.3.1, due to its higher share. The response time is still constant, also with variations in the Droop value. This allows for a reliable control of the grid voltage.

In modern power grids, STATCOMs are not always installed on the same bus, but they can also be distributed in the grid. A line impedance is then between the STATCOMs, affecting their individual voltage controllers. The effect of this on the Gain calculation is shown in Section 2.3.3.

### 2.3.3 Gain adaption with two units at different buses

When two units are not located on the same bus, an impedance can be modeled between their buses. This means the reactive power output of one STATCOM does not directly affect the voltage at the other STATCOM's bus. Fig. 2.15 shows a Single-Line diagram of a system installation with two STATCOMs with distances between them. This setup is used to estimate the effect of STATCOM placement inside the grid on the Gain calculation.

The impedances $Z_{Grid\,1}$, $Z_{Grid\,2}$, and $Z_{Grid\,0}$ depend on the locations of the STATCOMs and on the transmission lines in the power grid. The impedance

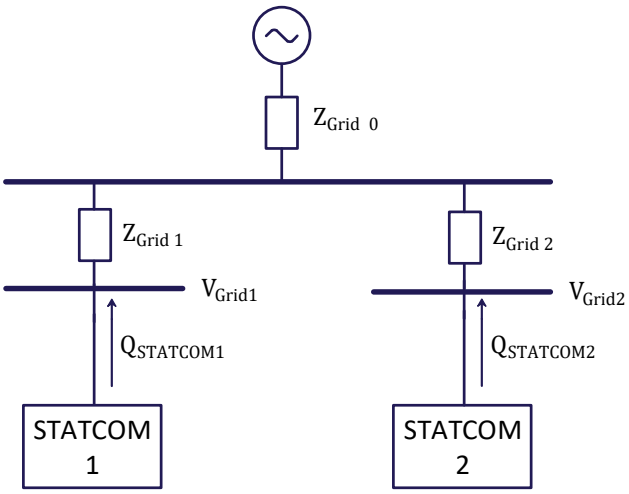


**Fig. 2.15:** Single-Line diagram of two STATCOM units installed at different buses.

values change during the system operation, whenever lines are being connected or disconnected. Lines could only be disconnected temporarily or forever. New lines can also be built and taken into operation, affecting the grid conditions.

To be consistent with the used system as before, the impedances can be set so that a single STATCOM in operation still operates in a power grid with SCL. This means for both units that:

$$Z_{Grid\,0} + Z_{Grid\,1} = Z_{Grid} = Z_{Grid\,0} + Z_{Grid\,2} \tag{2.22}$$

The impedances $Z_{Grid\,1}$ and $Z_{Grid\,2}$ are therefore set to be the same value. The sum of the two represents the impedance in the power grid between the STATCOMs. Determining $Z_{Grid\,0}$, $Z_{Grid\,1}$, and $Z_{Grid\,2}$ during the operation of the two STATCOM system in a real application is challenging, as the grid conditions can vary significantly, which is further addressed and solved by a proposed controller, presented in Chapter 3.

The other STATCOM's impact in (2.12) must be adjusted to determine its influence. The voltage lift by STATCOM 2 on the bus voltage of STATCOM 1 is reduced by:

$$\frac{Z_{Grid\,0}}{Z_{Grid\,0} + Z_{Grid\,2}} \tag{2.23}$$

The calculation of the voltage lift at the point of connection of STATCOM 1 changes (2.12) into:

$$\Delta V_{STATCOM\,1} = \frac{Q_{STATCOM\,1} + \frac{Z_{Grid\,0}}{Z_{Grid\,0}+Z_{Grid\,2}} Q_{STATCOM\,2}}{SCL} = \Delta V_0 - Q_{STATCOM\,1} \cdot \frac{Droop}{Q_{\mathrm{NOM}\,1}} \tag{2.24}$$

And for STATCOM 2:

$$\Delta V_{STATCOM\,2} = \frac{Q_{STATCOM\,2} + \frac{Z_{Grid\,0}}{Z_{Grid\,0}+Z_{Grid\,1}} Q_{STATCOM\,1}}{SCL} = \Delta V_0 - Q_{STATCOM\,2} \cdot \frac{Droop}{Q_{\mathrm{NOM}\,2}} \tag{2.25}$$

This can be solved again, with $Z_{Grid\,1} = Z_{Grid\,2}$.

$$Gain_1 \propto \frac{1}{\frac{1}{SCL} \cdot \frac{Q_{NOM\,1}+Q_{NOM\,2} \cdot \frac{Z_{Grid\,0}}{Z_{Grid\,0}+Z_{Grid\,1}}}{Q_{\mathrm{NOM}\,1}} + \frac{Droop}{Q_{NOM\,1}}} \tag{2.26}$$

The factor $X$ from (2.17) incorporating the influence of STATCOM 2 on STATCOM 1 can then be written as:

$$X_1 = \frac{Q_{NOM\,1} + Q_{NOM\,2} \cdot \frac{Z_{Grid\,0}}{Z_{Grid\,0}+Z_{Grid\,1}}}{Q_{\mathrm{NOM}\,1}} \tag{2.27}$$

When the impedance between the STATCOMs is lower, they interfere more, because $X$ is getting closer to (2.21). With a significant impedance between the STATCOMs, they will interfere less with each other. This causes $X$ then to be closer to one. The STATCOMs operate in such a case in a kind of stand-alone condition.

As an example, the impedances are chosen as:

$$Z_{Grid\,1} = Z_{Grid\,2} = \frac{1}{3} Z_{Grid\,0} \tag{2.28}$$

$$Z_{Grid\,0} = \frac{2}{3} Z_{Grid\,0} \tag{2.29}$$

Under this condition, the STATCOMs still see $Z_{Grid}$ as the grid impedance when operating stand-alone. SCL is then still 10 GVA, with only one unit being in operation. The STATCOM rated powers are again set to 100 MVar each. The STATCOMs interfere if both units are operating. In this case, the STATCOMs' influence on each other is reduced, as the voltage drop is shared between the two impedances to the grid voltage source. Under this condition, the factor $X$ is calculated as:

$$X = \frac{1 + \frac{2}{3}}{1} = \frac{5}{3} \tag{2.30}$$

In the studied condition, both STATCOMs do not 'share' the SCL. Instead, each STATCOM has to calculate the Gain with 60 % of the actual SCL, that the system has without the second STATCOM.

$$Gain = \frac{1}{\frac{1}{\frac{3}{5}SCL} + \frac{Droop}{Q_{NOM}}} \tag{2.31}$$

The system is again simulated with a step in the voltage reference value, and with a grid voltage disturbance. The results are shown in Fig. 2.16 and Fig. 2.17.

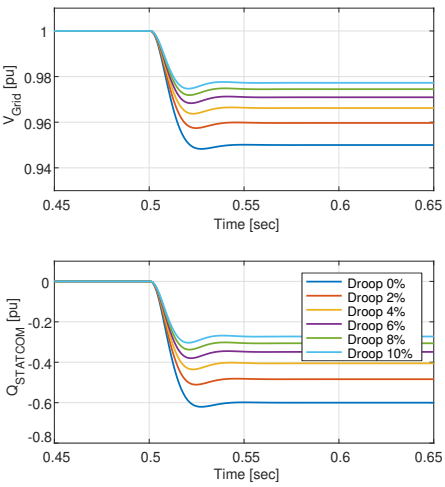


**Fig. 2.16:** Simulation of two STATCOMs at different locations during a voltage reference.

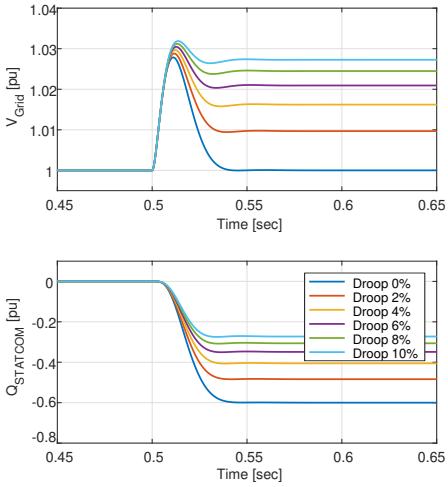


**Fig. 2.17:** Simulation of two STATCOM at different locations during a grid voltage change.

It can be seen, that the two-STATCOM system with the units being installed at different locations in the grid, still reliably provides voltage control. The reactive power coordination allows to stabilize the system voltage after a disturbance and the step-response time is also constant.

However, to utilize (2.26), a STATCOM in operation would have to determine the actual values of $Z_{Grid\,0}$, $Z_{Grid\,1}$, and $Z_{Grid\,2}$. The STATCOMs have to estimate their value for $X$, which leads to a reliable controller performance. Doing this requires knowing about the characteristics of the power grid, possibly together with other STATCOMs. The STATCOMs have to be flexible enough to adapt to grid changes, such as the activation or deactivation of other STATCOMs with an unknown impedance between them.

## 2.4 Summary

The adaption of one STATCOM to one or more other STATCOMs with the same dynamics has been discussed in this Chapter. First, the interactions of two identical STATCOMs installed at one location have been shown. Then, the Gain calculation was more generalized to calculate the correct Gain value for different grid conditions, such as different rated powers or unit locations. The main outcome is that the Gain has to take into account the influence of the other STATCOMs and not just use a constant factor as it is currently done. Instead, the factor has to be set to influence the value of SCL in the calculation. This means the STATCOMs have to estimate a lower value of SCL, when interfering with other STATCOMs.

All shown Gain calculations have one severe drawback: The amount of required information from the other STATCOMs. In particular conditions, this can be given, e.g., when multiple STATCOMs are installed at the same time by one vendor. When more dynamic voltage controlling units are added after years in close proximity, then the old ones do not have any of the required information. Partially, this could be compensated when the system operator collects all information and then distributes it to the different STATCOMs. But STATCOMs have, so far, not the option to receive data by the system operator to influence the Gain as desired.

In Chapter 3, a method is proposed that directly estimates the value of $SCL/X$ used in the Gain calculation. The proposed improvement allows adjusting the controller response to any other STATCOM size and location. However, it is also beneficial in stand-alone operation, where the SCL can also change during operation.

# Chapter 3

# Reliable observer-based voltage control

## 3.1 Background and Motivation

One important aspect that has to be solved is how to find the correct $SCL$ value throughout the operation of STATCOM's. The $SCL$ is required to ensure the adaption to changes in the grid strength during operation, as during transmission line changes or even system splits. And this has also to be done for other STATCOM units, which are close nearby like described in Chapter 2.

To adapt to changes in $SCL$, a grid strength estimation test is performed as state-of-the-art for the operation of STATCOM's. The test is done in regular intervals, such as once or twice per day. A reactive power perturbation is applied to the grid, affecting the system voltage in a negative way. However, this test is not designed to operate under the interaction of other, fast voltage controlling devices nearby, as described in Section 3.1.2.

Alternative solutions have already been proposed [78–86]. Nevertheless, they still have significant disadvantages in their capability to guarantee correct adaption to varying grid conditions in modern power grids.

### 3.1.1 Conventional grid strength test

The $SCL$ estimation is currently performed on a regular basis, often twice per day. During the test is the voltage control deactivated, and the reactive power output is changed by a fixed value, causing a voltage deviation in the power grid, which is measured and evaluated. The test procedure with the measured voltage and reactive power values are illustrated in Fig. 3.1.

The $SCL$ is proportional to the ratio between voltage and reactive power

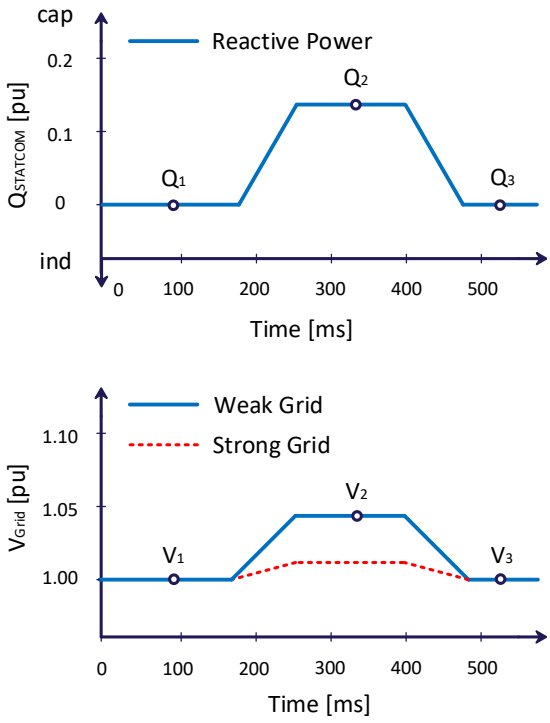


**Fig. 3.1:** Grid strength test performed by a STATCOM unit.

changes. The short-circuit strength can then be estimated as $SCL_{Est}$ by:

$$SCL_{Est} \propto \frac{|Q_2 - Q_1|}{|V_2 - V_1|} \tag{3.1}$$

$SCL_{Est}$ is taken into the PI-controller Gain calculation to ensure consistent dynamic performance of the unit like described in Chapter 2. The forced voltage disturbance caused by the perturbation test can be minor in a strong grid. In a weak grid, it can be significant, and it has to be ensured not to violate the grid voltage during the test. A control structure that can adapt to changes in the grid has severe advantages, especially in relatively weak power grids, without causing a voltage penetration.

### 3.1.2 Challenges with the grid strength test due to STATCOM interaction

When multiple voltage controlling units with roughly the same response time are close together, they interfere with each other during the test. When one

STATCOM performs the test and changes the local grid voltage, other units nearby measure this voltage change. These units then change their reactive power output to reduce the voltage disturbance, as shown in Fig. 3.2.

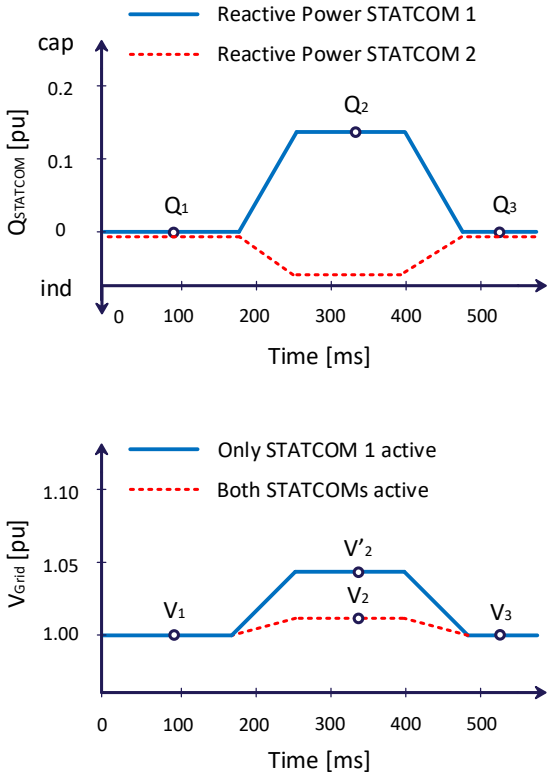


**Fig. 3.2:** Grid strength test performed with another unit in operation.

The testing STATCOM will measure a reduced voltage change $|V_2 - V_1|$ and is interpreting this as a stronger grid, by using (3.1). $SCL_{Est}$ is then higher than $SCL$. The Gain value is then set too high, according to (2.2), leading to voltage overshoots or even controller output oscillations. Hence, it has been shown in Chapter 2 that $SCL_{Est}$ for the Gain calculation is a share of the actual $SCL$ value to correctly adapt to other voltage controlling devices at the same bus or nearby.

One way to solve this issue is to implement communication between the units. All other units can then freeze their voltage controls during the phases of the test. $SCL_{EST}$ can then be calculated correctly, with the cost of no unit providing voltage control during the test. With communication it is also possible to estimate a value for the required adaption to other nearby units. However, as promising as this sounds, it is impractical for real applications,

where the units are often not planned to operate close to each other. Situations like this may occur when units are provided by different vendors, or when units are installed years after each other. It is also sometimes desired not to have communication links, for example, due to cyber-security constraints. Transmission system operators are at high risk, so they are becoming increasingly aware of the threats opposed by criminals. To prevent this, system operators reduce the communication links to critical infrastructures, such as STATCOMs.

### 3.1.3 Alternative solutions for the grid strength test

A new method has been proposed to estimate $SCL$ and reduce the influence of other STATCOMs to adapt the voltage control. A modified penetration test is performed with neuronal-networks, measuring the system voltage during the test [78]. The influence of other units seems to cause a characteristic shape of the grid voltage during the test, allowing to determine the number of nearby units. However, this still requires the penetration test with its disadvantages. The performance of the proposed neuronal network also severely depends on the training data that was utilized during the design phase.

The same is true for structures that use Fuzzy Controls, trained with a Teaching-Learning based Optimization Algorithm, as introduced in [79]. Other similar structures are also improving the control performance but often face the same drawbacks and limitations. Fuzzy controls that detect the dynamic performance during an event and adapt the PI-controller parameters $k_p$ and $k_i$, have been proposed [80]. However, the fuzzy-sets are tuned for specific tested grid configurations. Not all possible grid changes can be foreseen for sure during the unit's design phase. The dynamic adaption of the PI-controller parameters is also proposed in [81–86]. The change in controller parameters during a dynamic voltage event affects the response time, making it impossible to guarantee satisfying controller dynamics.

### 3.1.4 Requirements for the reliable voltage control

A control structure is required that can estimate the local grid strength as $SCL/X$, so it directly incorporates the influence of other units. In general, the requirements for the control are:

- No further need for causing grid perturbations.
- A safe adaption to a variety of grid conditions.
- A correct consideration of other nearby voltage control units.

- Robust to operate under fast-changing grid conditions in the grid structure, such as split-ups.

A control that can fulfill these requirements allows for better integration of STATCOMs with highly dynamic voltage control. More renewable power generation units, like wind power plants, can then be connected without violating the voltage maintenance. STATCOMs are also allowing to supply remote grid loads, only having a weak connection to the main grid.

## 3.2 Proposed voltage controller adaption

An observer-based controller adaption is proposed in [C2]. The adaption relies on the dynamic voltage control behavior after a grid voltage disturbance. The proposed control observes the voltage error signal $V_{Err}$ inside the control to determine the achieved fault clearing time and to detect unwanted control oscillations. The proposed control scheme is shown in Fig. 3.3.

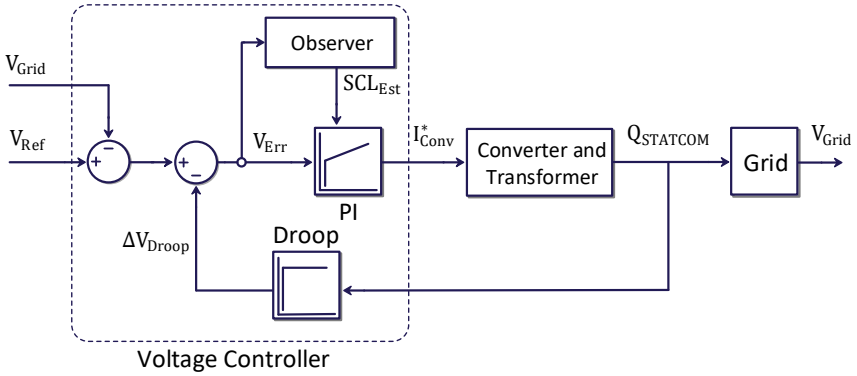


**Fig. 3.3:** Proposed voltage control scheme of STATCOMs with observer.

Observing $V_{Err}$ allows to incorporate the effect of the Droop control on the voltage reference setpoint. As the main controller is designed as a PI-controller, $V_{Err}$ is controlled to zero during steady-state. Any voltage deviation in the grid voltage deviates $V_{Err}$ from zero. The observer consists of three main parts that allow the adaptation to system changes, which is discussed in the following. The first two parts describe the detection of undesired system control performance. The third part is responsible for the change of $SCL_{Est}$, utilized in the Gain calculation. $SCL_{Est}$ is used in the Gain calculation, replacing $SCL/X$, directly incorporating the influence of nearby STATCOMs.

$$Gain = \frac{1}{\frac{1}{SCL_{Est}} + \frac{Droop}{Q_{NOM}}} \tag{3.2}$$

The STATCOM voltage controller is simulated with a cycle time of 1 ms in this study. The control blocks in the proposed observer have to be adapted to the cycle time if it is different in the respective application.

### 3.2.1 Detection of too slow control performance

The observer's first part has the purpose to detect if the voltage controller clears a grid voltage disturbance in a specified amount of time or if the controller takes too long. Then $SCL_{Est}$ and the used Gain have to be increased. $SCL$ can increase during operation when more lines and generation units are being connected. Nevertheless, it can also happen after a system split-up has been cleared, and the system is returning from a disturbed, weaker condition back to regular operation. Fig. 3.4 shows the simulation results of a single STATCOM being in operation during a grid voltage disturbance. The system conditions are as described in Chapter 2. The nominal grid voltage is 220 kV, $SCL$ is 10 GVA and the rated STATCOM power is 100 MVar, with the Droop being 4 %. The value of $SCL_{Est}$ is once correctly set to 10 GVA, in one simulation. Then it was set to 5 GVA to show the slowed-down controller response.

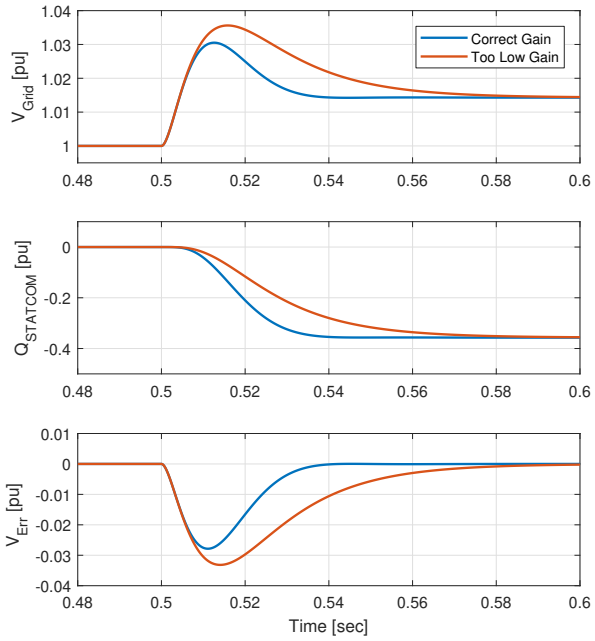


**Fig. 3.4:** System voltage control by STATCOM unit. Comparing correct and too small Gain value used in the controller.

The simulation results in Fig. 3.4 show the grid voltage $V_{Grid}$ and the re-

active power injected by the STATCOM, $Q_{STATCOM}$. The internal value of $V_{Err}$ is also shown to see its behavior during these two simulations. It can be seen, how the STATCOM response is slower when the Gain is set too low. Also, it takes a longer time to restore $V_{Err}$ back to zero after the grid voltage disturbance.

Any voltage disturbance that is measured by the control system is of unknown size. This uncertainty makes it impossible to determine whether the control is too slow during the initial phase of the disturbance. However, it can be detected when the disturbance is not cleared in a specified amount of time. Then, $V_{Err}$ does not return to zero as supposed (as shown in Fig. 3.4). The fault-clearing behavior is utilized to determine if the Gain is calculated correctly.

In the example, the STATCOM voltage controller is designed to have a step-response time of 30 ms [44]. The fault-clearing time is marginally larger than the step-response time, as the system has to measure the voltage disturbance first. Grid voltage disturbances are typically cleared with this kind of unit after 40 ms. The observer has to detect if the disturbance has been cleared at this time or not. When $V_{Err}$ is returned to zero in the specified time, then no further action is required. When $V_{Err}$ still deviates from zero, then the control system reacted too slow, and $SCL_{Est}$ has to be increased to speed up the controller.

This can be achieved in many different ways. In [C2], delay blocks are utilized to assess the dynamic system performance. With the delay-blocks, the currently measured $V_{Err}$ is compared with its delayed value. It can then be determined if $V_{Err}$ is cleared within a certain time by multiplying the current and the delayed value with each other. The basic control scheme for detecting too slow controller performance is shown in Fig. 3.5.

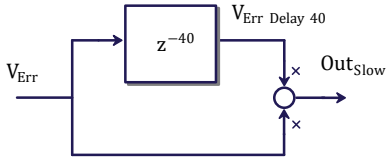


**Fig. 3.5:** Proposed observer part for detecting too slow voltage controller response [C2].

The multiplication $V_{Err} \cdot V_{Err\,Delay\,40}$ is zero during the steady-state operation, as both values are zero steady-state due to the integrator part in the PI-Controller. During a disturbance, the actual value of $V_{Err}$ deviates from zero. When the disturbance-clearing takes longer than the specified delay value of 40 ms, both inputs to the multiplier turn to non-zero. In this case, the sign of both $V_{Err}$ and $V_{Err\,Delay\,40}$ are the same, meaning the output is then positive.

In a real application, it is required to use a filter block at the $V_{Err}$ input

to neglect the influence of harmonics and measurement uncertainties on this adaption. In the proposed observer, this is done in the form of a dead-band. The dead-band is utilized to neglect the influence of harmonics and other, small voltage changes, which are too small to give valid information of the STATCOM's dynamic performance. In the performed simulations, the absolute value required to pass the dead-band is set to 0.001 pu. However, in a real STATCOM application, this threshold can be set higher, making the observer more robust.

$V_{Err}$ and its delayed value are dependent on the actual voltage change amplitude, which severely affects the product output magnitude. However, the controller adaption should be as independent as possible from the magnitude of the initial voltage disturbance. The Gain correction should be performed not with the absolute value of $V_{Err}$ but with its sign. The sign function is proposed as an addition to the control shown in Fig. 3.5 to be used directly after the dead-band. Nevertheless, it can also be included after the multiplication block. The improved control scheme is shown in Fig. 3.6.

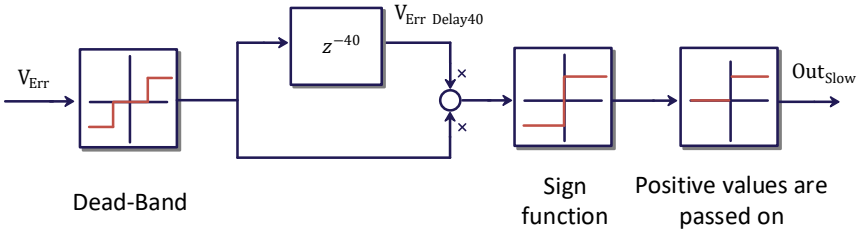


**Fig. 3.6:** Improved observer part for detecting too slow voltage controller response.

The performance of this control part is shown in Fig. 3.7 and Fig. 3.8. The simulation results in Fig. 3.7 show the behavior when the Gain is tuned correctly. Then $SCL_{Est}$ is $SCL/X$ and the STATCOM operates as desired. The observer block does not trigger any response, as it is not necessary in this case. Fig. 3.8 shows the observer behavior when $SCL_{Est}$ is smaller than $SCL/X$. The fault-clearing takes longer, triggering a response, after the delay time of 40 ms. It can be seen that the multiplication of the current and $V_{Err\,Delay\,40}$ value is positive.

The output value $Out_{Slow}$ is then later used in the third part of the observer, described in Section 3.2.3. With this, the observer is capable of adapting the STATCOM to power grids, which have an $SCL/X$ value that is higher than the controller initially estimated. In Section 3.2.2 is the next required part of the observer described, which is responsible for the detection of conditions, where the Gain is set too high for the current $SCL/X$ value.

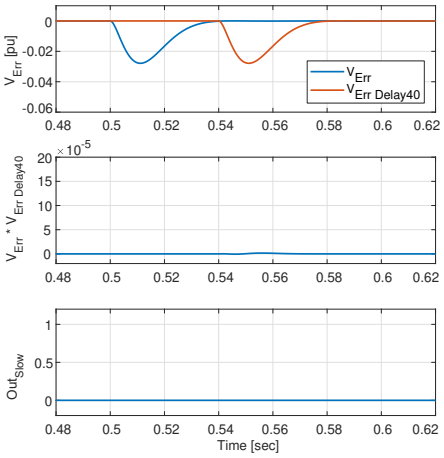


**Fig. 3.7:** Observer behavior at correct tuned Gain value.

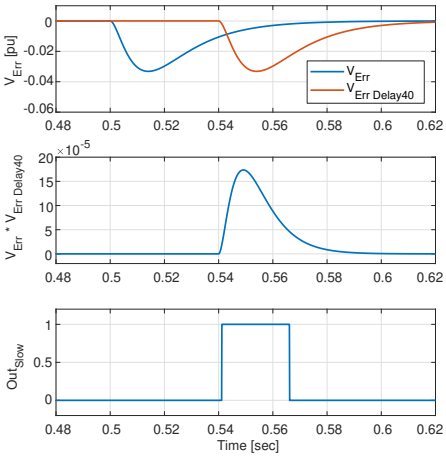


**Fig. 3.8:** Observer behavior at too low Gain value.

### 3.2.2 Detection of too fast control performance

The other case, which the observer has to detect, is when the $SCL_{Est}$ is higher than $SCL/X$. Then the controller reacts with too much reactive power on a voltage disturbance, causing voltage swings, and even oscillations, under severe circumstances. Under this condition, $V_{Err}$ is not going back to zero, as required, but it oscillates around zero, causing the STATCOM reactive power to swing. The system under this condition is simulated as before, only $SCL_{Est}$ is now set to 15 GVA. The results are shown in Fig. 3.9. It can be seen, that the initial deviation in $V_{Grid}$ is over-compensated, leading to a small swing in $V_{Err}$.

The observer has to detect the voltage disturbance caused by the internal dynamics of the STATCOM, due to the incorrect Gain. The detection is again realized with a delay block, as given in Section 3.2.1. The proposed control structure is shown in Fig 3.10. The delay time is chosen carefully to detect the repetitive change of signs of $V_{Err}$ due to the high Gain value. In the simulated STATCOM system is the delay time set to 20 ms. It is chosen according to the measured time, where $V_{Err}$ is positive in Fig 3.9. When the delay is chosen slightly larger or smaller, then the controller still works as required, only the final change in $SCL_{Est}$ is then slightly slower. However, this delay time is dependent on the designed control system's time constants, which do not change during operation.

The filter in Fig. 3.10, which only lets negative values pass, is a requirement even in the simplest controller design. Otherwise would $Out_{Fast}$ turn positive during any grid voltage disturbance, as the system is designed to restore the voltage after 40 ms and the delay is only 20 ms. Only the observer

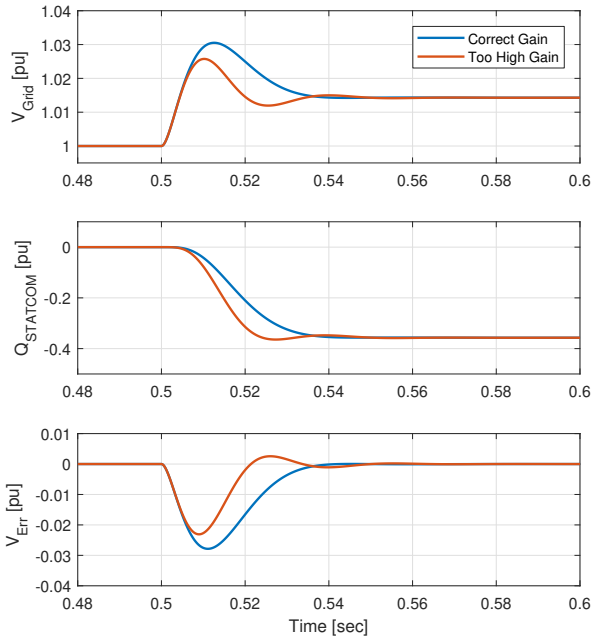


**Fig. 3.9:** System voltage control by a STATCOM unit, comparing correct and too high Gain value.

part from Section 3.2.1 has the possibility to increase the voltage controller Gain by having a positive output signal.

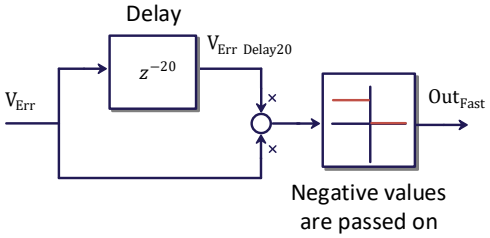


**Fig. 3.10:** Proposed observer for detecting too strong voltage controller response [C2].

Whenever the $SCL/X$ value is lower than $SCL_{Est}$, it will cause a controller swing in the $V_{Err}$ signal. These swings change the sign of the $V_{Err}$ after the initial clearing phase. These sign changes cause $V_{Err} \cdot V_{ErrDelay}$ to be negative. The negative value of $Out_{Fast}$ is forwarded to an integrator in the third part of the observer to decrease $SCL_{Est}$.

In a practical situation it is again advantageous to include a dead-band or a different type of filter, neglecting the influence of harmonics and small voltage measurement fluctuations. To improve the dynamics of the adapta-

tion, it is also beneficial to utilize the sign function, making the observer less dependent on the absolute value of the grid voltage disturbance but relying on the amount of Gain mismatch. The improved control scheme is shown in Fig. 3.11.

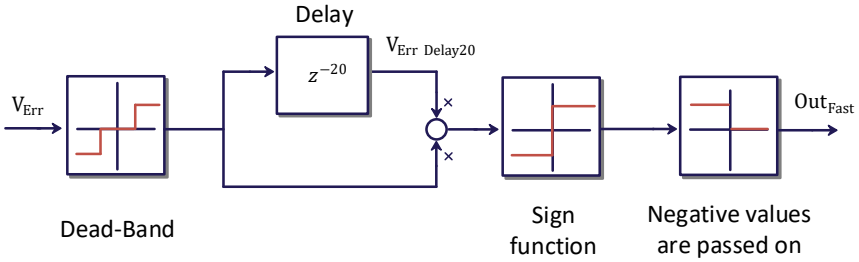


**Fig. 3.11:** Improved observer part for detecting too fast voltage controller response.

The system simulation results in Fig 3.12 show the observer behavior during a voltage disturbance with the Gain calculated correctly. $V_{Err} \cdot V_{ErrDelay}$ turns positive during the simulation, but this is not passed on to the output. Only, when $SCL_{Est}$ is set too high, as in Fig 3.13, then the resulting negative value is passed on to $Out_{Fast}$.

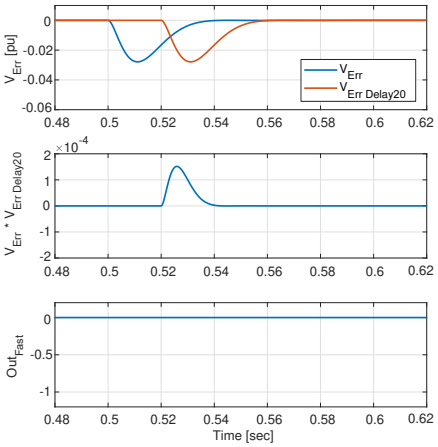


**Fig. 3.12:** Observer behavior with correctly tuned Gain value.

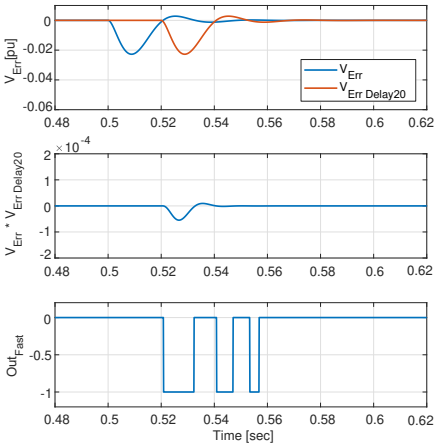


**Fig. 3.13:** Observer behavior with too high Gain value.

$Out_{Fast}$ is then further utilized in the $SCL$-Estimator, which is described in Section 3.2.3.

### 3.2.3 SCL estimation Block

The two previously described blocks can observe deviations between $SCL/X$ and $SCL_{Est}$ values. The third and last block needs to use the outputs $Out_{Slow}$ and $Out_{Slow}$ to adapt the controller. This is realized with an integrator block. The initial value of the integrator determines the STATCOM setting at the start-up.

Fig. 3.14 shows the proposed $SCL$-Estimator. The input $Out_{Slow}$ is only allowed to be zero or positive, causing an increase in $SCL_{Est}$. When $Out_{Fast}$ of the second block turns negative during a voltage disturbance, then this is used to decrease $SCL_{Est}$.

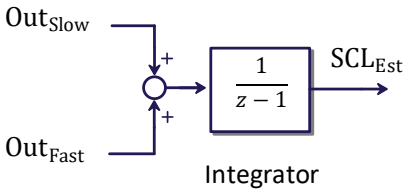


**Fig. 3.14:** Integrator, used to estimate $SCL$.

The overall control scheme for the observer is shown in Fig. 3.15. The dead-band and the sign function can be combined for the two different observers. The sign function is then used before the delay-blocks. The control scheme in [C2] does not include the sign function, as an improvement for the observer. As described above, allows the sign-function that the control is much less dependent on the initial grid voltage disturbance magnitude.

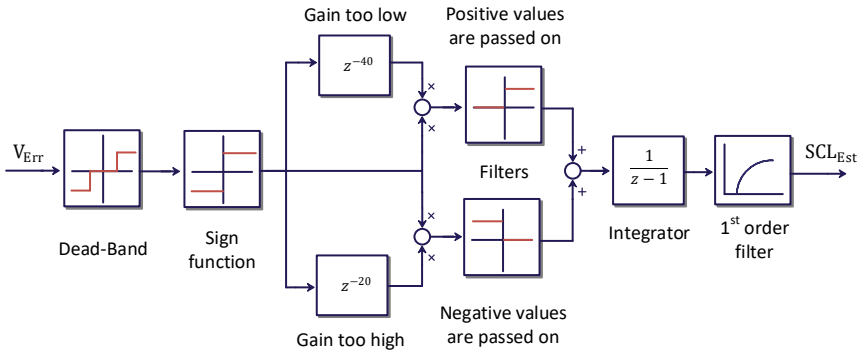


**Fig. 3.15:** Overall control scheme of the proposed observer.

The dynamic change of $SCL_{Est}$ for the Gain can also bring the system in danger when the changes are applied too fast. Fast-changing values of the Gain can otherwise cause interactions with the observer and the PI-controller.

In a real application, this has to be taken into account. Therefore should $SCL_{Est}$ be filtered before being further used. In [C2], a first-order low pass filter is utilized to smooth out the $SCL_{Est}$ being applied in the PI-Controller Gain calculation.

The observer behavior is simulated and evaluated in Section 3.3.

## 3.3 Verification of the proposed observer's performance

The proposed observer is now tested, to determine, how the adaption is done during the operation of a single STATCOM under changing grid conditions. Afterward, is the behavior together with a second STATCOM analyzed.

### 3.3.1 Observer performance during SCL changes

Simulation results are shown in Fig. 3.16 and Fig. 3.17. The STATCOM has a rated power of 100 MVAr, and the Droop value is set to 4 %. The power grid is again simulated with $SCL$ being 10 GVA. The first order filter block is set to a time constant of 150 ms, preventing interaction during the respective event. Voltage disturbances are simulated in the grid voltage to cause a reactive power response by the STATCOM.

The simulation results in Fig. 3.16 show $V_{Grid}$, $Q_{STATCOM}$, and $SCL_{Est}$. $SCL_{Est}$ is initially set to 4 GVA, causing the STATCOM response to be slower than desired. The STATCOM evaluates its own dynamic response to the applied voltage disturbances and adapts $SCL_{Est}$ accordingly. The slow reaction time causes the increase of $SCL_{Est}$ by the proposed observer. The adaption is slowed down, the closer $SCL/X$ and $SCL_{Est}$ are. The controller response is then as designed and the controller Gain does not have to be increased anymore.

The results in Fig. 3.17 show the observer behavior when $SCL_{Est}$ is initially set to 25 GVA. Conditions like this can be caused by a system split-up. It can be seen that the incorrect dynamics, identified as short voltage oscillations, are not occurring anymore when the voltage controller Gain is using the correct value for $SCL_{Est}$ of 10 GVA.

The STATCOM voltage controller can, with the proposed observer, adapt to changes in $SCL$. The passive behavior of the observer reduces the need to perform forced voltage disturbances, as before with the penetration-based test, as described in Section 3.1.1. This is already a significant improvement from the previous method. Another benefit is the continuous monitoring of the STATCOM behavior during operation, not only periodically, e.g., every 12 or 24 hours.

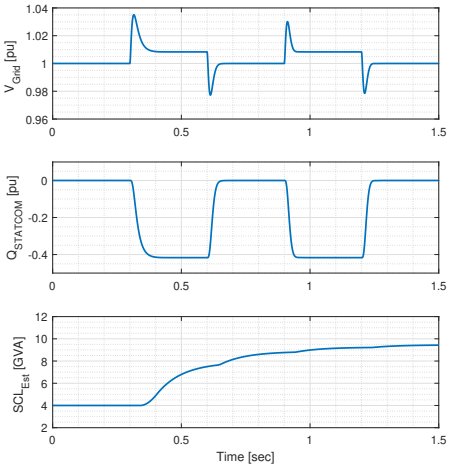


**Fig. 3.16:** STATCOM behavior, when the grid strength rises from 4 GVA to 10 GVA.

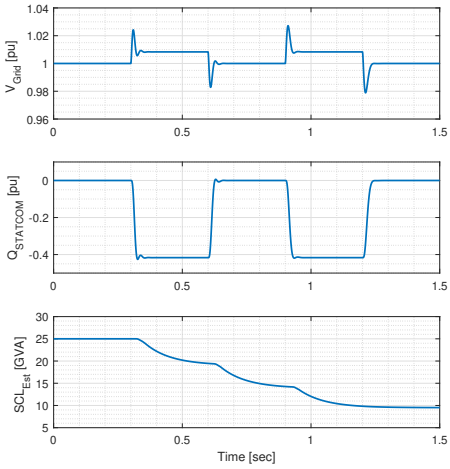


**Fig. 3.17:** STATCOM behavior, when the grid strength decreases from 25 GVA to 10 GVA.

However, the main task is the coordination of multiple STATCOMs, that are nearby in the power grid. It is evaluated in Section 3.3.2 if this is done with the proposed observer structure. Then $SCL_{Est}$ should not only be $SCL$ but $SCL/X$

### 3.3.2 Observer performance in a two-STATCOM system

The evaluated power system is changed to a system with two STATCOM at a single bus, as described in Section 2.1.2. The proposed observer is designed to detect the second STATCOM, as it detects a reduction $SCL$ as both STATCOMs operate in parallel, reducing the amount of required reactive power by the single STATCOM.

The simulation results from a STATCOM in operation in a grid with an $SCL$ of 10 GVA is shown in Fig. 3.18. In the simulation, a second STATCOM is activated, also with $SCL_{Est}$ set to 10 GVA. During the first grid voltage events, the controllers respond both with too much reactive power. $SCL_{Est}$ is changed in both STATCOMs, which in the end then splits the $SCL$ up between the two units.

Fig. 3.19 shows the dynamic STATCOM behavior when the second STATCOM is not installed at the same bus, but as described in Section 2.3.3 with an impedance between them. It can be seen, that $SCL_{Est}$ inside the observer is reduced, as each STATCOM has to control three-fifth of $SCL$.

The proposed observer makes the STATCOM voltage controller robust against any power grid changes, even after years of operation. The reliable maintenance of the grid voltage with STATCOMs is now possible with sig-

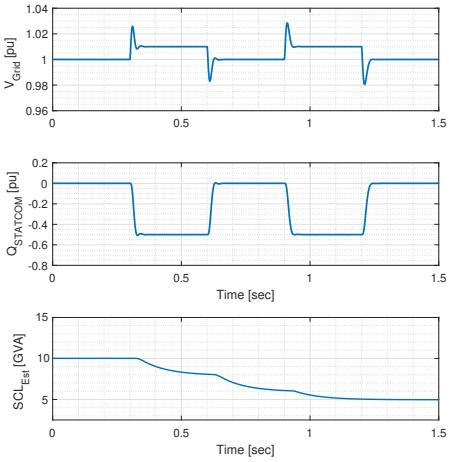


**Fig. 3.18:** STATCOM behavior during grid disturbances with a second STATCOM at the same bus.

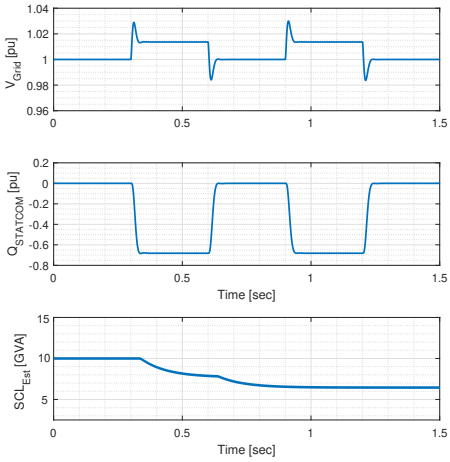


**Fig. 3.19:** STATCOM behavior during grid disturbances with a second STATCOM at a different location.

nificant improvements compared to the perturbation-based $SCL$-estimation. The interaction between multiple STATCOMs is also realized independent of the STATCOM placements in the grid.

## 3.4 Limitations of the proposed control adaption

STATCOMs can with the proposed observer-based control adapt to many different conditions in the power grid. But the observer has also limitations. Voltage control is not only performed by STATCOMs. Other units also contribute to the system voltage control, like conventional generators and converter-based units, such as wind power plants, or photovoltaic units. However, STATCOMs are typically the fastest units, which makes the proposed observer suitable.

The proposed control scheme can not be used in slower units, as wind power plants, that have a much slower voltage controller response time. Its dynamics are limited by the communication delay between the wind power plant controller (WPPC) and the wind turbines, as shown in Fig. 3.20. The possible interaction between fast STATCOMs and slow wind power plants causes changing dynamics for the voltage control in the wind power plant controller.

The observer is also limited when the STATCOM can not control the system voltage back to the desired operating point with its reactive power. The STATCOM can only provide a certain amount of reactive current and power, so a severe voltage disturbance may bring the STATCOM to its limits. Then,

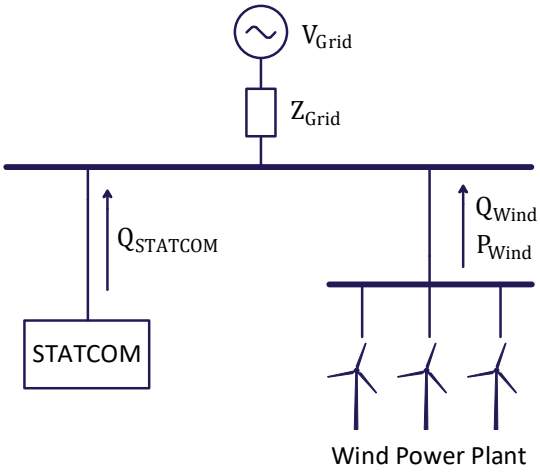


**Fig. 3.20:** One-Line diagram of a wind power plant with STATCOM.

$V_{Err}$ is not restored back to zero, giving the expression for the observer as a slow controller behavior. The observer should, in this case, not change the internal grid $SCL_{Est}$ which has to be included in the observer. For this, the STATCOM could block $Out_{Slow}$ and $Out_{Fast}$ as inputs to the integrator whenever the STATCOM is limiting its power and shortly thereafter. The STATCOM is then protected from an incorrect Gain increase.

## 3.5 Summary

The proposed control scheme with a passive observer allows to control the bus voltage reliably with STATCOMs. The observer can detect changes in the surrounding grid by analyzing the dynamic voltage controller's behavior during disturbance-clearing. The proposed control structure is also capable of detecting other voltage controlling units nearby, as this causes similar changes in the controller dynamics like changes in the grid strength.

The observer is active throughout the unit's operation. The permanent observation is advantageous to the solution currently used in industry where the strength of the power grid is only estimated twice per day. $SCL$ is not only determined after many hours and it does not require a grid voltage perturbation by the STATCOM. More importantly, the proposed observer incorporates other voltage controlling units, allowing the usage of STATCOMs and other fast voltage controlling devices in parallel at one bus or also distributed in the transmission grid. The further integration of more STATCOMs into the power grid allows reliable voltage control in modern power grids.

# Chapter 4

# Assessment of modern power system frequency reliability

## 4.1 Background and Motivation

The reliable operation of the power system is not only dependent on the maintenance of the system voltage. Many other criteria have to be fulfilled to ensure a reliable supply of all system loads and the safe operation of the entire power grid. Transmission system operators have named frequency control as the most challenging issue, that arises with the integration of power-electronic-based generation units on a large scale [14]. The reliable control of the power system frequency in modern power grids with a high renewable power penetration is the focus of this Chapter.

Modern power systems can no longer rely on conventional frequency controls using synchronous generators. The replacement of the synchronous machines with converter-based ones reduces the system inertia. The main issue with reduced inertia is, that the system frequency changes faster and the RoCoF is then higher. In a conventional power system with a high inertia, there is a longer time between an event and the frequency reaching the load shedding threshold. This allowed the conventional frequency controls to react and to stabilize the system frequency. With the reduced inertia, this time to react has decreased so that the conventional generation units can no longer adjust their power output in time to balance the power grid demand. This increases the risk of abnormal frequency conditions in the power grid. Also, the operation under emergency situations is seen as being more likely with the reduction of inertia [75].

In this study, the focus is on wind power plants assisting with the frequency control of the power grid. This is done, as wind power is the main

contributor to renewable energy in many countries worldwide, e.g. in Denmark. Wind power plants are also capable of contributing to frequency controls, assisting the power system during phases of high non-synchronous penetration. These frequency controls can be utilized as system services applied in different time frames, as steady-state power curtailments, or fast frequency controls during severe contingencies. The main advantage of using converter-based generation units for frequency controls is their flexibility in controls. Wind power plants can offer a variety of services to the grid, only limited by their physical properties. It is not possible to produce more energy than the wind provides, when the grid is in need for more energy. However, it is possible to initially curtail wind power or to utilize the rotational energy of the blades for short-term power increases. It is the system operator, that has to define in the grid code, which frequency controls shall be implemented. Modern wind power plants are also capable of having different controls available. The system operator can then choose, which one is required for the safe grid operation at the current grid state. Communication links are then used to vary the control schemes, or settings inside the controls to benefit the power system.

### 4.1.1 Study Test System

A power system that is often used for the assessment of the power system reliability, is the IEEE reliability test system (IEEE RTS). It is developed to allow for adequacy assessments and also the assessment of the system security. The system data are specified in [87,88]. The given load distributions and the generator data are given, which allows determining the system reliability during e.g. one year of operation.

This system is used for many different assessments of the power system's reliability. It is used in the original configuration, but also with additional equipment such as STATCOMs or changes in the transmission lines in operation [89]. The original IEEE RTS has no integration of wind power plants. Assessing the system reliability with this kind of additional equipment can be done by inserting additional wind power plants, as shown in Fig. 4.1 [J1].

The wind power plants have to be described with the turbine data and the natural conditions around them. The wind speed distribution throughout the yearly operation has to be given to determine the available power for the wind turbines. The turbine parameters also have to be given, as the rated turbine power and the cut-in, the rated, and the cut-out wind speed.

With this, it is possible to determine the available power in-feed of the wind power plants. The grid code requirement for the wind power plant in the evaluated power grid has to be defined, to determine the system performance with wind power integration.

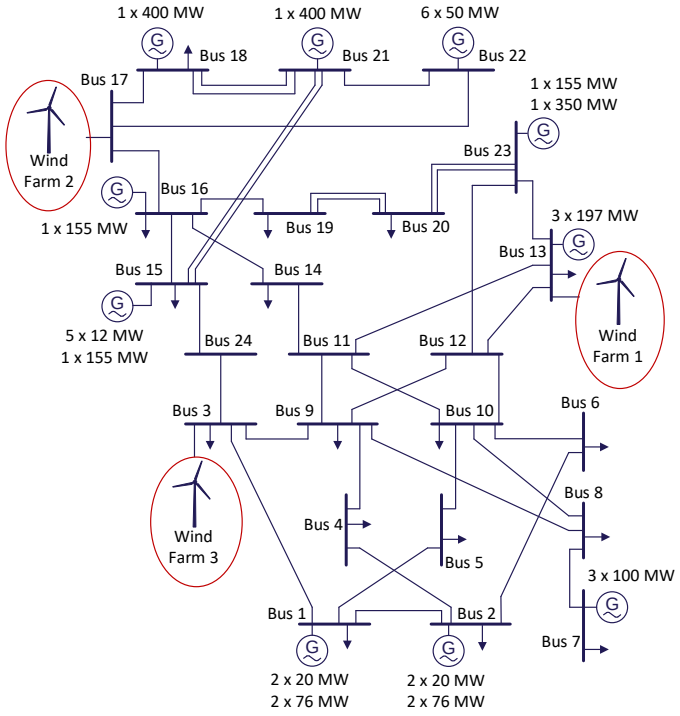


**Fig. 4.1:** Modified IEEE reliability test system with three additional wind power plants [J1].

### 4.1.2 Aim of this study

Utilizing these new kinds of services has to be evaluated concerning the increase in frequency performance and the additional frequency service effort. Frequency reliability indices are already used to describe the system performance. However, it can also be used to estimate the effect of changes on the grid's safe operation. These changes can be additional equipment, such as more conventional or more renewable power generation units. Also, the decision-making by the system operator may have a severe influence on the operational security, such as different generator scheduling schemes or a change in frequency controls by converter-based generation units.

The main open issues with fully including wind power plants into the frequency management by the system operators are:

- Quantification of the frequency control usage during operation.
- Ensuring an accurate assessment of the power system with additional frequency controls.
- Allowing fast assessment of the power system to compare multiple fre-

quency managements.

With these issues fulfilled, it is possible to effectively compare different frequency managements including wind power plants.

## 4.2 Frequency reliability assessments

The frequency reliability assessment procedure of wind-integrated power systems is proposed and shown in Fig. 4.2. The different steps in the assessment are further described in the following. This is required for system operators to decide on which control schemes should be used under which grid conditions to allow for the most reliable operation possible.

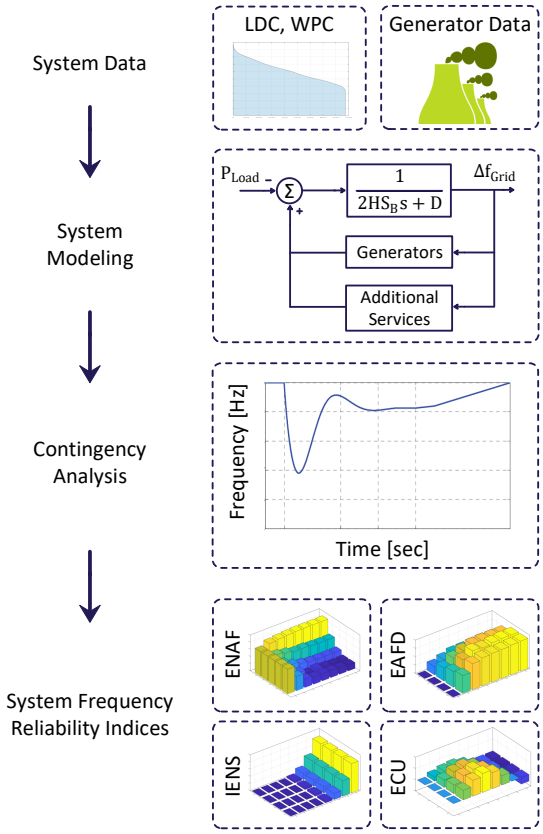


**Fig. 4.2:** Frequency security assessment procedure of wind-integrated power systems.

The process includes the gathering of system data, such as how the system load or the wind power behaves throughout the year. The system modeling is

the next step, as the system in all its possible states has to be described during steady-state, but also together with the functions, that are implemented into the grid. This has to be done carefully, to describe the system accurately enough, without increasing the computational burden too high. The system simulation under the influence of contingencies and the calculation of the reliability indices then allows quantifying the system health in regards to the frequency quality.

The system data required as input for the assessment are described in the following.

### 4.2.1 System data for the frequency reliability assessment

First, the system conditions during the yearly operation are described with the load duration curve (LDC) and the wind power curve (WPC). The load duration curve describes the distribution of the maximum hourly system load throughout the yearly operation of the grid. It changes minor from year to year, so it is often taken from a five-year average system data to have a good representation of the typical system behavior [90].

The WPC describes the amount of wind power injected into the system in one year of operation. It is also representing the maximum wind power per hour, sorted in descending order. An average of multiple years can again be used to determine the average system behavior.

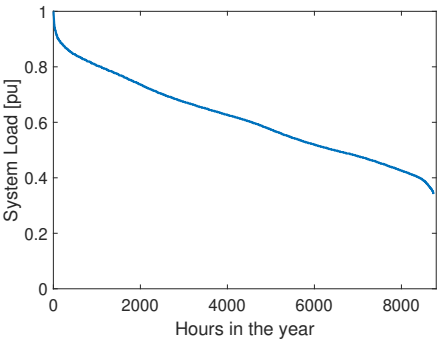


**Fig. 4.3:** Load duration curve of the IEEE Reliability test system [87].

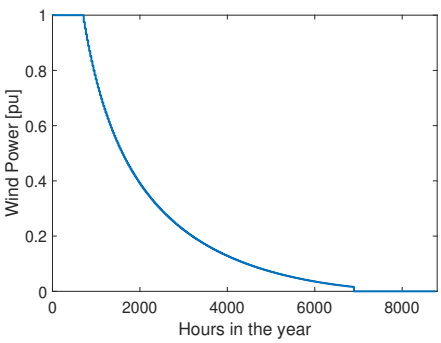


**Fig. 4.4:** Wind power curve, representing 2200 full-load hours [J1].

The generation units connected to the power system are also part of the input data. Their rated powers and time constants are essential to model the frequency response during active power imbalances. It is also important to respect the dynamic capability of the units to contribute to primary or secondary frequency controls. One of the most important pieces of information on the generators is how often they fail. For this, the mean time to failure, MTTF, can be utilized. It does not define, that a unit will always trip after a

certain number of hours in operation, but it is used to determine the probability of the event per year. MTTF is therefore only a statistical value, which is estimated from historical data.

The system states describe the different steady-state operation points of the grid. This means a certain amount of system load and system wind power injection together with the conventional units are in operation to fulfill the demand. The probability of this state can be calculated by the probabilities given in the LDC and WPC.

### 4.2.2 System modeling for reliability assessments

As it is shown in Fig. 4.2, the next step is to perform the power system modeling. Later the system models will be utilized for contingency simulations. The different system states have to be modeled, and then the contingencies are simulated. The dynamic system simulation has to be repeated for the different system states, such as load variations and wind power injections. Detailed system modeling is an essential part of the system security assessment design. The models of the dynamic processes and the number of incorporated system states have to be accurate enough. Otherwise, the influence on the power system reliability can not be estimated correctly, and the system operator can not determine the actual system performance. Fig. 4.5 shows the system model used to assess the frequency behavior during contingencies. The system model includes the system inertia, the $n$ different conventional generators, and the wind power plant behavior together with the under-frequency load shedding (UFLS).

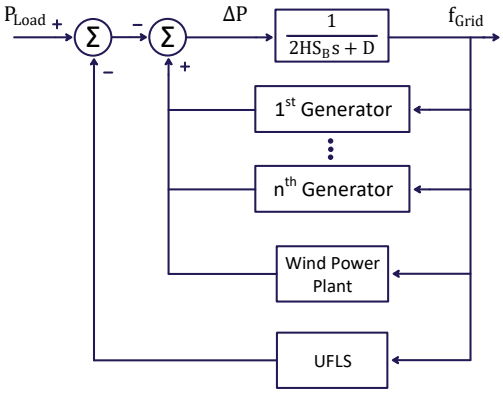


**Fig. 4.5:** Power system modeling for frequency operational security assessment [J2].

The different considered system states are determined following a fixed procedure. First, the system load is discretized for the simulation in steady-state. Different levels of loads are used with their probability to represent

the load distribution in one year, following the LDC, as shown in Fig. 4.3. The amount of demanded system load at simulation start, when the system is in steady-state is set as $P_{Load}$. Additionally, the behavior of the system loads during severe under-frequency occurrences is modeled concerning the system operator's UFLS. This protective function only gets activated during severe under-frequency events to protect the remaining grid from failing due to insufficient active power delivery.

The behavior of wind power plants is modeled next. In many countries renewable energy sources are allowed to inject their full available power, the conventional generation units are then 'filling up' the remaining grid demand. However, due to the rapid increase in renewable penetrations in several countries, there are now limitations in place to curtail the steady-state injection of converter-based generation units if the penetration levels are too high. This can be seen, e.g., in Ireland, where the SNSP, the system non-synchronous penetration, is utilized to keep the minimum inertia in operation [58]. In a wind integrated power system is the available wind power therefore not always the injected wind power as the system operator can curtail the wind power if the operation requires it. Through the inclusion of the wind power plant model, the influence of their active power change to the point of connection on the system frequency can be included as well. The model has to include the physical behavior of the turbines, with the wind speed as the input to determine the actual behavior during frequency disturbances. The additional frequency controls, demanded by the grid code, are implemented. The frequency-related protection functions are important to be modeled in these units as well, as they get deactivated under several grid conditions. The functions can also include over- and under-frequency thresholds or RoFoF based functions for disconnection. RoCoF is often included as a measure to prevent the units from operating in islanded situations.

Afterward, the conventional generation units are modeled. The number of conventional generators during the system operation depends on the remaining grid demand, not yet supplied by the renewable sources. The generator scheduling scheme is used to determine, which units are being activated first, and which ones are only allowed to run during high-demand periods. The generation units are modeled with their inertia and their frequency control behavior. Different levels of details are possible for their modeling. The choice of detail in the modeling depends on the study's aims. In some assessments, all generation units are combined into one unit, which is responsible for the power supply, and the primary, secondary and tertiary frequency controls.

To incorporate more details into the models such as unit-specific dynamic data can all generation units of one size be combined to one, with multiplication by the number of the units, as shown in Fig. 4.5 [J2]. The unit-specific dynamics can be the primary control response times or the ramp-rates of the

secondary frequency controls. This makes the model more accurate, resulting in a better representation of the dynamic system performance. The drawback is an increase in the simulation burden and a longer overall duration for the reliability assessment. The frequency swing equation from (1.5) is modeled with the combined rated power of all running conventional generators $S_B$, their time constants $H$, and the system damping coefficient $D$. These parameters have to be given for the connected conventional generation units and for the connected system loads [87,88]. The model input is the demanded active power in the system $P_{Load}$. The power imbalance between demanded and supplied power $\Delta P$ is then the input to the system frequency swing equation, resulting in the grid frequency $f_{Grid}$.

An important part of the modeling is also the correct representation of the protective functions, implemented in the generation units. The generation units are only designed to operate in a specific frequency band. If the frequency is too high or too low, then these units might be damaged, which can be avoided by disconnecting them before the critical thresholds are reached. The protection function of conventional generation units also contains the rate of change of rotational speed as a measure, as it is a sign of high mechanical stresses in these units.

### 4.2.3 Contingency analysis

The next step in the assessment of the power system's frequency reliability is the contingency analysis, as also shown in Fig. 4.2. The analysis determines the system's response to the considered contingencies. The reliability analysis requires evaluating a large number of steady-state grid operations. These depend on the different load levels, taken from the LDC and also on the states of the other equipment. In wind-integrated systems, the different levels of wind power injection have to be considered.

The contingencies can be the trip of feeders in the power grid, resulting in the loss of grid load. This is simply simulated with a reduction of the $P_{Load}$ value at the time, the contingency occurs. The following frequency rise causes the connected equipment to react according to the set frequency controls. The units performing primary and secondary frequency controls reduce their power production to stabilize the power grid frequency. When wind power plants are designed to contribute, then their active power change also causes the grid frequency to stabilize.

Under-frequency occurs when the active power production is reduced. This is caused by the sudden trip of generation units, both conventional or converter-based. The trip of conventional generation units also has to be respected in the parameters of the swing equation, as the total system inertia is then reduced, causing changes in $H$ and $S_B$, seen in Fig. 4.5.

In power grids with HVDC units connecting two different synchronous

areas, a sudden trip of the units also causes the grid frequency to change. The sign of frequency change is then dependent on the current HVDC line operation, importing, or exporting power.

The grid's frequency response and the frequency control actions are recorded to combine them into the reliability indices, describing the system's performance in one year.

### 4.2.4 Reliability indices for system reliability assessment

After the contingency analysis is done and the time-series simulation is performed, the results have to be interpreted into the reliability indices. Different indices quantify the behavior of the power system in one year of operation. These indices can be separated into two categories; the first one describes the power system's frequency quality, meaning the number and duration of abnormal frequency states [75]. Another index in this category is the total amount of load curtailment. The higher this index is, the more load curtailment is expected to happen during the system operation. These indices are listed in Table 4.1.

**Table 4.1:** Reliability indices describing the frequency quality [75,91].

| Index | Unit | Full Name |
|---|---|---|
| NOF | | Exp. Number of Over-Frequency Events |
| NUF | | Exp. Number of Under-Frequency Events |
| ENAF | | Exp. Number of Abnormal Frequency Events |
| OFD | min | Exp. Over-Frequency Duration |
| UFD | min | Exp. Under-Frequency Duration |
| EAFD | min | Exp. Abnormal Frequency Duration |
| EENS | MWh | Exp. Energy Not Served to Loads |

The other category describes the amount of energy being used for frequency control, indicating how much effort is required to keep the power system frequency reliable. The different indices used in conventional power systems are listed in Table 4.2 [91].

**Table 4.2:** Reliability indices describing the usage of frequency control [91].

| Index | Unit | Full Name |
|---|---|---|
| IENS 1 | MWh | Indirect Energy Not Supplied (for Primary Frequency Control) |
| IENS 2 | MWh | Indirect Energy Not Supplied (for Secondary Frequency Control) |
| ECU 1 | MWh | Unnecessary Energy Consumption (for Primary Frequency Control) |
| ECU 2 | MWh | Unnecessary Energy Consumption (for Secondary Frequency Control) |

The reliability indices are calculated for multiple system states $i$ and the respective contingencies $j$. The indices $X_{i,j}$ from the single simulations are combined dependent on their probabilities, where $p_i$ is the probability of the system state and $p_j$ is the probability of the contingency.

$$X_{L,W} = \sum_{i=1}^{N_i} \sum_{j=1}^{N_j} p_i \cdot p_j \cdot X_{ij} \tag{4.1}$$

The indices describing the frequency quality do not determine an actual system failure, as no equipment is damaged or disconnected at the used threshold of 0.2 Hz in the central Europe power grid, as shown in Fig. 4.6 [75]. Nevertheless, system operators can determine with these indices how their system reacts to changes over time, such as the further integration of renewable generation units. The increasing likelihood for abnormal frequency states has to be evaluated, and it may be required to make changes in the frequency controls. The expected number of under-frequency events can be calculated by:

$$NUF_{L,W} = \sum_{i=1}^{N_i} \sum_{j=1}^{N_j} p_i \cdot p_j \cdot NUF_{ij} \tag{4.2}$$

The amount of energy that is not supplied to the system loads indicates how often and how severe load curtailments occur. The policy for load curtailment is defined by the TSOs in one region and has to be coordinated with other protective functions in the power grid. The better the frequency controls are designed, the fewer UFLS are activated. Fig. 4.6 shows the frequency behavior and the conventional frequency controls following a generation unit outage. It can be determined if and how long the frequency is abnormal and how much frequency control is used.

The used energies for frequency control are indications of the status of the system. The indices are not a prediction of one year's system behavior, as the failure probability is not representing a fixed number of failures per year, but it only describes a certain probability of occurrence. Nevertheless, these indices allow a comparison of different controller settings, generation scheduling schemes, and the effects of integrating more converter-based generation units. System operators can use the reliability assessment results to determine the impact of changes in the frequency control on their operation of the power system. The balance between system frequency quality and the use of energy for frequency controls can then be found.

Converter-based units are nowadays also capable of contributing to reliable system frequency in many different ways. System operators have to incorporate the dynamic behavior of converter-based generation units, such as wind power plants, and include them in their system reliability analysis.

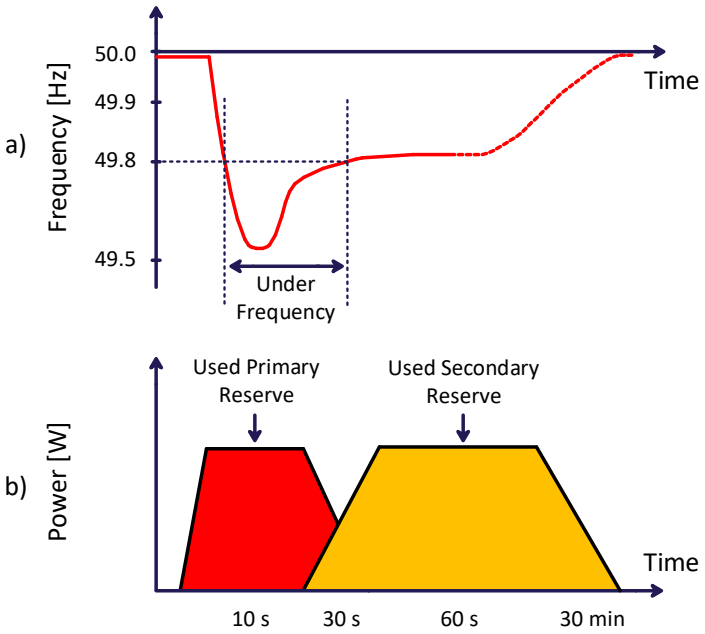


**Fig. 4.6:** Evaluating frequency reliability indices. a) System frequency during a generation outage. b) Active conventional frequency controls activation during a frequency event.

This allows the TSO to understand the Pros and Cons of different frequency services to improve the power system's frequency management and thereby system reliability.

In Section 4.3 the reliability indices are explained, which are required to evaluate the wind power plant's impact on the frequency reliability. Section 4.4 elaborates how system operators can ensure that their assessment is accurate enough while reducing the required computational burden. With the change in the frequency controls, this is essential, as control setting changes in these units may last for years and have to be evaluated offline before setting them into operation.

## 4.3 Reliability indices in wind-integrated power systems

The reliability indices as described previously are sufficient in a conventional power grid. In wind-integrated power grids, the evaluation of the wind power plant performance also plays an important role and has to be included in the assessment. The indices have to include the steady-state, as well as the active usage of frequency controls during the contingencies. These two time-

frames have to be considered to determine the impact of frequency controls in the wind power plants throughout the operation of the grid under all circumstances.

### 4.3.1 Incorporating frequency controls in steady-state

The curtailment of wind power during steady-state operation is a function that is nowadays often demanded in power grids. It is demanded to keep a minimum number of conventional generation units running, allowing to keep some spinning reserve under all conditions. The curtailed wind power has to be summed up to determine the amount of total wind energy wasted. The amount of curtailed wind power is dependent on many factors. These are the amount of wind power, the demanded amount of active power reduction in steady-state, and the TSO's strategy when to demand the curtailment. This is dependent on TSO's frequency management.

The index describing this expected wind energy wasted,e EWEW. EWEW measures the amount of wasted wind energy curtailed to keep the demanded minimum inertia in the power system. This is not part of a frequency service, but only a protective curtailment. When wind power is curtailed for a service, this energy can be part of an additional TSO tool for frequency reliability enhancement. The wind power is then not wasted but kept in 'reserve' for usage when required. Fig. 4.7 shows the available and the actually injected wind power into the IEEE RTS with 1 GW installed wind power capacity. The curtailment is done by reserving 0.2 pu wind power during phases of high wind power penetration levels above 50 %.

This curtailment is not representing wasted wind power for the plant operator. The wind power plant's frequency reserve has to be compensated by the TSO economically. In the modern power grid, these services are competing with the conventional generation units, currently providing the primary frequency controls.

Other frequency services do not require wind power curtailment during steady-state, but they are still influenced by grid operations. Then, the TSOs have to consider service availability. VSM-based controls, as an example, maintain the steady-state power at the maximum available wind power. However, they have the potential to provide additional short-term energy for frequency support. The same is true for under-frequency control, which is also provided by VSM-controls.

The amount of ordered VSM-services by the system operator can be determined by the demanded service power and on the duration, the service is demanded. This can be calculated with the state probability during the yearly operation $p_i$, in the same way as the wasted wind energy in steady-state is calculated. This can be seen in Fig. 4.8, where the distribution for the ordered VSM-service is shown. In this case, 20 % of the wind turbines deliver

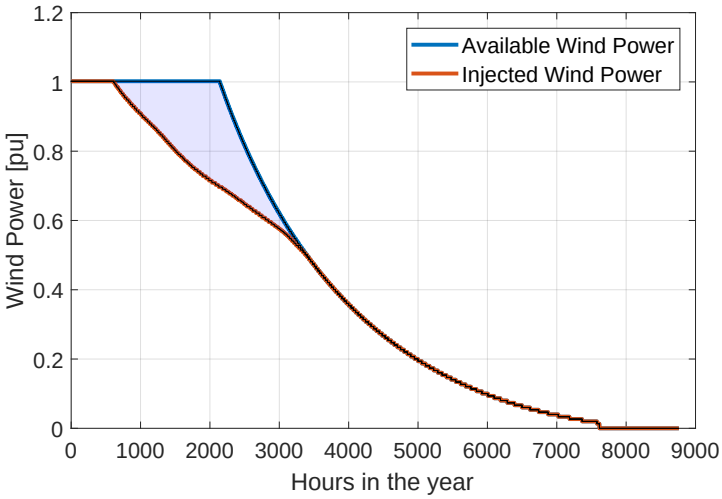


**Fig. 4.7:** Available and injected wind power distribution in the IEEE RTS with 1 GW wind power when the wind power is curtailed during operation.

the service when the wind power penetration has reached more than 40 % in the IEEE RTS. The LDC from Fig. 4.3 and the WPC shown in Fig. 4.4 define the ordering of the VSM-service.

The total ordered VSM-service energy can be calculated as shown in (4.3), where the expected ordered frequency service (EOFS) by the VSM controlled wind power plants is shown.

$$EOFS_{VSM} = \sum_{i=1}^{N_{states}} |VSM_i| \cdot p_i \tag{4.3}$$

As wind power plants are very flexible in the utilized controls, other frequency services can also be provided. Fig. 4.9 shows a frequency control that gets activated when the frequency is below a certain threshold, providing a fixed amount of power for several seconds, followed by a recovery period. As a service, this control puts high stress on the mechanical parts of the wind power plants, which has to be compensated for by the TSO. The periods, where the service is ready, but not actually used should nevertheless be evaluated as the payment in modern power systems also depends on the service availability and the service usage. This is also currently the case for the primary reserve.

All these service demands are to be evaluated by the system operator and to be incorporated into the system frequency reliability analysis. System operators are going to order these services only during weak power system states, where the wind power plants can improve the frequency behavior sig-

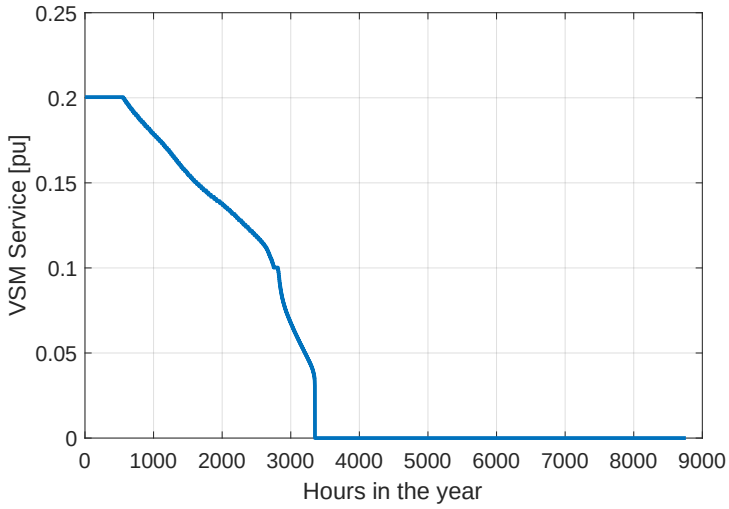


**Fig. 4.8:** Ordered VSM-service in the IEEE RTS with 1 GW wind power when the VSM-service is ordered at 30 % wind power penetration level.

nificantly. So the assessed additional frequency service has to be balanced with the improved frequency quality. Otherwise, the service is ordered without benefit for the system, only increasing the TSO's frequency control efforts. Nevertheless, it is also crucial to evaluate the dynamic efforts by wind power plants throughout the analysis, determining the positive effect on the system frequency and the amount of used service.

### 4.3.2 Incorporating additional frequency controls during contingencies

The curtailed wind power is wasted and not used during under-frequency events on a large scale. However, when wind power is curtailed in steady-state, then it is possible to increase the output power back to the maximum power point during phases of under-frequency. This is already included in several grid codes, such as in the Danish one [41].

The actual usage of wind power plants as frequency control units is determined by the dynamic contingency simulation. All kinds of frequency controls can be compared by representing the amount of wind energy, utilized for frequency control purposes [C3]. The system frequency is dynamically simulated, and the frequency controls inside the wind power plants get activated or not, dependent on the settings and the actual grid contingency.

Therefore, these service usages depend not only on the system state and its probability but also on the evaluated contingency $j$ and its probability $p_j$.

The expected delivered frequency service (EDFS) due to this converter-based frequency control power can be calculated with the additional frequency service power delivered during the contingency.

$$EDFS = \sum_{i=1}^{N_i} \sum_{j=1}^{N_j} ServiceEnergy_{i,j} \cdot p_i \cdot p_j \tag{4.4}$$

The used wind power for frequency control purposes can therefore be used to determine how often the service is actually demanded. Fig. 4.9 shows a generator outage in the power grid, which causes an under-frequency event. The frequency control in the wind power plant is triggered to give active power support for a short period, followed by a long recovery period.

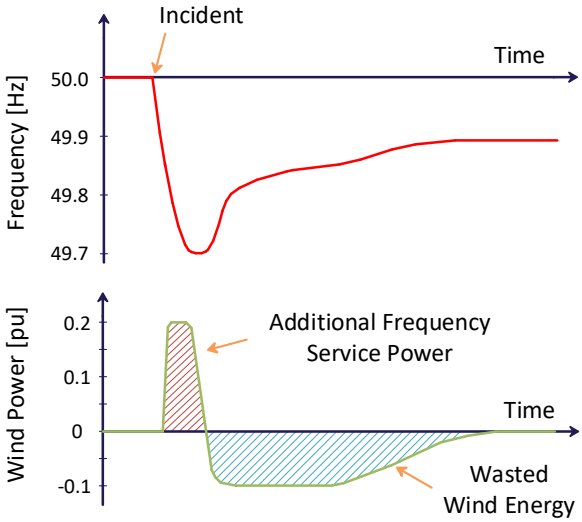


**Fig. 4.9:** Triggered frequency control due to under-frequency with a recovery phase in wind power plants.

The used additional energy provided by the wind power plant per year is an indication of how often the service is activated. Nevertheless, it is also dependent on how often the additional wind power is available for the service during these under-frequency events. The yearly additional frequency service energy usage is also dependent on the TSOs frequency management, as the additional power during the operation demands an agreement between TSO and wind power plant operator. The wind power wasted during the recovery phase should be measured in a similar way, as it indicates the dynamic efforts of the wind power plants to balance the benefits and drawbacks of certain frequency controls. The same dynamic index assessment has to be done when other frequency controls are used.

With these reliability indices, it is now possible to assess the effect of additional frequency controls in the power system. It has to be ensured that system operators can test many different frequency managements to compare them. System operators can affect the employed frequency controls in many different ways. An accurate and fast reliability assessment is essential to find the proper frequency control strategy for their specific power grid needs.

## 4.4 Ensuring an accurate frequency reliability assessment

The power system frequency reliability assessment has to incorporate the different system states that occur during the operation of the power grid. For this, the system model has to be accurate enough to represent the system data. These states are the different amounts of demanded active power from the loads in the system and, in the case of wind-integrated power systems, the supply of active power from the wind power plants. The system loads are represented with the LDC. Wind-integrated systems can use the distribution of wind speed and wind turbine parameters to calculate the WPC, as discussed before.

The reliability assessment has to be accurate with and without wind power integration. However, it is essential to determine if the computational efforts have to increase severely with this additional power grid equipment. In modern power grids using frequency controls performed by the converter-based units has to be determined, whether the details in the system modeling has to increase, to estimate the system reliability indices correctly. It is clear that frequency controls change the grid performance, but its impact on the accuracy of the calculated reliability indices needs to be verified.

Evaluating all hours of the system operation with all possible contingencies means an immense computational burden. Therefore, the reliability assessment is limited by the amounts of incorporated simulations. Deterministic reliability assessment uses a fixed number of load and wind power conditions for the system state. Monte-Carlo simulations set a fixed total number of simulations and assigning the load, wind, and contingencies in a random manner, but considering their likelihoods. With a high enough number of simulations, the results of this method tend to settle around the correct assessment value with a certain accuracy.

### 4.4.1 Error in system representation

The number of simulations to correctly estimate the indices has to be chosen carefully. With a deterministic reliability assessment, one can directly influence the system representation's accuracy going into the system modeling.

The two main input data that are evaluated are the LDC's and WPC's detail, going into the assessment.

The main issue is the over- and under-estimation of different system states, which influences the final reliability indices. Fig. 4.10 shows the LDC from the IEEE reliability test system (IEEE RTS). In this figure, five discrete steps are going into the reliability assessment. Fig. 4.11 shows the same LDC, but with ten discrete steps used to represent the power system load. This increases the details going into the reliability assessment but doubling the computational efforts. It can be seen that the number of discrete steps has a significant influence on the details in the system representation and, therefore, on the correct estimation of the system performance.

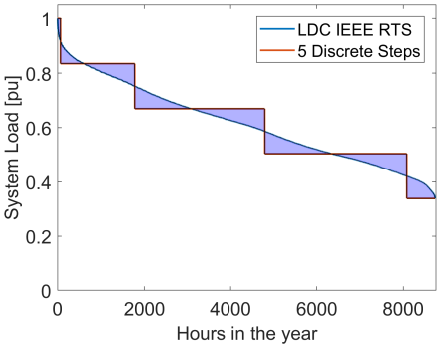


**Fig. 4.10:** Five discrete steps used to model the IEEE RTS load.

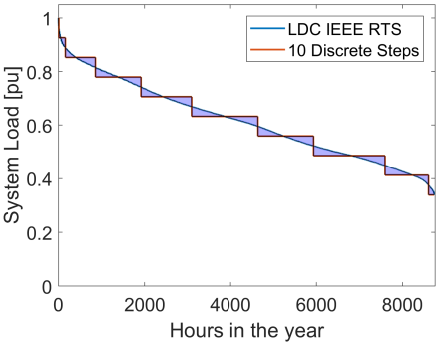


**Fig. 4.11:** Ten discrete steps used to model the IEEE RTS load.

The error between the actual LDC and the considered states can be calculated for all 8760 hours in one year as:

$$Error_{LDC} = \frac{\sum_{i=1}^{8760} |LDC_i - LDC_{discrete\,i}|}{\sum_{i=1}^{8760} LDC_i} \tag{4.5}$$

In Fig. 4.10 and Fig. 4.11, the steps are split up with even steps in the system load. Other strategies, such as the separation into constant probabilities, can be realized as well. The load values and probabilities have to be chosen so that the total system load consumed in one year is the same as described in the LDC. Otherwise, the total system load during the year is changed, and the system behavior is not evaluated correctly. The usage of different discrete step numbers has a severe influence on $Error_{LDC}$, as it can be seen in Fig. 4.12.

It has to be determined if the value of $Error_{LDC}$ can be used to determine the accuracy of the reliability assessment. If this is true, then the system operators can very fast define the number of required discrete steps without the need for performing an unnecessarily high number of simulations.

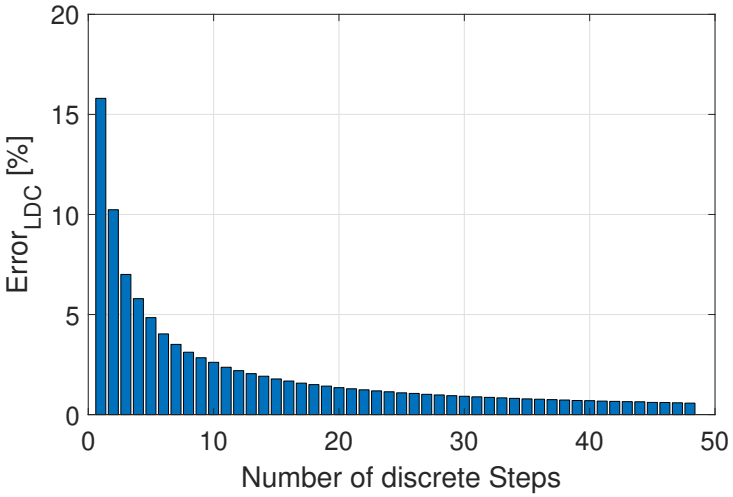


**Fig. 4.12:** Error in LDC with different numbers of discrete load steps.

The same considerations have to be done with the other system data, as the WPC in the wind integrated power systems. Here, $Error_{WPC}$ is utilized to estimate the influence of wind power modeling details on the accuracy of the assessment.

$$Error_{WPC} = \frac{\sum_{i=1}^{8760} |WPC_i - WPC_{discrete\,i}|}{\sum_{i=1}^{8760} WPC_i} \tag{4.6}$$

The total system error in the system representation is taken as the summation of both the LDC and the WPC representation error.

$$Error_{System} = Error_{LDC} + Error_{WPC} \tag{4.7}$$

It has to be evaluated on how to utilize $Error_{System}$ to guarantee the accuracy of the frequency reliability assessment. This error value can be calculated without the dynamic system simulation but only with the LDC and the WPC. So it is helpful to use it for the verification of the assessment whenever the WPC and LDC change, for example, due to changes in the frequency management, as shown in Fig. 4.7, or when the LDC changes over many years due to grid customer changes.

### 4.4.2 Accuracy of power system frequency reliability assessment

To determine the accuracy of the reliability assessment outcome, one has to evaluate the index values achieved with a certain number of load steps $L$ and

**Table 4.3:** ENAF values achieved with different numbers of simulation steps in the IEEE RTS.

| ENAF | Number of Load Steps $L$ | Accuracy [%] |
|---|---|---|
| 56.23 | 5 | 84.55 |
| 56.01 | 10 | 93.13 |
| 55.88 | 15 | 96.25 |
| 55.83 | 20 | 98.93 |
| 55.82 | 25 | 99.25 |
| 55.83 | 30 | 99.97 |
| 55.79 | 40 | 99.99 |
| 55.81 | 50 | 100 |

wind steps $W$. The index values are compared with the accurate solution, $Index_{ref}$, which is estimated using a very high number of wind and load steps. Then, the index values do not change anymore, even if the discrete steps are further increased, as shown in an example for ENAF in Table 4.3. The accuracy of reliability indices is calculated by the estimated index values assessed with a very high number of simulated system states as described by:

$$Acc_{Index_{L,W}} = 100\,\% - abs\left(\frac{Index_{L,W} - Index_{ref}}{Index_{ref}}\right) \tag{4.8}$$

This allows estimating whether the number of simulations is too low, and the accuracy of the reliability assessment is severely affected. The total error in the system representation can be assessed before the dynamic simulation. Therefore, it can be used before the time-consuming assessment step to evaluate if the expected system indices are within a certain accuracy.

An example is the values for ENAF from the IEEE RTS taken with 1 GW of installed wind power without frequency control. The number of wind power steps is constant at 50 in these assessments. The number of load steps is varied in Table 4.3. The reference value is determined with 50 wind and 50 load steps in this evaluation [J1].

The results from Table 4.3 show that ENAF, with the increasing number of load steps, is getting closer to the reference value. Above 20 load steps, ENAF does not change significantly anymore. A higher number of load steps in the reliability assessment is not improving the accuracy anymore.

The same assessment is done with all other reliability indices from Table 4.1 and Table 4.2 to determine how $L$ and $W$ influence the total reliability assessment. Certain indices may be more sensitive to the number of simulations than ENAF. When utilizing frequency controls in wind power plants,

this evaluation must include the indices describing the used control effort from Section 4.3.

For this, the reliability of a wind power integrated power system has been assessed with different numbers of discrete loads and wind power steps [J1]. The values for $Index_{ref}$ are assessed with 50 wind and load steps each. Higher numbers have been evaluated as well. However, the index values did not change anymore in the evaluated study case, when a further increase in the number of states is used.

The accuracy achieved with the different step numbers from all indices is combined to assess the total assessment accuracy. Fig. 4.13 shows the average accuracy of all assessed reliability indices. It can be seen that an average index accuracy of more than 95% can easily be achieved, even with a low number of evaluated system states. To guarantee that all indices are assessed correctly, all assessed indices' minimum accuracy, shown in Fig. 4.14, are used to evaluate the total accuracy of the reliability assessment.

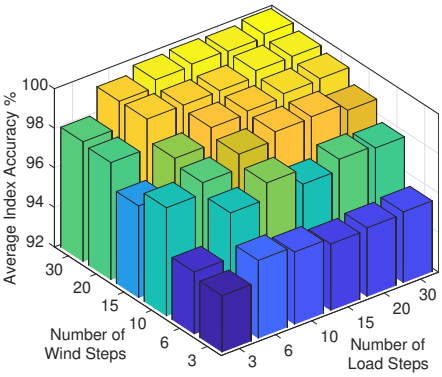


**Fig. 4.13:** Average accuracy of the reliability assessment with different steps of wind and load steps without frequency controls in the wind power plants [J1].

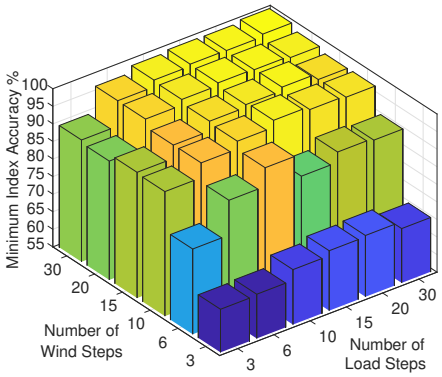


**Fig. 4.14:** Minimum accuracy of the reliability assessment with different steps of wind and load steps without frequency controls in the wind power plants [J1].

It can be determined with this method which number of considered system states leads to high accuracy. System operators can choose a threshold for the accepted level of accuracy required for the reliability assessment. With this, the balance between simulation details and simulation efforts can be found.

### 4.4.3 Influence of the system representation on the assessment accuracy

The next step is to determine if there is a direct correlation between the accuracy of the reliability assessment and the $Error_{System}$ used to make the assess-

**Table 4.4:** $Error_{System}$ [%] for different numbers of discrete Steps. Red: Accuracy is not sufficient. Green: Accuracy is sufficient.

| Wind Steps \ Load Steps | 3 | 6 | 10 | 15 | 20 | 30 |
|---|---|---|---|---|---|---|
| 3 | 17.03 | 13.03 | 10.95 | 9.75 | 9.11 | 8.45 |
| 6 | 14.06 | 10.03 | 7.98 | 6.78 | 6.14 | 5.47 |
| 10 | 12.64 | 8.64 | 6.56 | 5.36 | 4.72 | 4.06 |
| 15 | 11.81 | 7.81 | 5.73 | 4.53 | 3.89 | 3.22 |
| 20 | 11.38 | 7.37 | 5.29 | 4.09 | 3.45 | 2.79 |
| 30 | 10.95 | 6.94 | 4.86 | 3.66 | 3.02 | 2.36 |

ment. This would be helpful, as the error in the system representation can be assessed without dynamic system simulation, but only with a comparison of system LDC and WPC and the utilized discrete system states. Therefore, it is fast to calculate and changes in the load or wind behavior can be evaluated quickly.

Table 4.4 shows $Error_{System}$ with different numbers of discrete system states in the IEEE RTS system, as shown in Fig. 4.1, with Wind Farm 1 in operation, meaning 600 MW wind power plants are installed in the grid. The color in Table 4.4 indicates the accuracy of the reliability assessment outcome. When the reliability assessment is within the specified accuracy of 95%, it is marked green. When the assessment is not accurate enough, the cells are marked red. The minimum accuracy (as given in (4.8)) for all indices is used.

Table 4.4 shows that a sufficient low $Error_{System}$ can be used as a criterion for determining the reliability assessment accuracy. Nevertheless, the obtained results show only one specific case for one system frequency management with a defined system behavior. The minimum number of required system states in the assessment can be found with ten load steps and ten wind steps, so with a total of one hundred evaluated system states. The $Error_{System}$ value is, in this case, 6.56 %, and every further increase in load steps or wind steps will lead to a more accurate assessment with an even lower $Error_{System}$. The accurate reliability can also be obtained with six load steps and twenty wind power steps in the performed analysis. However, this leads to a higher number of simulations and a higher remaining value for $Error_{System}$, so this option provides no advantages.

It has to be determined if the relationship is the same when there are severe changes in the power system, as a further increase in wind power penetration, or in frequency management changes. As wind power plants are increasingly considered for frequency controls in the power system, is their effect further discussed in this work.

**Table 4.5:** Frequency reliability accuracy dependency on system data and installed wind power [J1].

| | Wind Power [MW] | Number of System States | $Error_{System}$ [%] |
|---|---|---|---|
| System Data 1 | 600 | 80 | 7.88 |
| | 1200 | 70 | 7.13 |
| | 1800 | 84 | 6.62 |
| System Data 2 | 600 | 140 | 8.28 |
| | 1200 | 88 | 9.44 |
| | 1800 | 130 | 8.37 |

### 4.4.4 Influence of LDC and WPC on the assessment accuracy

As a first step are the influences of different LDCs and WPCs discussed, as their characteristics are highly influencing the actual system states in the assessment and the outcome of the reliability assessment. Moreover, the increasing number of wind power plants is assessed, as it does influence the system behavior by reducing the required number of conventional generation units.

Table 4.5 shows the results from [J1]. Different load and wind distributions were implemented into the IEEE RTS to determine the correlation between accuracy and the $Error_{System}$, as a measure for the accurate system representation.

It can be seen that the amount of installed wind power affects the accuracy of the reliability assessment. Nevertheless, the influence is minor compared to the LDC and WPC changes, represented by the change from System Data 1 to System Data 2. The number of simulations required for the same accuracy increases significantly. $Error_{System}$, on the other hand, can be seen as being relatively constant. This concludes that a low value of $Error_{System}$ can be used to assess if the assessment outcome is being accurate. The influence of additional frequency services in the wind power plants is addressed in Section 4.4.5.

### 4.4.5 Influence of frequency controls on the assessment accuracy

The influence of frequency management changes on the reliability assessment accuracy is challenging to address. Different decision-makings at different states of the power grid, the change of demanded frequency services during operation, and the set-point changes all cause non-linearities in the reliability assessment. Nevertheless, the evaluation can be done for several critical changes, in order to understand the possible variations of accuracy caused

**Table 4.6:** Accuracy dependence on used frequency controls in wind power plants.

| | Wind Power [MW] | Number of System States | $Error_{System}$ [%] |
|---|---|---|---|
| No Control | 600 | 80 | 7.88 |
| | 1200 | 70 | 7.13 |
| | 1800 | 84 | 6.62 |
| With Control | 600 | 91 | 7.51 |
| | 1200 | 88 | 7.59 |
| | 1800 | 112 | 6.5 |

by this kind of grid operation changes.

The accuracy with different frequency controls and different levels of wind power penetration is evaluated [J1]. The used frequency control scheme is shown in Fig. 1.15 and is based on the Danish grid code. A wind power curtailment of 0.2 pu is used in this study.

The results in Table 4.6 show that the accuracy varies slightly with changes in frequency management. This means that one can determine the accuracy for some critical system conditions, by evaluating the relationship between accuracy and $Error_{System}$. Afterward, a slightly higher number of discrete system states can be found, which allows extending the accuracy above the desired value.

The required amount of evaluated system states and $Error_{System}$ have been shown to vary only slightly in the analysis. The impact of frequency controls on system reliability does, therefore, not influence the accuracy of the assessment. A high enough number of evaluated wind and load states is guaranteeing that the reliability assessment can be used to compare different frequency management methods.

The variations in the required value for $Error_{System}$ mean that there are still small variations for different frequency managements. Low assessment accuracy can be avoided with a slightly higher number of steps for the wind and load characteristics than the minimum system state numbers assessed by the proposed methodology.

In the used IEEE RTS with the load data given in [87], the required $Error_{System}$ for guaranteeing a correct frequency reliability assessment can be found to be at 7.2 % on average. The variation reaches from 6.5 % to 7.88 %. As the goal is to find the minimum number of evaluated system states, the used $Error_{System}$ has to be chosen carefully.

## 4.5 Conclusion

The presented methodology of assessing the wind power plant's influence on the frequency control allows the system operators to compare different frequency management strategies. There can be different control schemes, as well as different settings used in these controls. The indices describing the wind power plant's contributions to the frequency control during operation can be used to find the control options best suited for reliable control of the power system.

It is also possible to determine how many system states have to be incorporated to achieve the desired reliability assessment accuracy, which is important to reduce the computational burden while ensuring that the achieved results can be used to evaluate system reliability. $Error_{S_{System}}$ has been introduced as a quick estimation of the accuracy of the reliability assessment. This value is nearly constant for a required accuracy threshold, even when WPC and LDC change. The proposed methodology is therefore useful to plan, even years ahead, the requirements for frequency controls. This is required, as grid codes and the wind power plant controls can not change very frequently, as it can take many years to implement new control functions into equipment.

Previously, especially with using Monte-Carlo simulations, the number of simulations had to be set arbitrarily high to ensure high enough accuracy of the simulation. Now, the number of simulations can be reduced to the minimum, even when concerning a safety margin. This allows performing many frequency reliability assessments with changing frequency services by wind power plants and other converter-based units.

In a more converter-based power system, the frequency management has to go through fundamental changes. The accurate assessment is an essential part of reliable frequency management in modern power grids. The influence of new frequency controls, delivered by power electronic-based units, has to be balanced with the frequency quality improvements provided by these new services. As the number of possible frequency control schemes, their settings and the grid conditions under which they are utilized are endless, a way has to be found, that allows the system operators to compare a very high number of options. This is essential to find the best-suited usage of the frequency controls in wind power plants, but also in other converter-based units. Therefore, a method is proposed in Chapter 5, allowing TSOs to design their frequency management for improved reliability.

# Chapter 5

# Design method for improved frequency reliability

## 5.1 Background and Motivation

With the reliability indices describing the influence of wind power plants, one can determine the required frequency controls in these units, to ensure a high system frequency reliability. Chapter 4 has shown, how the accuracy of the reliability assessment can be guaranteed, allowing for a valid result, without increasing the simulation burden too high. System operators are now in the need of testing and evaluating multiple different frequency controls that can be realized in converter-based units. Different frequency management strategies can be utilized to improve the system frequency quality throughout the operation. However, every power system is different from its size, the change in load behavior, and the system operator's strategies for frequency controls.

System operators need to evaluate a large number of possibilities for the type of frequency controls, using the exact settings, and when to activate frequency services during operation. This requires multiple reliability assessments, including dynamic system simulation. For this, the number of simulations per assessment is significant, as the assessment has to be repeated often with variations in the frequency management.

The question now is, how can the system operators easily compare the different options they have for the frequency controls in wind power plants? And how can they determine the optimal solution for their grid operation?

To find the best usage of wind power plants for frequency controls, TSOs have to change the way, they utilize the flexibility that is offered by the controls in these units. The assessment has to meet the criteria in the following

to utilize the converter-based generation units in the most reliable way.

- Incorporating the effect of frequency controls in wind power plants on the entire system performance.
- Assessing a large number of frequency managements.
- Allowing an optimization process to find the best-suited solutions.

When these open issues are solved, it is possible for TSOs, to adjust the frequency control usage in wind power plants to their specific grid requirements. This allows reacting to grid changes with optimal corrective actions more easily.

## 5.2 Framework for the design for Frequency Reliability

System operators have to compare and evaluate different strategies of their remedial actions on the power system and their effects on frequency reliability. This can be achieved with a framework for the design for reliable frequency management, as shown in Fig. 5.1.

The central part is the known dynamic frequency-security assessment. The inputs to the assessment are fixed system descriptions, which do not change. On the other side are the variable additional services, that are compared with each other. The variables define an input vector of frequency managements, used in the dynamic frequency-security assessment. The evaluation of the assessed reliability indices is an essential step, that allows comparing the system reliability according to the transmission system operator's requirements and reliability goals.

### 5.2.1 Fixed System description data

Some parts of the power system data can be kept constant throughout the variation analysis in the system's frequency management. This can be actual data, such as the LDC or the WPC, or the number and type of generators in the system. The fixed system description data describes the equipment, that is connected to the power system and is not directly affected by the analyzed changes. Even if the conventional generators do not change, there can be an impact on the usage of the generation units throughout the operation. When a steady-state wind power curtailment is demanded, then the conventional generation units are utilized more to supply the system loads.

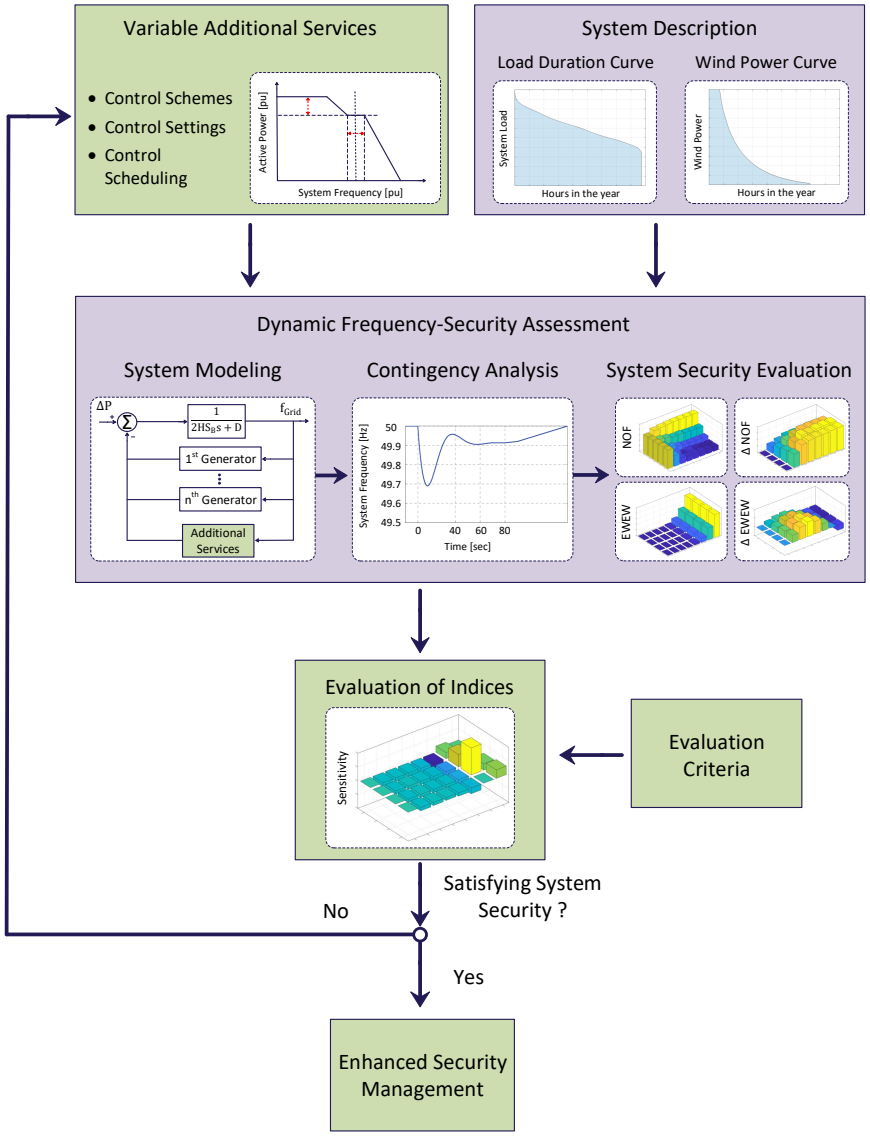


**Fig. 5.1:** Framework for the design for improved frequency reliability in power systems with wind power integration [J2].

Fixed system data can also be the number of installed wind power plants, depending on the variations used in the analysis. In these cases may the number of turbines change to see the impact of higher wind power penetrations on the frequency quality.

The fixed system inputs can also be policies used during system operation. This includes under-frequency load shedding strategies or settings for the protection of equipment in case of over- or under- frequency. Other strategies, that can be fixed, are the scheduling of conventional generation units, determining when to use which unit during which system conditions. Also, the amount and design of primary and secondary frequency controls can be kept constant. Still, the usage during operation is affected by the frequency management changes.

However, to compare different strategies, variable frequency managements are defined, and their influences on the system reliability are assessed.

### 5.2.2 Variations of frequency services

The system operator defines the variations at the beginning of the design process. Different frequency managements can be used for the assessment of their performance. The variations can include a wide variety of system operational decisions, as system operators can intervene during operation with different remedial actions, depending on the current system state.

The variations in the wind power plant usage for frequency controls include:

- Different frequency control schemes
- Different settings in these frequency controls
- Scheduling the activation of frequency controls

With this, the variations in the frequency controls can be realized with a very high degree of freedom for the system operator. All defined variations are evaluated in the dynamic frequency-security assessment, and the reliability indices are calculated. The dynamic simulation has to respect the system operator's decisions that are executed in the steady-state at simulation start to change the dynamic behavior of the connected wind power plants.

As an example, the influence of two different scheduling scheme for the usage of frequency control services provided by wind power plants is discussed in [J3]. The system operator's decision-making when to activate a VSM-based service is assessed. For this, different criteria for service activation are used. Once, the activation is based on the total system inertia in the power system, activating the service during weak grid conditions with the total system inertia being below different thresholds. Another scheduling

strategy uses the converter-based penetration, as this potentially leads to a service-activation when the wind power plants can contribute the most.

The evaluated variations are not restricted to renewable or converter-based units. Conventional generation units can also be changed in their participation in the system frequency control. It can be assessed, for example, how much primary controls can be replaced by wind power plants with frequency supporting functions. This is required in the further share of converter-based units into the power system required for the transition into a fully renewable-based system. The variations can be seen as an input vector going into the assessment procedure.

### 5.2.3 Evaluation

The evaluation procedure is important in order to decide which evaluated frequency management is the most reliable one. The evaluation method compares the reliability indices, that are calculated in the previous step with the requirements from the transmission system operators. These requirements

The evaluation takes as input all the indices from the dynamic system simulation. Simple evaluation strategies only compare a reduced number of indices with each other, such as the benefit of reduced load curtailment with the additionally ordered frequency service, like described in Section 4.3.2. More advanced evaluation methods include more indices, to see the frequency management's impact on the system operation as a whole. This requires much more consideration but allows to operate the system in the most reliable way.

#### Assessing a reduced number of indices

With wind power plants' usage for frequency controls, the main drawback is the non-injected wind power during operation when available. This potential energy is not sold to supply the system loads and is to be compensated by the transmission system operator and, finally paid by all consumers in the power grid. The benefit of the additional frequency controls is reducing the number and duration of abnormal frequency events and preventing system loads from being curtailed.

System operators can compare the effect of their tested frequency managements by the change in the index value. This is done in the study case shown in [J2]. For this, one reference system state is chosen, used as a benchmark for the system's operational frequency reliability. The effect of the variation in frequency controls can be expressed with the change in the selected index values.

$$\Delta Index = Index - Index_{ref} \tag{5.1}$$

The change in index value allows comparing the change in system behavior, caused by the additional frequency controls. The comparison of different indices will, in some cases, be challenging, as the indices describe different characteristics. As an example, the number of abnormal frequency occurrences and the wasted wind energy can be compared to evaluated the impact of frequency controls in wind power plants. These two indices are important to quantify the reliable operation of the system but describe entirely different behaviors in the power system. Therefore, the indices can be calculated relative to their reference value.

$$\Delta Index_{rel} = \frac{Index - Index_{ref}}{Index_{ref}} \tag{5.2}$$

The relative index change allows to compare the influence of frequency managements. However, this is not applicable for certain indices, such as the usage of frequency controls, where the index value is zero in the reference case, as described in Section 4.3. In such cases, purely the change in system index can be used for comparison. Sensitivity analysis allows further tuning, for example, control settings for the most efficient ratio between frequency quality improvements to the usage of frequency controls. This can be seen as the sensitivity of one index to another.

$$Sensitivity_{Index_1, Index_2} = \frac{\Delta Index_{1\,rel}}{\Delta Index_{2\,rel}} \tag{5.3}$$

This methodology can be used when system operators only aim to compare two index values, e.g., the increase in EWEW with the improved underfrequency quality, as done in [J2]. There, a Droop-based frequency control scheme originating from the Danish grid code is utilized [41]. The amount of curtailed wind power in steady-state is varied and the system reliability is compared.

$$Sensitivity_{NUF,EWEW} = \frac{\Delta NUF_{rel}}{\Delta EWEW_{rel}} \tag{5.4}$$

Fig. 5.2 shows the absolute value of the number of abnormal frequency occurrences in the evaluated case study in the IEEE RTS. This is influenced by the set value of wind power curtailment in steady-state. The total amount of wind power, wasted during operation is shown in Fig. 5.3.

The absolute values change with the amount of installed wind power plants in the system and with the decision of the system operator to change the amount of curtailed wind power. The change due to the frequency management variation is calculated according to (5.1), the results are shown in Fig. 5.4 and Fig. 5.5.

The ratio between the increased efforts and the improvements in frequency quality can be determined to find the most effective usage of the

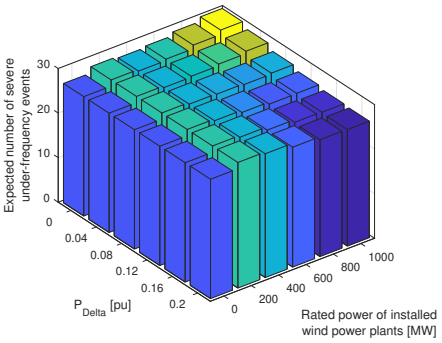


**Fig. 5.2:** Number of abnormal frequency states per year, changing with variations in the frequency control setting in the wind power plants [J2].

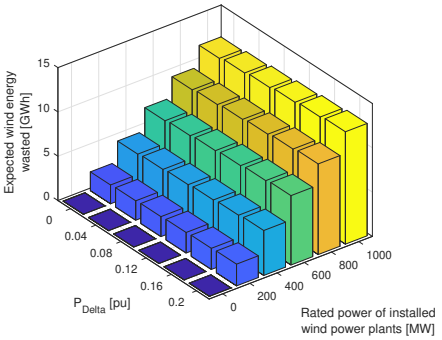


**Fig. 5.3:** Wind energy wasted per year, changing with variations in the frequency control setting in the wind power plants [J2].

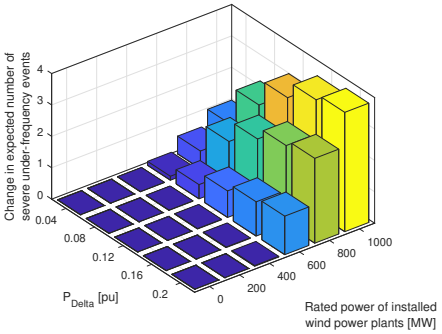


**Fig. 5.4:** Change in the number of abnormal frequency states per year, dependent on the variations in the frequency control setting in the wind power plants [J2].

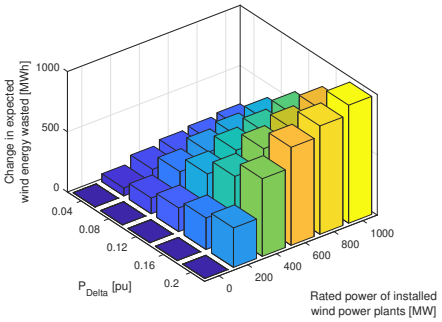


**Fig. 5.5:** Change in EWEW, dependent on the variations in the frequency control setting in the wind power plants [J2].

frequency control in the wind power plant. This is then the sensitivity of NUF to EWEW, allowing power system operators to decide on the best ratio of frequency quality improvement to the least amount of frequency control effort. The sensitivity is then used as a toll to find the most reliable operation of the grid with wind power contributing to frequency control.

Analyzing this sensitivity can help the system operators to determine the impact of different frequency controls on the system's reliability. However, this is limited to two indices that are compared to each other. When deciding for frequency control, based on the sensitivity of two indices, the other indices are ignored and do not contribute to the decision.

Another benefit of the additional frequency services can be that conventional frequency controls are used less when the frequency control is replaced

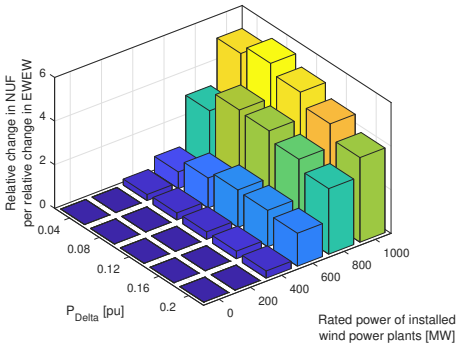


**Fig. 5.6:** Sensitivity of NUF to EWEW for different numbers of wind power plants and changed frequency control settings [J2].

by the frequency controls in wind power plants. This is clearly dependent on frequency management strategy. The shown example is limited to only consider a reduced number of indices to the system operator's decision. This ignores the other, maybe significant, effects of reliability changes on the evaluation.

### Assessing a large number of indices

The consideration of many indices allows studying the impact of the frequency management changes on the system operation as a whole. However, this requires looking at a list of parameters for each variation and to compare the differences in system performance. In [C3] is the impact of two different frequency controls compared and the reliability indices compared. One frequency control is Droop-based, so the active power change is proportional to the frequency deviation. The other one is emulating inertia, aiming to reduce the rate of change of the frequency. Both frequency controls aim to improve frequency quality, reducing the number and duration of abnormal frequency states, as well as reduce the total amount of curtailed system load due to UFLS. The reliability indices describe the system performance, as described in Section 4.3 with the IENS and ECU being used combined energies for primary and secondary frequency controls in the study case. The total wasted wind energy is the combined wasted wind energy in steady-state and due to the frequency control during contingencies.

The calculated system reliability indices in the used study case are shown in Table 5.1 for the Droop-based frequency control and in Table 5.2 for the frequency control using an inertia-based control scheme.

The variations do not only include the two control schemes, but also two different settings for each control scheme in order to see their impact on the system reliability.

**Table 5.1:** Reliability indices using Droop-based frequency control [C3].

| Parameter | No Wind | Wind Included | Droop 1 | Droop 2 |
|---|---|---|---|---|
| NOF | 5.84 | 6.44 | 5.86 | 5.73 |
| NUF | 80.1 | 82.24 | 81.34 | 79.5 |
| ENAF | 85.94 | 88.69 | 87.2 | 85.23 |
| OFD | 0.543 | 0.885 | 0.55 | 0.54 |
| UFD | 17.95 | 19.98 | 18.7 | 18.62 |
| EAFD | 18.49 | 20.83 | 19.25 | 19.16 |
| ENS | 348.6 | 370.2 | 347.97 | 339.1 |
| EWEW | 0 | 0.0766 | 0.0488 | 0.061 |
| EWES | 0 | 0 | 0.0623 | 0.0851 |
| IENS | 150.2 | 145.2 | 148.14 | 148.6 |
| ECU | 9.2 | 10.11 | 9.63 | 9.55 |

A large number of indices makes it difficult to determine, which evaluated frequency management is the most optimal one for the evaluated power system. Transmission system operators have to describe their aims for the different indices to evaluate the balance between frequency control effort and the risk of the system being in an abnormal state.

Another approach is to find the minimum of a total reliability function, that combines all indices, as shown in Fig. 1.18. The balance, in this case, can be found when a 'cost'-function is used to give each index a comparable value. The 'costs' for frequency quality and for frequency controls are then all added up. The global minimum is seen as being the most reliable frequency management. However, it has to be considered, that the indices that are evaluated and compared might be very different in nature. It is not easily possible to combine the number of abnormal frequency occurrences per year with the duration of these events, and also with the total amount of load not being supplied. From these three indices, only the energy not being supplied to system loads can be directly translated into costs, as under-frequency load shedding requires a payment to the customers for the energy not being supplied.

A method, that allows TSOs to combine multiple indices is shown in Section 5.3, where TSOs can combine different indices dependent on their relative change due to a frequency management variation [J3]. This can help to easily assess a larger number of frequency managements.

**Table 5.2:** Reliability indices using inertia-emulating frequency control [C3].

| Parameter | No Wind | Wind Included | Inertia 1 | Inertia 2 |
|---|---|---|---|---|
| ENOF | 5.84 | 6.44 | 5.86 | 5.62 |
| ENUF | 80.1 | 82.24 | 79.4 | 78.4 |
| ENAF | 85.94 | 88.69 | 85.26 | 84.02 |
| EOFD | 0.543 | 0.885 | 0.588 | 0.535 |
| EUFD | 17.95 | 19.98 | 18.46 | 18.2 |
| EAFD | 18.49 | 20.83 | 19.04 | 18.735 |
| EENS | 348.6 | 370.2 | 337.8 | 326.4 |
| EWEW | 0 | 0.0766 | 0.035 | 0.0398 |
| EWES | 0 | 0 | 0.12 | 0.153 |
| IENS | 150.2 | 145.2 | 149.6 | 149.7 |
| ECU | 9.2 | 10.11 | 9.63 | 9.62 |

### 5.2.4 Feedback for further improvement

After the evaluation of the system reliability, the system operator has to decide if the achieved operational frequency reliability matches the grid requirements or not. If not, then further changes to the frequency management are required. This can mean that other control strategies or scheduling strategies need to be implemented and tested.

The feedback can also be utilized to optimize the settings in frequency management, such as thresholds for activation or the settings inside the control schemes. With this, an optimization of the frequency management can be done, that narrows down from larger to smaller steps between the different iterations.

Fig. 5.7 shows an example of the possible optimization for the most reliable activation of VSM-based frequency services. It shows two rounds of iterations, where the system non-synchronous penetration value is taken to decide the frequency service's activation. In the first round, the evaluated threshold settings for the activation are chosen with a relatively wide distance between each other. When the outcome is not sufficient to the operator's reliability requirements, then the used threshold values are narrowed down around the current best solution. This defines the next round of iteration until the solution is sufficient. If the evaluated strategy does not find a suitable solution, then the system operator must repeat the process with a different frequency management setting.

This optimization process can be further improved by different optimization techniques. For example, improving the interpolation between the already tested variations for further narrowing down the values for the follow-

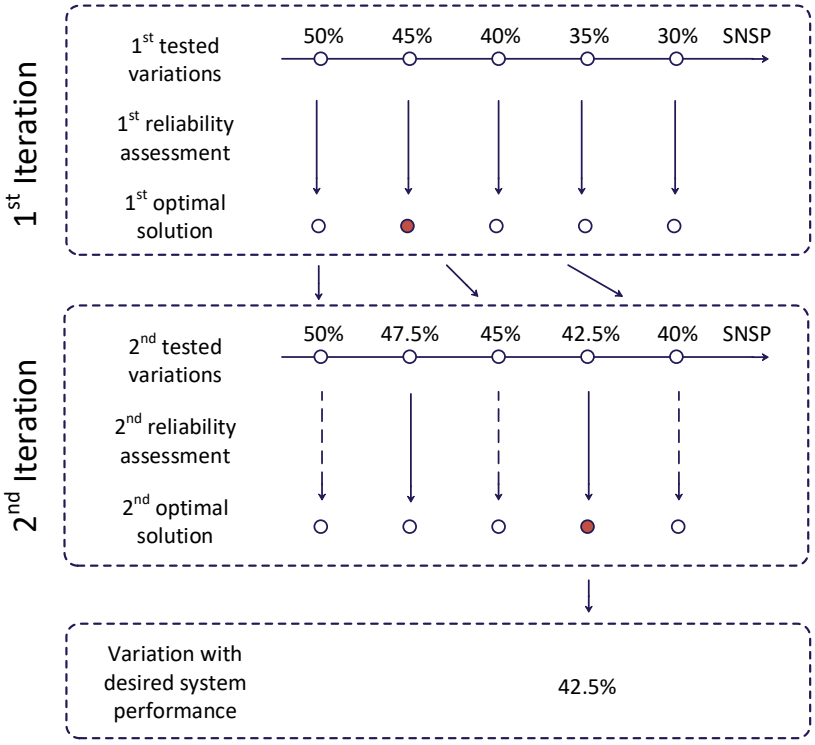


**Fig. 5.7:** Optimizing the frequency management to find the best setting for service activation.

ing iteration.

The same kind of optimization can be done with the settings inside the controls in parallel. With the VSM-based service, one can change the emulated time constant and the threshold to activate the service in parallel. This allows finding the global optimum usage of the frequency service during operation. The variation is then not only a vector of results, but it can be a two, or even a multi-dimensional matrix of solutions.

In order to evaluate this high number of system reliability results, a method is proposed, that allows to include all assessed reliability indices in a fast way.

## 5.3 Fuzzy-based reliability evaluation

As described in Section 5.2.3, an evaluation of all calculated reliability indices is required, when the system operator wants to guarantee the most reliable operation of the power grid.

A multi-index evaluation method that allows for customization to include specific TSO requirements is needed. One method to do this is presented in

[J3]. Fuzzy logic is used to combine all assessed indices into only two values, making the comparison more practical. These two values are the system Risk of not operating in a reliable way, and the Effort of the frequency controls. Fuzzy-logic is introduced to emulate language-based decision-making [92, 93]. It is already used for the reliability assessment procedure, describing the probability of the system states to reduce the simulation burden during the assessment [94–97]. The fuzzy-sets are thereby used to represent the system states' probability, such as load distribution. In some works [94–96], this is directly going into the assessment method; in others, the fuzzy-logic is utilized together with Monte-Carlo simulation to incorporate uncertainties in the system description [97].

However, until now, it is not utilized to evaluate the power system frequency reliability. Two values are calculated in [J3] to assess how the system reliability changes with additional frequency controls in wind power plants. The overall scheme for the proposed evaluation method is shown in Fig. 5.8.

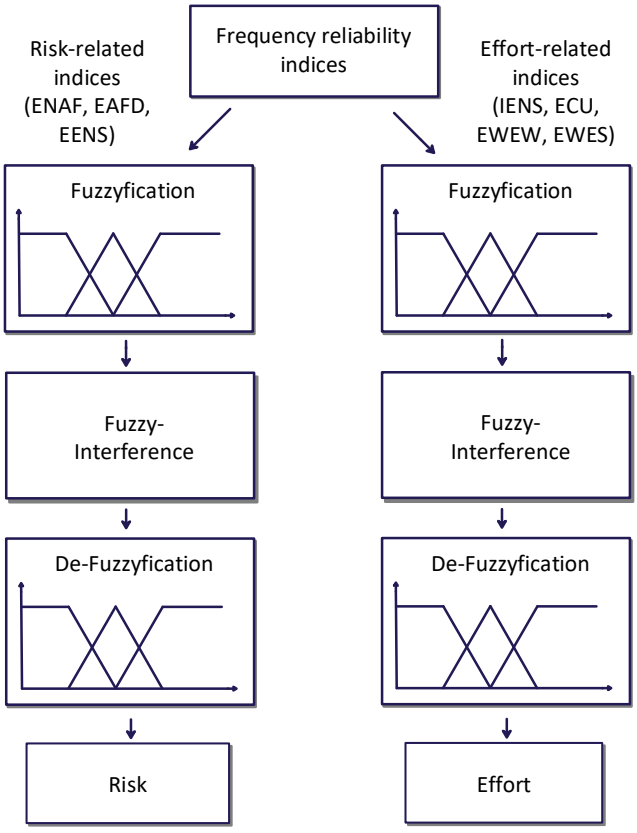


**Fig. 5.8:** Fuzzy-based evaluation method of system reliability [J3].

The indices are split up into two different categories. One describes the system frequency quality, including ENAF, EAFD, and the amount of load curtailment EENS. These indices describe the Risk of the system failing. Higher Risk indicates that the system performance decreases and the number and duration of abnormal states increases. Reduced Risk means that additional frequency controls benefit the system and abnormal or emergency states can be avoided.

The Effort calculated with the proposed methodology describes the number of used frequency reserves. This includes the curtailment of wind power in steady-state to maintain minimum system inertia and the actively used wind power during contingencies. The conventional frequency controls are included in the system Effort as well. This enables a fuzzy-based evaluation to describe more complicated changes to the system frequency reliability. It can easily be used to determine, which amount of conventional frequency controls could be replaced by wind power plants without negatively affecting the frequency quality.

The presented evaluation method is separated into three steps; fuzzification, interference, and defuzzification [92].

### 5.3.1 Fuzzification

The calculated reliability indices are fuzzified as the first step. The index values are assigned to certain fuzzy sets with a share dependent on their values. This is also referred to as the membership to a certain set. The index value compared to a reference scenario is evaluated to determine increasing or decreasing index values with variations in frequency management, as described in Section 5.2.3.

The three used fuzzy sets are 'Low', 'Normal', and 'High'. They are assigned for all calculated reliability indices separately. Fig. 5.9 shows the assignment of an index with a relative value of 93.33 %, meaning the currently evaluated frequency management variation has reduced the index value by 6.67 %. The index is, in this case, assigned by one-third to 'Normal' and two-thirds to 'Low', meaning the index value has decreased compared to the reference system assessment.

The shape and the number of sets can be defined by the system operator and his needs for the evaluation process, however, a linear assignment with three sets per index is fast to do in the evaluation and can be used with only minimal efforts.

An important feature of utilizing fuzzy-logic is, that the system operator can decide which indices are the most critical ones for his system. This is realized with two levels of importance or priority in [J3]. The most important indices are 'weighted' higher in the interference step to determine the evaluation outcome, so their change is taken more into account than variations of

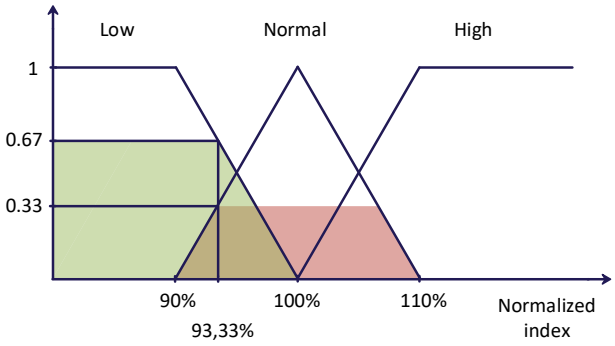


**Fig. 5.9:** Fuzzy-based evaluation of the system reliability [J3].

the lower priority indices.

In the study case, to determine the system Risk, the EENS is weighted with a higher priority than the indices ENAF and EAFD, as the loss of system loads weights higher than the frequency being in an abnormal state more often without losing any equipment. The assignment of all indices from the study case is shown in Table 5.3.

**Table 5.3:** Frequency reliability-related Indices.

| | Priority | Index |
|---|---|---|
| Risk | Reduced Priority | ENAF |
| | Reduced Priority | EAFD |
| | Increased Priority | EENS |
| Effort | Increased Priority | EVSM |
| | Increased Priority | EWEW |
| | Reduced Priority | IENS |
| | Reduced Priority | ECU |

When combining two indices, the average fuzzy membership is used. So, as an example, the membership of the Risk being 'Low' for the increased priority indices is:

$$M_{Risk,\,IncreasedPrio,\,Low} = M_{EENS,\,Low} \tag{5.5}$$

Whereas the reduced priority being influenced by the memberships of ENAF and EAFD.

$$M_{Risk,\,ReducedPrio,\,Low} = 0.5 \cdot (M_{ENAF,\,Low} + M_{EAFD,\,Low}) \tag{5.6}$$

The prioritization of indices allows the system operators to include their

requirements for a highly reliable system. This highly influences the calculations in the following step.

### 5.3.2 Interference

The interference combines the different sets and their memberships from the fuzzyfication step. The rules established in the interference matrix combine the previously assigned memberships with each other, as shown in Table 5.4. As a result, there are five sets with different memberships calculated. These five sets are named 'Very Low', 'Low', 'Normal', 'High', and 'Very High'.

**Table 5.4:** Interference matrix used to combine multiple input indices

| | | Increased Priority | | |
|---|---|---|---|---|
| | | Low | Normal | High |
| Reduced Priority | Low | Very Low | Low | High |
| | Normal | Low | Normal | High |
| | High | Low | High | Very High |

The combination is done by multiplying both the increased and reduced priority memberships to determine the outcome set membership value. As an example, the membership for 'Very Low' system Risk is determined by:

$$M_{Risk,\,VeryLow} = M_{Risk,\,ReducedPrio,\,Low} \cdot M_{Risk,\,IncreasedPrio,\,Low} \tag{5.7}$$

Or, when calculating it from the indices EENS, ENAF, and EAFD:

$$M_{Risk,\,VeryLow} = M_{EENS,\,Low} \cdot 0.5 \cdot (M_{ENAF,\,Low} + M_{EAFD,\,Low}) \tag{5.8}$$

The used combinations in Table 5.4 implement the relationship between increased and reduced priority indices. When two combinations are used to describe the system reliability, then the separate memberships are added to each other. This can be seen with the calculation of the 'Low' membership.

$$\begin{aligned} M_{Risk,\,Low} = {} & M_{Risk,\,ReducedPrio,\,Normal} \cdot M_{Risk,\,IncreasedPrio,\,Low} \\ & + M_{Risk,\,ReducedPrio,\,High} \cdot M_{Risk,\,IncreasedPrio,\,Low} \\ & + M_{Risk,\,ReducedPrio,\,High} \cdot M_{Risk,\,IncreasedPrio,\,Normal} \end{aligned} \tag{5.9}$$

The combination of the different reliability indices into the five output sets describe their relationship towards the reference system reliability. The five memberships are, in the last step, combined to one value, which allows a fast assessment. This process is done for the Risk-related indices to determine the total system Risk, and then separately for the Effort-related indices,

describing the total Effort of the system in regards to the frequency controls. The system Risk or Effort increase or decrease with the evaluated frequency management variations.

### 5.3.3 Defuzzyfication

The defuzzification is the last step in every fuzzy logic. In the proposed evaluation method, combines the defuzzyfication the different output membership functions from the interference matrix into one value, that is used as the result of the entire fuzzy logic.

The result is calculated by assigning five values to the five presented sets and then multiplying them with the respective membership functions. The set values for the study case are shown in Table 5.5.

**Table 5.5:** Values assigned to the five output sets.

| Set | Assigned Value |
|---|---|
| Very High | 5 |
| High | 2 |
| Normal | 1 |
| Low | 0.5 |
| Very Low | 0.2 |

This assignment results in an output value of one for the reference case, as then all indices are assigned 'Normal', leading to a 'Normal' output set membership of 100 %. When the indices rise in value, then the output is greater than one. This can occur, for example, when the frequency control usage rises with the more extensive usage of frequency controls in the wind power plants. In this case, is the frequency quality improved, so the Risk-related indices are decreasing, meaning the system Risk is lower than one.

The reduction to two values describing the Risk and Effort allows to easily compare different control variations, especially when many parameters evaluated for different settings. The evaluation of the study case from [J3] is described in the following, to give a guideline on how to utilize the achieved results.

### 5.3.4 Evaluation of results

The fuzzy-logic based evaluation allows for a fast comparison of different frequency management strategies. In the end, the operators have to look at the actual results. However, this method can be used to discriminate very fast between promising and ineffective frequency managements, as also shown in the study-case in [J3]. The scheduled activation of VSM-based frequency control is described. Two different scheduling strategies for determining if a

VSM-based service is required are compared. The first one is based on the remaining system inertia, so whenever the inertia in the system is below a certain threshold, is the service in the wind power plants activated. The other scheduling scheme calculates the percentage of converter-based penetration SNSP. Whenever the SNSP is above a given threshold, then the service is ordered.

**Evaluation of one reliability assessment**

One example of the reliability evaluation is given to illustrate the fuzzy-logic. The study case with VSM-control activated when the SNSP is at 50% is shown in detail in the following. The Risk-reliability indices of the reference case and of the evaluated study case with VSM-based frequency control in wind power plants are shown in Table 5.6.

**Table 5.6:** Risk-related reliability indices for the evaluation.

| Index | Reference Case | Analyzed Case |
|---|---|---|
| ENAF | 39.67 | 37.56 |
| EAFD [min] | 55.21 | 54.37 |
| EENS [GW] | 6.234 | 5.902 |

This causes the Fuzzy-membership of these indices according to the fuzzyfication described in Section 5.3.1. The memberships of these three indices to the three utilized sets are shown in Table 5.7.

**Table 5.7:** Memberships of the Risk-related reliability indices.

| Index | Low | Normal | High |
|---|---|---|---|
| ENAF | 0.5319 | 0.4681 | 0 |
| EAFD | 0.1521 | 0.8479 | 0 |
| EENS | 0.5326 | 0.4674 | 0 |

It can be seen in Table 5.7, that all indices are reduced due to the utilized VSM-based control in the wind power plants. In the next step are these indices combined with the interference matrix, shown in Section 5.3.2, resulting in five membership values for the Risk of the power system frequency.

**Table 5.8:** Fuzzyfied reliability indices

| | Very Low | Low | Normal | High | Very High |
|---|---|---|---|---|---|
| Risk | 0.1821 | 0.5103 | 0.3076 | 0 | 0 |

The five memberships from Table 5.8 are weighted as described in Section 5.3.3 to calculate the total Risk of the power system frequency reliability. The Risk is reduced due to the VSM-based control from 1 to 0.5627. This procedure is repeated for all analyzed variations to assess, which frequency management the most reliable one for the evaluated power system.

**Evaluation of multiple reliability assessment**

The results for the evaluated study case are shown in Fig. 5.10. Each point describes the evaluation result of a different threshold setting of the two used scheduling schemes. The reliability results calculated in the previous Section is marked in Fig. 5.10 with a black circle.

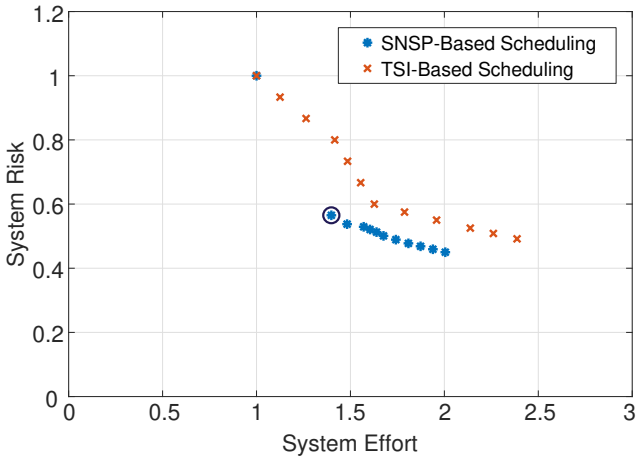


**Fig. 5.10:** Fuzzy-based reliability evaluation of SNSP and TSI-based service activation strategies [J3]. The black circle marks the result, calculated in the previous Section.

The results are obtained for various threshold settings to evaluate, which one activates the service more reliably. This means the service is demanded in cases where the grid is weak and can benefit the most. Higher reliability can also occur when the wind power plants are operated in a way, that allows them to contribute effectively during operation.

The system Risk and Effort without additional frequency control are taken as the reference system reliability, indicated with Risk and Effort values of one. The evaluated reliability with frequency control decreases the system Risk while increasing the Effort. The SNSP-based scheduling is more effective than the TSI-based one in the presented study case. The system Risk is reduced more with the SNSP-based scheduling with the same increase in Efforts. This means, that the service is demanded less often in conditions when it is not required [J3].

This kind of evaluation allows fast comparison of many different frequency management strategies, that respects all the assessed indices. Transmission system operators can then determine which strategies are fulfilling their reliability requirements.

## 5.4 Summary

In the modern power grid, which is dominated by converter-based generation, the frequency management is challenging. Converter-based units can implement various system services to assist the grid in different ways. System operators have to decide when to demand these services by the renewable power plants and when not to do. The control settings can also be adapted to the current grid needs, as communication links are already set in place. The proposed framework for the design for frequency reliability allows system operators to evaluate and compare multiple frequency managements. This allows determining the best-suited strategy for operating the power system with a strong influence of converter-based generation units to the frequency control.

The proposed fuzzy-based evaluation allows the combination of many very different reliability indices to find very fast the frequency managements which are the most beneficial for the reliable system operation. This is important, as modern power systems have to consider the influence of multiple equipment types. The reliability indices describe different operational time frames and policies, as described in Section 4.3. The exact settings and strategies still require a more in-depth consideration of all evaluated indices. However, the combination of indices with the fuzzy-logic allows identifying the frequency managements worth considering in more depth. The feedback-loop in the proposed framework in Fig. 5.1 introduces the option for optimization for frequency quality enhancements with the required effort in frequency controls.

The reliable operation of the power grid with increasing penetration of renewable sources puts the power system under severe pressure. The replacement of conventional generation units with power electronic-based ones reduces the system inertia and increases the risk of abnormal frequency variations. The design for additional frequency services from converter-based units can highly benefit the system operation. But they have to be designed carefully to balance the frequency improvement with the effort by the controls.

# Chapter 6

# Conclusion

This chapter summarizes the main results and research outcomes of the Ph.D. project *Reliable Control of Power-Electronic-based Power Systems*. Initially, a brief summary of the thesis is given, then the research contributions are highlighted. Finally, future research perspectives are discussed.

## 6.1 Summary

Increasing the penetration of renewable power generation units puts the existing operation of the power grid under high stress. The main focus of this Ph.D. is to improve the grid operation with the support of converter-based units. Voltage and frequency are two important values that define the health of the power grid. Power-electronic-based converters cause new challenges to arise, but they can also be the solution. The modern-day challenges of utilizing the flexibility these units offer regarding frequency and voltage support have been discussed in this Ph.D. thesis. The results and research outcomes of this Ph.D. project have been summarized in the form of a Ph.D. thesis based on a collection of six papers. A brief summary of the Ph.D. thesis is given in the following.

In *Chapter 1*, the main challenges related to the reliable power system operation with a high penetration of renewable generation are discussed. Transmission system operators have named the system frequency and system voltage maintenance as their most serious concern in the modern, power-electronic dominated power grid. To keep the system voltage under control, converter-based units are already contributing to the voltage controls at their point of connection. However, this arises new challenges, especially with the interaction of parallel voltage controlling units with a fast response time. The faster the voltage is controlled, the more care has to be taken to design these controls.

Additionally, the system frequency control sees severe changes. The replacement of conventional generation units causes a significant reduction in the physical inertia during high renewable penetration phases. Here, converter-based units can contribute, but this has to be managed and coordinated by the transmission system operator. The inclusion of wind power plants into frequency management is currently in progress but has to be further improved under the changing grid conditions.

The dynamic voltage control by power-electronic converters offers significant potential to increase the system voltage's stability during operation. Fault-ride-through and reactive current injection during transients are already a vital part of handling under-voltage situations. However, it is an entirely different task to reliably control the system voltage around the normal operating band during dynamic grid disturbances. This is typically assisted by FACTS units, which are often installed together with large wind power plants or at remote locations in the grid. The further integration of many of these units in one area causes the problem of coordinating their reactive powers for the reliable control of the system voltage. In *Chapter 2* of this Ph.D. thesis, the voltage controllers' adaption to a variety of parallel operations of these units is discussed. The controller interaction of the units at the same location is shown and also how to calculate the new settings to mitigate them. This guarantees constant controller dynamics and stable control of the grid voltage. The distributed installation of these units causes a reduced controller interaction, due to the impedance between the units. Nevertheless, it is essential for safe system operation to consider these states and to adapt the controller response for these cases. Therefore, this is included in the controller adaption, allowing to operate multiple units near to each other. This allows for wider usage of this kind of unit, stabilizing the system voltage at critical buses for a more reliable grid operation.

Another issue related to voltage control is the estimation of the grid strength. Units today perform a penetration test to determine the voltage deviation related to a forced reactive power change. This test is no longer viable when multiple units operate in parallel, as they interact and change the measured grid strength significantly. A control scheme is proposed in *Chapter 3* that allows improving the unit's control of the grid voltage behavior. One main advantage is, that the proposed control is no longer dependent on the grid perturbation test, as it is nowadays required to estimate the grid strength. The proposed control compares the designed and the achieved control dynamics to determine if the estimated and the real grid stiffness match. The control allows parallel operation of multiple units at different grid locations or the same bus. It incorporates the findings from *Chapter 2* and allows for fast but reliable voltage control that is required in modern power grids. The control includes different improvements to its performance, like the filtering of minor voltage disturbances, while making the control adaptation

speed independent from the initial grid voltage disturbance. This control makes it possible to install more fast voltage controlling units in one area, making all units only committing as required. This further allows for higher integration of renewables, even in remote locations.

The focus of *Chapter 4* is the assessment of the operational frequency reliability of wind-integrated power systems. Transmission system operators face new challenges with the wind power plants' usage as a vital part of the frequency management in modern power grids. During operation, the operators have to decide if their frequency reserves are sufficient or if wind power plants have to be included in the active power balancing. Wind power plants are capable of a variety of frequency services. However, their contribution has to be balanced with the increase in frequency quality throughout the operation. This is done by introducing new reliability indices that determine the amount of frequency control usage throughout the yearly operation of the wind power plant. It incorporates the impact of frequency controls during the steady-state, such as the curtailment of wind power injection, as well as the usage of frequency controls during contingencies during operation. Another important aspect is the reliability assessment design. One central question is, if the change in frequency management from a conventional to a converter-based one influences how the system has to be modeled for ensuring an accurate assessment outcome. It is discudded in *Chapter 4* how wind power integration can be incorporated with a minimum number of evaluated system states to represent the power system behavior correctly.

The methodology presented in *Chapter 4* is utilized to propose a framework that allows transmission system operators to 'Design for frequency reliability'. This framework is described in *Chapter 5*. It can be utilized to compare variations of frequency managements, including different control schemes, controller settings, and service usage scheduling. The framework evaluated these different frequency managements and allows transmission system operators to find the frequency controls best suited for their specific grid conditions and operational goals. This is emphasized with a fuzzy-based evaluation step, which utilizes the different reliability indices calculated by the assessments. System operators can implement their goals and define which indices are the most critical ones without ignoring the rest of the indices. The reliable usage of converter-based units for frequency controls changes the way the system frequency is maintained. The transition to fully-renewable power systems is only possible if all components contribute to their ability. Power electronic-based units offer system operators a, before, unknown degree of freedom in how power systems are managed. This new freedom is just at the beginning of being used in power grids today.

## 6.2 Main Contributions

The main research contributions of this Ph.D. project are summarized below.

### Understanding the interactions of fast voltage controlling units

The analysis, how different STATCOM units, or other FACTS units performing fast voltage controls, interact is studied. It is shown that it is possible with conventional PI-Controllers to allow for a reliable voltage control under a wide span of grid conditions. The evaluated system constellations are the parallel operation of similar units at one bus, which is further extended to units of different rated powers, and finally to the placement of the units distributed more widely in the power grid.

### Adapting the voltage controls to a variety of different grid conditions

A voltage control scheme is proposed to optimize the dynamic system performance to mitigate system voltage errors. The proposed control is based on a PI-controller, which is also widely used in industry today. An observer is used to compare the desired and the real voltage dynamics in the power grid to increase or reduce the estimated grid strength and it is adapting the PI-controller settings. This makes other control changes, such as fuzzy-based controls or artificial intelligence-based solutions, obsolete. The proposed control is also advantageous, as it is based on only observing the grid conditions, rather than disturbing the grid with a reactive power penetration test, which is performed in the industry today.

### Including wind power plants into the operational frequency security assessment

The inclusion of wind power plants into the frequency controls requires determining the frequency control usage of these units during operation. Therefore, new reliability indices are proposed allowing to compare different frequency management methods for their operational frequency reliability. The impacts of wind power curtailments during the normal grid operation have to be considered, but also the frequency control usage during contingencies. This allows TSOs to balance the frequency improvements with the control efforts, which are required to achieve them.

### Balancing the computational burden with the achieved accuracy of the reliability assessment

A method is proposed to evaluate the assessment process for the system frequency's operational reliability. It is shown that the number of evaluated system states determines the respected details of the system modeling. This can be used to guarantee the accuracy of the frequency reliability assessment. Also, it is discussed how additional frequency controls in wind power plants impact the system's reliability assessment design.

### Design the system for frequency security with wind power plant contribution

Utilizing the reduced computational burden and including wind power plants into the frequency reliability offers the possibility to optimally design the frequency management. This work proposes a framework that compares different frequency control schemes, scheduling strategies, and controller settings. This puts transmission system operators in a position to evaluate, which frequency control strategy is the most suitable one for their specific power system aims and conditions. A special evaluation tool is also proposed that incorporates all assessed reliability indices with the specific requirements of the transmission system operator. This is required to compare a large number of possible frequency managements to find the most reliable one for maintaining the power system frequency.

## 6.3 Research Perspectives

Despite investigating several aspects of the controls of power electronic-based units that allow a reliable system operation, there are still potential issues and challenges, which need to be addressed for the power system operation:

### Hardening the voltage controller design

The proposed voltage control adaption can find some limitations when used in real power grids. Whenever the system strength value deviates severely from the estimated one, the proposed voltage control adaption technique can be too slow. This may prevent the unit from protecting the system from initial voltage overshoots. For this case, additional safety measures should be implemented. It has also to be evaluated how the controller behaves when even faster voltage control devices are being developed. The dynamic voltage behavior may then change severely, violating the defined rules of the control.

As mentioned in *Chapter 3*, it is still an open question of how to tune much slower voltage controls, as implemented in wind power plants today. These units can not rely on the proposed solution, as the much faster FACTS units may have partially already restored the system voltage. The control can be designed slower in this case, but there are not always FACTS units installed together with wind power plants, so there are various possible grid conditions, that have to be considered.

## Further improving the operational frequency reliability assessment

This work has shown a method to reduce the simulation burden for the frequency reliability assessment. However, other methods can reduce the burden even more, when the wind and load states are modeled differently. The error in system representation can then even further be reduced without an increase in the number of simulations. This allows for a faster assessment procedure or one with higher accuracy with the same number of simulations. It should also be discussed, which grid contingencies are going into the reliability assessment, as this can also allow for a reduction in the needed simulations. This is needed, as, in modern power grids, multiple different frequency control schemes have to be tested and compared with each other in order to have a complete mapping of the system reliability.

## Evaluating different indices for frequency reliability

The used indices for frequency reliability may not be sufficient in modern power grids to determine the abnormal system states. Especially the evaluation of the RoCoF is becoming of more importance when the system inertia is further reduced with higher penetration of converter-based generation. However, evaluating the RoCoF in a probability-based assessment, as used in this work, is not used so far. With RoCoF, system operators have to decide on normal and abnormal system states. These are signs of the system being at a higher risk of failing. Also, RoCoF is a much more local phenomenon than NaDir. Areas with only a small amount of inertia see much higher values of RoCof than the rest of the power grid. Then, local violations of thresholds lead to the misbehavior of equipment in certain grid areas. To better evaluate these effects, a larger multi-bus system must be modeled and used in the reliability assessment, simulating this behavior.

# References


[1] United Nations, United Nations Framework Convention on Climate Change, "Paris Agreement," 2015. [Online]. Available: https://www.unfccc.int

[2] KEFM, Danish Ministry of Climate, Energy and Utilities, "Energy Agreement of 29 June 2018," 2018. [Online]. Available: https://en.kefm.dk

[3] BMWi, German Federal Ministry for Economic Affairs and Energy, "Second Progress Report on the Energy Transition, The Energy of the Future, Reporting Year 2017," 2019. [Online]. Available: https://www.bmwi.de

[4] A. M. Hava, T. A. Lipo, and W. L. Erdman, "Utility Interface Issues for Line Connected PWM Voltage Source Converters: A Comparative Study," in *Proc. of 1995 IEEE Applied Power Electronics Conference and Exposition - APEC'95*, vol. 1, Dallas, Texas, USA, 1995, pp. 125–132.

[5] Ł. Huchel and H. H. Zeineldin, "Planning the Coordination of Directional Overcurrent Relays for Distribution Systems Considering DG," *IEEE Transactions on Smart Grid*, vol. 7, no. 3, pp. 1642–1649, 2015.

[6] A. Yazdaninejadi, A. Hamidi, S. Golshannavaz, F. Aminifar, and S. Teimourzadeh, "Impact of Inverter-Based DERs Integration on Protection, Control, Operation, and Planning of Electrical Distribution Grids," *The Electricity Journal*, vol. 32, no. 6, pp. 43–56, 2019.

[7] S.-E. Razavi, E. Rahimi, M. S. Javadi, A. E. Nezhad, M. Lotfi, M. Shafie-khah, and J. P. Catalão, "Impact of Distributed Generation on Protection and Voltage Regulation of Distribution Systems: A Review," *Renewable and Sustainable Energy Reviews*, vol. 105, pp. 157–167, 2019.

[8] C. F. Jensen, "Harmonic Background Amplification in Long Asymmetrical High Voltage Cable Systems," *Electric Power Systems Research*, vol. 160, pp. 292 – 299, 2018.

[9] K. Lee, W. Yao, D. Carnovale, and Y. Huang, "Harmonics Performance and System Stability Evaluation between 18-Pulse and LCL Filter based Active Front end Converters under Weak Grid Condition," in *Proc. of 2017 IEEE Energy Conversion Congress and Exposition (ECCE)*. Cincinnati, USA: IEEE, 2017, pp. 2476–2483.

[10] X. Wang and F. Blaabjerg, "Harmonic Stability in Power Electronic-Based Power Systems: Concept, Modeling, and Analysis," *IEEE Transactions on Smart Grid*, vol. 10, no. 3, pp. 2858–2870, 2019.

[11] K. Creighton, M. McClure, R. Skillen, J. O'Higgins, T. McCartan, and A. Rogers, "Increased Wind Generation in Ireland and Northern Ireland and the Impact on Rate of Change of Frequency," in *Proc. of the 12th Wind Integration Workshop*, London, UK, 2013, pp. 1–6.

[12] J. Cochran, M. Miller, O. Zinaman, M. Milligan, D. Arent, B. Palmintier, M. O'Malley, S. Mueller, E. Lannoye, A. Tuohy *et al.*, "Flexibility in 21st Century Power Systems," National Renewable Energy Lab.(NREL), Golden, CO (United States), Tech. Rep., 2014.

[13] US Department of Energy, "Maintaining Reliability in the Modern Power System," 2016. [Online]. Available: https://www.energy.gov

[14] Tennet, "Migrate D1.1 Report on Systemic Issues," 2017. [Online]. Available: https://www.h2020-migrate.eu

[15] Energinet, "System Perspective 2035," 2018. [Online]. Available: https://www.energinet.dk

[16] EirGrid and SONI, "All Island TSO Facilitation of Renewables Studies," 2010. [Online]. Available: http://www.eirgridgroup.com

[17] R. Billinton and R. N. Allan, *Reliability Assessment of Large Electric Power Systems*. New York, US: Springer Science & Business Media, 2012.

[18] N. Hatziargyriou, J. Milanović, C. Rahmann, V. Ajjarapu, C. Cañizares, I. Erlich, D. Hill, I. Hiskens, I. Kamwa, B. Pal *et al.*, "Stability Definitions and Characterization of Dynamic Behavior in Systems with High Penetration of Power Electronic Interfaced Technologies," *IEEE PES Technical Report PES-TR77*, 2020.

[19] R. Billinton and T. Medicherla, "Overall Approach to the Reliability Evaluation of Composite Generation and Transmission Systems," in *IEE Proceedings C (Generation, Transmission and Distribution)*, vol. 127, no. 2. IET, 1980, pp. 72–81.

[20] R. Billinton, *Power System Reliability Evaluation*. New York, US: Taylor & Francis, 1970.

[21] W. Li *et al.*, *Reliability Assessment of Electric Power Systems using Monte Carlo Methods*. New York, US: Springer Science & Business Media, 2013.

[22] R. Billinton, M. Fotuhi-Firuzabad, and L. Bertling, "Bibliography on the Application of Probability Methods in Power System Reliability Evaluation 1996-1999," *IEEE Transactions on Power Systems*, vol. 16, no. 4, pp. 595–602, 2001.

[23] M. Čepin, "Evaluation of the Power System Reliability if a Nuclear Power Plant is replaced with Wind Power Plants," *Reliability Engineering & System Safety*, vol. 185, pp. 455 – 464, 2019.

[24] R. Yokoyama, T. Niimura, and N. Saito, "Modeling and Evaluation of Supply Reliability of Microgrids including PV and Wind Power," in *Proc. of 2008 IEEE Power and Energy Society General Meeting - Conversion and Delivery of Electrical Energy in the 21st Century*, Pittsburgh, Pennsylvania, US, July 2008, pp. 1–5.

[25] X. Wang, H. Dai, and R. J. Thomas, "Reliability Modeling of Large Wind Farms and Associateed Electric Utility Interface Systems," *IEEE Transactions on Power Apparatus and Systems*, vol. PAS-103, no. 3, pp. 569–575, March 1984.

[26] J. Wen, Y. Zheng, and F. Donghan, "A Review on Reliability Assessment for Wind Power," *Renewable and Sustainable Energy Reviews*, vol. 13, no. 9, pp. 2485 – 2494, 2009.

[27] J. Lin, L. Cheng, Y. Chang, K. Zhang, B. Shu, and G. Liu, "Reliability Based Power Systems Planning and Operation with Wind Power Integration: A Review to Models, Algorithms and Applications," *Renewable and Sustainable Energy Reviews*, vol. 31, pp. 921 – 934, 2014.

[28] S. Sulaeman, M. Benidris, and J. Mitra, "A Method to Model the Output Power of Wind Farms in Composite System Reliability Assessment," in *2014 North American Power Symposium (NAPS)*, Sep. 2014, pp. 1–6.

[29] J. Lin, L. Cheng, Y. Chang, K. Zhang, B. Shu, and G. Liu, "Reliability Based Power Systems Planning and Operation with Wind Power Integration: A Review to Models, Algorithms and Applications," *Renewable and Sustainable Energy Reviews*, vol. 31, pp. 921–934, 2014.

[30] P. Zhang, W. Li, S. Li, Y. Wang, and W. Xiao, "Reliability Assessment of Photovoltaic Power Systems: Review of Current Status and Future Perspectives," *Applied Energy*, vol. 104, pp. 822 – 833, 2013.

[31] S.-T. Cha, D.-H. Jeon, I.-S. Bae, I.-R. Lee *et al.*, "Reliability Evaluation of Distribution System Connected Photovoltaic Generation Considering Weather Effects," in *Proc. of 2004 International Conference on Probabilistic Methods Applied to Power Systems*. Ames, Iowa USA: IEEE, 2004, pp. 451–456.

[32] E. Collins, M. Dvorack, J. Mahn, M. Mundt, and M. Quintana, "Reliability and Availability Analysis of a Fielded Photovoltaic System," in *Proc. of 34th IEEE Photovoltaic Specialists Conference 2009 (PVSC)*. Philadelphia, Pennsylvania, US: IEEE, 2009, pp. 2316–2321.

[33] B. Fardanesh, "Optimal Utilization, Sizing, and Steady-State Performance Comparison of Multiconverter VSC-based FACTS Controllers," *IEEE Transactions on Power Delivery*, vol. 19, no. 3, pp. 1321–1327, 2004.

[34] A. Phadke, M. Fozdar, and K. Niazi, "A new Multi-Objective Fuzzy-GA Formulation for Optimal Placement and Sizing of Shunt FACTS Controller," *International Journal of Electrical Power & Energy Systems*, vol. 40, no. 1, pp. 46–53, 2012.

[35] S. O. Faried, R. Billinton, and S. Aboreshaid, "Probabilistic Technique for Sizing FACTS Devices for Steady-State Voltage Profile Enhancement," *IET Generation, Transmission & Distribution*, vol. 3, no. 4, pp. 385–392, 2009.

[36] Y. Del Valle, J. Hernandez, G. Venayagamoorthy, and R. Harley, "Optimal STATCOM Sizing and Placement using Particle Swarn Optimization," in *Proc. of 2006 IEEE/PES Transmission & Distribution Conference and Exposition: Latin America*. Caracas, Venezuela: IEEE, 2006, pp. 1–6.

[37] S. A. Jumaat, I. Musirin, M. M. Othman, and H. Mokhlis, "Optimal Placement and Sizing of Multiple FACTS Devices Installation," in *Proc. of 2012 IEEE International Conference on Power and Energy (PECon)*. Kota Kinabalu, Malaysia: IEEE, 2012, pp. 145–150.

[38] L. L. Grigsby, *Power System Stability and Control*. CRC press, 2016.

[39] P. Kundur, N. J. Balu, and M. G. Lauby, *Power System Stability and Control*. New York, US: McGraw-Hill, 1994, vol. 7.

[40] R. M. Mathur and R. K. Varma, *Thyristor-based FACTS controllers for electrical transmission systems*. Hoboken, NJ, USA.: John Wiley & Sons, 2002.

[41] ENERGINET, "Technical Regulation for Wind Power Plants, Denmark," (Date last accessed 24-March-2020). [Online]. Available: https://en.energinet.dk

[42] L. Gyugyi, "Power Electronics in Electric Utilities: Static VAR Compensators," *Proceedings of the IEEE*, vol. 76, no. 4, pp. 483–494, Apr 1988.

[43] N. G. Hingorani, L. Gyugyi, and M. El-Hawary, *Understanding FACTS: Concepts and Technology of Flexible AC Transmission Systems*. Wiley Online Library, 2000, vol. 2.

[44] SIEMENS AG, "Parallel compensation - Comprehensive solutions for safe and reliable grid operation," 2016. [Online]. Available: https://assets.siemens-energy.com/siemens/assets/api/uuid:65b2b83a-a5a7-442f-b5d3-803bb5a629d2/emts-b10018-00-7600.pdf

[45] E. Acha, V. Agelidis, O. Anaya-Lara, and T. J. E. Miller, *Power Electronic Control in Electrical Systems*. U.K., Oxford: Newnes Power Engineering Series, 2002.

[46] CIGRE Working Group and others, "Coordination of Controls of Multiple FACTS/HVDC Links in the Same System," *CIGRE Technical Brochure*, no. 149, 1999.

[47] ENTSO-E, "Frequency Stability Evaluation Criteria for the Synchronous Zone of Continental Europe," 2018. [Online]. Available: https://www.energinet.dk

[48] ENTSO-E, "P5–Policy 5: Emergency Operations," 2015, (Date last accessed 30-Aug-2019). [Online]. Available: https://docstore.entsoe.eu

[49] ENTSO-E, "High Penetration of Power Electronic Interfaced Power Sources (HPoPEIPS)," 2017. [Online]. Available: https://docstore.entsoe.eu

[50] EirGrid, "EirGrid Grid Code Version 6.0," 2015, (Date last accessed 24-March-2020). [Online]. Available: https://www.eirgridgroup.com

[51] Tennet TSO GmbH, "Offshore-Netzanschlussregeln (O-NAR)," 2019, (Date last accessed 24-March-2020). [Online]. Available: https://www.tennet.eu

[52] G. Chown, J. G. Wright, R. P. Van Heerden, and M. Coker, "System inertia and rate of change of frequency (rocof) with increasing non-synchronous renewable energy penetration," in *Proc. of Cigré 2017: 8th Southern Africa Regional Conference*. Somerset West, Cape Town, South Africa: Cigré, Nov 2017, pp. 1–20.

[53] P. Gupta, R. Bhatia, and D. Jain, "Active rocof relay for islanding detection," *IEEE Transactions on Power Delivery*, vol. 32, no. 1, pp. 420–429, 2016.

[54] X. Ding and P. A. Crossley, "Islanding detection for distributed generation," in *2005 IEEE Russia Power Tech*. IEEE, 2005, pp. 1–4.

[55] C. Li, C. Cao, Y. Cao, Y. Kuang, L. Zeng, and B. Fang, "A review of islanding detection methods for microgrid," *Renewable and Sustainable Energy Reviews*, vol. 35, pp. 211–220, 2014.

[56] D. J. Burke and M. J. O'Malley, "Factors Influencing Wind Energy Curtailment," *IEEE Transactions on Sustainable Energy*, vol. 2, no. 2, pp. 185–193, 2011.

[57] E. Nycander, L. Söder, J. Olauson, and R. Eriksson, "Curtailment Analysis for the Nordic Power System Considering Transmission Capacity, Inertia Limits and Generation Flexibility," *Renewable Energy*, vol. 152, pp. 942–960, 2020.

[58] EirGrid and SONI, "System Non Synchronous Penetration - Definition and Formulation," pp. 1–7, August 27, 2018. [Online]. Available: https://www.eirgridgroup.com/site-files/library/EirGrid/SNSP-Formula-External-Publication.pdf

[59] D. Fernández-Muñoz, J. I. Pérez-Díaz, I. Guisández, M. Chazarra, and Álvaro Fernández-Espina, "Fast Frequency Control Ancillary Services: An International Review," *Renewable and Sustainable Energy Reviews*, vol. 120, p. 109662, 2020.

[60] ENTSO-E, "Frequency Measurement Requirements and Usage, Final Version 7," 2018. [Online]. Available: https://docstore.entsoe.eu

[61] J. Van de Vyver, J. D. M. De Kooning, B. Meersman, L. Vandevelde, and T. L. Vandoorn, "Droop Control as an Alternative Inertial Response Strategy for the Synthetic Inertia on Wind Turbines," *IEEE Transactions on Power Systems*, vol. 31, no. 2, pp. 1129–1138, March 2016.

[62] H. Shao, X. Cai, D. Zhou, Z. Li, D. Zheng, Y. Cao, Y. Wang, and F. Rao, "Equivalent Modeling and Comprehensive Evaluation of Inertia Emulation Control Strategy for DFIG Wind Turbine Generator," *IEEE Access*, vol. 7, pp. 64 798–64 811, 2019.

[63] J. Brisebois and N. Aubut, "Wind Farm Inertia Emulation to fulfill Hydro-Québec's Specific need," in *Proc. of 2011 IEEE Power and Energy Society General Meeting*, July 2011, pp. 1–7.

[64] L. Miao, J. Wen, H. Xie, C. Yue, and W. Lee, "Coordinated Control Strategy of Wind Turbine Generator and Energy Storage Equipment for Frequency Support," *IEEE Transactions on Industry Applications*, vol. 51, no. 4, pp. 2732–2742, July 2015.

[65] Y. Sun, Z. Zhang, G. Li, and J. Lin, "Review on Frequency Control of Power Systems with Wind Power Penetration," in *Proc. of 2010 International Conference on Power System Technology*, Zhejiang, Hangzhou, China, Oct 2010, pp. 1–8.

[66] I. D. Margaris, S. A. Papathanassiou, N. D. Hatziargyriou, A. D. Hansen, and P. Sorensen, "Frequency Control in Autonomous Power Systems With High Wind Power Penetration," *IEEE Transactions on Sustainable Energy*, vol. 3, no. 2, pp. 189–199, April 2012.

[67] U. Tamrakar, D. Shrestha, M. Maharjan, B. Bhattarai, T. Hansen, and R. Tonkoski, "Virtual Inertia: Current Trends and Future Directions," *Applied Sciences*, vol. 7, p. 654, June 2017.

[68] S. D'Arco and J. A. Suul, "Virtual Synchronous Machines — Classification of Implementations and Analysis of Equivalence to Droop Controllers for Microgrids," in *Proc. of 2013 IEEE Grenoble Conference*, Grenoble, France, June 2013, pp. 1–7.

[69] M. Guan, W. Pan, J. Zhang, Q. Hao, J. Cheng, and X. Zheng, "Synchronous Generator Emulation Control Strategy for Voltage Source Converter (VSC) Stations," *IEEE Transactions on Power Systems*, vol. 30, no. 6, pp. 3093–3101, Nov 2015.

[70] J. Zhu, C. D. Booth, G. P. Adam, A. J. Roscoe, and C. G. Bright, "Inertia Emulation Control Strategy for VSC-HVDC Transmission Systems," *IEEE Transactions on Power Systems*, vol. 28, no. 2, pp. 1277–1287, May 2013.

[71] Q. Zhong, P. Nguyen, Z. Ma, and W. Sheng, "Self-Synchronized Synchronverters: Inverters Without a Dedicated Synchronization Unit," *IEEE Transactions on Power Electronics*, vol. 29, no. 2, pp. 617–630, Feb 2014.

[72] G. Ramtharan, N. Jenkins, and J. Ekanayake, "Frequency Support from Doubly Fed Induction Generator Wind Turbines," *IET Renewable Power Generation*, vol. 1, no. 1, pp. 3–9, 2007.

[73] W. Binbing, X. Abuduwayiti, C. Yuxi, and T. Yizhi, "Rocof droop control of pmsg-based wind turbines for system inertia response rapidly," *IEEE Access*, vol. 8, pp. 181 154–181 162, 2020.

[74] T. Liu, W. Pan, R. Quan, and M. Liu, "A Variable Droop Frequency Control Strategy for Wind Farms that considers Optimal Rotor Kinetic Energy," *IEEE Access*, vol. 7, pp. 68 636–68 645, 2019.

[75] ENTSO-E, "Incident Classification Scale," 2018. [Online]. Available: https://docstore.entsoe.eu

[76] B. Singh, N. Sharma, and A. Tiwari, "Coordinated Control and Interactions between FACTS Controllers in Multi Machine Power System Environments: An Overview & Issues," in *Proc. of 15th National Power Systems Conference (NPSC)*, Bombay, India, 2008, pp. 1–11.

[77] G. Romegialli and H. Beeler, "Reactive Compensation. Problems and Concepts of Static Compensator Control," in *IEE Proceedings C (Generation, Transmission and Distribution)*, vol. 128, no. 6. IET, 1981, pp. 382–388.

[78] A. J. Hernandez M, J. Lottes, D. Abhay, and M. Steger, "Artificial Neural Network Based Online Network Strength Estimation," in *Proc. of IEEE PES Innovative Smart Grid Technologies Conference Europe (ISGT-Europe)*, Sarajevo, Bosnia, 2018, pp. 1–6.

[79] V. Talavat, S. Galvani, and S. R. Marjani, "Robust Design of PSS and SVC using Teaching-Learning based Optimization Algorithm," in *Proc. of 10th International Conference on Electrical and Electronics Engineering (ELECO)*, Bursa, Turkey, 2017, pp. 72–75.

[80] J.-x. Xu, L.-c. Xiu, C.-c. Hang, C. Li, Q.-r. Jiang, and Z.-h. Wang, "PI Control of STATCOM using Fuzzy Set and Auto-Tuning Techniques," *IFAC Proceedings Volumes*, vol. 32, no. 2, pp. 7340–7345, July 1999.

[81] Y. Xu and F. Li, "Adaptive PI Control of STATCOM for Voltage Regulation," *IEEE Transactions on Power Delivery*, vol. 29, no. 3, pp. 1002–1011, June 2014.

[82] Y. Xu, F. Li, Z. Jin, and C. Huang, "Flatness-Based Adaptive Control (FBAC) for STATCOM," *Electric Power Systems Research*, vol. 122, pp. 76–85, 2015.

[83] S. Mohagheghi, Y. del Valle, G. K. Venayagamoorthy, and R. G. Harley, "A Proportional-Integrator Type Adaptive Critic Design-Based Neurocontroller for a Static Compensator in a Multimachine Power System," *IEEE Transactions on Industrial Electronics*, vol. 54, no. 1, pp. 86–96, 2007.

[84] A. A. AL-Gailany, I. I. Ali, and A. K. Mahmood, "Voltage Stability Improvements using Adaptive Controller for STATCOM," *Journal of Engineering and Sustainable Development*, vol. 21, no. 2, pp. 129–148, 2017.

[85] A. M. Eltamaly, Y. S. Mohamed, A.-H. M. El-Sayed, and A. N. A. Elghaffar, "Adaptive Static Synchronous Compensation Techniques with the Transmission System for Optimum Voltage Control," *Ain Shams Engineering Journal*, vol. 11, no. 1, pp. 35–44, 2020.

[86] S. O. Shewatkar and V. M. Harne, "Design of Adaptive PI Controller of STATCOM for Voltage Stability," *Journal of Electrical and Power System Engineering*, vol. 5, no. 2, pp. 1–11, 2019.

[87] P. M. Subcommittee, "IEEE Reliability Test System," *IEEE Transactions on Power Apparatus and Systems*, vol. PAS-98, no. 6, pp. 2047–2054, Nov 1979.

[88] C. Grigg, P. Wong, P. Albrecht, R. Allan, M. Bhavaraju, R. Billinton, Q. Chen, C. Fong, S. Haddad, S. Kuruganty, W. Li, R. Mukerji, D. Patton, N. Rau, D. Reppen, A. Schneider, M. Shahidehpour, and C. Singh, "The IEEE Reliability Test System-1996. A report prepared by the Reliability Test System Task Force of the Application of Probability Methods Subcommittee," *IEEE Transactions on Power Systems*, vol. 14, no. 3, pp. 1010–1020, Aug 1999.

[89] S. Peyghami, P. Davari, M. Fotuhi-Firuzabad, and F. Blaabjerg, "Standard Test Systems for Modern Power System Analysis: An Overview," *IEEE Industrial Electronics Magazine*, vol. 13, no. 4, pp. 86–105, Dec 2019.

[90] C. Liang, P. Wang, X. Han, W. Qin, R. Billinton, and W. Li, "Operational Reliability and Economics of Power Systems With Considering Frequency Control Processes," *IEEE Transactions on Power Systems*, vol. 32, no. 4, pp. 2570–2580, 2017.

[91] C. Liang, P. Wang, X. Han, W. Qin, R. Billinton, and W. Li, "Operational Reliability and Economics of Power Systems With Considering Frequency Control Processes," *IEEE Transactions on Power Systems*, vol. 32, no. 4, pp. 2570–2580, July 2017.

[92] L. A. Zadeh, G. J. Klir, and B. Yuan, *Fuzzy Sets, Fuzzy Logic, and Fuzzy Systems: Selected Papers*. World Scientific, 1996, vol. 6.

[93] L. A. Zadeh, "Fuzzy Sets," *Information and Control*, vol. 8, no. 3, pp. 338–353, 1965.

[94] M. Fotuhi and A. Ghafouri, "Uncertainty Consideration in Power System Reliability Indices Assessment using Fuzzy Logic Method," in *2007 Large Engineering Systems Conference on Power Engineering*. IEEE, 2007, pp. 305–309.

[95] A. R. Abdelaziz, "A Fuzzy-Based Power System Reliability Evaluation," *Electric Power Systems Research*, vol. 50, no. 1, pp. 1–5, 1999.

[96] X. Liu, Z. Wang, S. Zhang, and J. Liu, "A Novel Approach to Fuzzy Cognitive Map based on Hesitant Fuzzy Sets for Modeling Risk Impact on Electric Power

System," *International Journal of Computational Intelligence Systems*, vol. 12, no. 2, pp. 842–854, 2019.

[97] B. Canizes, J. Soares, Z. Vale, and H. Khodr, "Hybrid Fuzzy Monte Carlo Technique for Reliability Assessment in Transmission Power Systems," *Energy*, vol. 45, no. 1, pp. 1007–1017, 2012.

# Part II

# Selected Publications

# Conference Publication 1 [C1]

## Tuning of Voltage Controller Gain for Multiple STATCOM Systems

Joachim Steinkohl, Xiongfei Wang

The paper has been published at
*COMPEL 2018* Padua, Italy, 2018.

# Tuning of Voltage Controller Gain for Multiple STATCOM Systems

Joachim Steinkohl* and Xiongfei Wang†
*Department of Energy Technology*
*Aalborg University*
Aalborg, Denmark
*joa@et.aau.dk, †xwa@et.aau.dk

***Abstract*—STATCOMs with voltage control are known for their fast reaction time to stabilize the grid voltage. For optimal dynamic performance it is essential to use the correct gain settings for the PI voltage regulation controller, adapted for different states of operation. This paper shows the equation to calculate the accurate value for the gain setting in the voltage controller. The inner control behavior with enabled droop control is considered as well as the strength of the grid. After this the influences between STATCOMs installed in parallel in one bus is shown and the adaption of the gain to take this into account is calculated. The equations are validated by analytic aspects as well as by simulations. This enhances the existing control solution in industry and allows constant dynamic performance under various system changes in future grids.**

***Index Terms*—FACTS, STATCOM, Voltage Control**

## I. Introduction

A Static Compensator (STATCOM) is a device for advanced reactive power compensation to vontrol the voltage in the power grid [1]. It can be used to control power factor, regulate voltage, stabilize power flow, and improve the dynamic performance of power systems. It has been well understood that the voltage control of a STATCOM is highly dependent on the conditions in the grid it is connected to, especially to system strength [2] and to other dynamical voltage controlling devices. Without adapting to these conditions control instabilities occur [3]. Other research has focused on adaptive controller settings [4]–[6] or fuzzy control [7]. All these control techniques lack on the calculated adjustment of the voltage controller gain to the influences of other STATCOMs.

To prevent instabilities and to maintain optimal dynamic performances, communications between the FACTS devices are installed to reduce the gain of the voltage controllers by a constant factor [3]. But this control adaption does not guarantee constant dynamic performances. This paper shows the calculation for the optimal gain adaption for the voltage controller in a multiple STATCOM system. This allows to have constant dynamic performances for different system conditions.

978-1-5386-5541-2/18/$31.00 ©2018 IEEE

## II. STATCOM Gain Calculation

The gain calculation for a single STATCOM installation is determined at first. For this, the needed reactive output of a STATCOM due to a voltage deviation is calculated. Then the influences of other STATCOMs are taken into account as well.

### A. Single STATCOM installation

The control scheme of the STATCOM voltage controller with droop control is shown in Fig. 1. The inner current control is not shown, it can be neglected for this analysis, due to the slower dynamics. The reactive output of the STATCOM is fed back to change the voltage reference value. This is beneficial for keeping dynamic reserve in the system and to avoid instabilities with multiple voltage controlling devices.

The proportional-integral (PI) controller of the voltage controller has the form

$$Gain \cdot \left(1 + \frac{1}{T_{\mathrm{N}} \cdot s}\right) \tag{1}$$

With this form of the PI controller is it possible to adapt to changes in the grid strength and the Droop control. $T_N$ has to be set according to internal time constants such as the measurement delays. The Droop control is used to allow load sharing between multiple units. This allows the operators to reduce the impact of the STATCOMs under normal operating conditions [8].

The controlled positive phase sequence grid voltage in steady state is expressed in (2). This shows the deviation from the reference voltage due to the Droop control.

$$V_{\mathrm{GRID}} = V_{\mathrm{REF}} - Q_{\mathrm{STATCOM}} \cdot \frac{Droop}{Q_{\mathrm{NOM}}} \tag{2}$$

Fig. 2 shows the crossing of the Grid Line (determined by the grid strength) and the Control Line (determined by the Droop control) in a single STATCOM system. The point of crossing determines the operating point of the STATCOM under steady state conditions.

The Droop control has to be taken into account for the gain calculation, because it has a severe impact on the needed reactive power output due to a change in the grid voltage. It therefore changes the point of operation in the steady state. If it is not taken into account, the step response time and settling time of the STATCOM do not forfill the specifications for the

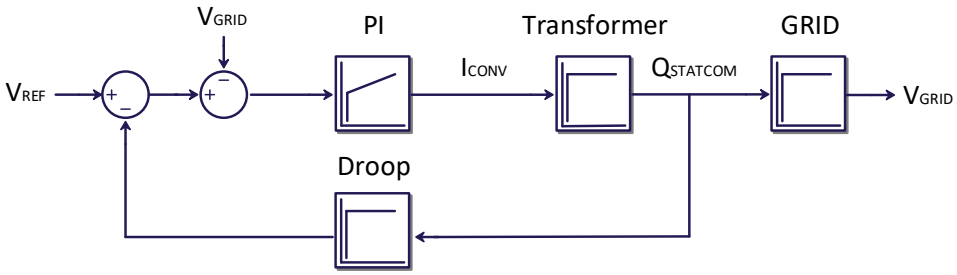


Fig. 1. STATCOM control scheme with Droop control.

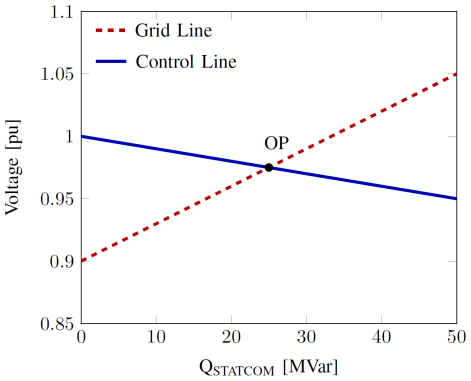


Fig. 2. Single STATCOM System.

voltage controlling dynamics [2]. The equation for the reactive power flow can be used to express the impact of the reactive output power of a STATCOM to the voltage difference, that is caused by this output.

$$Q = \frac{E \cdot V \cdot \cos\theta - V^2}{X} \tag{3}$$

Assumed, that the angle $\theta$ is small, the equation can be rewritten as

$$Q = \frac{E - V}{X} \cdot V \tag{4}$$

This can be rewritten so that the strength of the grid is an expression of the grid reactance $X$. (4) can be linearized around a stable operating point and the gain of the PI voltage controller can then be calculated using (5). This equation shows the relationship between a voltage drop in the grid and the needed reactive output change to compensate it.

$$Gain = \frac{\Delta Q_{\text{STATCOM}}}{\Delta V_0} \tag{5}$$

The needed change of reactive output for a voltage deviation with Droop control consists of two terms as can seen in (6). The first term represents the reactive output that is needed to fully compensate a voltage deviation. The second term represents the change of the voltage reference setpoint due to the Droop control.

$$\Delta Q_{\text{STATCOM}} = \Delta V_0 \cdot SCL - \Delta Q_{\text{STATCOM}} \cdot \frac{Droop}{Q_{\text{NOM}}} \cdot SCL \tag{6}$$

After solving (6) to $\Delta V_0$ and setting it into (5) leads to:

$$Gain = \frac{1}{\frac{1}{SCL} + \frac{Droop}{Q_{\text{NOM}}}} \tag{7}$$

With (7) it is possible to adapt the gain of the controller to keep the optimal dynamic performance of the STATCOM even with changes in the control parameters or changes in the grid strength.

### *B. Multiple STATCOM Installation*

This section describes the adaption of the gain to the influence of other STATCOMs.

The equation used in the industry [3] is shown in (8).

$$Gain = \frac{1}{\frac{1}{SCL} + \frac{Droop}{Q_{\text{NOM}}}} \cdot 0.55 \tag{8}$$

The reduction of the controller gain is done, by multiplying a constant factor to the previously calculated gain as in the single STATCOM system.

The voltage change due to the other STATCOM affects the reactive output, that is needed to control a voltage deviation.

$$\Delta Q_{\text{STATCOM 1}} = \left(\Delta V_0 - \frac{\Delta Q_{\text{STATCOM 2}}}{SCL}\right) \cdot SCL -$$

$$\Delta Q_{\text{STATCOM 1}} \cdot \frac{Droop_1}{Q_{\text{NOM 1}}} \cdot SCL \tag{9}$$

(9) can also be done for the second STATCOM. By solving the equations to the outputs of the separate STATCOMs leads to the following two equations

$$\Delta Q_{\text{STATCOM 1}} = \frac{\Delta V_0 - \frac{\Delta Q_{\text{STATCOM 2}}}{SCL}}{\frac{1}{SCL} + \frac{Droop_1}{Q_{\text{NOM 1}}}} \tag{10}$$

$$\Delta Q_{\text{STATCOM 2}} = \frac{\Delta V_0 - \frac{\Delta Q_{\text{STATCOM 1}}}{SCL}}{\frac{1}{SCL} + \frac{Droop_2}{Q_{\text{NOM 2}}}} \tag{11}$$

With these equations it is possible to determine the optimal change of reactive output of the two STATCOMs depending on the voltage deviation in the grid even with unequal ratings and control settings. Solving the two equations (10) and (11) with the same STATCOM ratings ($Q_{\text{NOM}}$) and control settings (Droop) entered in (5) leads to (12) as a gain for both STATCOM units.

$$Gain = \frac{1}{\frac{2}{SCL} + \frac{Droop}{Q_{\text{NOM}}}} \tag{12}$$

Therefore a second STATCOM changes the gradient of the grid line shown in Fig. 3 following (12).

For this, the diagram for the STATCOM effect on the system voltage has been redrawn to take the effect of a second STATCOM into account. This is done by changing the slope of the grid line.

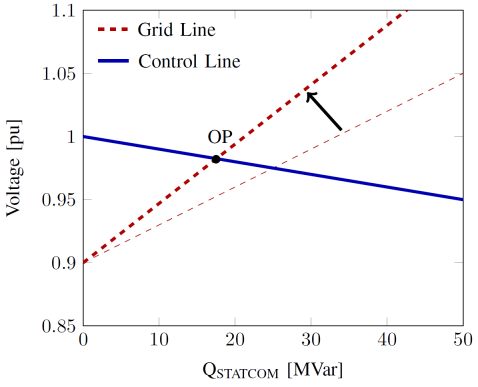


Fig. 3. Multiple STATCOM System.

The influence of a second STATCOM is taken into account in (6). The other STATCOM changes the voltage in the grid, but not the reactive output that is taken into consideration in the Droop control term. This can be seen also in [3], where the time constant of the control system is changed according to the droop, the grid strength and the existence of other voltage controlling devices.

This equation is not exactly the equation, that is used in the industry, both solutions are further analyzed in Section IV.

The gain can now be calculated for all values of the SCL and Droop settings. The proposed equation allows constant dynamic performances even with changed control parameters and grid conditions. This is shown in simulations in Section IV.

### C. Not equally sized STATCOMs

If there are STATCOMs installed close to each other with different reactive output ratings, then the equation has to change according to the nominal reactive power to the sum of all nominal reactive powers together.

$$Gain_1 = \frac{1}{\frac{1}{SCL} \cdot \frac{Q_{\text{NOM 1}} + Q_{\text{NOM 2}}}{Q_{\text{NOM 1}}} + \frac{Droop}{Q_{\text{NOM}}}} \tag{13}$$

and

$$Gain_2 = \frac{1}{\frac{1}{SCL} \cdot \frac{Q_{\text{NOM 1}} + Q_{\text{NOM 2}}}{Q_{\text{NOM 2}}} + \frac{Droop}{Q_{\text{NOM}}}} \tag{14}$$

The calculated gains in (13) and (14), that can be calculated from (10) and (11) allow the correct control of STATCOMs with different ratings in the same power grid. It is assumed that the Droop control is the same in both units, because they are installed in one power system with the same grid code. If the Droop control set points are different, it is still possible to calculate the optimal gain following the equations from above.

### D. Multiple STATCOM Installation

With more than two STATCOMs installed at one bus, the influence of these STATCOMs can also be taken into account for the gain calculation. The voltage deviation that has to be controlled by the different STATCOMs can be calculated to get an expression for the influences of all other STATCOMs to the individual ones. (15) demonstrates the influence of all other STATCOMs to one STATCOM.

$$\Delta Q_{\text{STATCOM 1}} = \left( \Delta V_0 - \sum_{i=2}^{N} \frac{\Delta Q_{\text{STATCOM i}}}{SCL} \right) \cdot SCL -$$

$$\Delta Q_{\text{STATCOM 1}} \cdot \frac{Droop_1}{Q_{\text{NOM 1}}} \cdot SCL \tag{15}$$

The gain of the voltage controllers can be calculated following the same calculations as for (12). Solving these equations again with the same ratings and controller settings leads to (16).

$$Gain = \frac{1}{\frac{N}{SCL} + \frac{Droop}{Q_{\text{NOM}}}} \tag{16}$$

With N in (16) being defined as the total number of identical STATCOMs in one bus. This formula is only applicable with the same Droop control settings and ratings of all STATCOMs installed in one bus. Different STATCOM ratings can also be expressed and calculated with respect to (17).

$$Gain_{\text{i}} = \frac{1}{\frac{1}{SCL} \cdot \frac{\sum_{i=1}^{N} Q_{\text{NOM i}}}{Q_{\text{NOM i}}} + \frac{Droop}{Q_{\text{NOM i}}}} \tag{17}$$

This allows the constant dynamic performance of a wide variety of possible STATCOM configurations.

## III. Analysis

To determine the impact of the different gain calculation methods, an analytic approach is needed. For this, the control system from Fig. 1 is analyzed. The filter for the measurement of the reactive output and also for the grid voltage is simplified to a first order low-pass filter. This slows down the control in such a way, that the step response of the closed loop control meets the dynamics as in a modern transmission STATCOM installation.

The bode diagrams of the closed-loop system with the gain reduction method as in (8), used in industry, are shown. For this, the system is analyzed with a droop of $10\,\%$ (in Fig. 4) and $4\,\%$ (in Fig. 5). The strength of the power system is changed in 5 GVA steps from 0.5 GVA to 20.5 GVA in both cases.

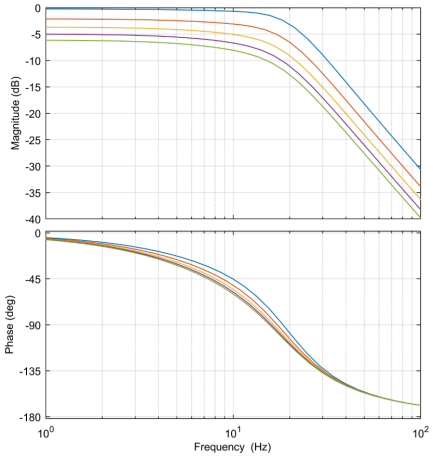


Fig. 4. Bode plot with SCL variations with fixed reduction factor with 10 % Droop.

It can be seen in the lower graphs in Fig. 4 that the time response of the system is not constant with the variation of the grid strength. This causes unwanted dynamics in the operation of the STATCOM system in a wide variety of grid conditions, if there are other voltage controlling devices nearby. The droop control affects the steady state operation point as one can see by the deviation of 0 db in the upper graph.

With reduced droop control setpoint the system variations in steady state are smaller than with 10 % droop. Nevertheless, the dynamic variations are still visible and the dynamics of the system are not constant under changing grid conditions.

Afterwards, the closed-loop behavior with the proposed gain reduction as in (12) is analyzed. Fig. 6 and Fig. 7 show the bode plots of the closed-loop system with the proposed gain tuning equation. The SCL variations are the same as in the previous analysis.

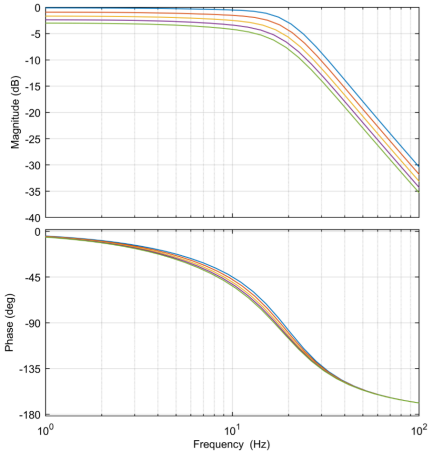


Fig. 5. Bode plot with SCL variations with fixed reduction factor with 4 % Droop.

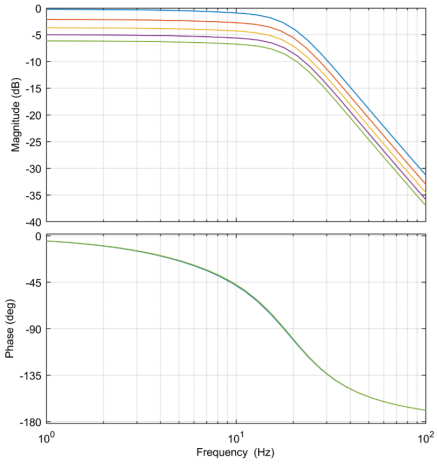


Fig. 6. Bode plot with SCL variations with proposed gain tuning with 10 % Droop.

The time response of the system shown in Fig. 6 is constant and does not change with the SCL variations. The steady state operation point is still varying due to the different effects of the STATCOM output to the grid voltage under droop control. The deviations under steady state are exactly the same as in Fig. 4, because the gain control adaption only affects the dynamics of the control system.

Fig. 7 proves also the constant dynamic behavior of the system under changed grid and control conditions. The steady state operation points are again the same as in Fig. 5.

The proposed gain tuning is therefore enhancing the dy-

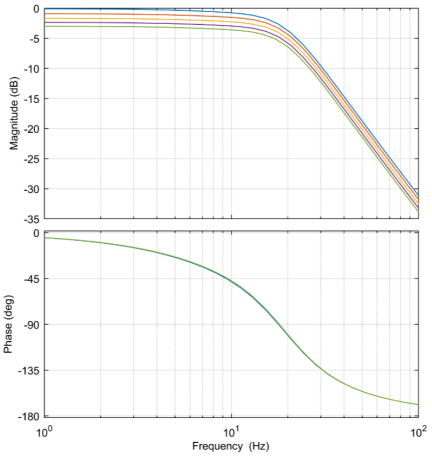


Fig. 7. Bode plot with SCL variations with proposed gain tuning with 4 % Droop.

namic behavior of the voltage in the power grid. This system behavior is also tested with step response tests in simulations, to further verify the performance under more detailed conditions.

## IV. Simulation

The theoretical results have been verified with simulations to see if the equations for the gain calculation are correct and that they improve the dynamic response of the STATCOM compared to the adaption that is used in the industry. The dynamic response of the STATCOM control has been tested with step response tests. For this test the reference voltage setpoint is changed at the time 4 sec in the simulation for all STATCOMs. All STATCOMs have identical ratings of 50 MVar and the Droop value is always set to $4\,\%$.

The simulation is performed with EMTDS / PSCAD. The STATCOMs are simulated with a controlled voltage source as the converter in a delta configuration. The model includes synchronization and current control. Also the positive sequence voltage is filtered and measured for the voltage control to get a more realistic system behavior.

The PI controller of the voltage control is tuned in a single STATCOM condition and afterwards also tested with the influence of a second STATCOM at the same bus.

### A. Single STATCOM installation

In the first simulations the gain adjustment for a single STATCOM installation is tested to verify (7). For this, the STATCOM is installed with a fixed Droop setting of $4\,\%$ in different grids.

Fig. 8 and Fig. 9 show the adaption of the voltage controller gain to a change in the grid strength with droop control. The dynamic response to the changed reference value is constant.

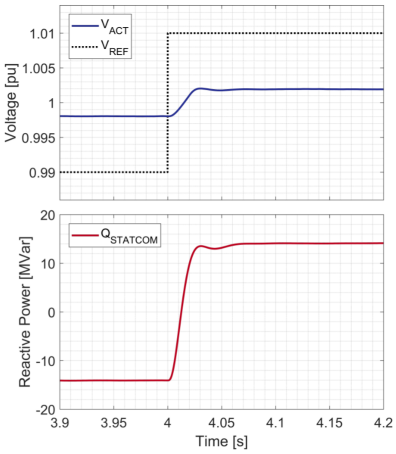


Fig. 8. Single STATCOM in 5 GVA grid.

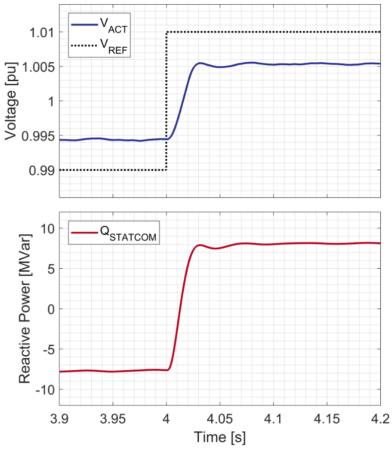


Fig. 9. Single STATCOM in 1 GVA grid.

Further simulations are performed with varying control and system conditions. The results are shown in Table I.

The simulation results in Table I show that a single STATCOM unit can be adapted to changes in future system strength and droop control conditions with constant voltage control dynamics.

### B. 2 STATCOM installation with fixed reduction

In these simulations two STATCOMs are installed in the same bus. The gain is reduced as proposed in industry by 45 % compared to the single STATCOM simulations, as shown in [3].

The simulation results in Fig. 11 prove, that with a fixed gain reduction factor it is possible to achieve good dynamic results

TABLE I
Simulation Results with single STATCOM installation

| | Droop | Rise Time | Overshoot |
|---|---|---|---|
| 1 GVA | 1 % | 25 ms | 2 % |
| | 2 % | 25 ms | 3 % |
| | 4 % | 26 ms | 2 % |
| 5 GVA | 1 % | 27 ms | 1 % |
| | 2 % | 25 ms | 2 % |
| | 4 % | 26 ms | 2 % |
| 10 GVA | 1 % | 26 ms | 2 % |
| | 2 % | 27 ms | 1 % |
| | 4 % | 25 ms | 3 % |

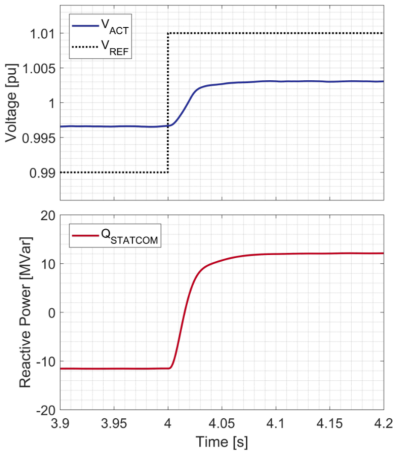


Fig. 10. 2 STATCOMs in 5 GVA grid.
With fixed Gain adaption as used in industry.

with some constellations of SCL and Droop control. But the system dynamics shown in Fig. 10 do not have a sufficient dynamic behavior. In this case the system response is too slow. This proves incorrect controller settings, if the gain is reduced with a constant factor. A pure change of the reduction factor can not be applied with respect to the other simulations results shown in Table II. A reduced reduction factor can speed up the control in some grid conditions, other conditions in the grid will then lead to high overshoots that are not allowed for a stable grid operation (as in the first test result in Table II).

Table II shows the dynamic behavior of the tested setup with the constant gain reduction of 45%. This adaption is not sufficient under all conditions. The overshoots are in the specified limits, due to the value of the reduction. But the rise time increases to very high values (up to 44 ms in the performed simulations). This method will therefore limit the optimal dynamic operation range of the STATCOM voltage control.

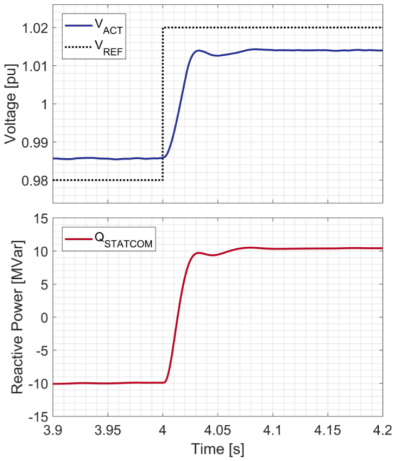


Fig. 11. 2 STATCOMs in 1 GVA grid.
With fixed Gain adaption as used in industry.

TABLE II
Simulation Results with double STATCOM installation with fixed Gain Reduction as used in industry

| | Droop | Rise Time | Overshoot |
|---|---|---|---|
| 1 GVA | 1 % | 25 ms | 4 % |
| | 2 % | 26 ms | 3 % |
| | 4 % | 27 ms | 1 % |
| 5 GVA | 1 % | 26 ms | 1 % |
| | 2 % | 31 ms | 0 % |
| | 4 % | 38 ms | 0 % |
| 10 GVA | 1 % | 29 ms | 0 % |
| | 2 % | 37 ms | 0 % |
| | 4 % | 44 ms | 0 % |

### *C. 2 STATCOM installation with proposed calculation*

In the following simulations the proposed gain reduction is used.

The simulation results shown in Fig. 12 and Fig. 13 prove the correct adaption of the STATCOM controller to the influence of a second STATCOM installed in the same bus with the proposed gain tuning. The time to reach the new steady state operation is constant and the overshoots of the controller are always low enough to fulfill the requirements for stable grid operation.

The results of the dynamic analysis are shown in Table III. It can be seen, that the proposed gain tuning method allows

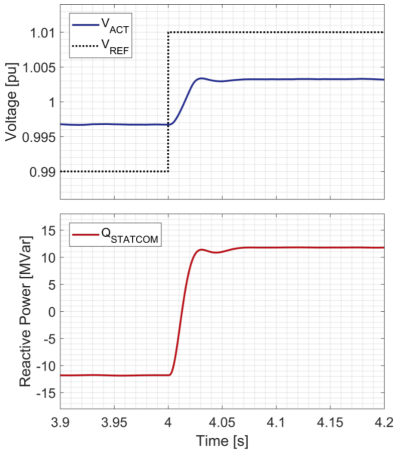


Fig. 12. 2 STATCOMs in 5 GVA grid.
With proposed Gain adaption.

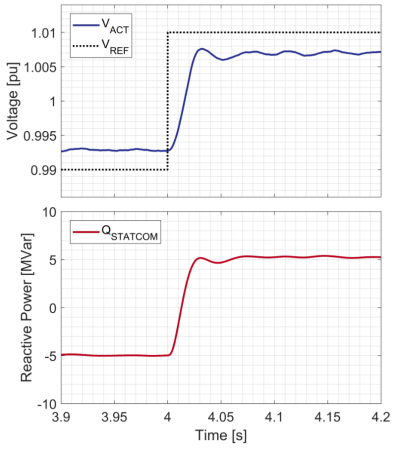


Fig. 13. 2 STATCOMs in 1 GVA grid.
With proposed Gain adaption.

to keep a constant dynamic performance, even with the installation of a second STATCOM unit close nearby.

Also simulations are performed with different STATCOM nominal reactive outputs. This leads to the conclusion, that (13) and (14) are valid and enable constant system dynamics. The used nominal reactive outputs used for the simulations are 50 MVar in one STATCOM and then variations in the second STATCOMs nominal reactive power (50 MVar, 25 MVar and 10 MVar). The simulation results are not shown here, they correspond almost to the results shown in Table III.

TABLE III
Simulation Results with double STATCOM installation with proposed Gain Reduction

| | Droop | Rise Time | Overshoot |
|---|---|---|---|
| 1 GVA | 1 % | 25 ms | 2 % |
| | 2 % | 25 ms | 3 % |
| | 4 % | 26 ms | 2 % |
| 5 GVA | 1 % | 27 ms | 1 % |
| | 2 % | 25 ms | 2 % |
| | 4 % | 26 ms | 2 % |
| 10 GVA | 1 % | 26 ms | 3 % |
| | 2 % | 27 ms | 2 % |
| | 4 % | 27 ms | 2 % |

## V. Conclusion

The simulations performed in this paper proves the correctness of the equation for adapting the controller gain. So it is possible to achieve optimal dynamic response to voltage deviations from the STATCOM in all analyzed system conditions with the proposed gain adaption method. The equation used in the industry right now is not sufficient to adapt to multiple STATCOMs in a correct way. This can lead to unwanted behavior during severe grid events.

Further investigation is needed to the influence of distances and therefore impedance between different STATCOM units. This changes the impact of the reactive power of one STATCOM to the measured voltage on the other STATCOM. Therefore it affects the optimal gain that is needed for constant dynamics. Due to the high number of possible grid configurations has it not been included.

## References


[1] N. G. Hingorani, L. Gyugyi, and M. El-Hawary, *Understanding FACTS: concepts and technology of flexible AC transmission systems*. Wiley Online Library, 2000, vol. 2.

[2] G. Romegialli and H. Beeler, "Reactive compensation. Problems and concepts of static compensator control," in *IEE Proceedings C (Generation, Transmission and Distribution)*, vol. 128, no. 6. IET, 1981, pp. 382–388.

[3] *Coordination of Controls of Multiple FACTS/HVDC Links in the Same System*, ser. Brochures thématiques: International Conference on Large High Voltage Electric Systems. CIGRE, 1999.

[4] Y. Xu and F. Li, "Adaptive PI Control of STATCOM for Voltage Regulation," *IEEE Transactions on Power Delivery*, vol. 29, no. 3, pp. 1002–1011, June 2014.

[5] J.-x. Xu, L.-c. Xiu, C.-c. Hang, C. Li, Q.-r. Jiang, and Z.-h. Wang, "PI control of STATCOM using fuzzy set and auto-tuning techniques," *IFAC Proceedings Volumes*, vol. 32, no. 2, pp. 7340–7345, july 1999.

[6] Y. Xu, F. Li, Z. Jin, and C. Huang, "Flatness-based adaptive control (FBAC) for STATCOM," *Electric Power Systems Research*, vol. 122, pp. 76–85, 2015.

[7] S. A. Al-Mawsawi, M. Qader, and G. Ali, "Dynamic controllers design for STATCOM," *Iranian journal of electrical and computer engineering*, vol. 3, no. 1, pp. 16–22, 2004.

[8] L. Gyugyi, "Power electronics in electric utilities: static VAR compensators," *Proceedings of the IEEE*, vol. 76, no. 4, pp. 483–494, Apr 1988.

# Conference Publication 2 [C2]

## Gain Optimization for STATCOM Voltage Control under Various Grid Conditions

Joachim Steinkohl, Xiongfei Wang

The paper has been published at
*EPE'18 ECCE Europe* Riga, Latvia, 2018.

# Gain Optimization for STATCOM Voltage Control under Various Grid Conditions

Joachim Steinkohl and Xiongfei Wang
Aalborg University
Pontoppidanstrde 111
9220 Aalborg, Denmark
Phone: +45 93562489
Email: joa@et.aau.dk and xwa@et.aau.dk

## Keywords

FACTS , STATCOM , Non-linear control , Optimal control

## Abstract

Static Compensators (STATCOMs) with voltage control are known for their fast reaction time to stabilize the grid voltage. For optimal dynamic performance it is essential to adjust the gain settings for the voltage controller, for different states of operation. This paper presents a new gain adaption algorithm to passively adapt to changes in the grid stiffness as well as to other dynamic voltage controlling devices, in order to provide stable STATCOM behavior in all system conditions. The proposed control will not need communication between the FACTS units. Which consequently simplifies and enhances the control systems even under severe grid changes.

## Introduction

A Static Compensator (STATCOM) is a device for advanced reactive power compensation [1]. It can be used to regulate the grid voltage, stabilize the power flow and improve the harmonic performance of power systems, such as wind parks.

It has been well understood that the voltage control of STATCOMs is highly dependent on the conditions in the grid, especially on the system strength, also called short circuit level (SCL) [2] and on other dynamic voltage controlling devices (e.g. other STATCOMs) installed nearby. If the devices can not adapt to these changing conditions, they can not guarantee optimal dynamic performances [3]. To allow the adaption to grid changes, a communication link between the voltage controlling devices is installed nowadays to adapt the gain of the voltage controllers [3]. Also the placement of the STATCOMs in the power grid has a huge effect on the interactions, as mentionned in [4].

Some researchers have focused on adaptive controller settings [5] or fuzzy control [6, 7, 8]. These control techniques are dynamically adapting the controller during the event to optimize the STATCOM's reactive output due to an external voltage change. Some take the effect of multiple nearby STACOMs into account as well [9]. However, after the event all controller settings will be set back to the preset values. Also, these controllers are used to optimize the step response behavior of a STATCOM. Yet this is not the main purpose of the STATCOM. The main purpose is the reduction of voltage changes due to other grid events.

Other researchers use neuronal grid techniques [10] or other techniques, where the controller is trained in a huge number of simulations [11] to obtain the controller optimal behavior under various system

conditions. These methods may lead to unsatisfying operation, if there are grid situations that have not been foreseen by the engineers in the design phase.

This paper proposes a new algorithm for the optimal gain adaption of the voltage controller to system strength changes for single and multiple STATCOM systems. This method guarantees constant dynamic performances for a wide variety of system conditions. The proposed controller enables to place voltage controlling devices, as STATCOMs, without the need of communication or prior knowledge about grid parameters, such as distances to other voltage controlling devices. The proposed method allows therefore cost-effective and communication-failure-free dynamics over a wide range of possible future grid conditions. This superior feature is attractive to prevent critical infrastructure from failures and to improve the interoperability of dynamic voltage controlling devices from different vendors.

## STATCOM Voltage Control

The main task of STATCOMs is to stabilize the voltage in the power grid. STATCOMs are capable of providing both capacitive and inductive reactive currents and is therefore capable of lifting and lowering the grid voltage.

The strength of the power grid is a key value that has to be known to adjust the voltage controller to operate with its specified dynamics under all system conditions. Fig. 1 shows the control diagram of a STATCOM in voltage control mode with droop control.

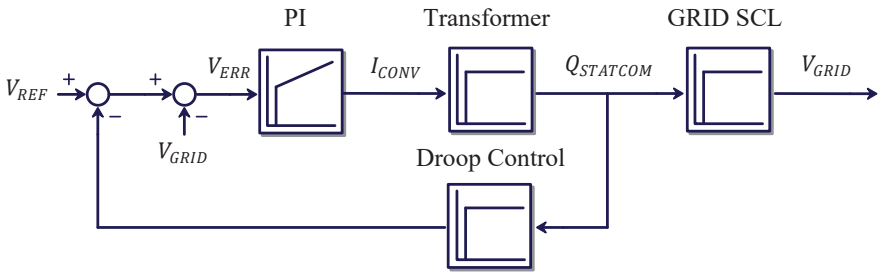


Fig. 1: STATCOM control scheme with droop control

The voltage reference setpoint is changed by the Droop factor (in %) multiplied with the reactive output of the STATCOM, which is normalized according to the rated reactive output of the STATCOM. Hence, a Droop of 1 % allows a voltage reference change in the steady state of 1 % when the STATCOM operates at nominal reactive output.

The equation of the Proportional-Integral (PI) controller is given by (1).

$$Gain \quad 1 \quad \frac{1}{T_N \ s} \tag{1}$$

In this form the time constant $T_N$ has to be set according to the filter time constant for the grid voltage measurement. Also a Proportional-Integral-Derivative (PID) control can be used with the proposed control. To achieve optimal response to voltage deviations [3], the gain value for the controller has to be set as below.

$$Gain \quad \frac{1}{\frac{1}{SCL} \quad \frac{Droop}{Q_{NOM}}} \tag{2}$$

With this gain adaption it is possible to have an optimal dynamic behavior between two steady state operation points. However, one main difficulty is the estimation of the SCL in the STATCOM controller and the interactions with different other voltage controlling devices.

The strength of the grid can be related to the impact of a reactive power change of a STATCOM on the resulting voltage deviation, which is given by

$$SCL \quad \frac{\Delta Q_{\mathrm{STATCOM}}}{\Delta V_{\mathrm{GRID}}} \tag{3}$$

If there are multiple dynamic voltage controlling devices (e.g., other STATCOMs) installed close to each other, the different voltage controllers have to be coordinated to prevent oscillations [3]. The coordination means a reduction of the calculated gain value from (2). This will then slow down the STATCOMs' dynamic responses to voltage deviations and lead to a stable behavior in the grid. To calculate the reduction, there has to be a communication link between the STATCOM controllers. This requires communication protocols between different vendors, as well as refurbishments when there are new STATCOM installed close to old installations.

The proposed controller allows the calculation of the optimal gain value without the need of communication with respect to other voltage controlling devices nearby.

## Proposed Control

The purpose of the proposed control is to optimize the dynamic response of the STATCOM to voltage disturbances. Fig. 2 illustrates the structure of the proposed gain adaption controller, which consists of three main blocks.

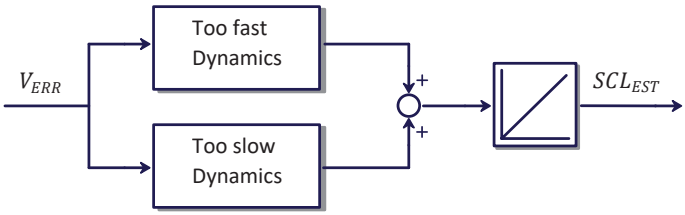


Fig. 2: Gain adaption controller overview

The block 'Too slow Dynamics' detects, if the strength of the power grid has increased since the last adaption. This implies that the STATCOM needs more reactive output to control the voltage in the grid accurately. The estimated SCL value for the gain calculation has to increase to compensate this.

The 'Too fast Dynamics' block is responsible for the detection of an SCL reduction in the grid since the last adaption. Then the estimated SCL value in the controller for the gain calculation has to be decreased. The used method to detect this behavior is described in the related Section.

The last block is an integrator. The output of the integrator is an estimation for the short circuit level of the grid. This value is then taken into (2) to calculate the gain for the PI controller also with respect to the droop control settings.

### Too slow Dynamics Block

The block 'Too slow Dynamics' is activated, when the stiffness of the grid has increased since the last adaption (e.g., due to the activation of loads and generation during daytime). The block detects, if the time to compensate a voltage disturbance is longer than the optimal compensation time. This time is highly dependent on the internal dynamics of the voltage controller. Especially the filters for the voltage measurement signal will affect the dynamics of the voltage controller. The time for the optimal voltage

disturbance compensation can be determined through simulations by tuning the voltage controller with step response tests and then applying voltage disturbances in the grid.

Fig. 3 shows the grid voltage (upper graph) and voltage error (lower graph) behavior during a grid voltage disturbances (load rejection). The figure shows the results with optimal gain settings and also the reaction of the STATCOM with increased grid strength and therefore too low gain settings.

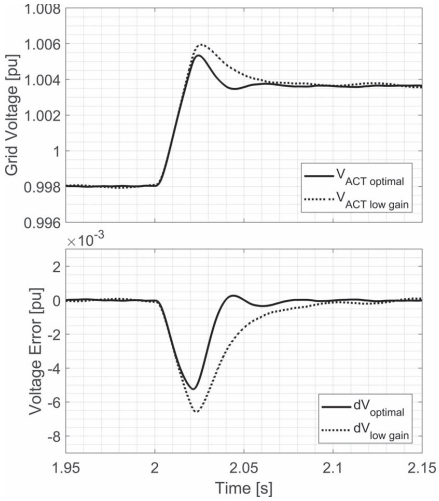


Fig. 3: Voltage error behavior after SCL increase

Fig. 4 shows the control diagram for the block 'Too slow Dynamics'. The only input for this block is the voltage error signal. It is used to detect, if the system strength has increased.

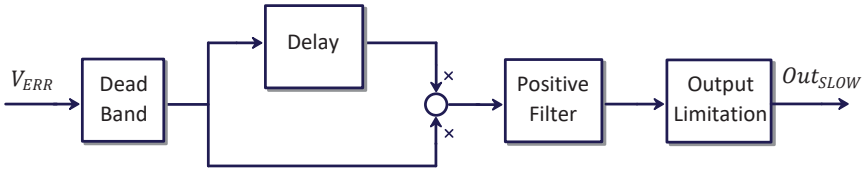


Fig. 4: Too slow dynamics block diagram

The control structure filters out small disturbances in the grid, e.g. due to measurement uncertainties, with the dead-band. Then the sign of the error value will be multiplied with itself delayed by the defined time constant. The resulting value will be filtered in a way that only positive values are allowed. This structure has been chosen, because it can also be used for the detection of fast controller dynamics.

The Output Limitation block in Fig. 4 is added to detect, if the STATCOM output is at its current limit. The current output has to be within the limits for a minimum 50 ms to be released. The STATCOM is not able to fully compensate the voltage error during severe events, like a grid fault. This would lead to a high output value of this controller structure, that is misinterpreted as an increase of the grid strength.

In the performed simulations, the voltage error can be compensated in 35 ms with the STATCOM reactive output change. This means, the error signal shall return to zero after a disturbance in 35 ms. If the error value is for a long time different from zero, then the output of detection block will be positive hence both the error signal and the delayed error signal will have the same sign.

The simulation results shown in Fig. 5 (a) represent the controller behavior under optimal gain settings. The upper graph shows the voltage error signal and the voltage error signal with time delay. The lower

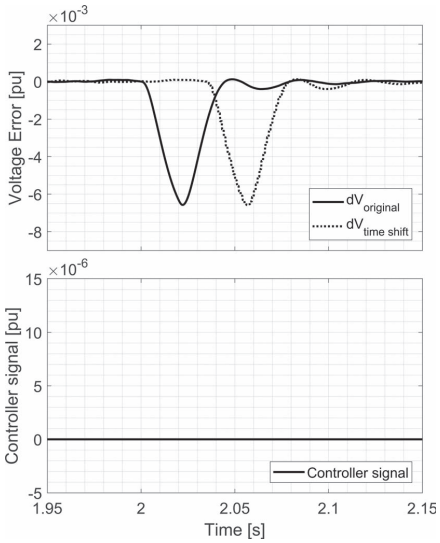


( (a)) SCL increase block with adapted grid strength

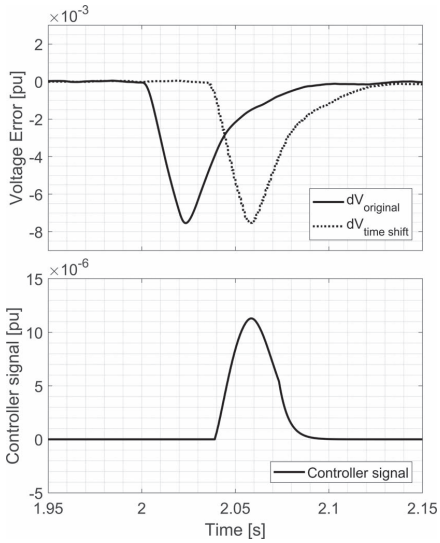


( (b)) SCL increase block output with increased grid strength

Fig. 5: Simulation results for the behavior under too slow dynamics

graph shows the output of 'Too slow Dynamics' block. In this simulation, there is no need to adapt the gain, because the system strength has not increased since the last adaption. If the STATCOM operates under optimal conditions, then the estimated SCL value will not be increased further.

In contrast, it can be seen in Fig. 5 (b), how the block behaves, if the grid strength has increased since the last adaption. Then, the output value of the block (Seen in the lower graph in Fig. 5 (b)) will be positive. This indicates that the estimated SCL has to increase to adapt to the increased grid strength.

The output of this logic is further processed in the integrator block. There it will increase the estimated SCL value for the gain calculation. Simulations with increased grid strength and the correct gain adaption is further shown in the Simulation Section.

### Too fast Dynamics Block

If the strength of the grid has decreased since the last adaption (e.g., during the night, when loads and generation units are reduced), then the STATCOM voltage control responds with too high reactive output change to a voltage disturbance. Therefore, it will cause overshoots in the grid voltage and damped oscillations with defined time constants will occur.

Fig. 6 shows the grid voltage (upper graph) and the voltage error signal (lower graph) with a STATCOM under optimal and too fast dynamics. The higher dynamics due to a high gain value will result in overshoots in the grid voltage and in oscillations around zero in the error signal. The block 'Too fast dynamics' has the purpose to detect these oscillations in the error signal. The block diagram is shown in Fig. 7. The limitation block is not needed for the detection of voltage overshoots.

The time delay for this detection block has been chosen to 20 ms, due to the simulation results shown in Fig. 6. Then, positive and negative values will overlap to result in a negative value after the multiplication. If the voltage measuring system time constant and the controller time constant are different from the simulations performed in this study, then the time delay has to be adapted to the changed STATCOM system time constants. The output of the block is filtered in a way that only negative values can pass. This block can therefore never increase the estimated SCL value.

The upper graph in Fig. 8 (a) shows the voltage error signal and the error signal with time delay of 20 ms. This simulation shows the controller behavior under optimal conditions, there is no need to adapt the

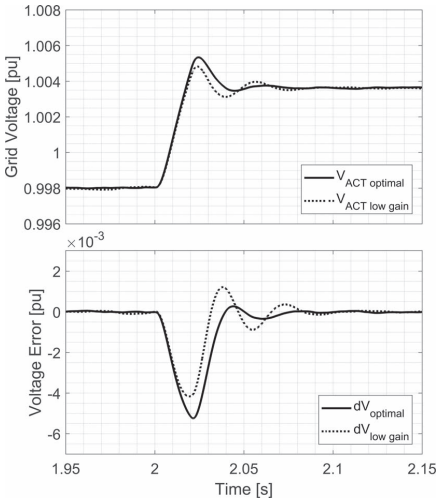


Fig. 6: Voltage error behavior after SCL decrease

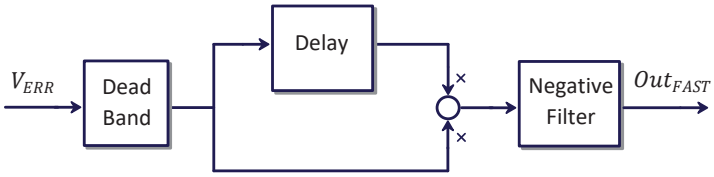


Fig. 7: Too fast dynamics block diagram

gain. The lower graph shows the output of the oscillation detection. It is zero all the time, because there is no adaption needed. These simulation results prove, that the estimated SCL value in the controller will not be reduced further, if it is not needed.

Fig. 8 (b) shows the block behavior if the strength of the grid has decreased severely. Then, there will be overshoots in the STATCOM reactive output, in the grid voltage and also in the resulting voltage error signal. The resulting negative output of the 'Too fast Dynamics' block (as shown in the lower graph in Fig. 8 (b)) will be a negative input to the integrator block. This will result in a reduction of the voltage controller gain and thus to a better dynamic performance.

These overshoots and error oscillations do not only occur if the grid strength decreases. They can also be seen if other dynamic voltage controlling devices, such as a second STATCOM, are activated close to the first STATCOM unit. These overshoots will then also lower the estimated SCL value for both voltage controllers. So the proposed algorithm can guarantee stable adaption to other voltage controlling devices as well as to grid strength changes. This will be further shown in the simulation results in the related Section.

### Integrator Block

The integrator block integrates the sum of the outputs of the two detection blocks. The detection blocks have the output zero almost all the time. This means, that the output of the integrator block will be a constant value for most of the time. The input of the integrator will only be not zero during grid voltage disturbances and then only, if the strength of the grid has changed. This will then change the estimated SCL value and the gain of the voltage controller accordingly.

This estimated SCL value will automatically be adapted to the influence of other dynamic voltage controlling devices as well. So the voltage controllers will adapt their dynamics themselves, if there are

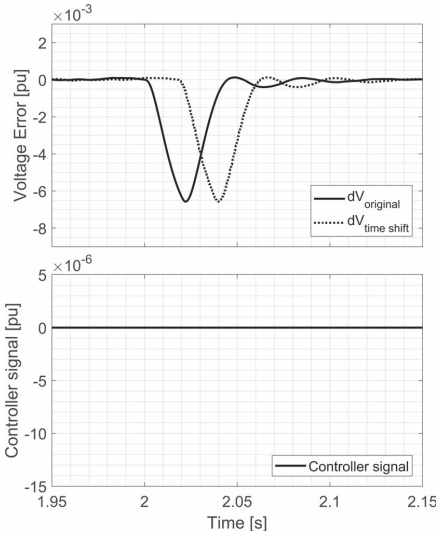


( (a)) SCL decrease block with adapted grid strength

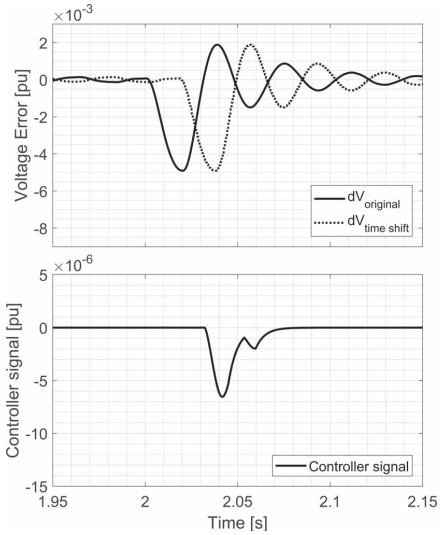


( (b)) SCL decrease block output with decreased grid strength

Fig. 8: Simulation results for the behavior under too fast dynamics

other voltage controlling devices energized or taken out of operation nearby.

## Simulation Verification

To verify this new proposed controller several simulations have been performed. The simulations are performed with EMTDS / PSCAD. A model for a delta configuration STATCOM has been used with controllable voltage sources as representations of the converter arms. The voltage will be simulated in 1 kV steps to represent the output of a converter with 1 kV submodules. The STATCOM is located behind a step-up transformer connected to a 220 kV AC voltage source with a series impedance to simulate different system strength conditions. For the simulations the grid strength will be set to different levels to show the adaption of the controller to these changes.

Step response tests are not a representation for the real system behavior. In a STATCOM application it is not allowed to periodically perform step response tests, because this would cause voltage fluctuations in the grid. So, for a real application test, the behavior due to a change in the grid voltage due to a disturbance is a better controller dynamics test. This voltage disturbance can be either due to a load switching or a line switching event. Several different voltage setpoint, droop control settings, grid SCL values and voltage disturbance levels have been set to verify the behavior under different conditions as well.

### Single STATCOM

The simulations for a single STATCOM installation have been performed with both an increase and a decrease of the grid strength at the beginning of the simulation. At first, the grid strength was increased from 1 GVA to 2 GVA at 3.5 sec. After this, small disturbances in the grid voltage are simulated and the proposed control is validated. The disturbances are the connection and disconnection of an inductive load.

Fig. 9 (a) shows the adaption of the controller behavior according to Section . The upper graph shows the grid voltage change due to the disturbance and then the control back to the reference value. The response of the STATCOM is too slow during the first distortion. After the first adaption of the estimated

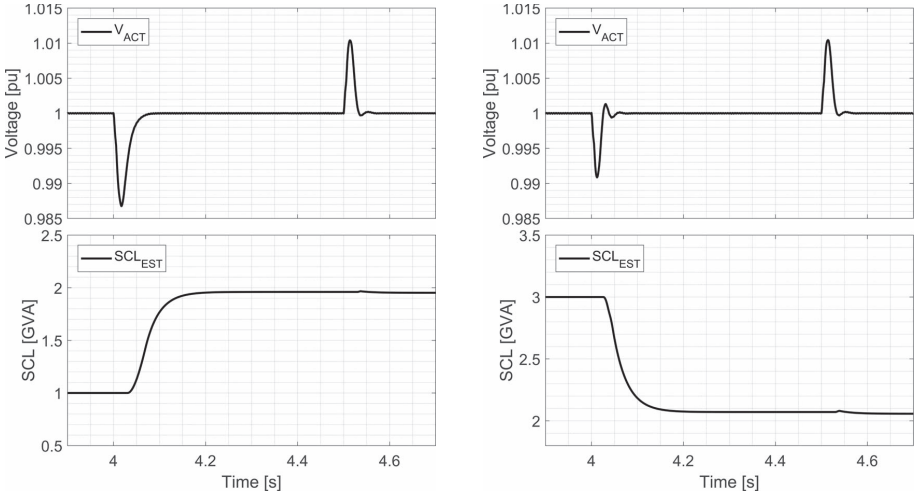


( (a)) Simulation gain value increase needed ( (b)) Simulation gain value reduction needed

Fig. 9: Simulation results for the behavior under too fast dynamics

SCL value (shown in the lower graph) it can be seen, that the control is faster, but stable. The dynamic parameters are listed in Table I.

Table I
Simulation Results with SCL Increase

| | Disturbance Rejection Time | Overshoot |
|---|---|---|
| $1^{st}$ Distortion | 52 ms | 0 % |
| $2^{nd}$ Distortion | 35 ms | 4 % |

After this, the simulations have been performed with decreased grid strength. In the beginning, the grid strength has been set to 3 GVA, then it has been reduced to 2 GVA at 3.5 sec. Afterwards small disturbances (load switching) in the grid voltage are simulated and the control adaption is validated.

The simulation results in Fig. 9 (b) shows that the estimated SCL value decreases if needed. The control dynamics are listed in Table II.

Table II
Simulation Results with SCL Decrease

| | Disturbance Rejection Time | Overshoot |
|---|---|---|
| $1^{st}$ Distortion | 30 ms | 15 % |
| $2^{nd}$ Distortion | 34 ms | 3 % |

The simulation shows that the overshoots in the grid voltage due to a too high STATCOM output have been reduced from 15 % to 3 %.

### Two STATCOMs

If there is one STATCOM already in operation in the grid and then another STATCOM will be enabled nearby, then the gain has to adapt to this new grid condition. In this simulation one STATCOM (STATCOM 1) is in operation in the grid with a short circuit level of 2 GVA. Then, at the simulation time 4.1 sec,

the second STATCOM (STATCOM 2) will be energized and operational at the same bus. Therefore both STATCOMs will control the voltage in the grid. Both STATCOMs have the same voltage reference set-point (1 pu), the same rating (70 MVar) and also the same droop control settings (1 %). The result of this simulation is shown in Fig. 10 (a).

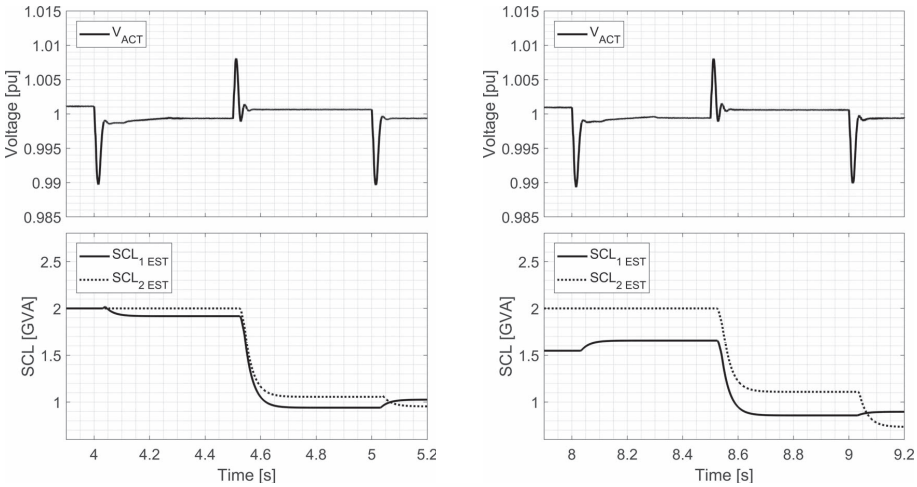


( (a)) Simulation Start-up of second STATCOM

( (b)) Simulation Start-up of second STATCOM with distance

Fig. 10: Simulation results for the behavior under too fast dynamics

As shown in Fig. 10 (a) both STATCOMs adapt independently to the new grid condition and will lower their gain values in the controller to achieve satisfying dynamics after the adaption, as shown in Table III. This will allow both STATCOM units to operate with optimal dynamic performances and the grid voltage can be controlled as requested.

Table III
Simulation Results with two STATCOMs

| | Disturbance Rejection Time | Overshoot |
|---|---|---|
| $1^{st}$ Distortion | 35 ms | 3 % |
| $2^{nd}$ Distortion | 25 ms | 20 % |
| $3^{rd}$ Distortion | 36 ms | 4 % |

Also the performance of the adaption with distances between the different STATCOMs has been analyzed. For this, there is a 20 % additional grid impedance added before the connection points of the two separate STATCOMs. Fig. 10 (b) shows the results of this simulations. It can bee seen, that the first STATCOM has settled to a different starting value, due to the additional impedance.

Table IV shows the performance of the STATCOMs at the connection point of STATCOM 1. When STATCOM 2 is also operational, both will adapt to the new grid constellation independently. It can be seen that the response fulfills the required dynamics and that the controller helps to stabilize also this kind of STATCOM placement in the power grid. This increase of performance is possible without communication being installed between the two units. Therefore, this new controller adaption, if installed in both STATCOMs, will allow the installation of multiple more dynamic voltage controlling devices nearby and with distances, if all have an adaption of the gain value as described in this paper.

Table IV
Simulation Results with two STATCOMs and Distance

| | Disturbance Rejection Time | Overshoot |
|---|---|---|
| $1^{st}$ Distortion | 34 ms | 1 % |
| $2^{nd}$ Distortion | 28 ms | 18 % |
| $3^{rd}$ Distortion | 35 ms | 4 % |

## Conclusions

The paper has discussed a new control method for a stable STATCOM voltage control. One advantage of this new controller is that it needs no communication between the STATCOMs or between the STATCOM and other dynamic voltage controlling devices. If all STATCOMs have this control, then future FACTS devices will no longer cause unwanted dynamic performances or the need of refurbishment with communication between the units.

The new control method is superior to other gain adaptions, because it provides an automated adaption of the gain value, not only cyclical, but whenever there is a severe event in the grid that forces the STATCOM to operate at a different point of operation. This controller adaption operates passively without any forced disturbance in the grid voltage caused by a triggered reactive output change. This new proposed controller has been verified by several simulations with many different setups.

## References


[1] N. G. Hingorani, L. Gyugyi, and M. El-Hawary: Understanding FACTS: Concepts and Technology of Flexible AC Transmission Systems, Wiley Online Library, 2000, vol. 2

[2] G. Romegialli and H. Beeler: Reactive Compensation. Problems and Concepts of Static Compensator Control, IEE Proceedings (Generation, Transmission and Distribution), 1981, vol. 128, no. 6., pp. 382- 388

[3] Coordination of Controls of Multiple FACTS / HVDC Links in the Same System, ser. Brochures thématiques: International Conference on Large High Voltage Electric Systems, CIGRE, 1999, Chapter 4

[4] B. Singh, N. Sharma, and A. Tiwari: Coordinated Control and Interactions between FACTS Controllers in Multi-Machine Power System Environments: An Overview & Issues, Fifteenth National Power Systems Conference (NPSC), IIT Bombay, 2008

[5] Y. Xu and F. Li: Adaptive PI Control of STATCOM for Voltage Regulation, IEEE transactions on power delivery, 2014, vol. 29, no. 3, pp. 1002- 1011

[6] S. A. Al-Mawsawi, M. Qader, and G. Ali: Dynamic Controllers Design for STATCOM, Iranian journal of electrical and computer engineering, 2004, vol. 3, no. 1, pp. 16- 22

[7] J.-x. Xu, L.-c. Xiu, C.-c. Hang, C. Li, Q.-r. Jiang, and Z.-h. Wang: PI Control of STATCOM using Fuzzy Set and Auto-Tuning Techniques, IFAC Proceedings Volume, 1999, vol. 32, no.2, pp. 7340- 7345

[8] A. K. Mahmood, I. I. Ali, and A. A. AL-Gailany: Voltage stability Improvements using Adaptive Controller for STATCOM, Journal of Engineering and Sustainable Development, 2018, vol. 21, no. 2, pp. 129- 148

[9] L. Qing and W. Zengzing: Coordinated Design of Multiple FACTS Controllers Based on Fuzzy Immune Co-Evolutionary Algorithm, Power & Energy Society General Meeting, IEEE, 2009, pp. 1- 6

[10] S. Mohagheghi, Y. del Valle, G. K. Venayagamoorthy, and R. G. Harley: A Proportional-Integrator Type Adaptive Critic Design-Based Neurocontroller for a Static Compensator in a Multimachine Power System, IEEE Transactions on Industrial Electronics, 2007, vol. 54, no. 1, pp. 86- 96

[11] V. Talavat, S. Galvani, and S. R. Marjani: Robust design of PSS and SVC using Teaching-Learning Based Optimization Algorithm, International Conference on Electrical and Electronics Engineering, IEEE, 2017, pp. 72- 75

.

Conference Publication 3 [C3]

# A Frequency Security Analysis of Wind Integrated Power Systems with Frequency Controls

Joachim Steinkohl, Xiongfei Wang, Pooya Davaari, Frede Blaabjerg

The paper has been published at
*18th Wind Integration Workshop 2019* Dublin, Ireland, 2019.


*The layout has been revised.*

# A Frequency Security Analysis of Wind Integrated Power Systems with Frequency Controls

Joachim Steinkohl, Xiongfei Wang, Pooya Davari and Frede Blaabjerg
Department of Energy Technology
Aalborg University, Denmark
Email: joa@et.aau.dk,xwa@et.aau.dk, pda@et.aau.dk and fbl@et.aau.dk

***Abstract*—A power grid with a high penetration of renewable power generation faces new issues that have not been there before. The frequency in the power system is highly related to the mass and the rotational speed of the operational synchronous machines. With more and more power electronic converters as energy generation units, the mechanical rotating mass is decreasing, which causes more and higher frequency disturbances. Several controls for short term frequency controls in the power electronic based generation units have been proposed, but their impact on the frequency reliability is only a minor researched topic. This paper will analyze different basic control strategies in power electronic converters to enhance operational reliability of the power system regarding the short term frequency reliability.**

## I. Introduction

Large amounts of wind and solar power are installed in power grids in power grids all over the world [1]. The high amount of renewable power generation is now at a critical point, where they define the more and more the behavior of the power grid.

One of the challenges with the usage of power electronic converter based generation units is the reduction of rotating mass in the power system, causing higher frequency swings in the power grid [2]. This is based on the power system swing equation, that takes the rated power of all operating synchronous machines ($S_B$) and their time constants ($H$) into account.

$$\dot{f} = (P_{Gen} - P_{Load}) \cdot \frac{f_{nom}}{2 \cdot S_B \cdot H} \tag{1}$$

with

$$S_B = \sum_{n=1}^{N} S_{B\,n} \tag{2}$$

and with

$$H = \frac{1}{S_B} \sum_{n=1}^{N} H_n \cdot S_{B\,n} \tag{3}$$

Often H is called TSI, the total system inertia, the time constant of an entire synchronous area. This TSI, as well as $S_B$ is reduced, when large parts of the loads are supplied by converter based generation units instead of synchronous generators, changing the system behavior during transient active power events.

The power system frequency changes from the nominal range when severe events, such as generator failures, transmission line trips or big load outages occur. A lack of injected power causes the conventional generators to slow down. An excessive amount of generated power speeds up the generators, increasing the system frequency. The wide usage of converter based generation units already causes the deactivation of some conventional units during a high renewable penetration situation, changing the rated power and the time constant H in the swing equation.

Frequency controls have been set in place to keep the frequency at the nominal value. These frequency controls balance the produced and consumed power by adjusting the generated power of the conventional generation units. This takes part in different time frames, reaching from up to 10 seconds (primary control) to several minutes (secondary and tertiary control) [2]. Primary frequency control is droop based, changing the power output from the running generation units depending on the frequency deviation. The activation of reserve generation units, for additional support during under frequencies is also a strategy for maintaining a stable system frequency. Nevertheless this is not considered in this frequency security analysis.

These frequency controls have, due to the increasing renewable generation, come to a point where the system frequency can not be reliably maintained only by changing the power output of the conventional units. This has been reported by TSOs (Transmission System Operators) being one of the main challenges in future power grids [3]. To overcome these issues, the curtailment of wind power during abnormal over frequency situations is already in place in many grid codes worldwide. This supports the conventional generation units in the handling of these events, showing the awareness of TSOs for this issue. And it shows also the capabilities of the converter based units to participate in maintaining a high system operational reliability.

Other, more advanced control strategies are also highly researched, reaching from the emulation of inertia or virtual synchronous machines [4]–[6] up to fixed output increase for short time periods, as certified in [7]. These controls are feasible, but have not been implemented on a wide scale and are not part of any grid codes so far. Especially [7] proofed, that the short term power output increase is possible without further equipment, with respect to converter current limitations and other factors. This paper focuses two control schemes. The first is a droop based control, the other one uses the frequency deviation as control input.

The reliable supply of electric energy to the customers is the goal of the entire power system. It can be analyzed in its performance under different aspects. One is the adequacy of the system, meaning the ability of the system to supply the loads under all possible steady state operation points. Another one is the operational security, which is the capability of the system to withstand a severe disturbance

with minimum impact to the system operation. This paper will focus on the system security, especially the ability of the system to maintain a reliable system frequency with a high penetration level of wind power. An overview of the different aspects of the system reliability with focus on the dynamic security is shown in Fig. 1.

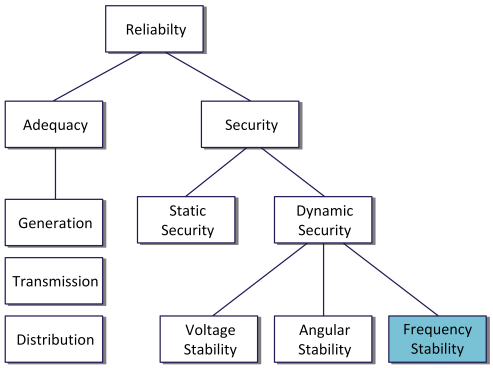


Fig. 1: Scheme of the System Reliability Analysis.

The impact of wind power to system adequacy has been intensely studied [8]. Also the impact on the short term frequency reliability has been intensively studied before [9]–[11]. These studies include the requirements of wind turbines to curtail their power output under abnormal over frequency situations, as it is nowadays present in many grid codes all over the world. The probabilistic based system security assessment uses time series simulation with respect to the occurrence rate of possible events under different system conditions. Because the system load is not constant and the wind is not always fully available, there are changes in the system behavior to the same disturbances at different points of operation.

The number and duration of abnormal frequency events is measured from the simulation outcome. Also the amount of wind energy curtailment, and the amount of curtailed system load. These indexes allow a probabilistic verification of the system security, hence the ability of the system to withstand a severe active power disturbances.

The influence of additional frequency controls in the power electronic based generation units on the power system frequency security is not evaluated for now. This paper analyzes the system behavior with additional, basic control strategies, providing a guideline for a more and more power electronic converter based power system.

## II. Methods

The used power system for the reliability calculation is a modified version of the IEEE-9 Bus system [12], as it can be seen in Fig. 2, with detailed load variations as in [13]. This system is well established for different types of reliability analysis, from security to adequacy assessment. Also the integration of wind turbines into the system has been done before, as in [14], [15]. In [14] they also focus on the frequency security due to the power electronic based unis, but without additional frequency support functionality in the respective units.

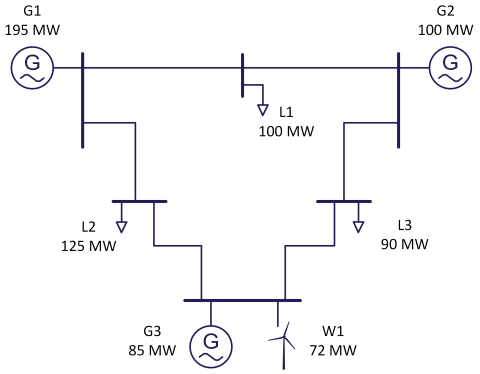


Fig. 2: Modified IEEE 9-Bus System with Wind Integration.

For the frequency reliability evaluation, the system can be expressed with a single bus, taking all loads, conventional generation units and additional equipment into the one bus [16]. The different parts of the power system will be further analyzed in the following sections.

### A. System Load

The power system load is not fixed during the daily or yearly operation, but changes over time. The system load can be represented by the maximum load during every hour of a year, as in [12], which will be used in this analysis as well. This results in a load duration curve (LDC) as shown in Fig. 3, where the peak load throughout the year is 315 MW, as in the IEEE 9-Bus system.

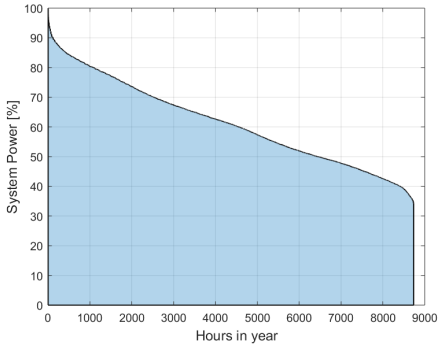


Fig. 3: Load Duration Curve of the Power System.

For the system security assessment the probability of higher and lower load demands throughout the operation has to be taken into account, hence the load level determines the active conventional power generation units in the steady state with respect to the actual wind power injected to the power grid. This load duration curve is discretized in order to start the time series simulation from a stable steady state value. Load trips can occur during the system operation, which can be caused by tripping transformers, lines or buses or internal issues. These load trips cause rising frequencies, which has to be controlled by reducing the output power

of the generation units. These load reduction are parts of the rated system loads with respect to the load duration curve. Also load curtailment during under frequencies has been implemented, stabilizing the system frequency after a severe generation outage [17].

### B. Generation Units

The conventional generation units in the modified IEEE 9-Bus test system have a total capacity of 380 MW. The power rating has been slightly increased from the original IEEE 9-Bus system (320 MW), allowing n-1 security and spinning reserve capability. Hence all units are simulated in one bus, it is not necessary to distribute the generation units exactly as in the three generation buses. In the proposed test grid, each generator has a certain probability of a trip every year, calculated with the mean time to failure (MTTF) [12], as shown in Table I.

TABLE I: Generator Data

| Rated Power $[MW]$ | Number of Units | MTTF $[hrs]$ | MTTR $[hrs]$ | H $[s]$ |
|---|---|---|---|---|
| 5 | 4 | 2940 | 60 | 2.5 |
| 10 | 4 | 450 | 50 | 3.0 |
| 20 | 5 | 1960 | 20 | 3.5 |
| 30 | 2 | 1960 | 40 | 4.0 |
| 40 | 4 | 1200 | 50 | 4.3 |

The generation units are capable of providing primary and secondary control as used in [11].

### C. Wind Power

The actual Wind Power injected into the power system is also not constant, but determined by the actual wind speed blowing and the limitations of the turbines. The wind speed probability has been determined for different locations around the world. Its probability can be expressed with a Weibull-Distribution with varying parameters [18], which can be compared with the capacity factor [19]. This wind speed has to be recalculated to the wind power output, respecting cut-in wind speed, cut out wind speed and maximum wind power. This leads then to the wind power duration curve from Fig. 4. In this analysis, the wind turbines operate with 2500 full load hours, the capacity factor is therefore 28.5 %.

For the reliability evaluation of wind integrated power systems, the different levels of wind speed and their probabilities have to be taken in consideration. The installed wind power is 72 MW power. The actual injected power is based on the probability of wind speed and the resulting produced power of the wind turbine. The wind speed is assumed to be constant at all wind turbines, an independent wind speed for many smaller units can be a part of future research. The wind turbine control is includes the grid requirement for over frequency output reduction (frequency response) as in the Danish grid code [20] (seen in Fig. 5).

This control reduces the output power during over frequency situation to support a stable operation of the grid. This control has a limited range and its response time has to be smaller than 10 sec. Nevertheless, it does not impact the frequency derivative, hence other controls may be needed

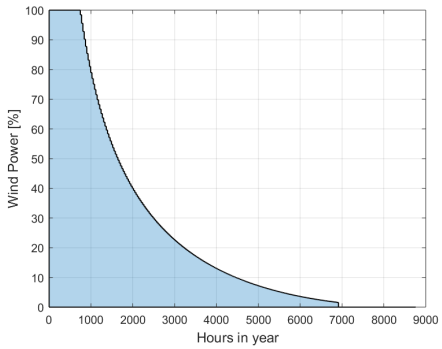


Fig. 4: Wind Power Duration Curve.

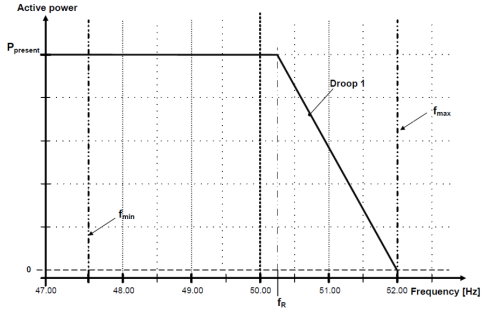


Fig. 5: Danish Grid Code requirement regarding the frequency response of Wind Power Plants.

with a wider integration of converter based units in power grids.

The system TSI changes with the wind power installed. This is due to the reduction of rotating mass during the wind power injection, as shown in Fig. 6. The base case refers to the IEEE 9-Bus System, without wind turbines, so all generated power is produced by conventional generation units. When the wind turbines are included, they displace some generation units, reducing the TSI during wide parts of the operation time. The minimal TSI changes therefore from 3.5 sec to only 2.5 sec, meaning a severe weakening of the system during these hours of operation.

The shown reduction in the transmission system inertia shows the weakened system capability to withstand active power imbalances. especially the reduction of the lowest value from 3.5 sec to 2.5 sec verifies this. The TSI shown in Fig. 6 describes the generation units being in operation during the steady state. The trip of a generation unit can cause a further drop of the transmission system inertia.

### D. Additional Frequency Controls

The rate of change of frequency (RoCoF) is mainly dependent on the rotating mass of the synchronous generators and the active power imbalance. The replacement of the conventional generators with power electronic based units is increasing the RoCoF during active power imbalances, leading also to increased frequency deviations.

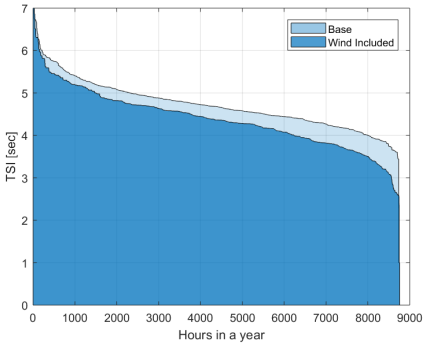


Fig. 6: TSI of the IEEE 9-Bus System with and without Wind Power Generation.

Different additional frequency controls have been proposed in the past. These range from droop controls, over inertia emulating controls to virtual synchronous machines or constant power injections at certain frequency thresholds.

This paper focuses on droop based frequency controls and Inertia emulating controls. These controls are set up with different parameters to change their behavior. The utilization of active power increase during low frequency events requires additional costs. To take this into account, both strategies will be once tested with the possibility of active power increase and once without. This helps to determine the value of this enlarged control range.

*1) Droop Control:*

The droop based control structure is shown in Fig. 7.

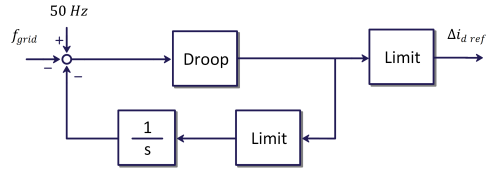


Fig. 7: Droop Control Structure.

The initial response follows the droop characteristic, hence on the long term the output is brought back to the maximal output with the limiter and the integrator, bringing the frequency deviation back to zero in steady state. This control is designed to help the conventional generation units during the initial frequency deviation, but minimizes the long term output reduction of the wind turbines.

The maximal power reduction in this control is 0.2 pu. The limit for the power output increase is once set to 0, allowing no power increase. Later, this limiter is changed, allowing a 0.1 pu power increase. This additional power can come from the rotational energy of the blades or from battery solutions. In this study, the origin of the additional power is not determined, nor of further interest.

The droop value has been set to 1, causing a power reduction of 0.1 pu at a frequency deviation of 0.1 Hz. Meaning, the control is fully active, before the frequency response, as required in the grid code (as in Fig. 5), is activated. The second evaluation uses a droop value of 2, causing a reduction of 0.1 pu at a frequency deviation of only 0.05 Hz.

*2) Emulation of Inertia:*

The direct reduction of the frequency deviation, the RoCoF, is the aim of the second tested control. The control structure with the controller gain is shown in Fig. 8.

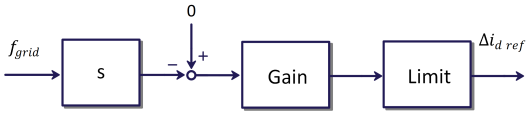


Fig. 8: Inertia Emulating Control Structure.

The controller is limited the same way as with the droop control, allowing a 0.2 pu power reduction in the first evaluation. The power increase is there deactivated. Afterwards, 0.1 pu additional power can be provided for a short duration to stabilize the system during frequency drops. The first controller gain is chosen to allow a 0.1 pu power change at a RoCoF of 0.2 Hz/sec. The second controller gain higher, causing a 0.1 pu power change at a RoCoF of just 0.1 Hz/sec

### *E. Reliability Evaluation*

Following the reliability parameters presented in [11], the abnormal frequency events can be compared with and without additional frequency controls in the wind turbines. The reliability indexes are the number and duration of abnormal frequencies and the energy used for frequency regulation by the conventional generation units. Also the not used wind energy and the surplus wind energy due to additional controls are monitored. Also the load curtailment is taken into consideration, measuring the amount of not supplied energy. The nominal frequency of the tested power system is 50 Hz, with the abnormal frequency occurring at a frequency deviation of $\pm 0.2$ Hz.

The parameters are evaluated, taking the probabilities of the active load, actual wind speed and the probability of the disturbances into consideration, combining it up to indexes for the evaluated operational frequency security. As an example, the calculation of the expected number of over frequency events (ENOF) is shown in (4).

$$ENOF = \sum_{n=1}^{N} p_{Load,n} \cdot p_{Wind,n} \cdot p_{Event,n} \cdot ENOF_n \quad (4)$$

All determined indexes are shown in Table II, where ”Exp.” stands for the expected system index.

The IENS is the energy, which is provided by the conventional generation units for primary and secondary control. ECU is the amount of energy that has been not produced due to frequency controls by the conventional generators. These energies have a severe influence on the economic operation of the power system. Therefore, they have to be considered for the reliability evaluation of the system.

TABLE II: Reliability Evaluation Indexes

| Index | Unit | Full Name |
|---|---|---|
| ENOF | | Exp. Number of Over Frequency Events |
| ENUF | | Exp. Number of Under Frequency Events |
| ENAF | | Exp. Number of Abnormal Frequency Events |
| EOFD | min | Exp. Over Frequency Duration |
| EUFD | min | Exp. Under Frequency Duration |
| EAFD | min | Exp. Abnormal Frequency Duration |
| EENS | MWh | Exp. Energy Not Served to loads |
| EWEW | MWh | Exp. Wind Energy Wasted |
| EWES | MWh | Exp. Wind Energy Surplus Supplied |
| IENS | MWh | Indirect Energy Not Supplied |
| ECU | MWh | Unnecessary Energy Consumption |

## III. Comparison of tested Control Strategies

Several simulations have been performed with the different events and varying wind power injected into the power grid and load consumed by the system. The results of these scenarios are shown in the following sections. First some time series results and afterwards the reliability comparison of the droop control implementations. The shown simulation show all the same steady state operation, where the system load is 190 MW and the injected wind power is 72 MW.

### A. Frequency behavior with Droop Control

The following figures show the system behavior with additional droop control in the wind turbines. In Case 1 only power reduction is possible, whereas the controller setup in Case 2 has the possibility to increase the power output as well.

#### 1) Case 1: Only Power Reduction:

The simulation results in Fig. 9a show the frequency behavior after a load disconnection of 8 MW. The reduced wind power injected into the grid by the additional droop controls is shown in Fig. 9a.

The simulation results of this case shows the reduction of the maximum frequency deviation in Fig. 9a. Nevertheless, the frequency still rises over 50.2 Hz, mening an abnormal frequency event. But the duration of this event is severely reduced with this control, resulting a slightly reduced reliability index for this simulation outcome. The wind energy (shown in Fig. 9b), which is wasted increases from 5 MW to 8 MW with the increased droop parameter. It can also be noted, that the initial RoCoF is not changing, due to the response time of the control of around 2 sec.

#### 2) Case 2: Power Increase Possible:

The second shown event is the same initial grid condition and wind injection, but with a generation loss of 7 MW. Now, the droop control is also able to increase the output by 0.1 pu.

Fig. 10a shows the enhanced system frequency during the disturbance, hence the frequency drop is less severe. It can be noted, that the increased controller gain only slightly enhances the frequency behavior, a higher value has even potential to cause more oscillations in the system. Fig. 10b shows the increase of wind output during the low frequency duration. The higher controller gain is not causing a higher power output in the first swing, even though the limit of 7.2 MW has not been reached jet.

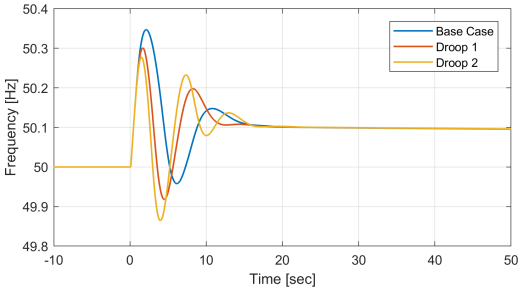


(a) System Frequency during Disturbance in Case 1.

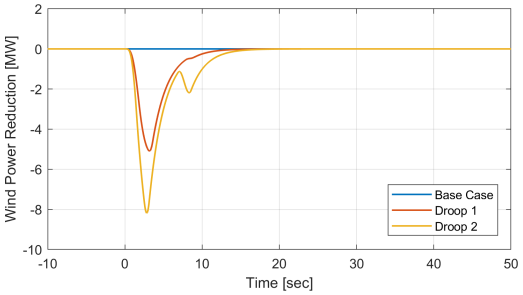


(b) Reduced Wind Power during Disturbance in Case 1.

Fig. 9: Simulation Case 1 with Droop Control.

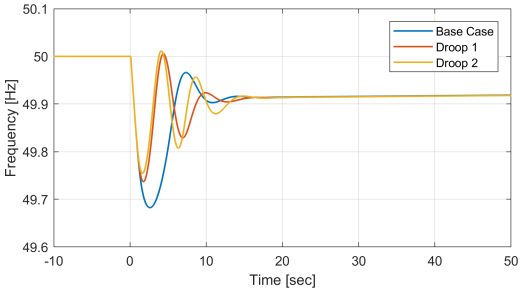


(a) System Frequency during Disturbance in Case 2.

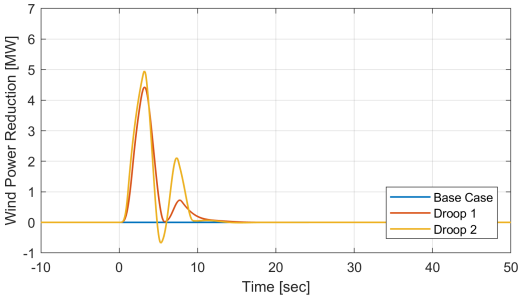


(b) Increased Wind Power during Disturbance in Case 2.

Fig. 10: Simulation Case 2 with Droop Control.

These, and many more time-series results are then transformed into reliability parameters in the following section to

see the overall effect of the different controls to the system performance during transient frequency events.

### B. Reliability with Droop Control

The reliability indexes of the wind integrated power system is compared with and without the droop control in Table III. The wind integration reduces the inertia in the system due to the deactivation of conventional generation units, when not needed.

TABLE III: Reliability with Droop based Control (Only Reduction)

| Parameter | No Wind | Wind Included | Droop 1 | Droop 2 |
|---|---|---|---|---|
| ENOF | 5.84 | 6.44 | 5.67 | 5.48 |
| ENUF | 80.1 | 82.24 | 81.95 | 81.94 |
| ENAF | 85.94 | 88.69 | 87.62 | 87.42 |
| EOFD | 0.543 | 0.885 | 0.588 | 0.569 |
| EUFD | 17.95 | 19.98 | 19.94 | 19.93 |
| EAFD | 18.49 | 20.83 | 20.51 | 20.50 |
| EENS | 348.6 | 370.2 | 369.9 | 369.9 |
| EWEW | 0 | 0.0766 | 0.0466 | 0.0553 |
| IENS | 150.2 | 145.2 | 145.2 | 145.2 |
| ECU | 9.2 | 10.11 | 10.11 | 10.11 |

It can be seen in Table III, how the installation of the wind turbines without further control affects the system frequency security compared to the system without wind turbines installed. Mainly, the expected energy not served goes up, meaning more and longer load curtailments. But also the number and duration of abnormal frequency events rises. The ECU, the energy used by the conventional units to control over frequency events rises, meaning a higher need for power reductions during the operation. This can be explained with the amount of load curtailments. during the events, where load curtailments occur, there is a lesser need for the generation units to increase their power, because there are fewer loads in the system.

The usage of additional output reduction controls depending on the frequency deviation is severely reducing the expected number and duration of over frequency events. The under frequency occurrences and duration are not severely affected, hence the added controls are not able to provide additional energy during these events. Interesting is the change of the expected wind energy wasted, which is reduced during the usage of the first droop parameter, but increased again slowly with the higher droop. This indicates an optimal droop coefficient for the wasted energy.

Table IV shows the frequency security indexes with also power increase possible for the wind turbines.

The option to increase the power output even for a short time has a severe effect on the system security. The load curtailment is severely reduced, even below the original system without wind turbines. Also the number of under frequency events is slightly reduced, compared to the initial value. This enhances system behavior comes with the drawback of the energy that has to be provided by the converter based units.

The energy used by the conventional generation units for the frequency control (IENS and ECU) is almost not changed with the additional frequency controls. This is primarily due to the short time of the control interactions compared to the long control duration of primary and secondary frequency control. The IENS is not increasing, because the wind turbines can clear the critical frequency deviations in a short period of time.

TABLE IV: Reliability with Droop based Control

| Parameter | No Wind | Wind Included | Droop 1 | Droop 2 |
|---|---|---|---|---|
| ENOF | 5.84 | 6.44 | 5.86 | 5.73 |
| ENUF | 80.1 | 82.24 | 81.34 | 79.5 |
| ENAF | 85.94 | 88.69 | 87.2 | 85.23 |
| EOFD | 0.543 | 0.885 | 0.55 | 0.54 |
| EUFD | 17.95 | 19.98 | 18.7 | 18.62 |
| EAFD | 18.49 | 20.83 | 19.25 | 19.16 |
| EENS | 348.6 | 370.2 | 347.97 | 339.1 |
| EWEW | 0 | 0.0766 | 0.0488 | 0.061 |
| EWES | 0 | 0 | 0.0623 | 0.0851 |
| IENS | 150.2 | 145.2 | 148.14 | 148.6 |
| ECU | 9.2 | 10.11 | 9.63 | 9.55 |

### C. Frequency behavior with Inertia based Control

The frequency behavior with additional inertia based control is the point of interest in this section. The control is supposed to reduce the rate of frequency change and therefore also the maximum frequency deviation, resulting in a more reliable system. The shown simulations are the same circumstances as in Section III-A.

#### 1) Case 1: Pure Power reduction:

The results of the simulation for this case is shown in Fig. 11. Fig. 11a shows the frequency behavior after the load disconnection of 8 MW. The reduced wind power injected into the grid due to the additional control is shown in Fig. 11b. An increase of wind power is not possible here.

These simulation results show the change wind power reduction (Fig. 11b) compared to the droop based control. The power reduction here is lower than with the droop control in Fig. 9b (6 MW compared to 8 MW), but it decays faster due to the control characteristics. This faster response is responsible for the improved frequency behavior with lesser wasted wind energy during this system setup and disturbance.

#### 2) Case 2: Power Increase Possible:

The second shown event is the same initial grid condition and wind injection, but with a generation loss of 7 MW. Now, the droop control is also able to increase the output by 0.1 pu.

The Fig. 12a shows the system frequency during the weakened grid condition with a more dynamic inertia control. The wind power change is shown in Fig. 12b. Further increase of the controller gain constant (MW change due to Hz/sec change) can nevertheless lead to system instabilities and oscillations in very weak grid conditions. The balance is therefore to design the control parameters together with the changing system dynamics.

### D. Reliability with Inertia

The reliability indexes of the IEEE 9 Bus wind integrated system with control schemes to emulate inertia are shown in Table V. This control only reduces the injected wind power,

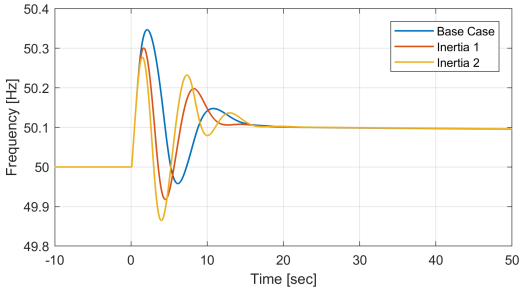


(a) System Frequency during Disturbance in Case 1.

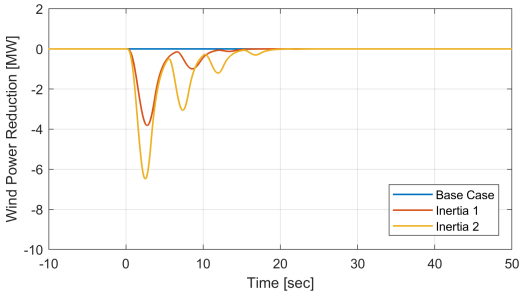


(b) Reduced Wind Power during Disturbance in Case 1.

Fig. 11: Simulation Case 1 with Inertia Control.

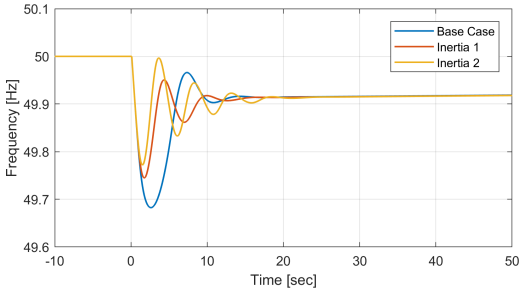


(a) System Frequency during Disturbance in Case 2.

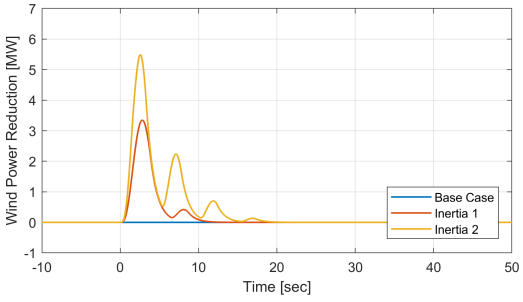


(b) Increased Wind Power during Disturbance in Case 2.

Fig. 12: Simulation Case 2 with Inertia Control

therefore the control is limited in its performance regarding under frequency events.

TABLE V: Reliability With Inertia Control (Pure Reduction)

| Parameter | No Wind | Wind Included | Inertia 1 | Inertia 2 |
|---|---|---|---|---|
| ENOF | 5.84 | 6.44 | 5.94 | 5.67 |
| ENUF | 80.1 | 82.24 | 81.94 | 81.88 |
| ENAF | 85.94 | 88.69 | 87.88 | 87.55 |
| EOFD | 0.543 | 0.885 | 0.607 | 0.576 |
| EUFD | 17.95 | 19.98 | 19.92 | 19.92 |
| EAFD | 18.49 | 20.83 | 20.53 | 20.50 |
| EENS | 348.6 | 370.2 | 369.9 | 369.9 |
| EWEW | 0 | 0.0766 | 0.0754 | 0.0822 |
| IENS | 150.2 | 145.2 | 145.2 | 145.2 |
| ECU | 9.2 | 10.11 | 10.11 | 10.11 |

The inertia based control with only power output reduction has, as well as the droop based control, the potential to reduce the number and duration of over frequency events. It has to be noted, that the expected wind energy wasted is nevertheless not severely dropping as in Table III. This means, that some over frequency events can be avoided with this control structure, but the majority of load trips still causes frequency rises over 50.2 Hz.

The system reliability parameters change with as shown in Table VI, when the control is designed to also allow a 0.1 pu power increase with emulated inertia. Now it is possible to control the system frequency over a much wider range, enhancing the system performance during the loss of active power generation.

TABLE VI: Reliability with Inertia Emulating Control

| Parameter | No Wind | Wind Included | Inertia 1 | Inertia 2 |
|---|---|---|---|---|
| ENOF | 5.84 | 6.44 | 5.86 | 5.62 |
| ENUF | 80.1 | 82.24 | 79.4 | 78.4 |
| ENAF | 85.94 | 88.69 | 85.26 | 84.02 |
| EOFD | 0.543 | 0.885 | 0.588 | 0.535 |
| EUFD | 17.95 | 19.98 | 18.46 | 18.2 |
| EAFD | 18.49 | 20.83 | 19.04 | 18.735 |
| EENS | 348.6 | 370.2 | 337.8 | 326.4 |
| EWEW | 0 | 0.0766 | 0.035 | 0.0398 |
| EWES | 0 | 0 | 0.12 | 0.153 |
| IENS | 150.2 | 145.2 | 149.6 | 149.7 |
| ECU | 9.2 | 10.11 | 9.63 | 9.62 |

The possibility to increase the power output with the emulation of inertia has a severe effect on the load curtailment. The expected energy not supplied index is severely dropping. But in order to achieve this, more energy has to be supplied by the wind turbines during short periods. Nevertheless, this control seems to have a more severe effect on the overall system performance than droop based control structures.

It can be seen in Table VI, as well as in Table reftab:InertiaReliabilityResultUp, that the control has a much higher influence on avoiding load curtailments (at frequencies below 49 Hz) than on avoiding frequency drops below only 49.8 Hz. The response time of the converter controls seems to give severe limitations to in avoiding the majority of abnormal under frequency states.

## IV. Conclusion

The paper shows the impact of two different frequency control schemes in a highly wind integrated power system

to the system frequency security. The converter based generation units have the possibility to contribute to a stable system operation with controlled power reduction, but this comes together with wasted wind energy and therefore high economic drawbacks. The installation of energy storage or the usage of rotational energy from the blades seems to be a viable step to contribute to a power electronic based power system, reducing the need for load curtailment.

Different kinds of controls can be implemented in power electronic based generation units, all changing the system frequency behavior. This paper is therefore not a finished analysis of all possible controls, but it shows trends, which controls are effective with respect to the system frequency security. The finding of an optimal balance between wasted energy, additional equipment and system performance depends on the system structure as well as on the amount of wind generation and has to be further researched.

A high integration of converter based units, replacing a severe number of conventional generation units, can be realized with different approaches. One of them is the usage of additional frequency control schemes, another is an increase of spinning reserve in the power system. An economical evaluation of the different possibilities has to be done in future research, allowing a secure system operation with reasonable costs.

## ACKNOWLEDGMENT

This work is supported by the Reliable Power Electronic-Based Power Systems (REPEPS) project at the Department of Energy Technology, Aalborg University as a part of the Villum Investigator Program funded by the Villum Foundation.

## REFERENCES

[1] REN21. (2018) Renewables 2018 Global Status Report. (Date last accessed 30-Aug-2019). [Online]. Available: http://www.ren21.net/gsr-2018

[2] P. Kundur, N. J. Balu, and M. G. Lauby, *Power System Stability and Control*. McGraw-Hill New York, 1994, vol. 7.

[3] MIGRATE. (2016) Deliverable D1.1, Report on Systemic Issues. (Date last accessed 30-Aug-2019). [Online]. Available: https://www.h2020-migrate.eu/downloads.html

[4] P. Keung, P. Li, H. Banakar, and B. T. Ooi, "Kinetic Energy of Wind-Turbine Generators for System Frequency Support," *IEEE Transactions on Power Systems*, vol. 24, no. 1, pp. 279–287, Feb 2009.

[5] N. R. Ullah, T. Thiringer, and D. Karlsson, "Temporary Primary Frequency Control Support by Variable Speed Wind Turbines Potential and Applications," *IEEE Transactions on Power Systems*, vol. 23, no. 2, pp. 601–612, May 2008.

[6] J. M. Mauricio, A. Marano, A. Gomez-Exposito, and J. L. Martinez Ramos, "Frequency Regulation Contribution Through Variable-Speed Wind Energy Conversion Systems," *IEEE Transactions on Power Systems*, vol. 24, no. 1, pp. 173–180, Feb 2009.

[7] Ørsted A/S. (2018) Enhanced Frequency Control Capability (EFCC) - Wind Package Report - Frequency Support Outlook. (Date last accessed 30-Aug-2019). [Online]. Available: https://www.nationalgrideso.com/document/136161/download

[8] R. Billinton, R. Karki, Y. Gao, D. Huang, P. Hu, and W. Wangdee, "Adequacy Assessment Considerations in Wind Integrated Power Systems," *IEEE Transactions on Power Systems*, vol. 27, no. 4, pp. 2297–2305, 2012.

[9] P. Wang, Z. Gao, and L. Bertling, "Operational Adequacy Studies of Power Systems with Wind Farms and Energy Storages," *IEEE Transactions on Power Systems*, vol. 27, no. 4, pp. 2377–2384, 2012.

[10] N. Farrokhseresht, H. C. Orestica, and M. R. Hesamzadeh, "Determination of Acceptable Inertia Limit for Ensuring Adequacy under High Levels of Wind Integration," in *11th International Conference on the European Energy Market (EEM), 2014*. IEEE, 2014, pp. 1–5.

[11] C. Liang, P. Wang, X. Han, W. Qin, R. Billinton, and W. Li, "Operational Reliability and Economics of Power Systems with Considering Frequency Control Processes," *IEEE Transactions on Power Systems*, vol. 32, no. 4, pp. 2570–2580, 2017.

[12] P. M. Subcommittee, "IEEE Reliability Test System," *IEEE Transactions on Power Apparatus and Systems*, vol. PAS-98, no. 6, pp. 2047–2054, Nov 1979.

[13] Reliability Test System Task Force of the Application of Probability Methods Subcommittee, "The IEEE Reliability Test System-1996," *IEEE Transactions on Power Systems*, vol. 14, no. 3, pp. 1010–1020, Aug 1999.

[14] H. Ahmadi and H. Ghasemi, "Maximum Penetration Level of Wind Generation Considering Power System Security Limits," *IET Generation, Transmission & Distribution*, vol. 6, no. 11, pp. 1164–1170, 2012.

[15] M. EL-Shimy, M. A. L. Badr, and O. M. Rassem, "Impact of Large Scale Wind Power on Power System Stability," in *2008 12th International Middle-East Power System Conference*, March 2008, pp. 630–636.

[16] R. Billington and R. N. Allan, "Reliability Evaluation of Power Systems," 1984.

[17] ENTSO-E. (2015) P5Policy 5: Emergency Operations. (Date last accessed 30-Aug-2019). [Online]. Available: https://docstore.entsoe.eu

[18] K. Conradsen, L. Nielsen, and L. Prahm, "Review of Weibull Statistics for Estimation of Wind Speed Distributions," *Journal of Climate and Applied Meteorology*, vol. 23, no. 8, pp. 1173–1183, 1984.

[19] N. Boccard, "Capacity Factor of Wind Power realized Values vs. Estimates," *Energy Policy*, vol. 37, no. 7, pp. 2679 – 2688, 2009.

[20] "Technical Regulation for Wind Power Plants, Denmark," (Date last accessed 30-Aug-2019). [Online]. Available: https://en.energinet.dk

.

# Journal Publication 1 [J1]

## Assessment Accuracy of Power System Frequency Security with Additional Frequency Controls in Wind Turbines

Joachim Steinkohl, Xiongfei Wang, Pooya Davaari, Frede Blaabjerg

The paper is in press at
*IET Renewable Power Generation* 2021.


*The layout has been revised.*

IET Renewable Power Generation

*Research Article*

IET Journals
The Institution of Engineering and Technology

ISSN 1751-8644
doi: 0000000000
www.ietdl.org

# Assessment Accuracy of Power System Frequency Security with Additional Frequency Controls in Wind Turbines

*Joachim Steinkohl*[1*], *Xiongfei Wang*[1], *Pooya Davari*[1], *Frede Blaabjerg*[1]

[1] *Department of Energy Technology, Aalborg University, Pontoppidanstræde 111, Aalborg, Denmark*
** E-mail: joa@et.aau.dk*

**Abstract:** Power grids all over the world are nowadays facing high penetrations of renewable power generation. The converter based generation units play a major role in system behavior and operation. Thereby, also the reliability of the power system is impacted in many different aspects. It has to be verified whether the frequency reliability assessment, which is often studied by simulations, is still accurate, every time a new control structure is considered. For this, the number of simulations should not be further increased if possible, in order to keep the computational efforts low. In this study, we verify that the assessment outcome will be accurate when the LDC and WPC of a system are described well enough. This is shown to be true for different frequency controls, implemented in wind power plants in the system. Besides, the effect of different LDCs and WPCs are analyzed, as they can change over time. The used methodology is validated on the IEEE-reliability test system (IEEE RTS).

## Nomenclature

| | |
|---|---|
| LDC | Load Duration Curve |
| MCS | Monte-Carlo-Simulation |
| TSO | Transmission System Operator |
| WPC | Wind Power Curve |
| IEEE RTS | IEEE Reliability Test System |
| NOF | Expected Number of Over-Frequency Events |
| NUF | Expected Number of Under-Frequency Events |
| ENAF | Expected Number of Abnormal Frequency Events |
| OFD | Expected Over-Frequency Duration, min |
| UFD | Expected Under-Frequency Duration, min |
| EAFD | Expected Abnormal Frequency Duration, min |
| ENS | Expected Energy Not Served to loads, MWh |
| EWEW | Expected Wind Energy Wasted, MWh |
| EWES | Expected Wind Energy Surplus Supplied, MWh |
| IENS 1 | Indirect Energy Not Supplied by Primary Frequency Control, MWh |
| IENS 2 | Indirect Energy Not Supplied by Secondary Frequency Control, MWh |
| ECU 1 | Unnecessary Energy Consumption by Primary Frequency Control, MWh |
| ECU 2 | Unnecessary Energy Consumption by Secondary Frequency Control, MWh |

## 1 Introduction

Large amounts of wind and solar power are installed in power grids all over the world [1]. The level of penetration has reached a point where it severely affects the behavior of the power grid. One of the main challenges with this extensive usage of wind and solar power is the reduction of rotating mass in the power system. This reduction is seen as a major concern from TSOs to ensure the reliable operation of the grid. Reduced inertia is causing faster and more severe frequency deviations when a disturbance occurs [2]. Extensive studies on the changing frequency behavior are performed, meaning increasing maximum frequency deviations, as well as faster rates of change of frequency (RoCoF) [3, 4]. It is shown that the conventional frequency controls (as described in [5–7]) are not enough to keep a high system frequency quality [8, 9].

The TSOs are therefore going through a fundamental transition in their requirements for grid connections. Several grid codes demand power curtailment of renewable generation units depending on frequency deviations that are now established in many countries all over the world. The demanded controls base on classical current-controlled units, with frequency controls dependent on the measured system frequency deviation [10–13]. So far, synchronous machine emulation controls (as in [14–17]) are not yet seen in the grid requirements and are therefore not considered in this study.

The system operational reliability can be used to verify the adequate supply of all loads in the power system. The effect of wind generation on the power system reliability is well understood [18–22]. In addition, over-frequency control using power curtailment is taken into consideration in these studies [23–25]. The effect of the additional controls is evaluated by making a contingency analysis. There, different steady-state operations are considered, and then the dynamic system performance during contingencies is analyzed. The number of system states and analyzed contingencies varies in the studies.

Often, the evaluation of the system reliability can be done analytically [26] or by using MCS [21, 22]. Other approaches are using artificial intelligence to determine the state of the system [27]. The system reliability is determined with a deterministic approach in this study to achieve comparable results. Multiple system states with a certain probability are chosen for the steady-state operation. MCS has the drawback of adding additional uncertainty to the assessment process, which is usually neglected by a high number of states considered. Ref. [28] uses MCS with a defined number of 1000 simulations, but it is not verified how this number is found. On the other hand, in [29], 100 simulations with MCS is used as a benchmark to describe the system capability to accommodate uncertain wind power generation. Ref. [30] uses 5000 simulations to determine the system load-flow in a wind-integrated power system. Then,

the authors use data clusters to reduce the computational burden. However, the minimum number of simulations required to achieve a valid assessment is not discussed; 5000 simulations are assumed to be enough. Fifty thousand different scenarios for frequency security evaluation of wind integrated systems are used in [31]. There, the impact of wind power plants on the load-curtailment is studied in detail. Until now the number of MCS is often just increased by researchers up to the number, where the solution settles enough to satisfy the requirement for the given study. These studies could potentially reduce their simulation numbers significantly without loosing accuracy in the assessment outcome.

The additional frequency controls are needed, as the power system inertia is reduced in many hours of the system operation nowadays, when converter-based units penetrate the power grid [32]. These controls can be very different in their characteristics [33], but they all severely change the grid ability to maintain a reliable system frequency. However, it is not fully understood how these additional frequency controls affect the accuracy of the assessment method. This means how the assessment process has to be adapted to the inclusion of wind power plants with additional frequency controls to achieve a valid estimation of the system performance. This paper closes this research gap by determining the number of system states that are needed during the assessment to estimate the system behavior within reasonable accuracy.

To determine the minimum number of states required for a given accuracy, a deterministic analysis is used to give results, that can be compared more easily. The system states are defined by different considered load and wind states. The number of simulations required for a valid system estimation is determined with and without modern frequency controls in power electronic-based units. The analysis validates if the additional equipment and control increase the requirements for the system assessment strategy. The aim is to determine if more or fewer simulations are needed to be performed to estimate the system behavior with additional frequency controls correctly. This of importance, as system operators have to rely on the assessment outcome in order to design their frequency control designs for the next decades.

The outcome of this study is used to reduce the simulation burden as much as possible, without losing accuracy during the assessment. The relative impact can also be utilized for MCS, adapting the number of considered system states when additional frequency controls are tested. Typically, with modern computers, the numbers of simulations used during the system reliability assessment is set very high, as simulation time is not the most critical resource. However, when TSOs aim to compare different frequency controls with each other, then the simulations have to be repeated for all tested control options, which increases the simulation numbers significantly. So a reduction of simulation numbers becomes of significant importance with the further integration of converter-based generation units and their usage for frequency control purposes.

In summary, this paper provides the following novelties:

- A method to determine the required number of simulations for valid assessment of the system frequency security.
- Introduction of a value representing the accuracy of system representation, which can be utilized to guarantee the accuracy of the reliability assessment.
- A comparison of the requirements for a system without and with additional frequency support from wind power plants in the system analysis.

The rest of the paper is organized as follows. Section 2 introduces the methodology used to assess the accuracy of the reliability estimation. It is explained how the desired threshold can be set to validate the needed number of simulations. Section 3 shows the specifics of the used test system, especially the frequency controls in the conventional generation units, the load behavior, and the wind turbines. Section 4 shows the assessment results and discusses the outcome. Finally, conclusions are drawn in Section 5.

## 2 Methods

### 2.1 Reliability indices

The reliability of the power system frequency is typically assessed with a number of different indices [24]. Some of these indices describe the system frequency behavior, others, the system effort to maintain the system frequency.

The frequency quality can be assessed with the number and duration of abnormal frequency states, where the deviation of the actual grid frequency from the nominal grid frequency exceeds the normal operating range within $\pm\,0.2$ Hz. The NUF is a measure of the system capability to handle the loss of a generation unit. It is highly dependent on the number and the sizes of the different installed generation units. In this study, the generation units are inserted depending on the needed active power in a hierarchical order.

The NOF, on the other hand, describes how the trip of large feeders influences the system frequency. Reduced inertia in the power system due to high wind power penetration leads to higher frequency deviations. As the frequency rises faster, it can also lead to an increase in NOF, as the frequency controls take time to counteract the feeder loss. The ENAF is of importance, as many TSOs have specific limits in their grid operations, how high this value is allowed to be [34]. If the ENAF is too high, significant changes in the grid operations have to be planned. The indices NOF and NUF are then indications, how these changes can be done to adapt the system operation. The duration of these abnormal events is evaluated using the OFD and the UFD. The total abnormal frequency duration is the EAFD, which is also used for the assessment of frequency quality by TSOs [34].

The index EWES is the short-term wind power that is released during the under-frequency events when the respective control is enabled. This controller action is only possible in this system when the wind power is already curtailed during steady-state operation. EWEW, EWES, IENS 1, IENS 2, ECU 1, and ECU 2 are indices that describe the economic impact of a given frequency control that is tested. With these indices, it is possible to estimate the smallest economic impact on the desired frequency quality.

All used frequency reliability indices are listed in the nomenclature section.

### 2.2 Discrete system states

In this work, two variables are changed for the analysis. First, the number of discrete load states ($L$). Second, the number of discrete steady-state wind power levels in the system ($W$). Together, these values describe the number of system states considered for the reliability assessment. The value of $L$ represents the discrete level of system load in the steady-state grid operation before the contingency occurs. Therefore, a higher value for $L$ takes more discrete system states regarding the system load before a contingency into account. A very high number of $L$ results in an almost ideal representation of the distribution of loads in the power system over time, often described by the load duration curve (LDC).

The error between the discrete load steps and the ideal LDC decreases with a higher number of discrete steps. Hence, it increases the desired number of simulations too. This value is calculated, as described in (1).

$$Error_{LDC} = \frac{\sum_{i=1}^{8760} |LDC_i - LDC_{discrete\,i}|}{\sum_{i=1}^{8760} LDC_i} \qquad (1)$$

It is assumed that a sufficiently low value of $Error_{LDC}$ will lead to high accuracy of the system load variations throughout the operation. Besides, the number of discrete wind power production states $W$ is varied in the analysis method. The wind power levels are then dependent on the wind power curve (WPC) of the wind turbines. A high value of $W$ results in an accurate representation of the available wind power in the system. The error of the discrete steps to $Error_{WPC}$ is calculated in the same way as for the LDC to see its impact on the assessment on the frequency reliability.

The addition of these two error values describes the error of the system representation $Error_{System}$. It is used to verify that the system analysis is sufficiently good, which will further lead to a correct system reliability estimation. The value of $Error_{System}$ is dependent on the LDC curve, the number of LDC steps, as well as on the WPC of the power grid and the number of discrete wind power steps.

### 2.3 Assessment outcome verification

The critical value of $Error_{System}$, leading to a valid reliability assessment, is determined by changing the number of system states. The total number of analyzed system states $N_{States}$ is given as:

$$N_{states} = L \times W \tag{2}$$

The number and type of system contingencies are dependent on the system states. It depends mainly on the number of running wind turbines, as well as on the number of generation units being in operation during each system state. The number of simulated system states is increased until the results settle and do not vary outside the desired accuracy.

The accuracy of the reliability assessment quantifies if the outcome matches the expected value. The precision of the simulation outcome is dependent on the validity of data as a system input, as there can be uncertainties in the yearly load distribution in the power system, the probability of the certain wind speeds, or the occurrence rate of a contingency. This analysis uses a deterministic method, meaning all possible system states and all contingencies are simulated and therefore taken into account. The precision of the assessment method is only an essential factor when MCS is used, where not all possible system states and contingencies are combined.

The accuracy of a simulation set is validated in this work, as shown in (3). Here, the reliability indices for a given number of states $X_{L,W}$ are compared to the indices estimated with a high number of states $X_{ref}$. $L$ and $W$ are increased until the assessment outcome does not vary anymore. Further increase of the number of simulations does not change the accuracy in the assessment anymore.

$$Acc_{X_{L,W}} = 100\,\% - abs\left(\frac{X_{L,W} - X_{ref}}{X_{ref}}\right) \tag{3}$$

It is necessary to compare the lowest accuracy for all given indices for any given number of simulation states to decide if one simulation outcome is valid or not. The minimum accuracy ($Min_{Acc}$) of any index is a value that describes the lowest of all determined indices. This minimum accuracy can be used to determine whether a simulation outcome can be trusted to a certain degree.

A threshold, e.g., 95 %, can be set and shows how accurate a simulation set has to be. Then, the outcome is considered as valid. Otherwise, the number of simulations was not sufficient. This is described in (4). Afterwards, the different reliability indices are combined to determine how many simulation steps are needed so that all indices match the expected value within the threshold. The calculated index is valid with the following expression.

$$Valid_{X_{L,W}} = \begin{cases} 1 & , Min_{Acc_{X_{L,W}}} > threshold \\ 0 & , Min_{Acc_{X_{L,W}}} \leq threshold \end{cases} \tag{4}$$

Simulation sets with all indices meeting the validation criterion in (4) are counted as a valid set. With this analysis, the accuracy of all indices can be assessed, and the simulation sets can be effectively compared.

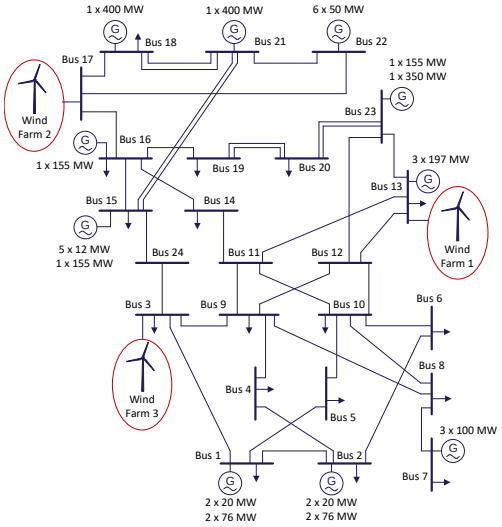


**Fig. 1**: IEEE 24-bus reliability test system [35], used for the system analysis, with three additional wind farms.

## 3 Test system modeling

The system design has a significant effect on the calculated system frequency reliability. The system states, as well as the considered contingencies, determine the frequency behavior. The power system used in this analysis is the IEEE RTS, as shown in Fig. 1 [35]. IEEE RTS is a commonly used power system and it is easily comparable [36].

It contains detailed information on the load level throughout the year, as well as generator models with failure rates and frequency control parameters [35, 37]. Three wind farms have been additionally added to the system to determine the effect on the system reliability assessment. They are further described in Section 3.3.

The used power system is modeled as a one-bus system like done in [24], using MATLAB Simulink, version R2018b. The system loads are connected to the bus, as well as the wind power plants and the conventional generation units, when in use.

The steps include the system description, including wind and load curves, but also the data of the generation units. The system modeling step implements then the different units of the power grid to a model of the power grid with its frequency behavior. The contingency analysis is then simulating the system frequency after the considered active power imbalances are applied. The simulation results are afterwards combined with the used reliability indices. The different steps of the frequency security assessment are shown in Fig 2.

### 3.1 Modeling of system load

The hourly peak loads with seasonal, weekly, and daily data are given for the IEEE RTS [35]. The LDC sorts these data points in a descending order to determine the probability of a load peak value throughout the observation period. In this study, two LDCs are used to compare the number of simulations needed to provide an accurate assessment outcome: the LDC of the IEEE-RTS System (LDC 1) and an alternative LDC (LDC 2) that represents a grid with lower overall power consumption, but the same maximum system load. Both LDCs are shown in Fig. 3.

The maximum peak load of both LDCs is given with 2,850 MW. The total power consumption of all loads in one year for LDC 1 is 15,300 GWh. The average load is 60 % of the peak value. The total power consumption per year with LDC 2 is 11,200 GWh.

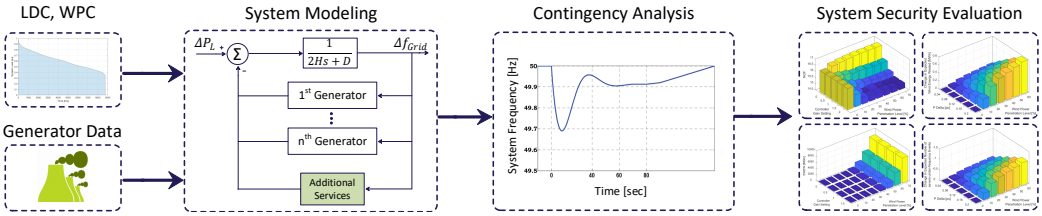


**Fig. 2**: Frequency security assessment procedure.

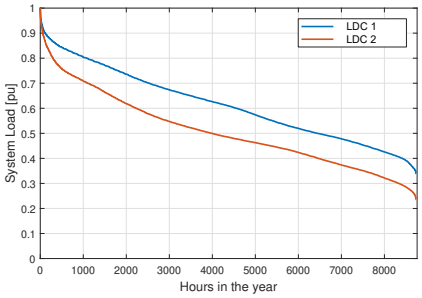


**Fig. 3**: LDC Curve of the IEEE Reliability Test System.

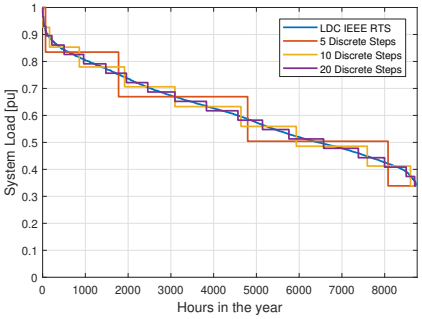


**Fig. 4**: LDC 1 with different used numbers of discrete load levels.

To perform the time series simulation of a contingency, the respective LDC has to be divided into discrete steps to achieve steady-state system operations before the events. These steps are the maximum load, minimum load, and balanced power levels in between. Different numbers of discrete steps of LDC 1 are shown in Fig. 4.

The duration of these discrete steps is chosen to keep the energy consumption of the test system throughout the operation constant. A higher number of simulation steps fits the original LDC more accurately than the use of only a few discrete steps, as shown in Fig. 4. As a drawback, the simulation time increases linearly with the higher number of discrete simulation steps.

### *3.2 Modeling of generation units*

The data for the generation units, including all needed parameters for estimating the frequency behavior, are taken directly from the IEEE RTS as it is specified in [35, 37].

The unit commitment order under different load and wind conditions is heuristically determined, preferring units with higher rated power to operate. This ensures a higher power system inertia than mixed generator scheduling and, therefore, a more stable system

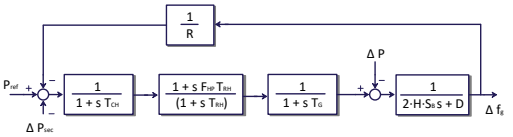


**Fig. 5**: Primary frequency control block diagram of conventional generation units, used in the IEEE RTS in Fig. 1.

Table 1: Stages of Wind Power installed in the IEEE RTS.

| | Installed Capacity | Number of installed Turbines |
|---|---|---|
| Wind Stage 1 | 600 MW | 100 |
| Wind Stage 2 | 1200 MW | 200 |
| Wind Stage 3 | 1800 MW | 300 |

operation. The control scheme of the primary frequency control is given in Fig. 5.

The generator parameters $T_G, T_{CH}, T_{RH}$, and $F_{HP}$ for the generation units committed to the frequency control are set to 0.2 s, 0.3 s, 7.0 s, and 0.3 respectively. The purpose of the primary frequency control is to restore a frequency deviation into the normal operation condition. The parameters and the droop $R$ are given in [5]. The secondary frequency control restores to the nominal value. The dynamics of the secondary control is highly dependent on the limited ramp rate in the conventional generation units. It is slowed down for the purpose of minimizing the dynamic requirements for the participating units. The secondary control influences the active power reference setpoint, as shown in the primary control scheme in Fig. 5. The parameters are given for the IEEE RTS [37].

### *3.3 Modeling of wind power plants*

Wind power is included in the IEEE RTS system in three stages. Stage one adds Wind Farm 1 with one hundred 6 MW wind turbine generators with a total rated power of 600 MW, according to Fig. 1. Stage two includes Wind Farm 1 as well as Wind Farm 2 with again one hundred 6 MW wind turbines. In stage three, Wind Farm 3 is also installed with again 600 MW rated power, which means a penetration level of up to 60 % wind power in stage three during high load situations. The amount of installed wind power in the test system in described in Table 1.

The injected wind power is determined by the wind speed and the turbine parameters. The cut-in wind speed is given as 3 m/s. The rated and cut-out wind speed are 13 m/s and 25 m/s, respectively. The simulated wind turbines have 1600 full-load hours, being a representation of onshore wind power generation units [38]. The probability of injected wind power into the system during steady-state is given in the wind power probability curve (WPC). This curve is further referred to as WPC 1, as shown in Fig. 6. A second WPC (WPC 2), representing 2200 full-load hours, is used to

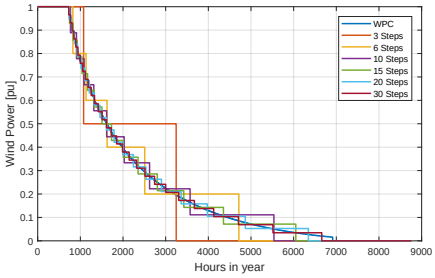


**Fig. 6**: Wind power probability curve for 2200 full-load hours with discrete simulated steps.

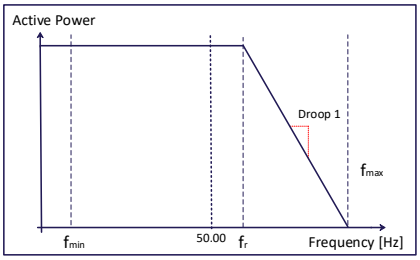


**Fig. 7**: 'Frequency response' of the wind turbines as specified in the Danish grid code [10].

compare the effect of the estimation error on the outcome of the assessment. This second WPC is ensuring that the assessment accuracy is not dependent on the one system condition, but that this assessment evaluation can be utilized for other system conditions as well.

The wind power plants are modeled as always being available. This means that the wind turbines are producing power whenever the wind speed allows for it. Otherwise, the WPC has to be adjusted by increasing the probability of lower wind power states. For the proposed methodology, changing the shape of the WPC slightly is not expected to influence the accuracy of the assessment, but only the value of the system reliability.

The power system frequency security is only affected by wind turbines when wind power is currently injected. Otherwise, the loads are supplied by conventional power plants. Higher availability of wind power, as in this study with the second used WPC, causes system states with a lower inertia and a system frequency that is less secure to maintain.

The discrete levels are chosen to keep the overall injected wind energy over the observation period constant and to minimize the error to the original WPC. The step number varies from $L = 3$ to $L = 30$.

The wind turbines are controlled using the over-frequency power curtailment as it is described in the Danish grid code as 'frequency response' [10]. The scheme of this frequency behavior is shown in Fig. 7. The settings are fixed and given in the grid code.

The scheme of the analyzed additional frequency control is shown in Fig. 8. This control can be realized with the respective settings when incorporating the control scheme 'frequency control' in the Danish grid code for wind power plants [10]. The variables shown in the scheme can be set during the system operation by the TSO. In the grid code, default settings are given, which are used in this study. The dead-band is set to 50 mHz, avoiding control interactions for small disturbances. The maximum positive power change $\Delta P_{max}$ is set to 0.2 pu, with a droop coefficient, so that the maximum available active power is requested at a frequency reduction

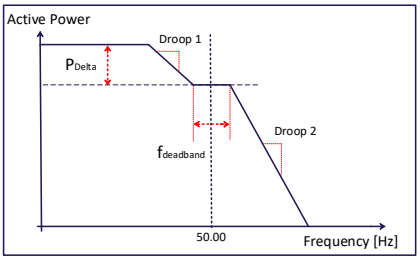


**Fig. 8**: Specification of the 'Frequency control' of the wind turbines as in the Danish grid code [10].

of 1 Hz. The full power reduction is set to be at 52 Hz grid frequency. Wind power plants contribute during the first phase of a frequency disturbance, which means they possibly prevent abnormal frequency conditions during both frequency drop as well as during frequency rise events.

The change in operational reliability is highly dependent on the used power system. Therefore, the change in frequency security due to the changed control is not directly applicable to other systems with different conditions. Nevertheless, the accuracy, determining the duration of the evaluation can be compared more easily.

Section 4 describes the results of these different simulation step numbers to the calculated system frequency reliability.

## 4 Results

.

This study shows the impact of the number of simulated system states on the reliability assessment accuracy. The results for stage 1 wind power penetration with the LDC 1 and the WPC 1 without additional frequency control is shown in Section 4.1. This illustrates the method and shows the verification of outcome accuracy. The system with 'frequency control' active is shown in Section 4.2.

The results for a system behaving as described by LDC 1 and WPC 1 is shown in Section 4.3. Section 4.4 describes then the results that are obtained when using LDC 2 and WPC 2.

### *4.1 Analysis of the system with LDC 1 and WPC 1, without 'frequency control'*

In this Section, the wind turbines in Wind Farm 1 behave with the 'frequency response' specified in the Danish grid code. This control gets active during frequencies above 50.2 Hz. A certain amount of wind power is curtailed to reduce the impact of over-frequency events. This case is shown in detail; all other used cases are only showing the final result to compare the needed $Error_{System}$ and the needed number of simulations.

The average accuracy of all indices of the wind power integrated system is shown with the used discrete steps in Fig. 9 with the different number of discrete wind and load steps used in the simulation.

Second, the minimum accuracy of any index used in the reliability analysis of the wind power integrated system is shown with the different number of simulation steps in Fig. 10. This value is used to verify whether the number of simulated system states is sufficient to achieve valid reliability results.

Fig. 10 shows the lowest index accuracy for each given discrete step number. A broad set of $W$ and $L$ values provides an accuracy of at least 90 % for all indices. The minimum accuracy of all indices is compared with a threshold to determine if the simulated outcome is valid or not, as described in Section 2. This threshold is set to an accuracy of 95 % in this study. The number of indices within this range is shown in Fig.11.

The state with the least amount of wind and load states needed to reach the 95 % accuracy can be found at $L = 8$ and $W = 10$. Also,

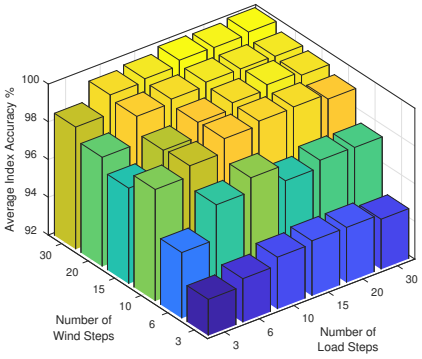


**Fig. 9**: Average index accuracy depending on the number of performed simulations, without frequency controls in wind turbines.

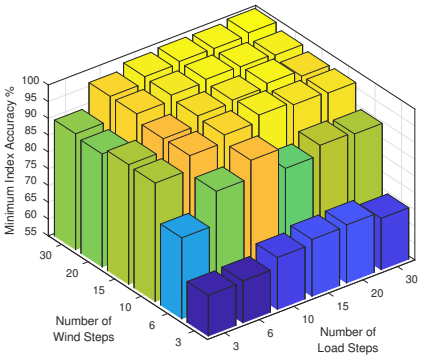


**Fig. 10**: Minimum index accuracy depending on the number of performed simulations, without frequency controls in wind turbines.

the combination of $L = 6$ and $W = 18$ has a valid accuracy, but with a higher number of simulations in total.

Fig. 12 shows the value of $Error_{System}$, for the different values of load and wind power steps. It can be seen that it decreases continuously with higher step numbers.

The values of $Error_{System}$ are shown in Table 2. There, it can also be seen which simulation leads to a valid system reliability assessment for the considered case. The green color indicates a reliability result within the specified accuracy of 95 %, whereas red indicates an invalid result in the evaluation. The shown discrete step numbers are only a selection to show the general behavior of $Error_{System}$.

The highest value of $Error_{System}$ leading to a valid assessment is 7.88 %, whereas the lowest value causing a wrong assessment can be found at 5.01 %. So the value of $Error_{System}$ is in itself not sufficient to guarantee a valid assessment together with low simulation numbers. To reduce the number of simulations and, therefore, the computational time, the number of discrete wind and load steps has to be kept close to each other. For this system, the minimum number of needed simulated system states is 80, with an $Error_{System}$ value of 6.81 %.

### *4.2 Analysis of the system with LDC 1 and WPC 1, with 'frequency control'*

Afterwards, the 'frequency control' from the Danish grid code is enabled in the wind turbines. The other system conditions are kept the same. The accuracy of the assessment is done with the same procedure. The required $Error_{System}$ value is determined with the

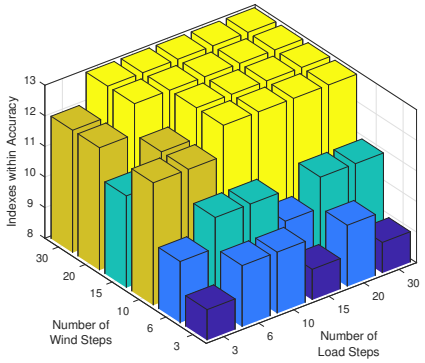


**Fig. 11**: Number of indices, where the simulation outcome matches the accurate value within the threshold of 95 % depending on the number of performed simulations, without frequency controls in wind turbines.

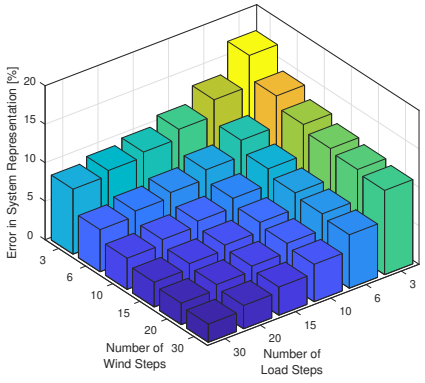


**Fig. 12**: System representation error, depending on the number of discrete wind power and load steps for LDC 1 and WPC 1.

Table 2: System Error Value [%] for different numbers of discrete Steps without 'frequency control'.

| Wind Steps \ Load Steps | 3 | 6 | 10 | 15 | 20 | 30 |
|---|---|---|---|---|---|---|
| 3 | 17.03 | 13.03 | 10.95 | 9.75 | 9.11 | 8.45 |
| 6 | 14.06 | 10.03 | 7.98 | 6.78 | 6.14 | 5.47 |
| 10 | 12.64 | 8.64 | 6.56 | 5.36 | 4.72 | 4.06 |
| 15 | 11.81 | 7.81 | 5.73 | 4.53 | 3.89 | 3.22 |
| 20 | 11.38 | 7.37 | 5.29 | 4.09 | 3.45 | 2.79 |
| 30 | 10.95 | 6.94 | 4.86 | 3.66 | 3.02 | 2.36 |

number of simulations needed to achieve the required accuracy for all reliability indices.

The mean accuracy of the reliability indices is shown in Fig. 13. This value is relatively high, even for low numbers of $L$ and $W$.

The mean index accuracy, however, can not be used to decide if all indices are calculated valid, so the minimum index accuracy is

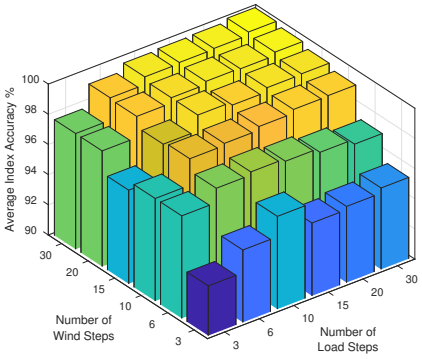


**Fig. 13**: Mean index accuracy depending on the number of performed simulations, with frequency controls in wind turbines.

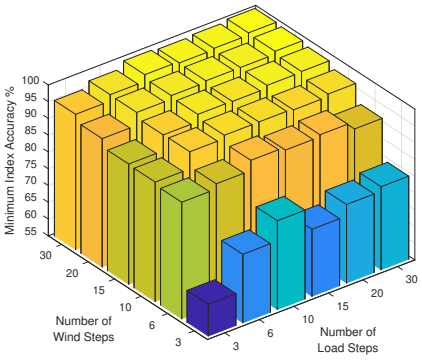


**Fig. 14**: Minimum index accuracy depending on the number of performed simulations, with frequency controls in wind turbines.

used to determine the accuracy of the assessment. The lowest index accuracy for the different values of $L$ and $W$ are shown in Fig. 10. The number of indices that are therefore considered valid is shown in Fig. 15.

The number of simulations, required to achieve a valid system reliability assessment, varies compared to the assessment without frequency controls. The value of $Error_{System}$ is the same as without 'frequency control' enabled as it is shown in Fig. 12.

The detailed results with the minimum required number of simulations comparing the assessment with and without the 'frequency control ' are shown in Section 4.3.

### *4.3 Results for LDC 1 and WPC 1*

The assessment of the IEEE RTS is repeated for the other two stages of wind integration, while still using LDC 1 and WPC 1. The wind power plants are analyzed with and without the frequency control, as described in Section 3.3.

The results of the validity assessment are shown in Table 3. This allows a comparison of the needed number of simulations required for a valid assessment. The minimum $Error_{System}$ for the correct assessment outcome is not fixed but depends on the control that is utilized and the wind power penetration level.

The results listed in Table 3 show the needed number of simulations when the grid conditions as described by LDC 1 and WPC 1. In the tested cases, the needed number of simulated system states varies from 70 to 112. Without 'frequency control', the average value of error at minimal step numbers is 7.30 %, ranging from 6.81 % to 7.95 %. With 'frequency control' enabled,

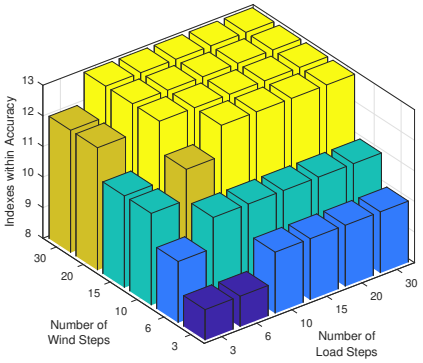


**Fig. 15**: Number of indices, where the simulation outcome matches the accurate value within the threshold of 95 % depending on the number of performed simulations, with frequency controls in wind turbines.

the $Error_{System}$ value has to be 7.20 % on average, 6.50 % at minimum and 7.59 % at maximum.

This indicates that the $Error_{System}$ value, allowing for an accurate system assessment, does not significantly change with the additional frequency control. When a safety margin is included, the accuracy can be kept high, even when testing an alternative controller setting.

### *4.4 Results for LDC 2 and WPC 2*

The results of the reliability assessment for the alternative set of wind and load behavior, are discussed in this section. Again, it is determined what the critical $Error_{System}$ value for an accurate result is and whether additional frequency control has a severe impact on the needed number of simulations.

Table 4 reveals that the needed number of simulations increases with LDC 2 and WPC 2. In the tested cases, the number of simulated system states is increased compared to Table 3. The average value of the needed $Error_{System}$ is 8.62 %, reaching from 8.28 % to 9.22 %, without 'frequency control'. With 'frequency control' enabled this changes to an average value of 7.72 %, a minimum value of 6.66 %, and a maximum $Error_{System}$ value of 8.28 %. The needed number of simulation increases severely with this system conditions; up to 150 system states have to be considered for the assessment.

Table 3 and Table 4 show that the accuracy is more dependent on the number of simulated wind power steps than on the number of load steps. This is obtained regardless of the wind power plants using additional frequency control for both tested system conditions. The results show that a system representation with $L$ and $W$ values to achieve an $Error_{System}$ value of less than 6 % is sufficient in any cases for the two given system conditions.

### *4.5 Results with a higher level of accuracy*

The simulation accuracy has also been tested for a higher level of the desired accuracy. The threshold has been increased from 95 % to 98 %. The simulation burden increased severely, as well as the required value for $Error_{System}$. For system condition 1, with WPC 1 and LDC 1, the value of $Error_{System}$ is determined to be 4.12 % at the minimum number of simulation, reaching from 3.81 % to 4.37 % for the different system variations, such as wind power plant changes as well as enabled and disabled frequency controls in the wind power plant. The minimum number of simulations is varying between 205 and 285, so it increased significantly compared to the previously tested threshold for accuracy.

When WPC 2 and LDC 2 are used for the system analysis, then the results change accordingly. The required $Error_{System}$ is

Table 3: System Representation Error for LDC 1 and WPC 1

| | Control Active | Max Error valid Result [%] | Minimal Sim Number (L: /W: ) | Error at Minimum Sim [%] |
|---|---|---|---|---|
| Wind Power Stage 1 | | 7.88 | 80 (8/10) | 6.81 |
| | X | 7.51 | 91 (7/13) | 7.51 |
| Wind Power Stage 2 | | 7.13 | 70 (7/10) | 7.13 |
| | X | 7.59 | 88 (8/11) | 8.17 |
| Wind Power Stage 3 | | 6.62 | 84 (6/14) | 7.95 |
| | X | 6.50 | 112 (8/14) | 8.13 |

Table 4: System Representation Error for LDC 2 and WPC 2

| | Control Active | Max Error valid Result [%] | Minimal Sim Number (L: /W: ) | Error at Minimum Sim [%] |
|---|---|---|---|---|
| Wind Power Stage 1 | | 8.28 | 140 (10/14) | 8.28 |
| | X | 8.30 | 182 (13/14) | 6.66 |
| Wind Power Stage 2 | | 9.44 | 88 (8/11) | 9.22 |
| | X | 8.28 | 140 (10/14) | 8.28 |
| Wind Power Stage 3 | | 8.37 | 130 (10/13) | 8.37 |
| | X | 8.21 | 150 (10/15) | 8.21 |

4.57 % on average, reaching from 4.02 % to 4.83 %. The required number of simulations to reach the demanded accuracy increase to the range between 255 to 372.

A system design that guarantees an $Error_{System}$ value of 3.5 % allows a significant margin of accuracy, whilst not wasting time for more simulations when the accuracy goal is set to 98 % in this study. This parameter can be verified and then used over a large course of analysis, as it verifies the assessment outcome even with variations in the frequency controls.

### *4.6 Discussion of results*

The analyzed power system reliability is highly affected by the simulation efforts that is performed. The balance between the number of simulations and the accuracy of the reliability assessment is shown. This balance has no linear behavior, as the system is highly non-linear, but influenced by the LDC, WPC, the used generation units, and the probability of failures. The performed analysis also determines the different effects of considered wind steps and load steps. It can be seen that the number of wind power steps has to be considered carefully, as it has a higher effect on the assessment accuracy than the number of load steps. So a higher value for $W$ than $L$ has to be chosen when the simulation burden is aimed to be reduced.

As the system is highly non-linear, the value of $Error_{System}$ during the design phase has to be chosen with a margin. This guarantees a high assessment accuracy even with severe changes in the frequency behavior of the wind power plants. However, the margin has to be chosen carefully to achieve a balance between the high accuracy and the simulation numbers.

The results for the two different system conditions show that the needed number of performed simulations severely changes when the LDC and WPC are changed. The reason for this is the different distribution of discrete states with the respective probability. The required $Error_{System}$ value for a defined level of accuracy, on the other side, is not changing severely between the two analyzed load and wind conditions. The same is true with the tested frequency control. It also has to be noted that a higher value of $W$ is needed when performing the reliability analysis, as it needs more discrete steps to model the system accurately.

## 5 Conclusion

The method presented in this work is able to analyze the severe impact of simulation numbers on the accuracy of frequency security assessment in wind-integrated power systems with additional frequency controls in wind turbines. The new method presented is helpful in determining the number of simulations by using the easily obtainable value of $Error_{System}$. This value can be calculated by comparing the actual LDC and WPC with the considered discrete system states. When higher accuracy is desired, the number of simulations has to be adjusted, and the critical value of $Error_{System}$ will change. The methodology presented in this paper can be repeated with any given power system for different wind power penetration levels and additional controls.

However, the methods are limited, as, so far, the methodology is only applicable for deterministic system assessment. With MCS, it is more challenging to achieve a correct estimation of $Error_{System}$, as the system states are varied randomly. The presented work is also only determining the impact of one specific frequency control, which is possible with wind power plants. Other control schemes can have a different impact on the assessment requirements. Also, the proposed methodology is only verified for one test power system. Applying it to other power grids may change the behavior of $Error_{System}$ and its application for accuracy verification. Further, the availability of wind power plants is not considered in this study. The availability of the wind power plants has an impact on the WPC, the $Error_{System}$, and also on the system reliability.

Nevertheless, the presented study allows for verification of the desired system reliability assessment performance under changing conditions without wasting valuable simulation time. For the given test system, there are no increased requirements when testing the frequency control in the wind turbines. Also, the level of penetration is not playing a major role in the desired number of simulations that have to be performed.

With the proposed method, TSOs can determine the required value of $Error_{System}$ for their system and for their demanded level of accuracy, before examining the impact of additional frequency controls to their grid operation. This helps to preserve computational effort without resulting in invalid reliability indices. It is then possible to compare the assessment outcome and to evaluate which frequency control scheme should be used in the respective power system to allow the highest system reliability.

Further research is needed to further reduce the required number of simulations by optimizing the discrete steps for LDC and WPC, to minimize the $Error_{System}$ value without increasing the number of considered states $N$. Other frequency control options, such as virtual synchronous machine emulations and alike, should also be tested for their requirements regarding the reliability assessment. This should be done before these functions are utilized in order to choose the design of these controls more carefully and to reliably utilize this kind of service. Also, a transformation of the given methodology to MCS would be beneficial, as MCS is also often performed for this kind of system assessment. The wind power plants are also not modeled in full detail, which can be addressed in future research, such as the availability. Additionally, the proposed method has to be tested in other power grids with changed system performance to see the impact on the reliability assessment.

## 6 Acknowledgments

This work is supported by the Reliable Power Electronic-Based Power Systems (REPEPS) project at the Department of Energy Technology, Aalborg University, as a part of the Villum Investigator Program funded by the Villum Foundation.

## 7 References

1 REN21. (2018) Renewables 2018 Global Status Report. [Online]. Available: http://www.ren21.net/gsr-2019
2 F. Milano, F. Dörfler, G. Hug, D. J. Hill, and G. Verbič, "Foundations and Challenges of Low-Inertia Systems (Invited Paper)," in *2018 Power Systems Computation Conference (PSCC)*, June 2018, pp. 1–25.
3 EirGrid and SONI, "All Island TSO Facilitation of Renewables Studies," 2010. [Online]. Available: http://http://www.eirgridgroup.com
4 ENTSO-E, "High Penetration of Power Electronic Interfaced Power Sources (HPoPEIPS)," march, 2017.
5 P. Kundur, N. J. Balu, and M. G. Lauby, *Power System Stability and Control*. McGraw-hill New York, 1994, vol. 7.
6 T. Sasaki and K. Enomoto, "Statistical and Dynamic Analysis of Generation Control Performance Standards," *IEEE Transactions on Power Systems*, vol. 17, no. 2, pp. 476–481, May 2002.
7 Ibraheem, P. Kumar, and D. P. Kothari, "Recent Philosophies of Automatic Generation Control Strategies in Power Systems," *IEEE Transactions on Power Systems*, vol. 20, no. 1, pp. 346–357, Feb 2005.
8 Tennet, "Migrate D1.1 Report on Systemic Issues," 2017. [Online]. Available: https://www.h2020-migrate.eu
9 US Department of Energy, "Maintaining Reliability in the Modern Power System," 2016. [Online]. Available: https://www.energy.gov
10 ENERGINET, "Technical Regulation for Wind Power Plants above 11 kW, Denmark," (Date last accessed 28-Jan-2020). [Online]. Available: https://en.energinet.dk/Electricity/Rules-and-Regulations/Regulations-for-grid-connection
11 C. Sourkounis and P. Tourou, "Grid Code Requirements for Wind Power Integration in Europe," in *Conference Papers in Science*, vol. 2013. Hindawi, 2013, pp. 1–11.
12 M. Altin, . GÃűksu, R. Teodorescu, P. Rodriguez, B. Jensen, and L. Helle, "Overview of Recent Grid Codes for Wind Power Integration," in *2010 12th International Conference on Optimization of Electrical and Electronic Equipment*, May 2010, pp. 1152–1160.
13 F. Diaz-Gonzalez, A. Sumper, and O. Gomis-Bellmunt, *Frequency Support Grid Code Requirements for Wind Power Plants*. John Wiley & Sons, Ltd, 2016, ch. 3, pp. 61–91. [Online]. Available: https://onlinelibrary.wiley.com/doi/abs/10.1002/9781118971291.ch3
14 M. Dreidy, H. Mokhlis, and S. Mekhilef, "Inertia Response and Frequency Control Techniques for Renewable Energy Sources: A Review," *Renewable and Sustainable Energy Reviews*, vol. 69, pp. 144 – 155, 2017.
15 M. F. M. Arani and E. F. El-Saadany, "Implementing Virtual Inertia in DFIG-based Wind Power Generation," *IEEE Transactions on Power Systems*, vol. 28, no. 2, pp. 1373–1384, 2012.
16 X. Liu and A. Lindemann, "Control of VSC-HVDC Connected Offshore Windfarms for Providing Synthetic Inertia," *IEEE Journal of Emerging and Selected Topics in Power Electronics*, vol. 6, no. 3, pp. 1407–1417, Sep. 2018.
17 M. Kheshti, L. Ding, M. Nayeripour, X. Wang, and V. Terzija, "Active Power Support of Wind Turbines for Grid Frequency Events using a Reliable Power Reference Scheme," *Renewable Energy*, vol. 139, pp. 1241–1254, 2019.
18 R. Billinton, R. Karki, Y. Gao, D. Huang, P. Hu, and W. Wangdee, "Adequacy Assessment Considerations in Wind Integrated Power Systems," *IEEE Transactions on Power Systems*, vol. 27, no. 4, pp. 2297–2305, 2012.
19 R. Billinton and R. N. Allan, *Reliability Assessment of Large Electric Power Systems*. Springer Science & Business Media, 2012.
20 N. Farrokhseresht, H. C. Orestica, and M. R. Hesamzadeh, "Determination of Acceptable Inertia Limit for Ensuring Adequacy under High Levels of Wind Integration," in *European Energy Market (EEM), 2014 11th International Conference on the*. IEEE, 2014, pp. 1–5.
21 W. Li and R. Billington, *Reliability Assessment of Electric Power Systems using Monte Carlo Methods*. Springer Science & Business Media, 2013.
22 R. Billinton and W. Wangdee, "Predicting Bulk Electricity System Reliability Performance Indices using Sequential Monte Carlo Simulation," *IEEE Transactions on Power Delivery*, vol. 21, no. 2, pp. 909–917, 2006.
23 R. Billinton, Y. Gao, and R. Karki, "Application of a Joint Deterministic-Probabilistic Criterion to Wind Integrated Bulk Power System Planning," *IEEE Transactions on Power Systems*, vol. 25, no. 3, pp. 1384–1392, Aug 2010.
24 P. Wang, Z. Gao, and L. Bertling, "Operational Adequacy Studies of Power Systems with Wind Farms and Energy Storages," *IEEE Transactions on Power Systems*, vol. 27, no. 4, pp. 2377–2384, 2012.
25 C. Liang, P. Wang, X. Han, W. Qin, R. Billinton, and W. Li, "Operational Reliability and Economics of Power Systems With Considering Frequency Control Processes," *IEEE Transactions on Power Systems*, vol. 32, no. 4, pp. 2570–2580, 2017.
26 A. M. L. L. da Silva, W. S. Sales, L. A. da Fonseca Manso, and R. Billinton, "Long-term Probabilistic Evaluation of Operating Reserve Requirements with Renewable Sources," *IEEE Transactions on Power Systems*, vol. 25, no. 1, pp. 106–116, 2010.
27 J. Ferrero Bermejo, J. F. Gomez Fernandez, F. Olivencia Polo, and A. Crespo Márquez, "A Review of the use of Artificial Neural Network Models for Energy and Reliability Prediction. A Study of the Solar PV, Hydraulic and Wind Energy Sources," *Applied Sciences*, vol. 9, no. 9, p. 1844, 2019.
28 M. Tajdinian, M. Allahbakhshi, M. Mohammadpourfard, B. Mohammadi, Y. Weng, and Z. Dong, "Probabilistic Framework for Transient Stability Contingency Ranking of Power Grids with Active Distribution Networks: Application in Post Disturbance Security Assessment," *IET Generation, Transmission & Distribution*, vol. 14, no. 5, pp. 719–727, 2019.
29 B. Liu, F. Liu, W. Wei, K. Meng, Z. Y. Dong, and W. Zhang, "Probabilistic evaluation of a power system's capability to accommodate uncertain wind power generation," *IET Renewable Power Generation*, vol. 13, no. 10, pp. 1780–1788, 2019.
30 M. R. Khalghani, M. Ramezani, and M. R. Mashhadi, "Probabilistic Power Flow Based on Monte-Carlo Simulation and Data Clustering to Analyze Large-Scale Power System in Including Wind Farm," in *2020 IEEE Kansas Power and Energy Conference (KPEC)*. IEEE, 2020, pp. 1–6.
31 A. Ashouri-Zadeh, M. Toulabi, A. Dobakhshari, and A. M. Ranjbar, "Frequency stability improvement in wind-thermal dominated power grids," *IET Generation, Transmission & Distribution*, vol. 14, no. 4, pp. 619–627, 2019.
32 L. Mehigan, D. Al Kez, S. Collins, A. Foley, B. Ó'Gallachóir, and P. Deane, "Renewables in the european power system and the impact on system rotational inertia," *Energy*, p. 117776, 2020.
33 A. Fernández-Guillamón, E. Gómez-Lázaro, E. Muljadi, and Á. Molina-García, "Power Systems with High Renewable Energy Sources: A Review of Inertia and Frequency Control Strategies Over Time," *Renewable and Sustainable Energy Reviews*, vol. 115, p. 109369, 2019.
34 H. Kuisti, M.Lahtinen, M.Nilsson, K.Eketorp, E.ÃŸrum, D.Whitley, A. Slotsvik, and A.Jansson, "NAG - Frequency Quality Report," (Date last accessed 11-Maj-2020). [Online]. Available: https://www.statnett.no
35 P. M. Subcommittee, "IEEE Reliability Test System," *IEEE Transactions on Power Apparatus and Systems*, vol. PAS-98, no. 6, pp. 2047–2054, Nov 1979.
36 S. Peyghami, P. Davari, M. Fotuhi-Firuzabad, and F. Blaabjerg, "Standard Test Systems for Modern Power System Analysis: An Overview," *IEEE Industrial Electronics Magazine*, vol. 13, no. 4, pp. 86–105, Dec 2019.
37 C. Grigg, P. Wong, P. Albrecht, R. Allan, M. Bhavaraju, R. Billinton, Q. Chen, C. Fong, S. Haddad, S. Kuruganty, W. Li, R. Mukerji, D. Patton, N. Rau, D. Reppen, A. Schneider, M. Shahidehpour, and C. Singh, "The IEEE Reliability Test System-1996. A report prepared by the Reliability Test System Task Force of the Application of Probability Methods Subcommittee," *IEEE Transactions on Power Systems*, vol. 14, no. 3, pp. 1010–1020, Aug 1999.
38 K. Conradsen, L. Nielsen, and L. Prahm, "Review of Weibull Statistics for Estimation of Wind Speed Distributions," *Journal of Climate and Applied Meteorology*, vol. 23, no. 8, pp. 1173–1183, 1984.

# Journal Publication 2 [J2]

## Frequency-Security Constrained Control of Power Electronic-Based Generation Systems

Joachim Steinkohl, Xiongfei Wang, Pooya Davaari, Frede Blaabjerg, Saeed Peyghami

The paper is in press at
*IET Renewable Power Generation* 2021.


*The layout has been revised.*

IET Renewable Power Generation

*Research Article*

IET Journals
The Institution of Engineering and Technology

ISSN 1751-8644
doi: 0000000000
www.ietdl.org

# Frequency-Security Constrained Control of Power Electronic-Based Generation Systems

*Joachim Steinkohl*[1*], *Saeed Peyghami*[1], *Xiongfei Wang*[1], *Pooya Davari*[1], *Frede Blaabjerg*[1]

[1] *Department of Energy Technology, Aalborg University, Pontoppidanstræde 111, Aalborg, Denmark*
** E-mail: joa@et.aau.dk*

**Abstract:** Power grids with high integration of power electronic converters face new issues that have not existed before. The frequency in the power system has been highly related to the inertia and the rotational speed of the operational synchronous machines. This is now changing, as the converter-based generation units are contributing increasingly to the balancing of active power in the modern power grid. Several frequency control designs for the power electronic-based generation units have been presented in the past, but optimal control structures and settings are dependent on the current power grid parameters and operation. The converter-based units allow the transmission system operators to change their behavior according to their grid requirements much more dynamical than ever before. This paper proposes a new framework that can be utilized to find the best-suited control settings in converter-based units to enhance the system frequency reliability. The proposed framework is demonstrated in a study case by varying the settings of one frequency control scheme currently used in wind power plants in the Danish grid codes and validated on the IEEE 24-Bus Reliability Test System with additional wind power integration.

## 1 Introduction

Large amounts of renewable power plants are installed in power grids all over the world [1]. The high amount of renewable power generation is now at a point where their power electronic converters define the behavior of the power grid. Also, other converter-based units are getting connected to the grid, such as battery systems, flexible AC transmission systems (FACTS), and high voltage DC transmission units (HVDC). One of the challenges with this extensive usage of these units is the reduction of inertia in the power system. An active power imbalance causes a change in the system frequency following (1), where the rated generator power $S_B$, and their time constant $H$ is used [2].

$$\dot{f} = (P_{Gen} - P_{Load}) \cdot \frac{f_{nom}}{2 \cdot S_B \cdot H} \tag{1}$$

The reliability of the power system in all aspects is severely affected by the converter-based units. Nevertheless, the change in system frequency behavior due to the proliferation of inertia-less units is a vast concern for transmission system operators (TSO) for reliable operation of modern power grids [3–5].

Modern power system reliability can be divided into two main aspects, adequacy and security, as shown in Fig. 1 [6]. The system adequacy describes the steady-state capability of the power system to operate. This can be the supply of system loads, even after the failure of any unit, and the system's capability to maintain a voltage at all buses within the allowed range.

The security of the system describes the dynamic capability of the system of withstanding a contingency. The analysis includes both the transient and static phases of the event. The TSO has to adjust the remedial actions depending on the grid conditions. These actions can be preventive (e.g., network topology changing, transformer tap changing, control changes) or corrective (e.g., load shedding, generator rejections). The steady-state voltage and thermal limits of the equipment are supposed not to deviate from the accepted operational limits. Otherwise, following events, like transmission line deactivation, can occur. The long term nature of these following events allows TSOs to perform corrective actions. This is considered in the static assessment of system security. Transient and dynamic events, on the other hand, are too fast for operators to interfere with corrective actions. Nevertheless, TSOs estimate the state of the grid in steady-state and the possible contingencies in these states. The operator ensures that enough reserves are available under all conditions by preventive actions. Hence, the operator has also to balance the benefits and the drawbacks of any used strategy. Every system operator has to consider the different aspects of voltage stability, angular stability, frequency stability, and converter driven stability [6].

Converter-based units allow a wide functionality in controlling the system voltage, as they are widely distributed, and they can inject controlled reactive power. The coordination of FACTS voltage controls for stable voltage control has been presented before [7], allowing a broader integration of these units in modern power grids. The proper local voltage control allows utilizing the faster control options that power electronic converters are capable of. In this field, converter based units are advantageous to conventional solutions, such as the activation of mechanically switched capacitors (MSCs). The angular stability describes the maintenance of a safe angle deviation between all conventional units when severe voltage collapses occur [2]. Converter based units can assist the grid during these events when using an assisting control method [8, 9].

This paper is dealing with frequency stability, assessing the impact and the possibilities of converter based units in maintaining a stable system frequency during contingencies. TSOs can order the curtailment of generated powers by the renewable units in cases of high penetration levels. This keeps a minimum number of conventional units in operation, therefore conserving a minimum inertia level [10]. Also, the operators directly control the HVDC units, adapting their frequency behavior to the system needs. The converter-based units, on the other side, are profiting from a reliable operation of the connected system as well. Wind power plants, as one of the main sources of renewable power generation, are capable of providing different frequency controls as their controls can be adapted to many requirements [11–13]. Grid codes are the way TSOs define the functions they demand from renewable generation units. It has been shown that wind, solar, and battery systems can provide a wide variety of services to assist the grid during frequency violation [14, 15]. Power electronic-based converters allow new flexibility with the usage of its controls that has not been seen before. It is now possible to activate and deactivate certain system services.

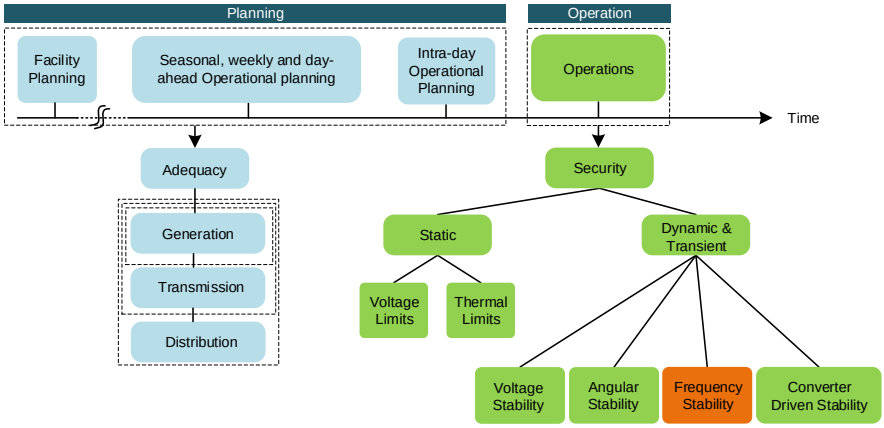


**Fig. 1**: Reliability assessment overview in modern power systems [6].

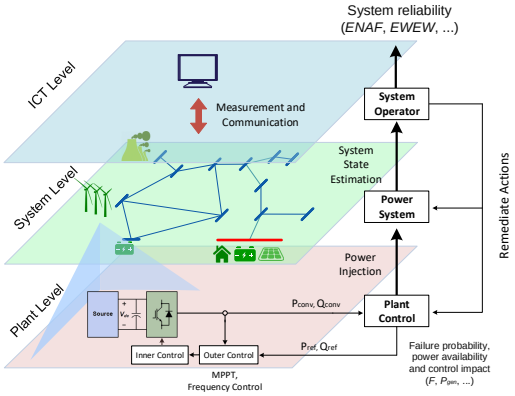


**Fig. 2**: The interactions between ICT, system, and plant level in the power grid. TSOs change plant control through remedial actions to support overall system security.

TSO can also change the settings inside the frequency services to further adapt them to the system needs. These new options for remedial actions allow TSOs to shape these units' frequency behavior to their needs, maintaining a high level of system reliability.

This relations between the system operator and the decentralized converter-based units are illustrated in Fig. 2. The three considered levels are the plant level, the system level, and the ICT level (Information and Communication Technology). The system operator can interfere with the converter-based units in the plant level via communication links. These actions are changes in power reference values, as well as control activation and deactivation commands, as well as setpoint changes.

System operators face the challenge of incorporating the flexibility converter-based units offer. In conventional systems, only a few units with a large capacity are committing to the frequency control. In modern power grids, thousands of units are assisting in the system frequency control in parallel, such as wind power plants with their grid code requirements [14]. This increased complexity requires the consideration of many more possible system states, where the flexibility in the converter-based units has to be set in focus. When determining the reliability impact of frequency services, only a small number of variations is evaluated so far [16–18]. This, however, is going through a fundamental change with the increase in frequency control flexibility in modern power grids.

To overcome this, this paper proposes a framework that can incorporate changes in frequency control schemes and settings for the converter units. The proposed framework allows a comparison of the impact of operative actions on frequency security. The benefits of the tested control schemes and settings are compared with their negative consequences, such as the reduced power produced by the renewable units. Thew framework can assist TSOs during the design process to find practical guidelines for improving frequency management.

## 2 Frequency-related security assessment

The procedure for a system frequency-related security analysis is shown in Fig. 3. The system is described with the given load duration curve and the other parameters that have to be considered, such as wind power distribution or solar irradiation characteristics. The conventional generation units and their frequency behavior have to be included as well [19–21]. The system model can be done with different levels of accuracy. For frequency-related security analysis, a one-bus multi-machine model is often used [16]. Additional services, such as frequency control in wind power plants are modeled as additional services. More detailed models are also possible, depending on whether the computational efforts are acceptable or not.

The system simulation incorporates the different possible system states. The different load conditions are considered with their probabilities in the load duration curve (LDC). The conventional generation units are modeled with primary and secondary frequency controls, as described in [16]. The single-bus multi-machine model has shown to be capable of analyzing the frequency behavior, as generator-dependent time constants and non-linearities can be implemented, such as ramp rates and limitations.

As generator failures, the considered contingencies cause frequency excursions in the system and it is followed by the control response to maintain the system frequency.

Following the reliability parameters presented in [16, 22–26], the abnormal frequency events are compared with different reliability indices. The reliability indices describe the number and duration of abnormal frequency in the power system. The power system' nominal frequency is 50 Hz in this analysis, with the abnormal frequency being counted at a frequency deviation of $\pm 0.5$ Hz, as the control gets activated at a frequency deviation of $\pm 0.2$ Hz.

Different indices can be used to describe the used energy for the frequency controls. The energy used for frequency regulation by the conventional generation units is taken as a metric, as well as the not used wind energy and the surplus wind energy due to additional controls [16]. Moreover, the under-frequency load curtailment is taken into consideration, measuring the amount of not supplied

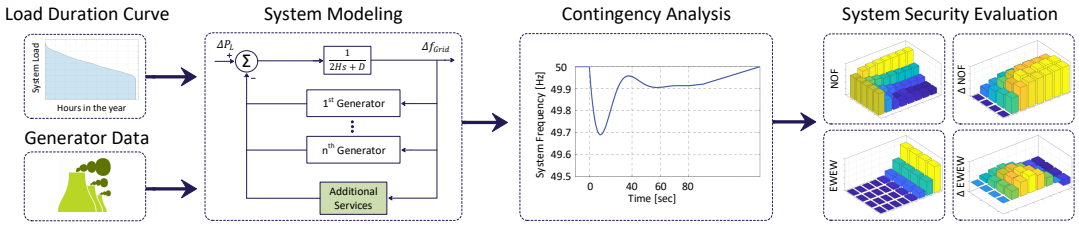


**Fig. 3**: Conventional system frequency security assessment [19–21].

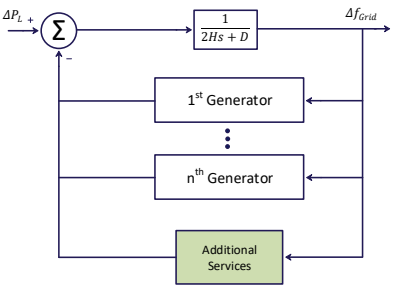


**Fig. 4**: System simulation model, including primary and secondary frequency controls in the generation units, as well as additional services provided by converter-based units.

Table 1: Reliability evaluation indexes used in the power system analysis [16].

| Index | Unit | Full Name |
|---|---|---|
| NOF | | Exp. Number of Over-Frequency Events |
| NUF | | Exp. Number of Under-Frequency Events |
| ENAF | | Exp. Number of Abnormal Frequency Events |
| EOFD | min | Exp. Over-Frequency Duration |
| UFD | min | Exp. Under-Frequency Duration |
| AFD | min | Exp. Abnormal Frequency Duration |
| EENS | MWh | Exp. Energy Not Served to Loads |
| EWEW | MWh | Exp. Wind Energy Wasted |
| EWES | MWh | Exp. Wind Energy Surplus Supplied |
| IENS | MWh | Indirect Energy Not Supplied |
| ECU | MWh | Unnecessary Energy Consumption |

load in the system due to severe under-frequency events. The indices are evaluated, taking the probabilities of system state and contingency into consideration. Often used indices for wind-integrated systems are listed in Table 1. For the system study performed in Section 4, the expected wind energy wasted, and the number of severe under-frequency is used to assess the system performance [16].

These indices represent the expected (Exp.) system behavior with the given parameters. They are used to compare the given system's capability concerning its frequency behavior and the spend and curtailed energy for maintaining it. It has to be noted that one can not directly link the cost for primary or secondary reserves with these indices. The indices described above are only reflecting the energy used during an analyzed contingency.

## 3 Proposed frequency-related security optimization framework

As the possibilities for different controller schemes, settings, and scheduling increases severely with the extensive usage of renewable power generation units, the assessment has to be adapted to this. Changing the input to the assessment, how these units behave during the operation of the grid, has a severe impact on the grid performance. System operators are in need of adapting their decision-making process to this change in the operation states. The aim is to reduce the frequency impact of the converter-based units while keeping the drawbacks as small as possible. Therefore, a framework for including multiple frequency managements and comparing their impact is proposed to find well-suited remedial actions for enhancing the frequency-related security. The proposed framework is shown in Fig. 5.

The additional parts of the proposed framework are described in the following subsections.

### *3.1 Design variations*

The first addition to the standard assessment of the system security is the variance in the tested system. This can be the usage of different control strategies, settings, or scheduling. A variety of frequency managements is defined, that is then implemented in addition to the conventional power system. The system description includes the load variation and the information of the conventional generation units, under-frequency load shedding strategies, and primary and secondary frequency control settings. The system is simulated with all defined variations. The study case in Section 4 varies one control parameter, resulting in a one-dimensional outcome. With more variations combined, the analysis can also result in multi-dimensional outputs, where different variations are evaluated together. The possible variations can include control setting changes, different control schemes, and different activation strategies by TSOs.

The reliability indices, as assessment outcomes, are compared in the following step to determine the best-suited frequency management variation. This step is further illustrated in the system study in Section 4.

### *3.2 Evaluation criteria*

The second addition to the classical frequency-related security assessment is the choice of an optimization strategy. The different indices that describe the abnormal frequency states and drawbacks in the frequency control processes have to be compared. Thus, multiple definitions are possible, such as the minimal needed energy used for reaching a certain frequency quality.

Another design goal is to find the highest efficiency between system benefits and the required drawbacks. Then, one can use a sensitivity analysis of the indices of interest. The change of the reliability indices for a given variation of input is given in (2). The reference value to compare with is the one where the control is deactivated.

$$\Delta Index_i = Index_i - Index_0 \tag{2}$$

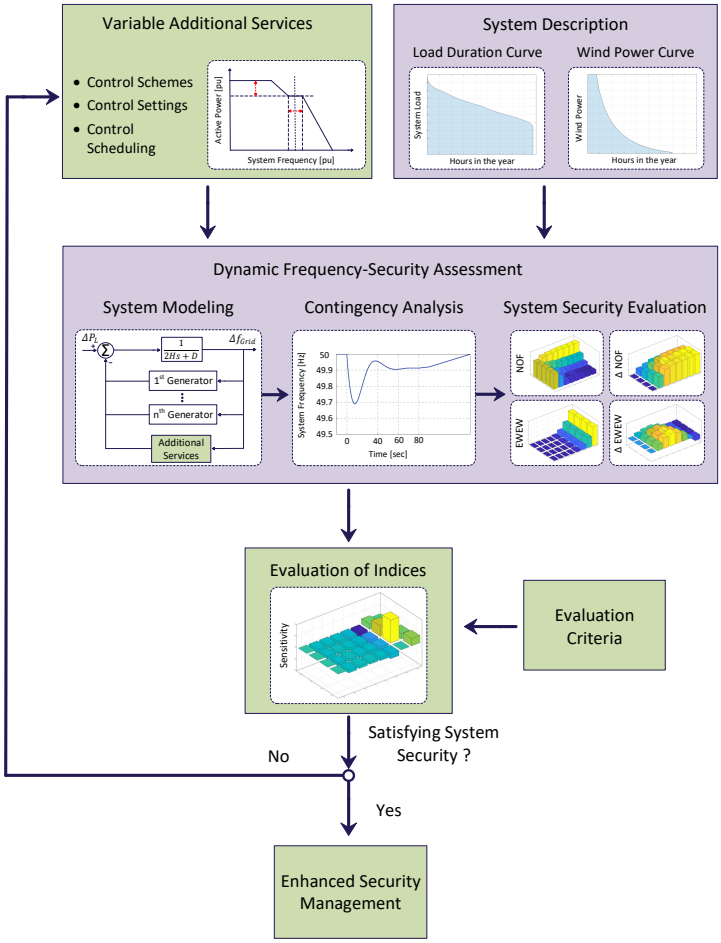


**Fig. 5**: Frequency-related security framework, to enhance system security management in modern power systems The proposed steps for improving the security management are indicated in green.

The change of an index value is an indication of how much the operational actions affect the system security. It allows seeing the effect of different controller settings or varying shares of converter-based penetration level. The relative change of a given index, described in (3), can be used to quantify the improvement due to the tested control.

$$\Delta Index_{Rel} = \frac{\Delta Index_i}{Index_0} \tag{3}$$

This relative change allows the combination of different frequency quality measures such as ENAF and EAFD to find operational strategies best suited for the given grid requirements. The relative frequency quality change is combined with other reliability indices of interest. This is done to achieve an optimal system performance and to incorporate the system efforts for this improvement. As described in [16, 23], the energy used for the frequency control in the different participating units is an essential factor when assessing the system performance and economics. This analysis allows a fast way of balancing the benefits and drawbacks of the applied system changes. For this analysis, the change in EWEW from the reference outcome is taken to determine the not produced power of the wind power plants as the control effort. The combination of benefits and costs is given with the sensitivity index is given in (4).

$$S_{Freq,Index} = \frac{\Delta Index_{Quality}}{\Delta Index_{Drawback}} \tag{4}$$

Other relevant indices can be the number of certain events, such as the number of occurring system splits, or the activation of different functions. The evaluated indices are based on the TSO design choice, determining which effect in the power grid is aimed to be optimized.

### *3.3 Design Evaluation*

In the last step, the optimization strategy is used to assess the system variations of interest. The strategy best suited for the TSO is determined, allowing an enhanced system performance. The outcome of the assessment can also be obtained by an iterative process. The iterations can include different frequency management choices, like control schemes, settings, and scheduling of usage. This step is the point where the proposed framework is changing from a descriptive process to a design tool, so operators can clearly see trends in their system reliability and the drawbacks of achieving it. Further changes, adapting to smaller system variations, can be incorporated.

The proposed framework is used on a test case in the following section, illustrating the proposed additional steps to the conventional

Table 2: Generator data [28]

| Rated Power $[MW]$ | Number of Units | MTTF $[hrs]$ | MTTR $[hrs]$ | H $[s]$ | Ramp Rate $[MW/hour]$ |
|---|---|---|---|---|---|
| 12 | 5 | 2940 | 60 | 2.5 | 60 |
| 20 | 4 | 450 | 50 | 3.0 | 80 |
| 50 | 6 | 1960 | 20 | 3.5 | 30 |
| 76 | 4 | 1960 | 40 | 4.0 | 304 |
| 100 | 3 | 1200 | 50 | 4.3 | 300 |
| 155 | 4 | 960 | 40 | 4.8 | 620 |
| 197 | 3 | 950 | 50 | 5.0 | 591 |
| 350 | 1 | 1150 | 100 | 5.5 | 350 |
| 400 | 2 | 1100 | 150 | 6.0 | 800 |

system assessment. With this, TSOs can better plan the remedial action needed to manage modern power system security.

## 4 System study

The framework is applied in a modified IEEE reliability test system (IEEE RTS) [27, 28]. The aim is to use frequency control in wind power plants to improve the system's frequency quality. The conventional parts of the system are described in details in [28]. This system is well established for different types of reliability analysis, from security to adequacy assessment [29]. For this study, an increasing number of installed wind turbines are considered to determine the change in operative actions. Wind power generation is chosen, as it is the main contributor to renewable generation in many countries. Nevertheless, the framework can also be applied to other converter-based units with frequency control capabilities. The integration of wind turbines into IEEE RTS and the respective reliability impact has been analyzed before, like in [16, 30]. In [16], they focus on the frequency-related security due to the power electronic-based units, but without additional frequency support functionality in the respective units. The software MATLAB Simulink is used to simulate the system behavior during the contingencies.

### *4.1 Conventional system components*

The conventional generation units in the IEEE RTS have a total capacity of 3405 MW. Each generator has a certain probability of a failure per year, as given in [28]. The dynamic generator parameters are shown in Table 2 with the mean time to failure (MTTF) and the mean time to repair (MTTR). This dynamic data describes the frequency behavior as well as the probability of the units for failing during operation.

The unit commitment order of the conventional generators under different system states is determined in a heuristical manner. The strategy includes the units with the highest time constant first, only activating the smaller units if needed. This results in a relatively high system inertia in the power system for any given load and wind situation. The generation units, which are committed to frequency control, can provide primary and secondary control, as discussed in [16]. There, the ramp rate restrictions for secondary control are considered.

The system load is not constant during the operation throughout the year. The system load can be represented by the hourly peak load, resulting in the load duration curve. In the IEEE RTS, the peak load throughout the year is 2850 MW, and the LDC is given in [27].

The under-frequency load-shedding (UFLS) follows the ENTSO-E guidelines [31]. This protective function stabilizes the system frequency after a severe generation outage [31]. The under-frequency load-shedding (UFLS) is the last option for the power system operation, keeping the remaining parts of the loads still supplied. The UFLS-scheme is fixed in this analysis, as it is implemented in the protection relays, and it is not changed dynamically during operation.

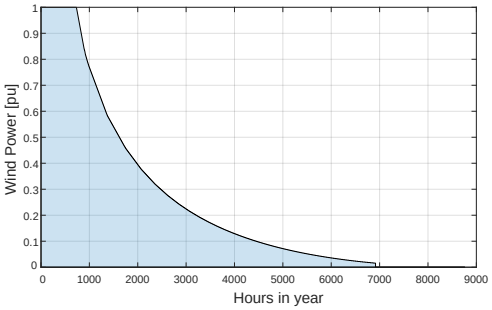


**Fig. 6**: Wind power duration curve, giving a capacity factor of 28.5 %.

### *4.2 Modeling wind power plants*

Wind power plants are additionally included into the IEEE RTS. The number of connected turbines is increased in this study to see the effect on the system reliability throughout different wind power penetration levels into the system. The rated power of installed wind power plants is increased from zero up to 1000 MW. The actual wind power injected into the power system is determined by the current wind speed and the design of the turbines. The rated wind turbine power is 5 MW. The cut-in, the rated, and the cut-out wind speed are 3 m/s, 11.4 m/s, and 25 m/s, as suggested in [32]. The produced wind power during every hour of a year can be combined to a wind power duration curve, as shown in Fig. 6. In this analysis, the wind turbines operate with 2500 full load hours, with a capacity factor of 28.5 % in a year [33].

The rated power of the wind turbines is varied in its share related to the peak load in a year. This is done to see the effect of the control parameters when more wind power plants are added to the system. The injection of wind power throughout the operation is curtailed above the maximum allowed penetration level of 70 %. The wind power plant deloading is realized as proposed in [34]. The rotor speed depends on the current wind situation, as well as on the amount of demanded power curtailment per turbine. This curtailment is in place to keep a minimum number of conventional units in operation, preserving minimum system inertia at all times.

The applied frequency control in this work is the 'frequency control' scheme, described in the Danish grid code [14], like illustrated in Fig. 7. It provides a high degree of flexibility, as many parameters ($P_{Delta}$, $Droop_1$, $Droop_2$, $f_{deadband}$) can be changed during the operation to adapt to the future grid needs. It can be realized in wind power plants without additional battery systems. The control scheme is included in all simulated wind power plants.

The setting in the control scheme that is varied in the assessment is $P_{Delta}$, the curtailed wind power in steady-state. It is increased linearly from zero up to 0.2 pu, severely deloading the wind power plants during operation, as described in [34]. The frequency control in the performed study is only activated by the TSO when the wind power plants currently inject more power than 50 % of the actual system load. Otherwise, $P_{Delta}$ is set to zero, resulting in over-frequency wind power curtailment, as it is mandatory in the Danish grid code for wind power plants. When power is curtailed during steady-state operation, the full wind power is injected into the grid at a fixed frequency value of 49.2 Hz. This control scheme aims to reduce the risk of UFLS. The dead-band value is fixed at 0.2 Hz, specified in the Danish grid code as the standard value. Full power

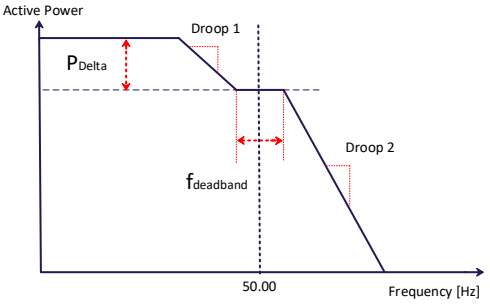


**Fig. 7**: Danish grid code requirement regarding the frequency response of wind power plants [14].

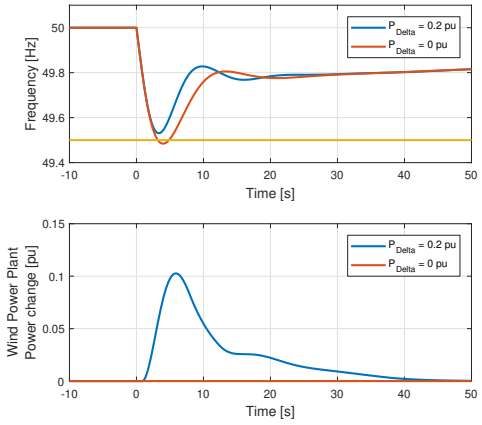


**Fig. 8**: System frequency and wind power during a 100 MW generator failure with changed frequency control behavior. The threshold for severe under-frequency occurrence is shown in yellow.

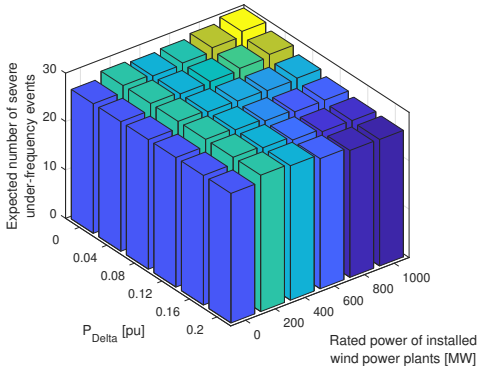


**Fig. 9**: Expected number of severe under-frequency events, dependent on the control setting.

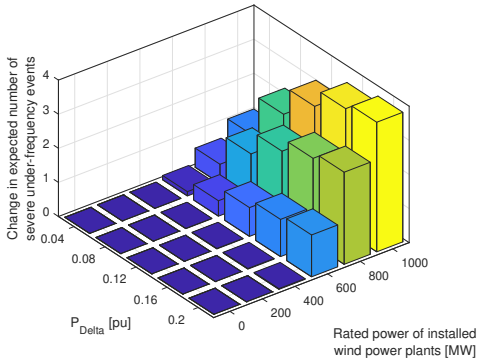


**Fig. 10**: Change in severe abnormal frequency occurrences during the operation. Wind power penetration level and control value are varied. Positive values indicate a reduction in abnormal frequency states.

curtailment is performed at a frequency of 52 Hz, protecting the system from over-frequency deactivation of equipment. The values for $Droop_1$ and $Droop_2$ are adjusted during this analysis, as $P_{Delta}$ is varied and the frequency set-points for zero and full power curtailment are fixed. This control is implemented in the wind power plant controller, receiving the controller setting from the TSO.

### *4.3 Results of the study case*

The IEEE RTS with the different capacities of installed wind power and the changed controller settings is simulated. The system frequency is highly affected by the additional frequency control in the wind power plants. In the shown contingency in Fig. 8, a 100 MW generator failed, causing a severe frequency drop in the system. The installed amount of wind power in the system is 1000 MW. Due to the control settings, the wind power reserve allows for a power increase during the frequency drop.

The simulation results in Fig. 8 shows one system state, where the power curtailment $P_{Delta}$ is set to 0.2 pu. This offers frequency control options during under-frequency contingencies. In the shown contingency, the frequency control is able to prevent a severe frequency drop below 49.5 Hz. This reduces the expected number of severe frequency events and therefore enhancing the frequency quality during operation. The reduction of wind power in steady-state causes a slightly higher system inertia, as more generation units have to be activated to supply the system load. In the shown result, this increased inertia is only marginal so that the rate of change of frequency is not severely affected.

The frequency-related security assessment results with all possible system states and contingencies allow an estimation of the system security during the grid operation of one year. The results of the assessment are illustrated in the following figures. The expected number of under-frequency drops below 49.5 Hz, ENUF, is shown in Fig. 9. The results are shown for the used values of $P_{Delta}$, which are varied in the analysis.

The change in the number of severe under-frequency events is twofold. The usage of wind power plants reduces the number of running conventional units, resulting in a reduction of inertia during high renewable power injection phases. Counteracting is the reduction of potential contingencies, as the generation units are less likely to be in operation during wind power injection. Therefore, the expected number of severe under-frequency events are not rising severely.

The influence of the used 'frequency control' in the wind turbines can be seen by calculating the change relative to the deactivated control, as described in Section 3.2. The improvement in the number of severe under-frequency events is shown in Fig. 10.

With rising wind power and increasing $P_{Delta}$, the values of the reduction due to this steady-state power curtailment is shown in Fig. 10. The positive control impact is dependent on the system and frequency control settings. Nevertheless, the control has a positive effect on the frequency quality under various system conditions.

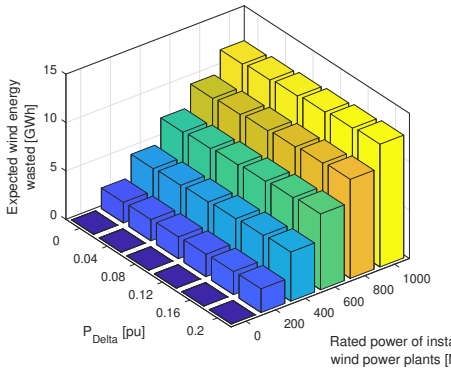


**Fig. 11**: Expected wind energy wasted for the tested system conditions. Wind power penetration level and control value are varied.

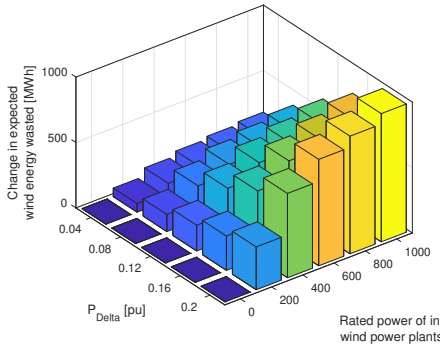


**Fig. 12**: Change in the expected wind power wasted during operation. Wind power penetration level and control value are varied.

Hence, the 'frequency control' has also drawbacks which have to be considered for reliable frequency management. The EWEW is shown in Fig. 11 for the different determined study cases. It is affected by the remedial actions of the TSO. These are the tested frequency control as well as the curtailment of wind power when the available injection is higher than the allowed share of the system load.

The results show that the EWEW increases severely with more wind power plants installed in the grid, but only slightly with the additional frequency control. The deviation caused by the 'frequency control' is determined by a change in EWEW for each assessed $P_{Delta}$ setting for the different wind power levels, which is illustrated in Fig. 12. This change due to remedial has to be balanced with the frequency quality gain, allowing for a reliable system operation.

The EWEW increases with the amount of installed wind power plants and curtailed wind energy in steady-state. The most reliable setting is determined in the following section by two different approaches to illustrate the capability of the framework to adapt to the TSO demands. One optimization strategy determines the wasted wind energy that is needed to restore the frequency quality that the system has without wind integration. The other one determines the most efficient ratio of wind energy curtailment with the enhancement in frequency quality.

### *4.4 Improved system security management*

Two strategies are used to determine the remedial actions best suited for enhancing security management.

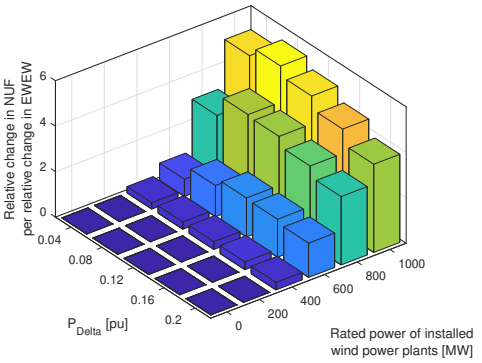


**Fig. 13**: Change in the expected wind power wasted during operation. EWEW depends on the amount of installed wind power and on the change in preventive action by the TSO.

*4.4.1 Optimizing for restoring frequency quality:* The first strategy assesses the needed amount of wasted wind energy to achieve the same frequency quality the system has without wind power penetration. The change in frequency-related security can be determined by comparing the results shown in Fig. 9 and Fig. 11. It can be seen that the additional frequency control service with 600 MW and lower are not capable of restoring the number of severe abnormal frequency events (26.8 occurrences per year) that the grid had before installing the wind turbines. With 800 MW installed wind power plants, this index can be achieved with a setting of 0.16 pu. The expected wasted wind energy is 9.88 GWh per year in this condition. With the full 1000 MW installed rated wind power, the abnormal frequency states can be reduced to the original value with $P_{Delta}$ set to 0.12 pu and 12.5 GWh wasted wind energy per year. The proposed assessment allows determining this quickly, giving a secure frequency management.

*4.4.2 Optimizing for effective wind energy usage:* When the goal of the optimization strategy is to determine the most efficient balance between frequency quality increase and wasted wind energy, one has to compare the relative changes the control variation causes. The control value, where the highest benefit in system quality is gained compared to the wasted wind energy, can be easily determined for the different wind integration levels. The relationship is shown in Fig. 13.

In this case study, a $P_{Delta}$ value of 0.08 pu is the most effective at a wind power penetration of 800 MW and 1000 MW, whereas it is more effective to use a power curtailment of 0.12 pu when wind power plants with a rated power of 600 MW are installed. The most effective setting, at lower penetration levels, can be found at 0.16 pu. Other combinations of indices used for the evaluation of the system performance can be chosen as well. This depends on the strategy a TSO decides for the respective grid performance evaluation.

## 5 Discussion

The proposed framework for enhancing the system's operational reliability can be used, as described in Section 4.4.2, to optimize the frequency controls in the evaluated power system. The framework is only assisting TSOs when all steps in the framework are designed carefully.

The power system modeling has to incorporate all important generation units with their dynamics and frequency controls. In the framework, it is also possible to implement demand-side controls that balance the system load throughout the operation, shifting the LDC in steady-state operation. Other load-shedding strategies are also a research target to assist reliable frequency management.

The evaluated contingencies have a severe impact on the reliability results. When too few contingencies are considered, it is not

possible to correctly estimate the system behavior. Including too many system states and grid disturbances but increases the computational burden severely. A balance has to be found that allows sufficient accuracy in the reliability evaluation in an acceptable simulation time.

The evaluation of the different frequency management strategies is done in the shown study by determining which control setting utilized the curtailment of wind power most effectively concerning the number of abnormal frequency states. Other evaluations may be more appropriate for the usage in real power grids. Often, TSOs have a maximal number of abnormal frequency states as a defined threshold that is not allowed to be violated. Then, the evaluation may consider the minimum EWEW to achieve this target.

## 6 Conclusion

The proliferation of power electronic-based generation units makes the coordination of frequency controls a more demanding task for system operators. Nevertheless, power converter-based units provide an unused degree of flexibility in frequency controls. The proposed framework for frequency security optimization in highly converter integrated power grids allows system operators to determine optimal strategies in the usage of these units. The framework adds different steps to the assessment process, beginning at the variable system input to choose the optimization strategy. This allows a strict procedure while keeping the assessment open to the requirements of the analyzed power grid. The combination of fixed and variable system parameters allows a fast assessment of the reliability of different scenarios. The costs and the benefits of the different scenarios can be evaluated and combined to estimate the control options that are suited the best for the given system demand.

The different steps in the proposed framework can be adapted to any grid that faces a high integration of converter-based units, allowing the operator to choose their remedial actions to manage the system's frequency-related security. Different power sources, such as photovoltaic, wind, and battery systems, can be included in the analysis, as well as HVDC transmission systems. For this, the possible variations increase even more, as frequency controls can be realized in all connected equipment. Then, other indices have to be respected, representing the not utilized solar energy or the amount of battery system usages.

In the study case, the power reduction in steady-state for a given frequency controller settings of a wind-integrated power system is shown. The test case shows that converter-based units can contribute, at least partially, to the frequency quality. The proposed framework can be combined with more advanced ways of optimizing the control, such as more iterative steps to further enhance the system frequency management.

## 7 Acknowledgments

This work is supported by the Reliable Power Electronic-Based Power Systems (REPEPS) project at the Department of Energy Technology, Aalborg University, as a part of the Villum Investigator Program funded by the Villum Foundation.

## 8 References

1 REN21. (2019) Renewables 2019 Global Status Report. (Date last accessed 15-July-2020). [Online]. Available: http://www.ren21.net/gsr-2019

2 P. Kundur, N. J. Balu, and M. G. Lauby, *Power System Stability and Control*. McGraw-Hill New York, 1994, vol. 7.

3 MIGRATE. (2016) Deliverable D1.1, Report on Systemic Issues. (Date last accessed 15-July-2020). [Online]. Available: https://www.h2020-migrate.eu/downloads.html

4 ENTSO-E. (2017) Need for Synthetic Inertia (SI) for Frequency Regulation. (Date last accessed 15-July-2020). [Online]. Available: https://consultations.entsoe.eu/system-development/entso-e-connection-codes-implementation-guidance-d-4

5 Ørsted A/S. (2018) Enhanced Frequency Control Capability (EFCC) - Wind Package Report - Frequency Support Outlook. (Date last accessed 15-July-2020). [Online]. Available: https://www.nationalgrideso.com/document/136161/download

6 N. Hatziargyriou, J. Milanović, C. Rahmann, V. Ajjarapu, C. Cañizares, I. Erlich, D. Hill, I. Hiskens, I. Kamwa, B. Pal *et al.*, "Stability Definitions and Characterization of Dynamic Behavior in Systems with high Penetration of Power Electronic interfaced Technologies," *IEEE PES Technical Report PES-TR77*, 2020.

7 J. Steinkohl and X. Wang, "Gain Optimization for STATCOM Voltage Control under Various Grid Conditions," in *2018 20th European Conference on Power Electronics and Applications (EPE'18 ECCE Europe)*. IEEE, 2018, pp. 1–6.

8 W. Du, Q. Fu, and H. Wang, "Power System Small-Signal Angular Stability affected by Virtual Synchronous Generators," *IEEE Transactions on Power Systems*, vol. 34, no. 4, pp. 3209–3219, 2019.

9 M. Edrah, K. L. Lo, and O. Anaya-Lara, "Impacts of High Penetration of DFIG Wind Turbines on Rotor Angle Stability of Power Systems," *IEEE Transactions on Sustainable Energy*, vol. 6, no. 3, pp. 759–766, 2015.

10 A. Fernández-Guillamón, J. I. Sarasúa, M. Chazarra, A. Vigueras-Rodríguez, D. Fernández-Muñoz, and A. Molina-García, "Frequency Control Analysis based on Unit Commitment Schemes with high Wind Power Integration: A Spanish Isolated Power System Case Study," *International Journal of Electrical Power & Energy Systems*, vol. 121, p. 106044, 2020.

11 Z. Wu, W. Gao, T. Gao, W. Yan, H. Zhang, S. Yan, and X. Wang, "State-of-the-Art Review on Frequency Response of Wind Power Plants in Power Systems," *Journal of Modern Power Systems and Clean Energy*, vol. 6, no. 1, pp. 1–16, 2018.

12 Y. Liu, S. You, and Y. Liu, "Study of Wind and PV Frequency Control in US Power Grids - EI and TI Case Studies," *IEEE Power and Energy Technology Systems Journal*, vol. 4, no. 3, pp. 65–73, 2017.

13 M. Dreidy, H. Mokhlis, and S. Mekhilef, "Inertia Response and Frequency Control Techniques for Renewable Energy Sources: A Review," *Renewable and Sustainable Energy Reviews*, vol. 69, pp. 144–155, 2017.

14 ENERGINET, "Technical Regulation for Wind Power Plants, Denmark," (Date last accessed 15-July-2020). [Online]. Available: https://en.energinet.dk

15 M. Altin, Ö. Göksu, R. Teodorescu, P. Rodriguez, B. Jensen, and L. Helle, "Overview of Recent Grid Codes for Wind Power Integration," in *2010 12th International Conference on Optimization of Electrical and Electronic Equipment*, May 2010, pp. 1152–1160.

16 C. Liang, P. Wang, X. Han, W. Qin, R. Billinton, and W. Li, "Operational Reliability and Economics of Power Systems with Considering Frequency Control Processes," *IEEE Transactions on Power Systems*, vol. 32, no. 4, pp. 2570–2580, 2017.

17 N. Nguyen and J. Mitra, "Reliability of Power System with high Wind Penetration under Frequency Stability Constraint," *IEEE Transactions on Power Systems*, vol. 33, no. 1, pp. 985–994, 2017.

18 J. Guo, T. Zhao, W. Liu, and J. Zhang, "Reliability Modeling and Assessment of Isolated Microgrid Considering Influences of Frequency Control," *IEEE Access*, vol. 7, pp. 50 362–50 371, 2019.

19 M. Vrakopoulou, K. Margellos, J. Lygeros, and G. Andersson, "A Probabilistic Framework for Reserve Scheduling and N-1 Security Assessment of Systems With High Wind Power Penetration," *IEEE Transactions on Power Systems*, vol. 28, no. 4, pp. 3885–3896, 2013.

20 Y. Wen, C. Chung, and X. Ye, "Enhancing Frequency Stability of Asynchronous Grids Interconnected with HVDC Links," *IEEE Transactions on Power Systems*, vol. 33, no. 2, pp. 1800–1810, 2017.

21 N. Balu, T. Bertram, A. Bose, V. Brandwajn, G. Cauley, D. Curtice, A. Fouad, L. Fink, M. G. Lauby, B. F. Wollenberg *et al.*, "On-line Power System Security Analysis," *Proceedings of the IEEE*, vol. 80, no. 2, pp. 262–282, 1992.

22 R. Billington and R. N. Allan, *Reliability Evaluation of Power Systems*. Plenum Publishing Corp., New York, NY, 1984.

23 P. Wang, Z. Gao, and L. Bertling, "Operational Adequacy Studies of Power Systems with Wind Farms and Energy Storages," *IEEE Transactions on Power Systems*, vol. 27, no. 4, pp. 2377–2384, 2012.

24 R. Billinton, R. Karki, Y. Gao, D. Huang, P. Hu, and W. Wangdee, "Adequacy Assessment Considerations in Wind Integrated Power Systems," *IEEE Transactions on Power Systems*, vol. 27, no. 4, pp. 2297–2305, 2012.

25 J. Dai, Y. Tang, and Q. Wang, "Fast Method to estimate Maximum Penetration Level of Wind Power considering Frequency Cumulative Effect," *IET Generation, Transmission & Distribution*, vol. 13, no. 9, pp. 1726–1733, 2019.

26 S. Peyghami, P. Palensky, and F. Blaabjerg, "An Overview on the Reliability of Modern Power Electronic Based Power Systems," *IEEE Open Journal of Power Electronics*, vol. 1, pp. 34–50, 2020.

27 P. M. Subcommittee, "IEEE Reliability Test System," *IEEE Transactions on Power Apparatus and Systems*, vol. PAS-98, no. 6, pp. 2047–2054, Nov 1979.

28 Reliability Test System Task Force of the Application of Probability Methods Subcommittee, "The IEEE Reliability Test System-1996," *IEEE Transactions on Power Systems*, vol. 14, no. 3, pp. 1010–1020, Aug 1999.

29 S. Peyghami, P. Davari, M. Fotuhi-Firuzabad, and F. Blaabjerg, "Standard Test Systems for Modern Power System Analysis: An Overview," *IEEE Industrial Electronics Magazine*, vol. 13, no. 4, pp. 86–105, Dec 2019.

30 J. M. Mauricio, A. Marano, A. Gomez-Exposito, and J. L. Martinez Ramos, "Frequency Regulation Contribution Through Variable-Speed Wind Energy Conversion Systems," *IEEE Transactions on Power Systems*, vol. 24, no. 1, pp. 173–180, Feb 2009.

31 ENTSO-E. (2015) P5 - Policy 5: Emergency Operations. (Date last accessed 15-July-2020). [Online]. Available: https://docstore.entsoe.eu

32 J. Jonkman, S. Butterfield, W. Musial, and G. Scott, "Definition of a 5-MW Reference Wind Turbine for Offshore System Development," National Renewable Energy Lab.(NREL), Golden, CO (United States), Tech. Rep., 2009.

33 N. Boccard, "Capacity Factor of Wind Power realized Values vs. Estimates," *Energy Policy*, vol. 37, no. 7, pp. 2679 – 2688, 2009.

34 C. Pradhan and C. Bhende, "Adaptive Deloading of Stand-Alone Wind Farm for Primary Frequency Control," *Energy Systems*, vol. 6, no. 1, pp. 109–127, 2015.

.

# Journal Publication 3 [J3]

## Fuzzy-Based Frequency Security Evaluation of Wind-Integrated Power Systems

Joachim Steinkohl, Xiongfei Wang, Pooya Davaari, Frede Blaabjerg, Saeed Peyghami

The paper currently under review at
*IET Energy Systems Integration* 2021.

IET Energy Systems Integration

*Research Article*

IET Journals
The Institution of Engineering and Technology

# Fuzzy-Based Frequency Security Evaluation of Wind-Integrated Power Systems

ISSN 1751-8644
doi: 0000000000
www.ietdl.org

*Joachim Steinkohl*[1*], *Saeed Peyghami*[1], *Xiongfei Wang*[1], *Pooya Davari*[1], *Frede Blaabjerg*[1]

[1] *Department of Energy Technology, Aalborg University, Pontoppidanstræde 111, Aalborg, Denmark*
* *E-mail: joa@et.aau.dk*

**Abstract:**
The transition to renewable energy-based power systems is in fast progress. One of the main challenges in keeping a power system with high operational reliability is to maintain the system frequency. As synchronous generator units are replaced with power-electronic converters, the rotating mass and the system inertia are decreasing. Virtual Synchronous Machine (VSM) control is a modern control technique that is aiming to compensate for the inertia reduction. The usage of power electronic-based converter units equipped with VSM control has to be managed and scheduled by system operators. An assessment of the operational frequency reliability is used to evaluate different service usages. A method is proposed that allows the comparison of different frequency management strategies. The proposed method uses fuzzy-logic to evaluate the system risk for abnormal frequency as well as the system effort in the form of frequency control usage. This allows to compare different frequency managements fast whilst respecting many different reliability indices together. The proposed method is validated with a modified IEEE Reliability Test System (RTS) with wind power capacity integrated.

## 1 Introduction

Modern power systems integrate more and more renewable generation units [1]. These use converters as the linking part between the renewable power source (solar or wind) and the power grid. The replacement of conventional, synchronous generation units with converters reduces the system inertia significantly during high renewable penetration phases. This weakens the system's capability of maintaining a normal frequency when contingencies occur, reducing the system operational reliability of the power grid. Transmission system operators (TSOs) have named reduced inertia the major concern for their operation in the modern power grids [2, 3]. Severe frequency incidents are recorded and analyzed by system operators to observe their grid operation and to improve their future handling of these incidents [4]. Modern frequency controls in wind power plants aim to contribute to the reliable system frequency. However, system operators have to evaluate when to utilize which additional frequency services. This is done by evaluating the system reliability with different frequency management strategies [5]. The evaluation of many different study cases is time-consuming and requires to consider many different factors on system performance. In this work, a method that allows fast comparison of multiple reliability assessments is proposed, which improves the decision-making process by system operators.

Fig. 1 shows the power system's hierarchical levels, which are taken into account to assess the operational frequency security. The ICT-layer (Information and Communication Technologies) describes the system operators' view of the system. The system operator evaluates the system and reacts with remedial action when necessary in order to change the behavior of the transmission network and the connected units at the plant level. These remedial system operator actions can be preventive or responsive. Responsive actions are, for example, the manual activation and deactivation of generation units. Preventive actions include the power curtailment of renewable sources during steady-state operation to maintain minimum inertia, and the change of set-points and control strategies. In this work, the impact of strategies to order VSM-service by wind power plants is discussed. The main question is how a system operator can decide which frequency management strategy is improving the system performance the best.

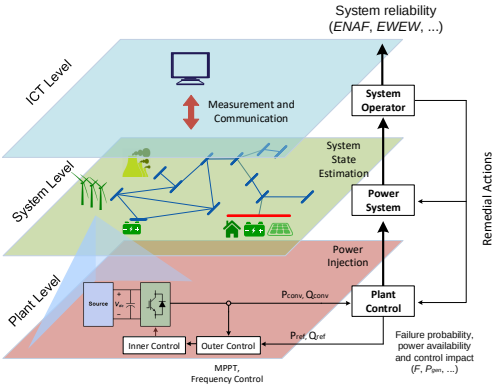


**Fig. 1**: Considered hierarchical Levels for the system reliability assessment and the interactions between them [6].

In conventional power systems, the needed amount of primary frequency reserves is only determined by the reference incident. This worst-case assumption for a system contingency varies for every power system and is defined in the system operator policies [7]. However, modern power grids with converter-based units offer the system operators a much wider variety of frequency services and how and when to utilize them. These modern units are capable of implementing modern frequency controls that can be changed according to the system's needs, even during the operation.

Modern controller designs in power electronic-based generation units aim to replace the conventional units and their system-supporting functions. Already now are these units contributing during the system operation with assisting controls, as demanded by grid codes [8, 9]. These units stay nowadays in operation and inject reactive power during transient grid events, e.g., lightning strikes. Renewable units are required to curtail their power injection during events of over-frequency [8, 9]. Virtual synchronous machines (VSMs) control converter-based units to mimic the synchronous

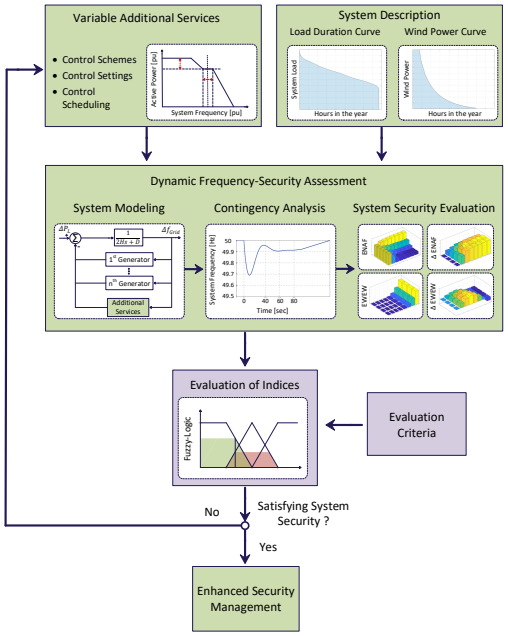


**Fig. 2**: Framework for enhancing the frequency management; the evaluation is highlighted in violet [6].

machine behavior. This control structure is promising, as it allows the system operator to maintain an acceptable frequency deviation (NaDir) as well as limit the rate of change of frequency (RoCof). Recent overviews of VSMs and their frequency-supporting capabilities are given in [10–12]. Other, very similar controls are fuzzy-based VSM Controls [13, 14], power-synchronization controls [15, 16], and inertia emulating adaptations for microgrids [17, 18]. So far, VSM controls are not used in many countries; only Hydro-Quebec demands inertia controls with 3.5 sec time constant emulation during severe frequency deviations [19]. However, many system operators discuss the need for converter based units to provide frequency support by emulating the inertia of synchronous machines and can soon be a more general demand.

TSOs have to decide when to utilize the new frequency controls as services to improve their frequency controls. Thus, the power system reliability assessment is utilized to compare multiple frequency management strategies to choose the most suitable one. A framework for enhancing the frequency management of modern power systems is given in Fig. 2 [6].

The framework describes the different steps of the system reliability enhancement design process. Parts of the system data are fixed to describe the constant grid conditions for the assessment. Frequency management variations are then implemented to change the frequency controls by converter-based units. The dynamic frequency-security assessment for all considered variations is performed. This is done by modeling the different controls and system states, performing the contingency-simulations, and then calculating the reliability indices from the simulation results. Afterward, the reliability indices have to be evaluated and compared, based on the defined evaluation criteria. A number of different indices are used to describe the system frequency performance and the utilized frequency controls [5, 20–24]. In this study, a fuzzy-logic based evaluation is utilized to combine the different indices for a fast comparison of the frequency management strategies.

Fuzzy-logic is introduced to emulate language-based decision-making [25, 26]. Until now, it is not used to evaluate the reliability assessment results. However, it is used for the reliability assessment procedure, describing the probability of the system states to reduce the simulation burden during the assessment [27–30]. The fuzzy-sets are thereby used to represent the system states' probability, such as load distribution. In some works [27–29], this is directly going into the assessment method; in others, the fuzzy-logic is utilized together with Monte-Carlo simulation to incorporate uncertainties in the system description [30].

The proposed evaluation method of system frequency management is presented in Section 2. A study case using the proposed method is described in Section 3; the results are given in Section 4. Finally, the conclusions are drawn in Section 5.

## 2 Methods

The evaluation of the system reliability is based on the indices as the result of the dynamic frequency-security assessment. The frequency controls aim to reduce the number, duration, and negative effects of severe frequency disturbances. Well-designed frequency management strategies only utilize additional frequency control effectively, so with well-chosen settings and only when required to keep the system operation economical.

### *2.1 Frequency reliability indices*

The reliability indices are obtained by combining the results of the dynamic system simulations. Different system states, $N_i$, are determined, and $N_j$ contingencies are applied to evaluate the system frequency, and the control performance. The results of the dynamic system simulation are evaluated in terms of abnormal frequency states, the curtailment of system loads, and the energy used for controlling the system frequency. A system reliability index is then calculated with the effect on the reliability index $Index_{i,j}$ during the system state $i$ and the contingency $j$, the probability of the respective system state $p_i$, an the probability for the simulated contingency $p_j$, as described in [5].

$$Index = \sum_{i=1}^{N_i} \sum_{j=1}^{N_j} Index_{i,j} \cdot p_i \cdot p_j \tag{1}$$

These indices are separated into two groups for evaluation. The first group describes the frequency quality as a measure of the system's Risk of failing or operating in an abnormal state. It is determined by the abnormal frequency states due to contingencies during operation. The number and duration of abnormal frequencies are taken as indices that determine if the frequency controls are sufficient for the safe system operation. An abnormal system frequency is in this work defined by a frequency deviation of more than 0.2 Hz. System operators use this threshold in the central Europe synchronous area [4]. The system risk of failing is also often described by the expected amount of energy not served to loads (EENS) [31]. This energy is not being served during severe frequency drops that cause activation of under-frequency load shedding functions [32]. The generation controls maintain the better the system frequency, the less this index is. Other evaluated indices are the number and duration of abnormal frequency events throughout the operation [5]. The indices used in this study for describing the system Risk are given in Table 1.

Table 1: Frequency reliability-related Indices

| Index | Unit | Full Name |
|---|---|---|
| ENAF | occur/year | Expected Number of Abnormal Frequencies |
| EAFD | min/year | Expected Abnormal Frequency Duration |
| EENS | GWh | Expected Energy Not Served |

The second group of indices is used to describe the system Effort by the frequency controls. Therefore are the energies estimated,

which are used by the frequency reserves (primary and secondary), and also the curtailed wind energy during operation (EWEW) [5]. In this work, a new index, EVSM, is introduced. This index describes the amount of VSM service ordered by the system operator throughout the operation. The index EVSM stands for the expected VSM service demanded. It measures how much the service is activated in the wind power plants, but not its actual energy delivery during operation. It is used to compare the effectiveness of different scheduling strategies for activating this service. Table 2 shows the used energy-related indices in this study.

Table 2: Frequency reliability-related Indices

| Index | Unit | Full Name |
|---|---|---|
| EVSM | GWh/year | Expected Amount of VSM service provided |
| EWEW | GWh/year | Expected Wind Energy Wasted |
| IENS | GWh/year | Indirect Energy Not Supplied |
| ECU | GWh/year | Expected Curtailed Energy |

These indices are used in the proposed fuzzy-based evaluation to describe the system control Effort and Risk. The system's Risk is an evaluation of the system's benefit by the additional frequency controls. The Effort-related indices are combined in fuzzy-evaluation to determine which frequency management uses the least amount of frequency controls. This aims to reduce the number of values to compare, but not only respecting one index for the Risk and only one for the system Effort.

### 2.2 *Fuzzy-Based Security Evaluation*

Fuzzy-logic has been introduced to emulate language-based decision-making processes [25]. Comparing different strategies by the TSO is challenging, as the given indices are all changed when the remedial actions are varied. The evaluation step from Fig. 2 is realized with the proposed fuzzy-evaluation. Therefore, the reliability indices are combined in the two groups from Section 2.1 to better evaluate the balance between System Risk and System Effort. This is possible using fuzzy-logic, as it allows multiple inputs. Fuzzy-logic is based on the three steps fuzzyfication, interference, and de-fuzzyfication, as shown in Fig. 3.

*2.2.1 Fuzzyfication:* The indices are normalized with a reference value to allow an easier comparison of variations in the system performance. In the presented study, the reference value is given for the system reliability without the evaluated additional frequency services by the wind power plants. The reference index values for the study case can be seen in Table 7 and Table 6 in the first row.

$$Index_{Normi} = \frac{Index_i}{Index_{Ref}} \tag{2}$$

In the fuzzyfication the indices are assigned to fuzzy-sets, describing the index behavior. The indices are thereby assigned to the sets not fully, but with a certain share, also called membership $M_{Index,Set}$. The assignment function of $M_{Index,Set}$ for the used three sets is shown in Fig. 4. The indices are assigned to three sets (Low, Normal, and High) with trapezoidal and triangle-shaped functions. The assignment of an index to the Low set is described with the respective function as in (3).

$$M_{Index,Low} = f_{Low}(Index_{Ref}) \tag{3}$$

The example in Fig. 4 assigns the relative index value of 93 % with 30 % to the Normal set and with 70 % to the Low set.

The three frequency-related indices are combined with different levels of importance. The proposed evaluation uses two different levels of importance, reduced priority, and increased priority. This

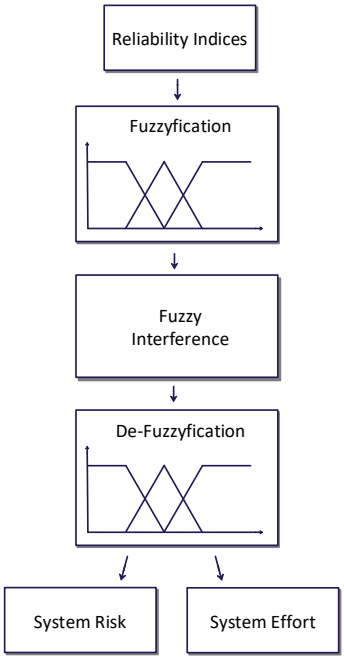


**Fig. 3**: Fuzzy-logic used for the evaluation of system Risk and system Effort with the indices from Table 1 and Table 2.

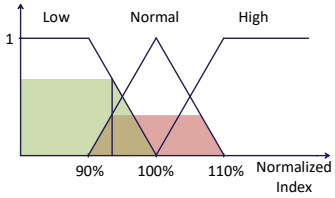


**Fig. 4**: Fuzzy-sets, describing the membership-functions of the system reliability indices.

allows a fast weighting of the indices by the system operator. In the study case, the amount of load curtailment is considered with increased priority, whereas the number and duration of abnormal frequency events are considered with reduced priority. Afterward, the set-values of the two priorities are combined with their averaged memberships. As a result of this, six sets are assigned with different shares, reduced and increased priority with each of the three sets Low, Normal, and High.

*2.2.2 Fuzzy-Interference:* The fuzzy-sets are, in this step, combined based on their memberships. The sets for reduced priority indices and the increased priority indices are used to achieve the set values for the five sets that are afterward used to describe the system Risk and Effort values. The five sets are Very Low, Low, Normal, High, Very High. These five sets' assignment is described with the relationships in Table 3 by multiplying the low priority and high priority set memberships.

As an example, the membership for Very Low system Risk is determined by the combined memberships of EENS, ENAF and EAFD as:

Table 3: Interference matrix used to combine multiple input indices

| | | Increased Priority | | |
|---|---|---|---|---|
| | | Low | Normal | High |
| Reduced Priority | Low | Very Low | Low | High |
| | Normal | Low | Normal | High |
| | High | Low | High | Very High |

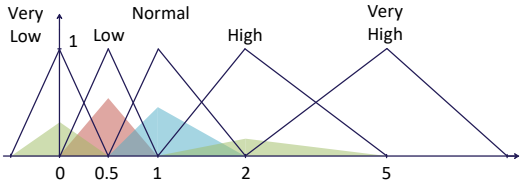


**Fig. 5**: Fuzzy-sets, used to calculate the outcome of the evaluation.

$$M_{RiskVeryLow} = M_{EENSLow} \frac{M_{ENAFLow} + M_{EAFDLow}}{2} \tag{4}$$

When output sets are assigned to multiple combinations, then the respective membership products are summed up. The five sets are used in the de-fuzzyfication step to the two values Risk and Effort.

*2.2.3 De-Fuzzyfication:* The five output fuzzy-sets achieved in the interference are translated back into a single value in the third and last step, the de-fuzzyfication. In this step, the sets are assigned to discrete values representing the state of the system. Hereby, the five sets are summed up with their memberships. This is done with the mean weighted value, determined with the membership values of the corresponding sets, as shown in (5).

$$\begin{aligned} Risk = {} & 0 \cdot M_{RiskVeryLow} + 0.5 \cdot M_{RiskLow} \\ & + 1 \cdot M_{RiskNormal} + 2 \cdot M_{RiskHigh} \\ & + 5 \cdot M_{RiskVeryHigh} \end{aligned} \tag{5}$$

Fig. 5 shows an example, where the Risk sets Very Low, Low, Normal, and High are assigned with a membership value. The outcome of the evaluation is thereby given as the summation of the share of the set with its assigned value. This means, the outcome of the system Risk and the system Effort, respectively, can vary between zero and five. A Risk value of zero indicates that all three frequency-related indices are totally assigned to the Low set, meaning the Risk in the system is severely reduced compared to the reference case. A Risk value of five indicates an assignment of these three indices to the High set, so the system frequency is worse than in the reference case.

The same relationship exists for the Effort of the system in maintaining the system frequency. A value of zero means that all determined energies have been significantly reduced, meaning they are assigned to the Low set. A system Effort of five, on the other hand, means that the frequency controls are utilized more often and more severely.

## 3 Case Study

The proposed evaluation method of multiple reliability assessments is tested on an IEEE reliability test system (RTS) with 1000 MW additional wind power plants. The system is described in detail in [33, 34]. The integration of VSM services provided by the wind power plants into the system aims to support the remaining synchronous machines to keep the frequency-related indices within an acceptable range.

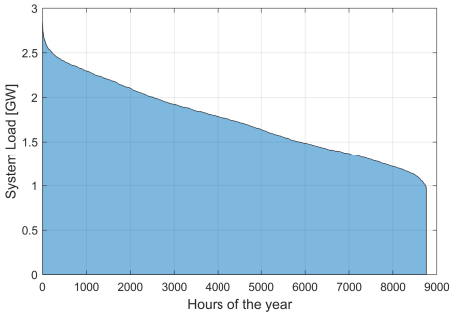


**Fig. 6**: Load duration curve in the IEEE reliability test system, data given in [33].

The main power system information is given in Section 3.1, together with the additional wind power plant information. The additional VSM service from the wind power plants, as well as the utilized scheduling scheme for the service, are described in Section 3.3.

### *3.1 Power system modeling*

The dynamic generator data to simulate the system frequency during contingencies are given in [34]. The system is represented as a one-bus system with multiple generation units. The unit commitment order of the conventional generators activates the generators with the higher time constants first, only activating the smaller units if needed. This results in the highest system inertia for any given load and wind power injection condition. Primary and secondary frequency controls are implemented in dedicated conventional generation units, as described in [5].

The system load is represented by the hourly peak load, resulting in the load duration curve (LDC). The data for the LDC is given in [33] and shown in Fig. 6. For the IEEE RTS, the maximum hourly peak load is 2850 MW.

Under-frequency load-shedding (UFLS) is implemented to determine the amount of load not supplied. This is the last option for the system operation during frequency drop contingencies. With the controlled load deactivation, still, the remaining parts of the system can be supplied. The UFLS-scheme is fixed in this analysis, as it is implemented in protection relays, and it is not changed dynamically over the operation of the grid. The used under-frequency load-shedding scheme follows the ENTSO-E guidelines [32]. The additional wind power plants in the test system are described in detail in Section 3.2.

### *3.2 Wind power plant modeling*

Wind power plants are additionally included in the IEEE RTS to analyze their impact on the frequency quality. The wind power plants included in the analysis have a total rated power of 1000 MW. The current power injection of the wind power plants depends on the wind speed distribution and the design and control of the turbines. The wind speed probability follows Gaussian distribution, a commonly used way of modeling wind power throughout the yearly operation [35]. The wind speed is translated to the wind power output, respecting cut-in wind speed, cut out wind speed, and maximum wind power. Two hundred wind turbines are included in the IEEE RTS with a rated wind turbine power of 5 MW. The cut-in, the rated, and the cut-out wind speed are 3 m/s, 11.4 m/s, and 25 m/s, the details of the turbine are described in [36]. The produced wind power in every hour of a year can be combined in a wind power duration

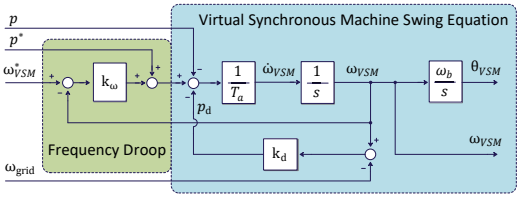


**Fig. 7**: Virtual Inertia control block of a wind turbine [12].

curve. The wind power plants together with the wind speed distribution are designed to have 4000 full load hours [37], representing offshore wind conditions.

### *3.3 VSM service by wind power plants*

Additional frequency controls in wind power plants are designed to improve the system frequency reliability in power electronic converter-based generation units. Wind power plants are also, in certain limits, capable of performing VSM services. However, when additional active power is supplied to the grid, then the wind turbines are slowed down and have to recover after the disturbance is cleared. The VSM control is described in Section 3.3.1, whereas the two compared scheduling schemes are described in Section 3.3.2.

*3.3.1 VSM control in the wind power plants:* Wind power plants in operation have a certain amount of kinetic energy available in the form of the rotating blade, gear, and generator. This allows the short-term power output to increase by reducing the rotational speed of the turbine. It has been shown that wind power plants are capable of delivering this kind of active power service [38–40].

Until now, converter-based units are current-controlled, meaning they synchronize to the grid voltage and then inject current into the grid. VSM control is changing the way converters behave severely. The active and reactive power flows of VSM-controlled machines are directly dependent on changing grid conditions. Reactive power loops change the magnitude of the converter output voltage, whereas the active power control is responsible for the voltage angle, emulating the inertia from machines. Different ways of VSM implementations are possible. In practice, however, inner current controls are still responsible for the equipment protection as well as for backup-purposes during grid faults, together with a phase-locked loop (PLL) for grid synchronization [12]. The virtual inertia and power control block is responsible for the frequency-dependent converter behavior. This control block is shown in Fig. 7. Two timeframes are given in this control block, the inertia-emulating part and then the steady-state droop-based control actions.

It can be seen in Fig. 7 that the measured active power flow $P$ into the grid is compared to the reference value $P^*$. Any deviation causes a change in the internal rotational speed value and, therefore, the angle of the output voltage and with this, the amount of produced active power. The internal frequency is also used in an internal loop so that the converter operates with a Droop characteristic, being defined with the control value $k_d$. This allows for finding a stable operating point after disturbances in systems with multiple machines. $T_a$ is the time constant that represents the time constant of the synchronous machine. The emulated time constant $T_a$ is set to 5 seconds, the damping $k_d$ is set to 50, as used in [41]. The possible active power change due to the enabled VSM service in the wind power plants is set to 0.2 pu. The VSM service is, when activated, used in 20 % of the wind power plants, as not all wind power plants may be equipped with the control option of the VSM service.

This study evaluates the active power delivery as a system service and does not give design proposals for the internal controls, such as the synchronization, current, and voltage controls. When system operator orders the service during operation, then the wind power plants can deliver more active power for a short time during frequency drops. During an increasing system frequency, the wind turbines curtail their power output, balancing the system's active power. The power reduction can be realized for a long duration without damaging the equipment.

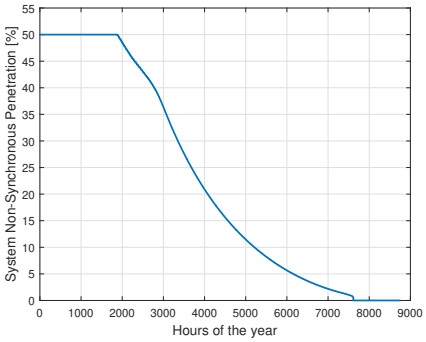


**Fig. 8**: SNSP of the IEEE RTS system with 1000 MW wind power installed.

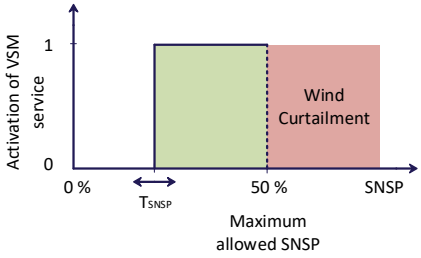


**Fig. 9**: Proposed VSM scheduling scheme based on the SNSP, with the variable $T_{SNSP}$ being changed during the reliability assessment.

*3.3.2 VSM Scheduling Strategies:* The VSM functionality is a system service ordered by the system operator. This service is to be scheduled to utilize it only when needed by the system during weak grid conditions. With the scheduling scheme, the TSO can decide when to activate this service and when it is not needed. For this, the system operators have to estimate the state of the power grid, so the amount of system load, the number of conventional generation units in operation, as well as the current number of converter based generation. The decision is based on the scheduling strategy, which considers the acquired information. Service activation is then distributed via communication links to the system equipment, changing the operating states.

The first analyzed scheduling scheme evaluates the SNSP, the System Non-Synchronous Penetration. With higher penetration of converters, this value is increased throughout the operation. However, it is not a direct measure of the remaining system inertia, as it only depends on the share of converter based injection, not on the total value of remaining synchronous generation units. It is given, as described in (6). The SNSP for the given IEEE RTS with the additional wind power plants is given in Fig. 8.

The scheduling scheme is illustrated in Fig. 9. The scheduling strategy activates the VSM service by the wind power plants whenever the actual SNSP is above a pre-defined threshold $T_{SNSP}$. The value of $T_{SNSP}$ is varied in this analysis from 50 % to 30 % to compare the different settings according to their impact on the system reliability. The wind power is always curtailed so that it never exceeds a penetration level of 50 %, so the service is first activated at this threshold. Reducing the threshold activates the service already at lower penetration levels, so the service is used more often during the operation.

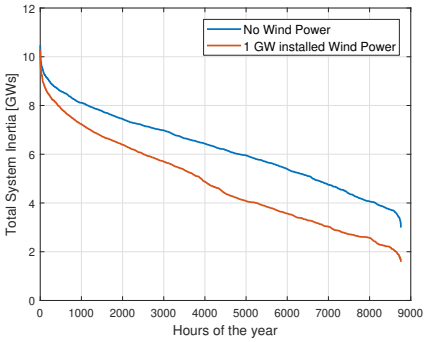


**Fig. 10**: TSI of the IEEE RTS system without and with 1000 MW wind power installed.

The second strategy for utilizing the VSM service is based on the remaining total system inertia (TSI). When the TSI is below a certain threshold $T_{TSi}$, then the system frequency is at greater danger of being in an abnormal state, and the VSM service is demanded. The TSI is defined by the conventional synchronous generation units in the system.

$$TSI = \sum_{i=1}^{N_i} SB_i \cdot H_i \tag{6}$$

The TSI of the IEEE RTS system without and with the 1000 MW wind power installed are shown in Fig. 10.

$T_{TSi}$, the threshold for demanding the VSM service, is varied in this analysis from 2 GWs to 4 GWs in order to determine the most reliable setting for frequency management. The results of the two compared scheduling schemes are illustrated in Section 4; the fuzzy-based evaluation for the study case is described in Section 4.3.

## 4 Results

### 4.1 Reliability with TSI-based scheduling

The system reliability is influenced by the value set for the scheduling scheme $T_{TSI}$. The Risk-based indices of the system are shown in Table 4. The results show how a higher threshold value changes the VSM service usage, which influences EENS, ENAF, and EAFD.

The used system Efforts for the different frequency management are shown in Table 5, with the indices EWEW, EVSM, ECU, and IENS. Other indices can help determine determining the optimal frequency management strategy when utilizing different frequency control schemes.

It can be seen that changing the scheduling strategy has an influence on all the determined frequency control-related indices. The comparison of the frequency performance and the control effort is further shown in Section 4.4. The proposed evaluation method is used to determine which scheduling strategy is better suited for reliable frequency management.

### 4.2 Reliability with SNSP-based scheduling

In this section, the system reliability using an SNSP-based scheduling strategy is evaluated. The threshold for activating the VSM service, $T_{SNSP}$ is varied in order to determine its influence on the system frequency reliability. The Risk-related indices are shown in Table. 6.

The Effort of the system with SNSP-based scheduling is shown in Table 7. $T_{SNSP}$ is varied in order to determine its influence on the frequency control effort by the system.

As different indices describe the system reliability for the tested management strategies, it is difficult to assess which one is suitable for TSO needs. The Effort has to be compared with the system's frequency behavior, described in Table 6. The proposed fuzzy-based evaluation method aims to allow this. It is shown in Section 4.3 how the fuzzy evaluation is adapted for the study case. The calculated System Effort and System Risk are then compared in Section 4.4.

Table 4: Results of the System Risk with TSI-based scheduling

| $T_{TSI}$ GWs | EENS GWh | ENAF occur | EAFD min |
|---|---|---|---|
| No VSM | 6.234 | 39.67 | 55.2 |
| 2 | 6.194 | 39.31 | 54.78 |
| 2.2 | 6.156 | 39.17 | 54.72 |
| 2.4 | 6.122 | 39.04 | 54.63 |
| 2.6 | 6.088 | 38.91 | 54.58 |
| 2.8 | 6.032 | 38.67 | 54.54 |
| 3 | 5.971 | 38.45 | 54.50 |
| 3.2 | 5.923 | 38.29 | 54.46 |
| 3.4 | 5.896 | 38.25 | 54.42 |
| 3.6 | 5.882 | 38.10 | 54.38 |
| 3.8 | 5.879 | 37.67 | 54.27 |
| 4 | 5.874 | 37.46 | 54.12 |

Table 5: Results of the System Effort with TSI-based scheduling

| $T_{TSI}$ GWs | EWEW GWh | EVSM GWh | ECU GWh | IENS GWh |
|---|---|---|---|---|
| No VSM | 518.19 | 0 | 0.447 | 0.2629 |
| 2 | 517.63 | 4.23 | 0.442 | 0.2621 |
| 2.2 | 517.41 | 6.73 | 0.438 | 0.2619 |
| 2.4 | 517.07 | 7.18 | 0.434 | 0.2619 |
| 2.6 | 516.87 | 8.91 | 0.433 | 0.2617 |
| 2.8 | 516.41 | 10.30 | 0.430 | 0.2614 |
| 3 | 515.90 | 11.59 | 0.428 | 0.2611 |
| 3.2 | 515.24 | 13.25 | 0.423 | 0.2609 |
| 3.4 | 514.48 | 15.93 | 0.418 | 0.2608 |
| 3.6 | 513.76 | 17.27 | 0.416 | 0.2606 |
| 3.8 | 513.32 | 19.89 | 0.414 | 0.2603 |
| 4 | 513.17 | 21.32 | 0.412 | 0.2601 |

### 4.3 Fuzzy-based evaluation in the study case

The fuzzy-based evaluation is adapted to the analyzed power system and the used frequency managements. The fuzzy-sets for the given study case allow for comparing the system frequency performance and load curtailment enhancement. The three indices for the system Risk description (EENS, ENAF, and EAFD) are fully assigned to the Low set when their values are reduced by 10 %; they are assigned as High when they increased more than 10 %. This value is dependent on the amount of change that system has in its reliability throughout the analyzed system conditions.

The Effort-related index EVSM changes severely for the different used scheduling strategies and settings. The assignment is Normal at zero VSM service usage. It is fully assigned to the High set when

Table 6: Results of the System Risk with SNSP-based scheduling

| $T_{SNSP}$ | EENS GWh | ENAF occur | EAFD min |
|---|---|---|---|
| No VSM | 6.234 | 39.67 | 55.21 |
| 50% | 5.902 | 37.56 | 54.37 |
| 48% | 5.887 | 37.49 | 54.10 |
| 46% | 5.883 | 37.42 | 54.08 |
| 44% | 5.879 | 37.36 | 54.06 |
| 42% | 5.875 | 37.29 | 54.04 |
| 40% | 5.870 | 37.16 | 54.04 |
| 38% | 5.866 | 37.03 | 54.03 |
| 36% | 5.862 | 36.89 | 53.97 |
| 34% | 5.860 | 36.83 | 53.89 |
| 32% | 5.858 | 36.76 | 53.82 |
| 30% | 5.856 | 36.69 | 53.80 |

Table 7: Results of the System Effort with SNSP-based scheduling

| $T_{SNSP}$ | EWEW GWh | EVSM GWh | ECU GWh | IENS GWh |
|---|---|---|---|---|
| 2 | 518.19 | 0 | 0.447 | 0.2629 |
| 2.2 | 516.57 | 16.63 | 0.425 | 0.2609 |
| 2.4 | 516.34 | 16.68 | 0.425 | 0.2607 |
| 2.6 | 516.03 | 16.81 | 0.423 | 0.2606 |
| 2.8 | 515.63 | 16.99 | 0.419 | 0.2604 |
| 3 | 515.27 | 17.16 | 0.417 | 0.2604 |
| 3.2 | 514.72 | 17.42 | 0.414 | 0.2604 |
| 3.4 | 512.89 | 17.68 | 0.409 | 0.2601 |
| 3.6 | 511.35 | 17.95 | 0.406 | 0.2599 |
| 3.8 | 510.61 | 18.13 | 0.404 | 0.2597 |
| 4 | 510.22 | 18.30 | 0.401 | 0.2597 |

it is at 36 GWh. This is the amount of VSM service that would be demanded when the service is ordered full-time. It depends on the power system behavior and has to be adapted when the VSM usage, control settings, and the scheduling strategy are varied. EWEW, IENS, and ECU are also assigned to the Low set when reduced by 10%. They are fully assigned as High when increased by 10%.

The interference matrix used in the study case is shown in Table 3. The interference is not dependent on the study case, as the fuzzy-sets themselves are adapted to the specific case study.

The de-fuzzyfication is performed as described in Section 2.2.3. The five sets, Very Low, Low, Normal, High, and Very High, are assigned with 0, 0.5, 1, 2, and 5, respectively. This is done to weight the rise of indices more than the reduction of indices due to frequency management changes. In the shown test case, this would mean an increase in system Risk if the ENAF rises by 10 % and the EAFD drops by 10 %. Other strategies for the evaluation can be chosen, such as a balanced rise to reduction ratio. This changes then the outcome values of the system Risk and Effort values.

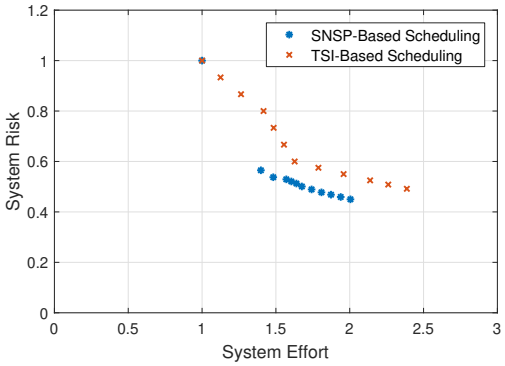


**Fig. 11**: Results of the reliability evaluation, allowing for comparison of different frequency management strategies.

### *4.4 Comparison of the scheduling strategies*

The reliability indices shown in Sections 4.1 and 4.2 are difficult to compare. Multiple indices have to be assessed in order to find the most reliable frequency management. The proposed fuzzy-based evaluation determines the Risk and Effort values of the respective scheduling settings and strategies. The results of both strategies in the evaluated study case with the utilized frequency managements are shown in Fig. 11.

It can be seen that both strategies reduce the system Risk by increasing the frequency management Effort. The reduction in Risk indicates that the additional frequency control reduces the amount of load curtailment, as well as abnormal frequency states and duration. However, the SNSP-based scheduling strategy is more effectively reduces the system Risk while not increasing the Effort too much. This indicates that the SNSP-based scheduling activates the VSM service more effectively in grid conditions, where it is more useful for frequency management in the evaluated power system and wind condition.

On the other hand, the TSI-based scheduling scheme allows a more gradient change in system frequency management. This can be explained by comparing Fig. 8 and Fig. 10. An increase in the threshold of the TSI-based scheduling causes a slow increase in the VSM service usage, whereas the SNSP-based scheduling is initially activated during larger shares of the system operation at the initial usage at SNSP being 50 %.

Comparing the different scheduling strategies allows TSOs to decide fast which frequency management strategies are worth investigating closer.

## 5 Conclusion

A new evaluation method for power system frequency assessments is proposed in this work. It utilizes fuzzy-logic to combine multiple different reliability indices to only two values, the system Risk and the system Effort. These two values allow a fast comparison of different frequency management strategies by the system operator. This allows finding the most reliable operational strategy for power systems with a high penetration of converter-based generation units.

Comparing two scheduling strategies with changing settings for VSM service by wind power plants has been evaluated in this study. It shows which strategy allows a more effective VSM service usage concerning the frequency management. The different schemes activate the service based on two different criteria, the remaining system inertia or the actual non-synchronous penetration level. Therefore, the VSM service can be utilized more effectively, and weaker grid conditions can be controlled in a more reliable way. The proposed fuzzy-based evaluation allows adapting to operator

preferences quickly by assigning the indices with different priorities. Under different grid conditions, the evaluation can be adapted very fast, by changing the shape of the fuzzy-memberships in the fuzzyfication step.

The proposed method is not only be used to compare different scheduling strategies as done in the shown study case. It can also be utilized to compare different control structures, settings in the controls, as well as service scheduling. The frequency management design for improved frequency reliability allows for a wider integration of renewable-based generation units into the system while maintaining high operational frequency reliability. Solar systems, as well as HVDC and battery systems, can also provide frequency-services to the system. Their effect on the system reliability has to be determined to guarantee the best system performance for the least frequency control effort.

Further research aims to utilize more advanced fuzzy-set shapes during the fuzzyfication. Different Interference strategies can also be utilized and compared in their ability to detect optimal frequency management strategies.

## 6 Acknowledgments

This work is supported by the Reliable Power Electronic-Based Power Systems (REPEPS) project at the Department of Energy Technology, Aalborg University, as a part of the Villum Investigator Program funded by the Villum Foundation.

## 7 References

1 REN21. (2019) Renewables 2019 Global Status Report. (Date last accessed 24-Nov-2020). [Online]. Available: http://www.ren21.net/gsr-2019

2 MIGRATE. (2016) Deliverable D1.1, Report on Systemic Issues. (Date last accessed 24-Nov-2020). [Online]. Available: https://www.h2020-migrate.eu/downloads.html

3 ENTSO-E. (2017) Need for Synthetic Inertia (SI) for Frequency Regulation. (Date last accessed 24-Nov-2020). [Online]. Available: https://consultations.entsoe.eu/system-development/entso-e-connection-codes-implementation-guidance-d-4

4 ——, "Incident Classification Scale," pp. 1–27, March 27, 2018.

5 C. Liang, P. Wang, X. Han, W. Qin, R. Billinton, and W. Li, "Operational Reliability and Economics of Power Systems with Considering Frequency Control Processes," *IEEE Transactions on Power Systems*, vol. 32, no. 4, pp. 2570–2580, 2017.

6 J. Steinkohl, S. Peyghami, X. Wang, P. Davari, and F. Blaabjerg, "Frequency-Security Constrained Control of Power Electronic-Based Generation Systems," *Accepted for publication at IET Renewable Power Generation*, pp. 1–8, 2020.

7 ENTSO-E, "Frequency Stability Evaluation Criteria for the Synchronous Zone of Continental Europe," 2018, (Date last accessed 24-Nov-2020). [Online]. Available: https://www.energinet.dk

8 ENERGINET, "Technical Regulation for Wind Power Plants, Denmark," (Date last accessed 24-Nov-2020). [Online]. Available: https://en.energinet.dk

9 TenneT TSO GmbH, "Offshore - Netzanschlussregeln (O-NAR)," pp. 1–90, August, 2019.

10 S. D'Arco and J. A. Suul, "Virtual Synchronous Machines âĂŤ Classification of Implementations and Analysis of Equivalence to Droop Controllers for Microgrids," in *2013 IEEE Grenoble Conference*, 2013, pp. 1–7.

11 H. Bevrani, T. Ise, and Y. Miura, "Virtual Synchronous Generators: A Survey and New Perspectives," *International Journal of Electrical Power & Energy Systems*, vol. 54, pp. 244–254, 2014.

12 S. D'Arco, J. A. Suul, and O. B. Fosso, "A Virtual Synchronous Machine Implementation for Distributed Control of Power Converters in SmartGrids," *Electric Power Systems Research*, vol. 122, pp. 180–197, 2015.

13 A. Karimi, Y. Khayat, M. Naderi, T. Dragičević, R. Mirzaei, F. Blaabjerg, and H. Bevrani, "Inertia Response Improvement in AC Microgrids: A Fuzzy-Based Virtual Synchronous Generator Control," *IEEE Transactions on Power Electronics*, vol. 35, no. 4, pp. 4321–4331, 2019.

14 Y. Hu, W. Wei, Y. Peng, and J. Lei, "Fuzzy Virtual Inertia Control for Virtual Synchronous Generator," in *2016 35th Chinese Control Conference (CCC)*. IEEE, 2016, pp. 8523–8527.

15 L. Zhang, L. Harnefors, and H.-P. Nee, "Power-Synchronization Control of Grid-Connected Voltage-Source Converters," *IEEE Transactions on Power Systems*, vol. 25, no. 2, pp. 809–820, 2009.

16 P. Mitra, L. Zhang, and L. Harnefors, "Offshore Wind Integration to a Weak Grid by VSC-HVDC Links using Power-Synchronization Control: A Case Study," *IEEE Transactions on Power Delivery*, vol. 29, no. 1, pp. 453–461, 2013.

17 S. D'Arco and J. A. Suul, "Virtual Synchronous Machines - Classification of Implementations and Analysis of Equivalence to Droop Controllers for Microgrids," in *2013 IEEE Grenoble Conference*. IEEE, 2013, pp. 1–7.

18 U. Bose, S. K. Chattopadhyay, C. Chakraborty, and B. Pal, "A novel Method of Frequency Regulation in Microgrid," *IEEE Transactions on Industry Applications*, vol. 55, no. 1, pp. 111–121, 2018.

19 AEMO, Australian Energy Market Operator, "International Review of Frequency Control Adaptation," pp. 1–179, October 14, 2016.

20 N. Nguyen and J. Mitra, "Reliability of Power System with high Wind Penetration under Frequency Stability Constraint," *IEEE Transactions on Power Systems*, vol. 33, no. 1, pp. 985–994, 2017.

21 J. Guo, T. Zhao, W. Liu, and J. Zhang, "Reliability Modeling and Assessment of Isolated Microgrid Considering Influences of Frequency Control," *IEEE Access*, vol. 7, pp. 50 362–50 371, 2019.

22 R. Billington and R. N. Allan, *Reliability Evaluation of Power Systems*. Plenum Publishing Corp., New York, NY, 1984.

23 P. Wang, Z. Gao, and L. Bertling, "Operational Adequacy Studies of Power Systems with Wind Farms and Energy Storages," *IEEE Transactions on Power Systems*, vol. 27, no. 4, pp. 2377–2384, 2012.

24 J. Dave, H. Ergun, and D. Van Hertem, "Incorporating DC Grid Protection, Frequency Stability and Reliability into Offshore DC Grid Planning," *IEEE Transactions on Power Delivery*, 2020.

25 L. A. Zadeh, G. J. Klir, and B. Yuan, *Fuzzy Sets, Fuzzy Logic, and Fuzzy Systems: Selected Papers*. World Scientific, 1996, vol. 6.

26 L. A. Zadeh, "Fuzzy Sets," *Information and Control*, vol. 8, no. 3, pp. 338–353, 1965.

27 M. Fotuhi and A. Ghafouri, "Uncertainty Consideration in Power System Reliability Indices Assessment using Fuzzy Logic Method," in *2007 Large Engineering Systems Conference on Power Engineering*. IEEE, 2007, pp. 305–309.

28 A. R. Abdelaziz, "A Fuzzy-Based Power System Reliability Evaluation," *Electric Power Systems Research*, vol. 50, no. 1, pp. 1–5, 1999.

29 X. Liu, Z. Wang, S. Zhang, and J. Liu, "A Novel Approach to Fuzzy Cognitive Map based on Hesitant Fuzzy Sets for Modeling Risk Impact on Electric Power System," *International Journal of Computational Intelligence Systems*, vol. 12, no. 2, pp. 842–854, 2019.

30 B. Canizes, J. Soares, Z. Vale, and H. Khodr, "Hybrid Fuzzy Monte Carlo Technique for Reliability Assessment in Transmission Power Systems," *Energy*, vol. 45, no. 1, pp. 1007–1017, 2012.

31 K. Bruvik and L. M. Hytten, "Probabilistic Reliability Analysis in the Norwegian Transmission System," in *2020 International Conference on Probabilistic Methods Applied to Power Systems (PMAPS)*, 2020, pp. 1–6.

32 ENTSO-E. (2015) P5 - Policy 5: Emergency Operations. (Date last accessed 24-Nov-2020). [Online]. Available: https://docstore.entsoe.eu

33 P. M. Subcommittee, "IEEE Reliability Test System," *IEEE Transactions on Power Apparatus and Systems*, vol. PAS-98, no. 6, pp. 2047–2054, Nov 1979.

34 Reliability Test System Task Force of the Application of Probability Methods Subcommittee, "The IEEE Reliability Test System-1996," *IEEE Transactions on Power Systems*, vol. 14, no. 3, pp. 1010–1020, Aug 1999.

35 K. Conradsen, L. Nielsen, and L. Prahm, "Review of Weibull Statistics for Estimation of Wind Speed Distributions," *Journal of Climate and Applied Meteorology*, vol. 23, no. 8, pp. 1173–1183, 1984.

36 J. Jonkman, S. Butterfield, W. Musial, and G. Scott, "Definition of a 5-MW Reference Wind Turbine for Offshore System Development," National Renewable Energy Lab.(NREL), Golden, CO (United States), Tech. Rep., 2009.

37 B. Hahn, S. Faulstich, and V. Berkhout, "Well, How are They Running?" in *Sea–Wind–Power*. Springer, 2017, pp. 159–167.

38 D. Yang, E. Jin, J. You, and L. Hua, "Dynamic Frequency Support from a DFIG-Based Wind Turbine Generator via Virtual Inertia Control," *Applied Sciences*, vol. 10, no. 10, p. 3376, 2020.

39 M. Krpan and I. Kuzle, "Dynamic Characteristics of Virtual Inertial Response Provision by DFIG-Based Wind Turbines," *Electric Power Systems Research*, vol. 178, p. 106005, 2020.

40 H. Shao, X. Cai, Z. Li, D. Zhou, S. Sun, L. Guo, Y. Cao, and F. Rao, "Stability Enhancement and Direct Speed Control of DFIG Inertia Emulation Control Strategy," *IEEE Access*, vol. 7, pp. 120 089–120 105, 2019.

41 K. Gu, F. Wu, X.-P. Zhang, P. Ju, H. Zhou, J. Luo, and J. Li, "SSR Analysis of DFIG-Based Wind Farm with VSM Control Strategy," *IEEE Access*, vol. 7, pp. 118 702–118 711, 2019.

ISSN (online): 2446-1636
ISBN (online): 978-87-7210-917-6 AALBORG UNIVERSITY PRESS